USAAVLABS TECHNICAL REPORT 68-47

ADVANCEMENT OF HELICAL GEAR DESIGN TECHNOLOGY

By

Wayne L. McIntire

Terry A. Lyon

July 1968

U. S. ARMY AVIATION MATERIEL LABORATORIES
FORT EUSTIS, VIRGINIA

CONTRACT DA 44-177-AMC-450(T)
ALLISON DIVISION-GENERAL MOTORS
INDIANAPOLIS, INDIANA

263

DEPARTMENT OF THE ARMY
U. S. ARMY AVIATION MATERIEL LABORATORIES
FORT EUSTIS, VIRGINIA 23604

This report represents a part of a continuing program to derive more accurate and uniform gear design formulae for aircraft propulsion systems than currently available. The report presents the results of an analytical and experimental program to derive a precise bending strength formula for helical gear teeth and to provide an IBM 7090 computer program for the use of this formula. Positive results were obtained from the program, and the information contained herein can be immediately considered by gear designers.

This command concurs in the conclusions made by the contractor.

Task 1G125901A01410

Contract DA 44-177-AMC-450(T)
USAAVLABS Technical Report 68-47
July 1968

ADVANCEMENT OF HELICAL GEAR DESIGN TECHNOLOGY

Final Report

by

Wayne L. McIntire
and
Terry A. Lyon

Allison Division Report EDR 5503

Prepared by

Allison Division ● General Motors
Indianapolis, Indiana

for

U.S. ARMY AVIATION MATERIEL LABORATORIES
FORT EUSTIS, VIRGINIA

SUMMARY

This report presents the results of an analytical and experimental program to derive and substantiate a bending strength design formula for helical gears. The program consisted of the following:

- Static single-tooth fatigue testing of four gear designs to determine the effect of two geometric variables (pressure angle and helix angle) and two tooth load positions (tip loading inboard of the tooth corner and tip loading at the tooth corner)
- Evaluation of the ability of five current calculation methods—AGMA, Lewis, Heywood, Almen-Straub, Cantilever Plate—to predict the relative ranking of the four fatigue test gear endurance limits for comparison with the basic material strength
- Statistical analyses of the fatigue test data to develop a predictive formula which reflects the basic material strength and relative significance values of the two geometric variables
- R. R. Moore rotating beam fatigue tests of the gear material to establish basic material strength for comparison with fatigue test endurance limits and the five calculation methods
- Strain gage measurements to determine the load distribution at the root fillet
- Measurement of the fatigue test gear crack location for comparison with location of the weakest section as predicted by the Lewis calculation method
- Metallurgical examination of fatigue test gears to verify material processing and mode of failure
- Dynamic testing at high pitch line velocity on helical gears (up to 20, 000 feet per minute) to determine the speed effect on gear tooth bending stress
- Development of a computer program to calculate gear tooth bending stress from the basic gear geometry

A modification to the existing AGMA method for calculating helical tooth bending strength was necessary to produce correlation between the calculated and actual endurance limit strength. The modification to AGMA Standard 221.02 consists of an accurate determination of the helical factor, C_H, and use of the factor as a direct stress modifier as presented in the Discussion of Results. This modification, in addition to speed effects, has been included in the final computer program.

The detailed results of the program are as follows.

- The AGMA and Cantilever Plate methods of calculating gear tooth bending stress accurately predicted the ranking of the strongest and weakest gear configurations. Both methods provided close correlation between calculated and actual gear fatigue life. The average endurance limit calculated by the Cantilever Plate method was 161,564 pounds per square inch, while the average calculated endurance limit for AGMA was 152,000 pounds per square inch.
- The average endurance limit of the gear material as determined by R. R. Moore rotating beam fatigue testing was 175,000 pounds per square inch for single directional loading. The Cantilever Plate method calculated the endurance limit to be within 8 percent of this established value, and the AGMA method was within 13 percent. A design stress value (1 percent failure) was statistically established to be 115,000 pounds per square inch for single directional loading.
- Dynamic testing of helical gears indicated a speed effect on tooth bending stress. The maximum bending stress measured was a squared function of speed. The calculated hoop stress was included in the computer program bending stress determination for high speed gears.
- The dynamic test measured dynamic fluctuating gear tooth bending stresses. The measured stresses indicated the stress to be increasing with the square of the speed. Testing to 20,000 feet per minute pitch line velocity resulted in a dynamic factor of 1.12.
- A comparison of the calculated endurance limits, based on applied load, was made by statistical tests of significance. Helix angle and pressure angle had a significant effect on gear tooth bending strength, and these effects were predicted by the AGMA and Cantilever Plate formulae. The effect of a change in load position was not proved to be significant.
- The strain gage stress values obtained were lower than values expected considering the R. R. Moore determined material strength. Actual crack locations on failed gears indicated that the area of maximum stress occurred approximately 0.030 inch below the location of the strain gages, accounting for the lower strain gage values. The measured strain gage stress values were within approximately 8 percent of Cantilever Plate stress calculations and within approximately 5 percent of AGMA calculations.
- Metallurgical examinations verified good processing of the fatigue test gears and fatigue as the mode of failure. Failures were initiated in the tooth root on the loaded side of the gear and were located in the general area of analytical maximum bending moment.

- Accurate determination of the helical factor used to modify the AGMA and Cantilever Plate bending stress formulae was found to be the most important criterion for correlating fatigue results, actual material strength, and calculated bending strength.
- The computer program developed accurately determined the root fillet configuration depending on tool (hob) dimensions. The tooth form factor is accurately determined by iteration. The gear tooth dimensions determined are used in a modification of the AGMA formula to determine bending stress. The modification consists of using the helical factor, C_H, to modify calculated stress directly rather than as an operator on the Lewis determined tooth form factor, X. A subroutine in the computer program accurately calculates the helical factor. A hoop stress at the root diameter is then calculated to account for the effect of speed on gear tooth bending stress. The steady hoop stress and the periodic bending stress are combined by means of a modified Goodman diagram to produce a combined stress and an expected failure life.

FOREWORD

This is the final report on the Allison project entitled "Advancement of Helical Gear Design Technology." This project was conducted during the 20-month period from 22 June 1966 through 22 February 1968 for the U.S. Army Aviation Materiel Laboratories (USAAVLABS) under Contract DA 44-177-AMC-450 (T).

USAAVLABS technical direction was provided by Mr. R. Givens.

The principal investigators at Allison were Mr. T. A. Lyon, Mr. F. G. Leland, Mr. M. R. Chaplin, Mr. K. V. Young, and Mr. W. W. Gunkel. The program was reviewed periodically by Mr. R. L. Mattson of General Motors Research for suggestions and comments.

Permission was obtained from the American Gear Manufacturers Association (AGMA) to print AGMA 221.02, Tentative AGMA Standard for Rating the Strength of Helical and Herringbone Gear Teeth, in this final report.

TABLE OF CONTENTS

LIST OF ILLUSTRATIONS

Figure		Page

Figure		Page

LIST OF TABLES

INTRODUCTION

The purposes of this project were to determine the effect of tooth geometry and tooth load position on helical gear tooth bending strength and to derive factors and formulae which can be used to appraise accurately helical gear tooth bending strength for aircraft applications.

The objectives of the project included substantiation of an accurate helical gear bending strength formula and the providing of an IBM 7090 computer program using the substantiation formula. Correlation of the basic material strength with this formula was also desired.

There are four common modes of gear failure: tooth breakage, surface pitting, scoring, and wear. Tooth breakage, which may be caused by foreign object interference or repetitive high bending stresses in the tooth root, is the most severe and often causes considerable secondary damage and catastrophic failure of an entire gear unit.

Many factors affecting the bending fatigue strength of gear teeth are not treated with precision in current helical gear design formula because the magnitude and interrelationship of the various factors involved have not been accurately assessed. Helical gear tooth bending strength is a function of geometric variables; i. e., pressure angle, helix angle, diametral pitch, tooth width, root fillet form, and root fillet radius. The bending strength is also influenced by manufacturing variables; i.e., surface finish, residual stress, material, and processing technique. Operating variables (i.e., speed, alignment, dynamic loading, and vibration) also affect the gear fatigue life. A thorough analysis of these variables will permit more accurate assessment of gear life expectancy.

Considerable research has been accomplished in analyzing gear tooth bending strength. Most of this research has been conducted on spur gears, and the results have been applied, often with modifying factors, to helical gears. There is a wide variation in the type of analysis, test data, and field experience. Application of these data to carburized gears designed to current standard geometric proportions often requires extensive extrapolation. The program described in this report was conducted in an effort to establish correlation between analytical methods and actual test results for lightweight aircraft gearing.

Current methods of calculating helical gear tooth bending stress are based on analytical studies and photoelastic tests conducted mainly on

spur gears. These methods produce calculated stresses which are appreciably lower than measured gear stresses and basic material strengths. Thus the calculations are most often used to compare similar designs. An "ideal" gear tooth bending strength formula would relate the operating gear tooth stress to the basic material strength to produce a gear life substantiated by standardized fatigue tests. It was the intent of this program to provide a more accurate bending stress formula by also relating calculated stress and fatigue test results to the basic material strength. R. R. Moore tests of carburized specimens were used to provide the basic material strength.

The following analytical and experimental analyses were conducted during this investigation:

- Design Analysis—An analytical review was made of current helical gear tooth bending strength formulae. Each formula was analyzed and compared to determine the effects of design variables.
- Experimental Evaluation—Each test gear configuration was instrumented with strain gages and statically loaded to obtain strain measurements for correlation with stress calculations.
- Gear Tooth Fatigue Tests—A single tooth fatigue test was conducted to investigate the effect of pressure angle, helix angle, and load position on fatigue life. Thirty-two gears were manufactured. Extreme care was taken to reduce all manufacturing variables which might affect fatigue life. Metallurgical investigations of the fatigue failures were made to ensure that the basic material was sound and was properly heat treated and that the failure mode was fatigue. Six teeth on each gear were available for fatigue testing.
- R. R. Moore Tests—R. R. Moore tests were conducted using the same heat material used to manufacture the test gears. The data obtained were used for comparison with the bending endurance strengths from the gear fatigue tests.
- Final Computer Program—Data collected during the program were formulated into an IBM 7090 computer program for helical gear bending strength.

ANALYSIS OF PROBLEM

HISTORICAL REVIEW

A review of helical gear tooth bending strength theory was made. The results of this review are discussed in the following paragraphs.

In 1892, Mr. Wilfred Lewis presented a paper which related gear tooth bending strength to tooth geometry. The Lewis method for computing tooth bending stress assumes that the tooth proportions approximate loading of a parabolic cantilever beam and determines the bending stress at an "assumed weakest section" of the tooth. The "assumed weakest section" is found by inscribing a uniform strength parabola in the tooth so that the vertex of the parabola is placed at the intersection of the load line with the radial center line of the tooth. The point of tangency of the parabola with the fillet of the tooth establishes the "assumed weakest section" of the tooth.

Mr. T. J. Dolan and Mr. E. S. Broghamer have established that the theory of flexure assumed by Mr. Lewis to determine the stress in the fillet is applicable only to constant cross-section members and that at any abrupt change in section of a stressed member (i.e., the root fillet of a gear tooth), localized stresses of relatively large magnitude are developed. Dolan and Broghamer conducted a photoelastic study of stresses in gear tooth fillets at the University of Illinois Engineering Experiment Station in 1942. This study resulted in a series of stress correction factors dependent on gear geometry which have been incorporated in the current AGMA Standard 221.02.

The existence of stresses other than bending stresses was recognized at an early date. The shear stress in the tooth root due to the tangential component of tooth load and the compressive stresses caused by the radial component of the tooth load are examples of these additional stresses. Several current tooth strength formulae include these stresses. These static stresses are present in the photoelastic models used to determine stress correction factors and are included in the stress correction factor employed in the AGMA formula. See Appendix IV.

This previous investigative effort has been directed toward the solution of spur gear problems, and the results are directly applicable primarily to spur gears. The most common method used to calculate bending stress in helical gear teeth has been to consider an infinitely thin section of the helical gear tooth as a spur gear tooth and to calculate bending stress using conventional spur gear equations.

This procedure ignores the fundamental difference between the tooth loading characteristics of the helical and spur gears. The helical gear tooth contact line is inclined to the tooth tip, while the spur gear tooth contact line is parallel to the tooth tip.

The effect of the inclined load line on the root bending moment distribution was investigated by Wellauer and Seireg.[1] A semiempirical method to determine the bending moment distribution was also advanced which gave good correlation between theoretical and actual strain-gage investigations. This investigation was based on prior work done by MacGregor,[2] Holl,[3] and Jaramillo[4] to define the moments and deflections of a cantilever plate caused by concentrated transverse loads. Wellauer and Seireg extended this work to include the bending moment distribution in cantilever plates caused by loads impressed on the plate at various inclination angles and load intensities. The result of the investigation was to develop a correction factor based on the maximum bending moment produced by load application on the inclined line and that which would be produced in a gear loaded "parallel to axis" at the tooth tip.

The correction factor (c) in the Cantilever Plate theory is simply the ratio of maximum bending moment produced by a loading applied along the oblique helical contact line to the root bending moment produced by the same intensity of loading applied parallel to and at the tooth tip. This correction factor is applied directly in the Cantilever Plate bending stress formula. The inverse of the same helical correction factor is used in the AGMA bending stress formula to modify the Lewis form factor which is used to calculate the geometry factor (J).

Several helical gear bending strength formulae use a stress modifying factor based on the tooth-to-tooth load transfer ability of helical gears. The Almen-Straub equation[5] uses the minimum length of the transverse line of action to modify the basic Lewis bending strength formula. The Cantilever Plate formula[1] uses a load sharing factor equivalent to the ratio of the minimum length of the oblique contact lines to the gear face width to modify the stress formula. The AGMA formula uses the same load sharing ratio in an inverse form as a modifier of J.

Five helical gear tooth bending strength formulae were evaluated and applied to the four fatigue test gear configurations: Lewis, Almen-Straub, Heywood, AGMA, and cantilever plate. The stresses for each configuration are listed in Table I. The stresses in each case are calculated using

TABLE I. COMPARISON OF GEAR TOOTH BENDING STRESSES CALCULATED BY VARIOUS METHODS

Gear No.	W_T**/F	Part Number	Helix Angle (degrees)	Pressure Angle (degrees)	AGMA* Bending Stress (psi)	Lewis Bending Stress (psi)	Lewis % AGMA	Almen-Straub Bending Stress (psi)	Almen-Straub % AGMA	Heywood Bending Stress (psi)	Heywood % AGMA	†Cantilever plate Bending Stress (psi)	†Cantilever plate % AGMA
Stress Per 1000-lb Applied Load													
1	939	EX-84117	20	20	$\boxed{20,700}$	$\boxed{15,483}$	74.8	13,525	65.3	$\boxed{27,935}$	135	$\boxed{21,751}$	105
2	905	EX-84118	20	25	14,300	11,966	83.7	$\boxed{11,926}$	83.4	24,555	171.7	16,255	113.6
3	939	EX-84119	35	20	20,000	10,270	51.4	$\boxed{15,036}$	75.2	26,124	130.6	19,194	96
4	905	EX-84120	35	25	$\boxed{13,500}$	$\boxed{7,877}$	58.3	13,735	101.7	$\boxed{24,372}$	180.5	$\boxed{13,729}$	101.7
Stress Per 6000-lb Unit Load													
1	6000	EX-84117	20	20	22,000	16,500	74.8	14,403	65.3	29,800	135	23,200	105
2	6000	EX-84118	20	25	15,800	13,200	83.7	13,181	83.4	27,100	171.7	18,000	113.6
3	6000	EX-84119	35	20	21,250	11,000	51.4	16,062	75.2	27,850	130.6	20,400	96
4	6000	EX-84120	35	25	14,900	8,700	58.3	15,168	101.7	26,900	180.5	15,200	101.7

†K_m = 1.10

*C_H—calculated per Cantilever Plate theory
K_m = 1.10

**W_T = define as tangential load at pitch diameter
W_T/F = unit load

a 1000-pound load applied normal to the tooth surface along the inclined load line and for a constant unit load of 6000 pounds per inch. Unit load is defined as the equivalent tangential load at the pitch diameter on a tooth having a diametral pitch of 1 and a face width of 1 inch.

All of the formulae, with the exception of the Almen-Straub formula, identified the same configurations as having the highest and lowest stresses (boxed numbers in Table I). The Heywood method calculates the highest stresses in all cases.

The geometric construction and formula for each of the five gear tooth strength calculation methods are shown in Figures 1, 2, and 3 and in Tables II and III. The Lewis and Almen-Straub methods use the Lewis geometric construction (Figures 1 and 2) in the normal plane of the gear. The AGMA and Cantilever Plate methods use the Lewis geometric construction in the normal plane at one diametral pitch. The Lewis and Almen-Straub methods do not include a stress concentration factor, while a stress concentration factor is included in both the AGMA and Cantilever Plate theory.

The Heywood construction method (Figure 3) locates the maximum fillet stress point as a function of the fillet radius of curvature only. It should be applicable, therefore, to any gearing system for which the fillet curvature is definable.

In summary, a review of the literature indicated that a wide variation of bending stress could be calculated for a given configuration. Limited data are available which attempt to correlate the actual endurance limit stress of a material as determined by laboratory tests and the calculated endurance limit stress of a gear manufactured from the material. It was apparent that a controlled fatigue experiment with full size tooth proportions could aid the development of a more accurate method of calculating helical gear bending strength. Correlation of the calculated endurance limit stress with basic material strength data from R. R. Moore fatigue tests would enhance the analysis.

DESIGN OF EXPERIMENT

Two factors of gear tooth geometry and two factors of tooth load position were investigated in a statistically designed experiment. Each of the factors was expected to affect gear tooth fatigue life. The experiment was designed to determine if these factors interact and if the observed results

were statistically significant. The factors evaluated were:

Factor	Levels	Values Assigned
Pressure angle	2	20 and 25 degrees
Helix angle	2	20 and 35 degrees
Load position	2	Load through tip of tooth at corner and load through tip of tooth 0.250 in. inboard from corner

$$S_b = \frac{W}{F\,Y\,p}$$

$$Y = \frac{2}{3}\,\frac{x}{p}$$

$$x = \frac{t^2}{4h}$$

$$S_b = \frac{6\,Wh}{Ft^2}$$

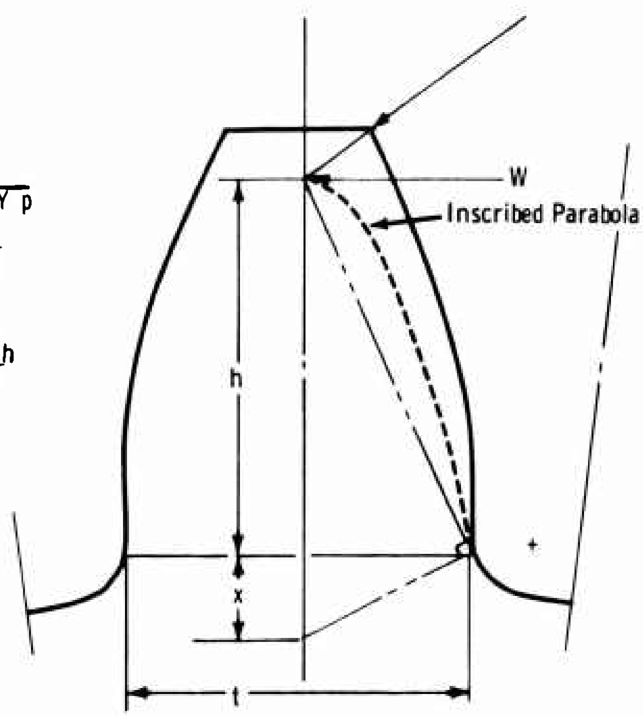

where

- W = tangential component of load applied at vertex of inscribed parabola
- F = face width of tooth
- S_b = maximum bending stress
- h = height of equivalent constant stress parabolic beam
- t = thickness of beam at weakest section
- p = circular pitch

Figure 1. Lewis Construction and Gear Tooth Bending Stress Formula.

$$S_b = \frac{3\pi\, T}{N\, F\, N_a\, X}$$

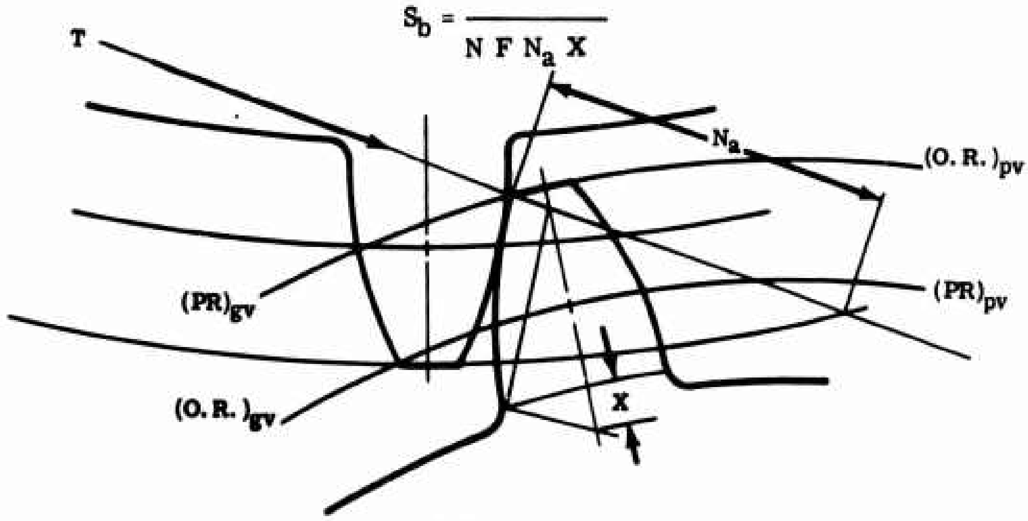

Normal Section Layout

where

S_b = bending stress of tooth
T = applied torque on driving gear
N = number of teeth
F = gear face width
N_a = length of line of action in plane of rotation

$$N_a = \left[(O.R.)_{pv}^2 - (PR)_{pv}^2 \cos^2\phi\right]^{1/2} + \left[(O.R.)_{gv}^2 - (PR)_{gv}^2 \cos^2\phi\right]^{1/2} - (PR_{pv} + PR_{gv}) \sin\phi$$

where

$O.R._{pv}$, $O.R._{gv}$ = outside radius of pinion, gear in plane of rotation

PR_{pv}, PR_{gv} = pitch radius of pinion, gear in plane of rotation

ϕ = pressure angle in plane of rotation

X = Lewis tooth form factor with load applied at tooth tip

Figure 2. Almen-Straub Construction and Gear Tooth Bending Stress Formula.

$$S_b = \left[1 + 0.26\left(\frac{e}{R}\right)^{0.7}\right]\left[\frac{1.5\,a}{e^2} + \left(\frac{0.36}{be}\right)^{0.5}(1 + 0.25\sin\gamma)\right]\frac{P}{F}$$

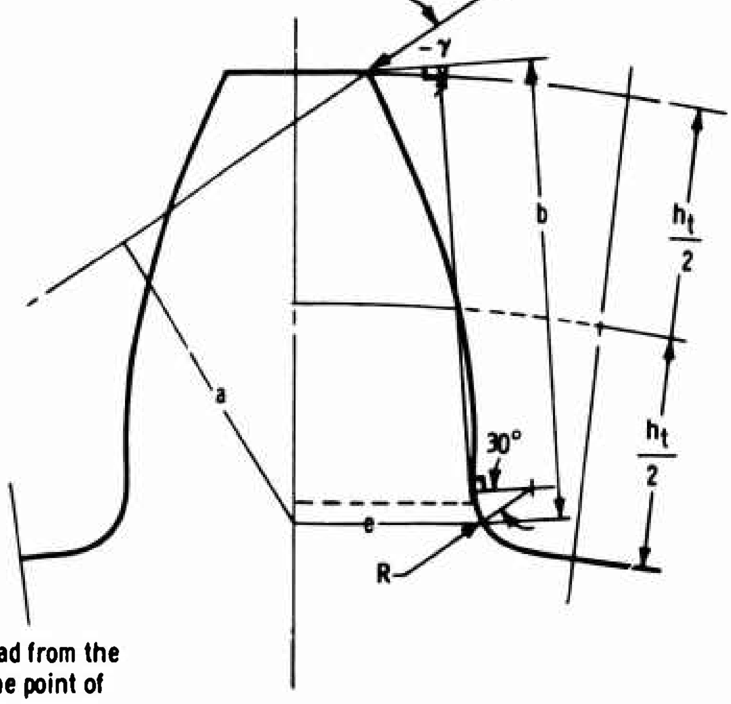

where

h_t = tooth depth

F = face width

a = moment arm

e = resisting material

R = fillet radius

P = normal load

γ = angle deviation of load from the point of loading to the point of maximum stress

b = distance parallel to equivalent straight-sided projection from the point of loading to the point of maximum stress

S_b = maximum fillet stress

Figure 3. Heywood Construction and Gear Tooth Bending Stress Formula.

The experiment planned involved cycling two teeth to failure at four stress levels for each of the eight possible combinations of the four geometric variables and two load positions investigated.

Evaluation of the two geometric factors and two load position factors was to be based on the infinite life portion of the resulting fatigue (S-N) curves.

DESIGN OF FATIGUE TEST GEARS

Drawings of the four fatigue test gears are presented in Appendix I. Table IV lists the pertinent dimensions for the four fatigue test gear configurations.

TABLE II. AGMA GEAR TOOTH BENDING STRESS FORMULA

$$S_t = \frac{W_t K_o}{K_v}\left(\frac{P_d}{F}\right)\frac{K_s K_m}{J}$$

where

S_t	= calculated tensile stress at the tooth root	
W_t	= transmitted tangential load at the operating pitch diameter	Load
K_o	= overload factor	Load
K_v	= dynamic factor	Load
P_d	= transverse diametral pitch	Tooth Size
F	= net face width	Tooth Size
K_s	= size factor	Stress Distribution
K_m	= load distribution factor	Stress Distribution
J	= geometry factor	Stress Distribution

$$J = \frac{Y_c \cos^2 \psi}{K_f M_n}$$

where

J	= geometry factor
Y_c	= tooth form factor
ψ	= helix angle, degrees
K_f	= stress correction factor
M_n	= load sharing

TABLE II. (cont)

$$K_f = H + \left(\frac{t}{r_f}\right)^J \left(\frac{t}{h}\right)^L$$ = Dolan-Broghamer Stress Correction Factor

	Pressure angle (degrees)
H = 0.22	14.5
= 0.18	20.0
= 0.14	25.0
J = 0.20	14.5
= 0.15	20.0
= 0.11	25.0
L = 0.40	14.5
= 0.45	20.0
= 0.50	25.0

t, h, and r_f from gear tooth layout at one diametral pitch for virtual number of teeth (Lewis construction)

$$M_n = \frac{F}{L_{min}}$$

where

F = net face width
L_{min} = minimum length of contact line

$$Y_c = \frac{1.0}{\dfrac{\cos\phi_{Ln}}{\cos\phi_n}\left(\dfrac{1.5}{X\,C_H} - \dfrac{\tan\phi_{Ln}}{t}\right)}$$

where

ϕ_{Ln} = normal load pressure angle at tip of tooth

ϕ_n = tooth normal pressure angle

TABLE II. (cont)

t = tooth thickness at section of maximum stress measured from layout

X = tooth form factor measured from layout at one diametral pitch for virtual number of teeth (Lewis construction)

C_H = helical factor—ratio of the root bending moment produced by tip loading to the root bending moment produced by the same intensity of loading applied along the oblique helical contact line

$$C_H = \frac{1.0}{1 - \sqrt{\frac{\nu}{100}\left(1 - \frac{\nu}{100}\right)}}$$

where

ν = load line inclination angle

$$\tan \nu = \tan \psi \sin \phi_n$$

where

ψ = helix angle
ϕ_n = normal pressure angle

$$S_t \leq \frac{S_a K_L}{K_T K_R}$$

where

S_a = allowable stress for material

K_L = life factor

K_T = temperature factor

K_R = factor of safety

TABLE III.

CANTILEVER PLATE GEAR TOOTH BENDING STRESS FORMULA

$$S_b = C \frac{W_t}{K_v F m_n} \frac{P_d}{Y \cos^2\psi} \times K_o \times K_s \times K_m$$

where

S_b = calculated bending stress at the tooth root

W_t = transmitted tangential load at the operating pitch diameter

K_o = overload factor

K_v = dynamic factor

K_s = size factor

K_m = load distribution factor

F = net face width

P_d = transverse diametral pitch

ψ = helix angle

m_n = load sharing factor

Y = tooth geometry factor obtained in normal plane, includes stress concentration and the nonsymmetrical stress distribution at the critical section due to pressure angle

C = helical factor—ratio of maximum bending moment produced by loading along the inclined load line to the maximum bending moment produced by the same intensity of loading applied along the tip of the tooth

TABLE IV. HELICAL GEAR DESIGN PARAMETERS

Gear Number	1	2	3	4
Drawing Number	EX-84117	EX-84118	EX-84119	EX-84120
Pitch	5.6382	5.6382	4.9149	4.9149
Number of teeth	24	24	24	24
Helix angle, degrees	20	20	35	35
Pressure angle, degrees	21.1724	26.3918	23.9569	29.6510
Distance over two 0.2880-in. balls, in.	4.6582	4.6589	5.2873	5.2871
Root diameter, in.	3.789	3.8057	4.4154	4.4321
Pitch diameter, in.	4.2567	4.2567	4.8831	4.8831
Outside diameter, in.	4.5900	4.5900	5.2164	5.2164
Normal pitch	6	6	6	6
Normal pressure angle, degrees	20	25	20	25
Lead, in.	36.7415	36.7415	21.9088	21.9088
Arc tooth thickness in plane of rotation, in.	0.2786	0.2786	0.3196	0.3196
Base circle diameter, in.	3.9694	3.8130	4.4624	4.2437
Back lash, in.	0	0	0	0
Face width, in.	0.9400	0.9400	0.8192	0.8192
Active profile diameter, in.	4.0433	4.0062	4.6380	4.0688

A normal diametral pitch of six was selected for all test gears. This pitch selection is consistent with current design practice for lightweight aircraft main power train gearing and would also allow comparison of test results with spur gear results from the investigation conducted under Contract DA 44-177-AMC-318(T) and reported in USAAVLABS Technical Report 66-85. All gears were protuberance hobbed. Pressure angles of 20 and 25 degrees were selected, since they represent current gear design practice.

Helix angles of 20 and 35 degrees were selected, since they represent current design practice and a reasonable variation in this factor.

Gear face widths were selected to produce a 1-in. face width in the normal plane.

All gears were shot peened in the root and black oxide treated prior to testing.

The fatigue test gears were made without a rim and web to eliminate possible complications. Twenty-four tooth gears were chosen to avoid undercutting and to provide reasonable gear sizes to make it possible to relate fatigue life results to the 24-tooth fatigue life results obtained on the aforementioned spur gear program.

MANUFACTURE OF FATIGUE TEST GEARS

Fatigue test gear manufacturing was controlled to minimize variation within and between each of the four groups and to maintain constant metallurgical microstructure and surface treatment. Specific items of control were as follows:

- The material used was of the same specification (AMS-6265) as the material used to conduct the spur gear program. The gears were manufactured from 6-in. bar stock of AMS-6265 material (supplied by Composite Forge—heat number 513C). The raw material record is given in Table V.
- All heat treatments and surface finish processes were accomplished at the same time on all test gears.
- All machining processes for each gear configuration were completed on the same machine and with the initial machine setup.
- Copper plating prior to hardening and stripping of copper plate after hardening were each accomplished simultaneously on all parts.
- Shot blasting and peening were accomplished simultaneously on all gears.

TABLE V. RAW MATERIAL RECORD

Allison Purchase Order Number K8-13020

STEEL SUPPLIER DATA—COMPOSITE FORGINGS, INCORPORATED

Material specification—AMS-6265
Heat number—513C
Material size—6-in. diameter

MICRO INCLUSION RATING

Inclusion Type	A		B		C		D	
Inclusion Size	Thick	Thin	Thick	Thin	Thick	Thin	Thick	Thin
Top	1	0	1	0	0	0	1.5	1
Bottom	1	0	1	1	0	0	1.5	1

Chemical analysis

C	M_N	P	S	Si	CR	Ni	Mo
0.09	0.50	0.007	0.004	0.28	1.25	3.20	0.15

ALLISON METALLURGICAL INSPECTION RECORD

Coarse etch—okay

Magnaflux step-down bars—okay

Chemical analysis

C	M_N	P	S	Si	CR	Ni	Mo
0.07	0.69	—	—	0.21	1.19	3.17	0.12

Many in-process and finished part measurements were made to define stock removal and to record the final geometry of each part. Tables VI, VII, VIII, and IX list the gear measurements and analysis. The root diameter, tooth thickness (dimension over pins), root radius, and protuberance undercut depth are the critical dimensions for the fatigue specimens.

TABLE VI. TABULATION OF PROTUBERANT FILLET GEAR MEASUREMENTS FOR 20-DEGREE PRESSURE ANGLE, 20-DEGREE HELIX ANGLE TEST GEAR EX-84117

Part Number	Root Fillet Radius (in.)		Root Diameter (in.)			Dimension Over Pins (in.)				Final (in.)	
	Print Minimum	Actual	Print (±0.002)	After Hob	After Solution Machining	Print (+0.0000 -0.0039)	After Hob	After Solution Machining	After Final Grind	Pins	Root Diameter
CXD-586	0.05	0.05	3.789	3.806	3.798	4.6582	4.6915	4.684	4.6570	4.6570	3.798
CXD-587	0.05		3.789	3.794	3.797	4.6582	4.686	4.682	4.6538	4.6538	3.797
CXD-588	0.05		3.789	3.794	3.798	4.6582	4.686	4.683	4.6572	4.6572	3.798
CXD-589	0.05		3.789	3.794	3.798	4.6582	4.6864	4.685	4.6548	4.6548	3.798
CXD-590*	0.05		3.789	3.799	3.796	4.6582	4.6865	4.683	4.6572	4.6572	3.796
CXD-591**	Involute error		3.789	3.794	3.798	4.6582	4.6865	4.677	4.630***	4.630	3.798
CXD-592	0.05		3.789	3.794	3.797	4.6592	4.6865	4.683	4.6548	4.6548	3.797
CXD-593	0.05	0.050	3.789	3.794	3.800	4.6582	4.6865	4.682	4.6580	4.6580	3.7915

*Not used for data.
**Scrapped for rig checkout.
***Out of limits either + or -.

TABLE VII. TABULATION OF PROTUBERANT FILLET GEAR MEASUREMENTS FOR 25-DEGREE PRESSURE ANGLE, 20-DEGREE HELIX ANGLE TEST GEAR EX-84118

Part Number	Root Fillet Radius (in.)		Root Diameter (in.)			Dimension Over Pins (in.)				Final (in.)	
	Print Minimum	Actual	Print (±0.0020)	After Hob	After Solution Machining	Print (+0.0[illegible]0 / -0.0[illegible]9)	After Hob	After Solution Machining	After Final Grind	Pins	Root Diameter
CXD-596	0.05	0.07	3.8057	3.840	3.840	4.6589	4.690	4.6852	4.655	4.655	3.840
CXD-597	0.05	—	3.8057	3.840	3.8398	4.6589	4.691	4.6855	4.6585	4.6585	3.8398
CXD-598*	0.05	0.07	3.8057	3.750**	3.7445	4.6589	4.635**	4.6285	4.6186	4.6186	3.7445
CXD-599	0.05	—	3.8057	3.840	3.8405	4.6589	4.690	4.685	4.6578	4.6578	3.8405
CXD-600*	0.05	—	3.8057	3.837	3.840	4.6589	4.691	4.6845	4.6576	4.6576	3.840
CXD-601	0.05	0.07	3.8057	3.844	3.842	4.6589	4.691	4.6867	4.6580	4.6580	3.842
CXD-602	0.05	—	3.8057	3.835	3.837	4.6589	4.6888	4.682	4.6561	4.6561	3.837
CXD-603	0.05	—	3.8057	3.840	3.837	4.6589	4.6885	4.6843	4.6585	4.6585	3.837

*Not used for data.
**Out of limits either + or -.

TABLE VIII. TABULATION OF PROTUBERANT FILLET GEAR MEASUREMENTS FOR 20-DEGREE PRESSURE ANGLE, 35-DEGREE HELIX ANGLE TEST GEAR EX-84119

Part Number	Root Fillet Radius (in.)		Root Diameter (in.)			Dimension Over Pins (in.)				Final (in.)	
	Print Minimum	Actual	Print (±0.002)	After Hob	After Solution Machining	Print (+0.0000 / -0.0039)	After Hob	After Solution Machining	After Final Grind	Pins	Root Diameter
CXD-522	0.05	0.080	4.4154	4.438	4.426	5.2873	5.314	5.311	5.2855	5.2855	4.426
CXD-523	0.05	0.080	4.4154	4.440	4.432	5.2873	5.315	5.312	5.2862	5.2862	4.432
CXD-524	0.05	0.080	4.4154	4.435	4.424	5.2873	5.314	5.311	5.2865	5.2865	4.425
CXD-525*	0.05	0.080	4.4154	4.440	4.426	5.2873	5.314	5.311	5.2860	5.2860	4.426
CXD-526	0.05	0.080	4.4154	4.435	4.4245	5.2873	5.316	5.311	5.2800	5.2860	4.4245
CXD-527	0.05	0.080	4.4154	4.425	4.427	5.2873	5.314	5.310	5.2870	5.2870	4.[illegible]26
CXD-528*	0.05	0.080	4.4154	4.435	4.428	5.2873	5.316	5.313	5.2859	5.2859	5.2859
CXD-529*	0.05	0.080	4.4154	4.435	4.424	5.2873	5.314	5.310	5.285	5.285	4.424

*Not used for data.

TABLE IX. TABULATION OF PROTUBERANT FILLET GEAR MEASUREMENTS FOR 25-DEGREE PRESSURE ANGLE, 35-DEGREE HELIX ANGLE TEST GEAR EX-84120

Part Number	Root Fillet Radius* (in.)		Root Diameter (in.)			Dimension Over Pins (in.)				Final (in.)	
	Print Minimum	Actual	Print (±0.002)	After Hob	After Solution Machining	Print $\binom{+0.0000}{-0.0039}$	After Hob	After Solution Machining	After Final Grind	Pins	Root Diameter
CXD-546	0.05	0.065	4.4321	4.463	4.460	5.2871	5.313	5.307	5.2863	5.283	4.460
CXD-547***	0.05	0.065	4.4321	4.463	4.462	5.2871	5.3127	5.308	5.2860	5.2860	4.462
CXD-548***	0.05	0.065	4.4321	4.463	4.436**	5.2871	5.3154	5.290	5.2855	5.2855	4.463
CXD-549	0.05	0.065	4.4321	4.463	4.461	5.2871	4.3138**	5.308	5.2862	5.2862	4.461
CXD-550	0.05	0.065	4.4321	4.461	4.465	5.2871	5.3147	5.309	5.2840	5.2840	4.464
CXD-551	0.05	0.065	4.4321	4.438	4.445	5.2871	5.2923	5.290	5.2588	5.2588	4.445
CXD-552	0.05	0.065	4.4321	4.463	4.465	5.2871	5.3164	5.310	5.2865	5.2865	4.462
CXD-553***	0.05	0.065	4.4321	4.462	4.459	5.2871	5.3123	5.308	5.2835	5.2835	4.459

*Minimum root fillet radius.
**Incorrect measurement.
***Not used for data.

Some gears had dimensional deviations; however, most were within the dimensional tolerance limits. In some cases, involute error, tooth thickness error, and root grinding marks were found. When this occurred, the gears or gear teeth in question were excluded from the fatigue test program. Tables VI through IX also list the discrepancies found and identify the excluded gears. Sample routing sheets for a typical fatigue test gear (EX-84117) are given in Appendix II.

TEST RIG DESIGN AND PROCEDURE

The test rig was designed for single tooth testing. Single tooth testing was selected to permit accurate control of test variables and to render the results applicable to previous single tooth testing performed on spur gears.[8] A tooth adjacent to each test tooth was removed from the gear to provide clearance for the load member.

A 30,000-pound Ling electromagnetic shaker was selected for the input loading device. This electromagnetic shaker loading device, which had excellent dynamic stability, allowed close control and accurate measurement of dynamic tooth load.

To achieve the designed operational requirements, the main design emphasis for the test rig was placed on method of loading, reacting, and indexing the test gear. The fatigue test rig was designed with high axial stiffness of the load reacting components. High radial stiffness of the fatigue test rig was inherent in the shaker armature design. A degree of flexibility was built into the load member-flexure assembly to ensure uniform tooth load distribution under dynamic conditions during tooth roll and unequal tooth deflections present in loaded helical gear teeth. The fatigue test rig was coupled to the Ling electromagnetic shaker. Operation at or near a system resonance of 115 c.p.s. was realized. The principle of operation of the fatigue test is shown schematically in Figure 4. The relative size and construction of the facility are shown in Figure 5.

The shaker driving force was applied directly by the mass of the shaker armature which loaded the gear tooth through a load cell. The mass (shaker armature) is flexibly supported in the axial direction with flexure plates built within the main structure of the electromagnetic shaker. Radial stabilization of the mass was ensured by the same disk-type flexible plates.

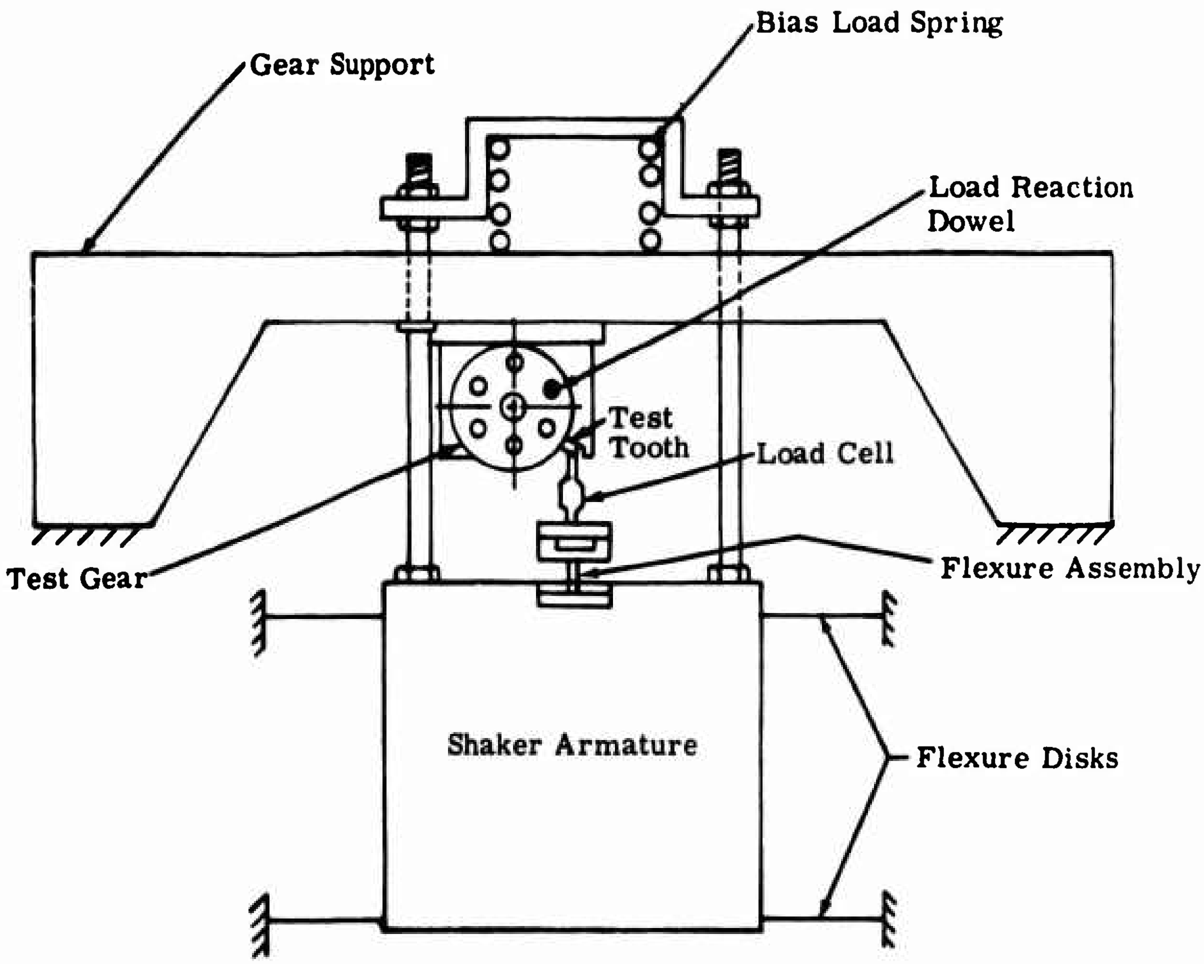

Figure 4. Test Rig Schematic.

The required static preload was provided by compressing a relatively low spring rate coil spring. Inertial loading of the tooth, using the moving mass, made possible considerable force amplification at and near the system axial resonance. The forced dynamic load was about the mean value—the static preload. Figures 6 and 7 show the gear mounted to the fatigue rig indexing fixture with the fixture coupled to the shaker and the load cell in position.

The load cell, an Allison-designed strain gage type cell, was incorporated at the point of tooth loading to provide accurate control of both static and

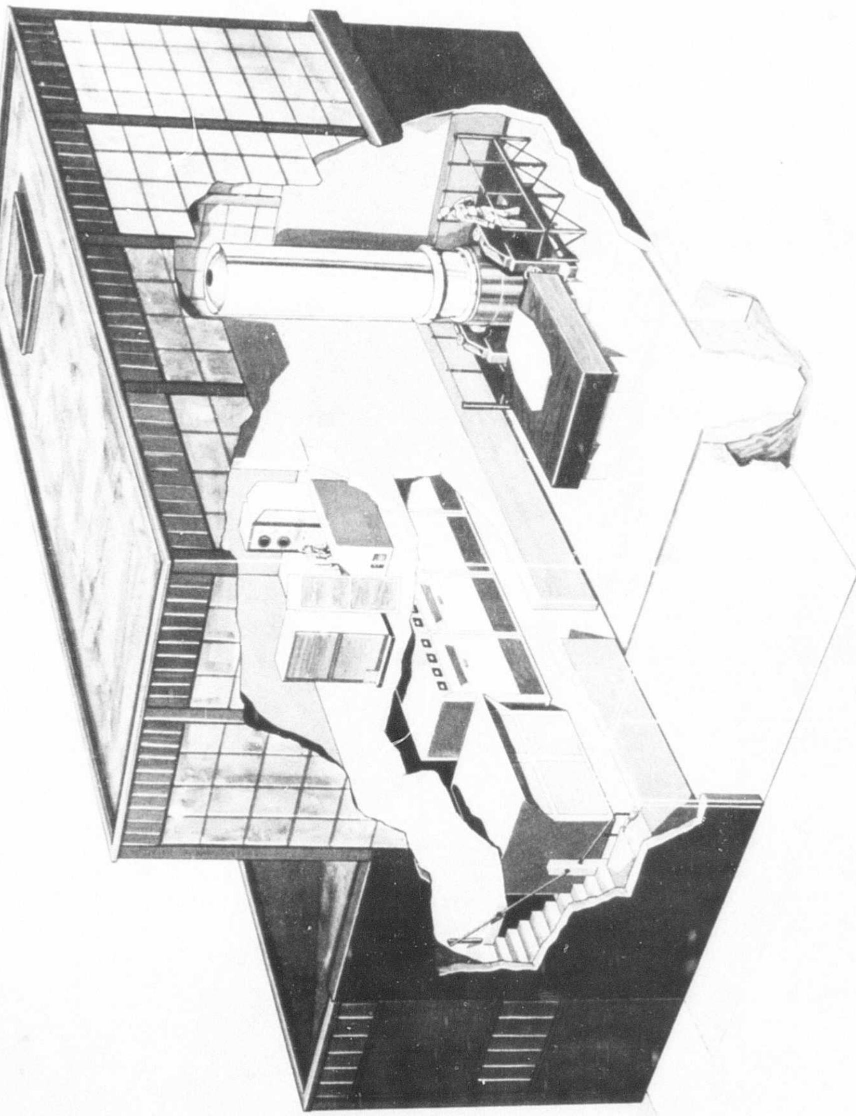

Figure 5. Allison Vibration Facility.

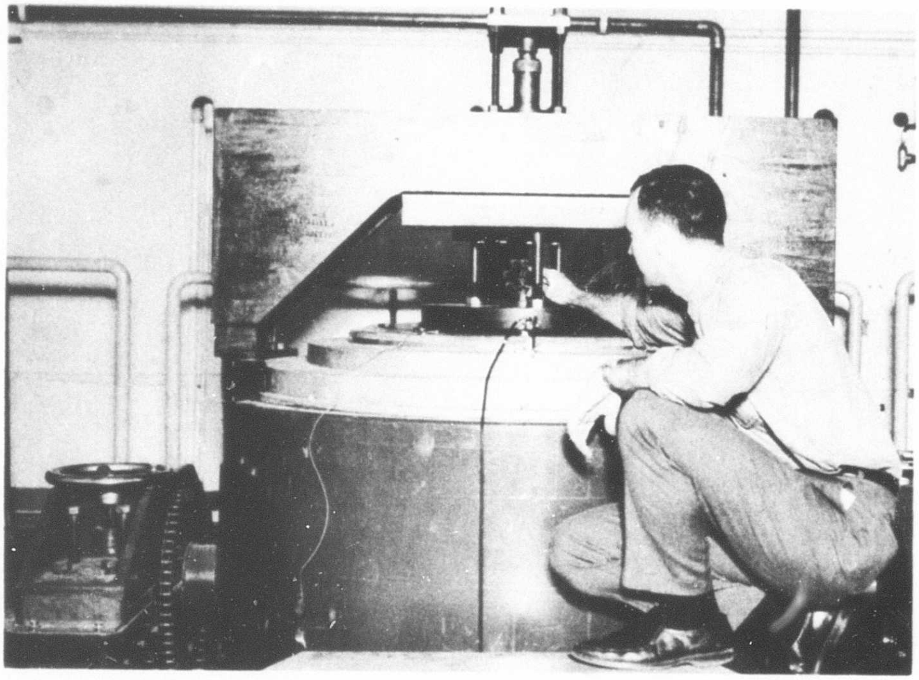

Figure 6. Fatigue Test Rig Mounted On Electromagnetic Shaker.

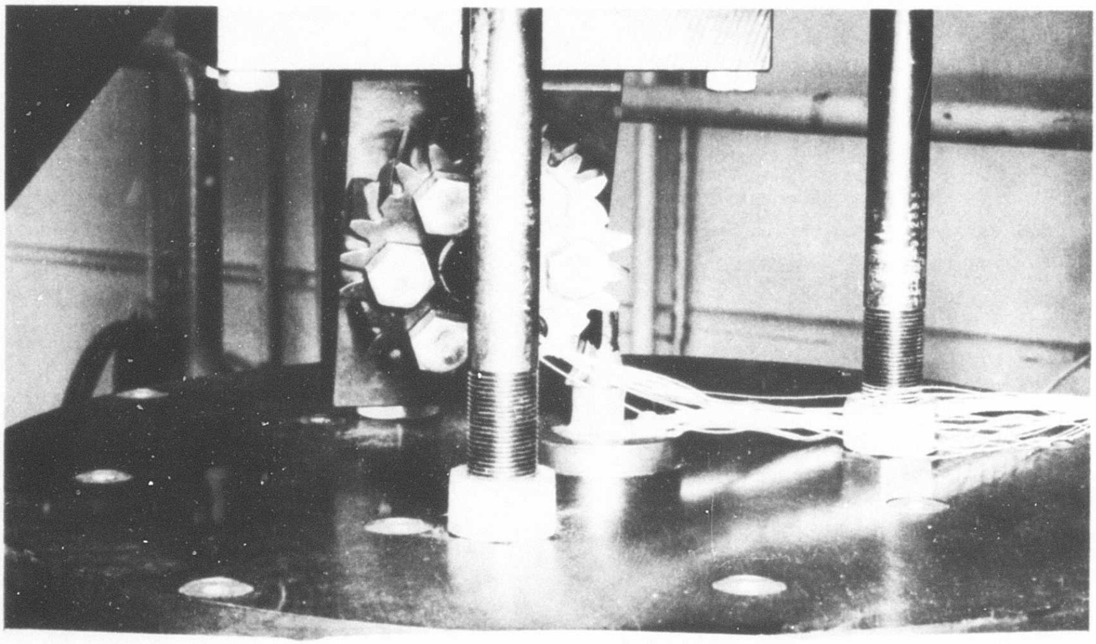

Figure 7. Fatigue Rig Indexing Fixture, Mounted Test Gear, and Load Member Shown in Test Position.

dynamic tooth loading during fatigue testing. Figure 8 shows the load cells instrumented with axial and circumferential strain gages. The strain gage hookup is a four-active arm bridge. The bridge signal output was directly proportional to the change in applied thrust—independent of load cell bending and temperature change and 2 $(1 + \mu)$ times as large as the corresponding output of a single strain gage. The symbol μ is Poisson's ratio.

A series of checkout procedures was performed prior to initiation of dynamic fatigue testing. The following paragraphs present the checkout procedures performed.

Radial Spring Rate of Fatigue Rig

The fatigue rig was installed on the electromagnetic shaker and instrumented with dial indicators referenced to ground. With test gear EX-84117 installed and loaded to 7000 pounds with the bias spring loading

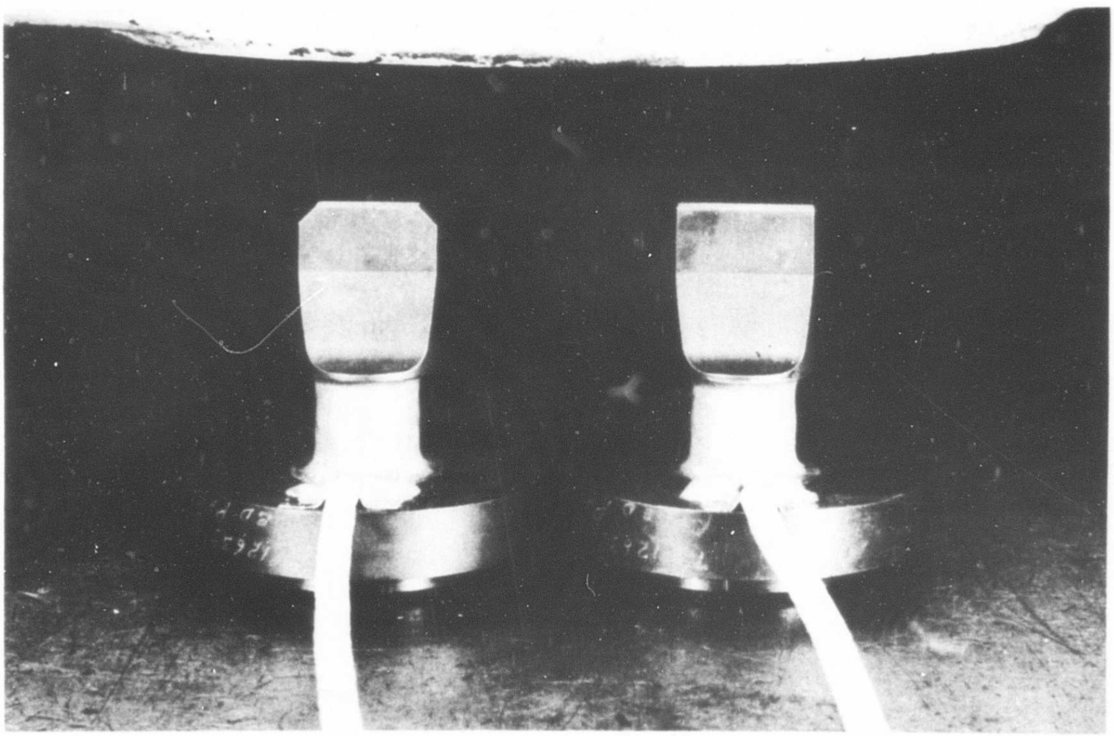

Figure 8. Fatigue Test Load Cell Load Member Showing Strain Gage Instrumentation.

device, the radial deflections were measured. The radial spring rate was determined to be 5,000,000 pounds per inch. This high radial spring rate verified the design objective of high system stiffness and allowed accurate load application and good alignment of all moving parts during operation.

Dimensional Checkout

The test fixture positioned the gear in such a manner that loading occurred along a straight line on the tooth profile tangent to the base circle. Measurements were made to verify center line locations of the gear mounting block pilot shaft with respect to the tip of the load cell. All parts were dimensionally checked to the drawing requirements, and no deviations were found.

Dynamic Resonance Frequency

To determine the system operating frequency, a frequency scan was made versus shaker drive current. The frequency scan was made between 50 and 300 c.p.s. with test gear EX-84117 installed and preloaded to 2000 pounds. The frequency scan indicated a system resonance of 115 c.p.s.

Dynamic Separation

To ensure continued contact between the gear tooth and the load member tip, it was necessary to determine the static/dynamic load margin necessary to maintain contact. The load cell output signal was displayed on an oscilloscope, and the dynamic load was cycled about a constant preload. Wave shape analysis of the output signal indicated that a minimum differential load margin of 50 pounds was required to maintain contact between the tooth and the tip of the load member.

Load Cell Calibration

To eliminate inaccuracies in the load, a precise static calibration of the load cell was performed. The load cell was loaded with a Baldwin press as shown in Figures 9 and 10. Incremental loads of 1000 pounds were applied to a maximum of 25,000 pounds, and the output of the load cell strain gage bridge was recorded. The procedure was repeated four times on each load cell to ensure repeatability. Figure 11 shows typical calibration data. Recalibration of the load cells was accomplished at 30 and 60 percent fatigue test completion points and cell output versus load data repeated within 1 and 2 percent, respectively.

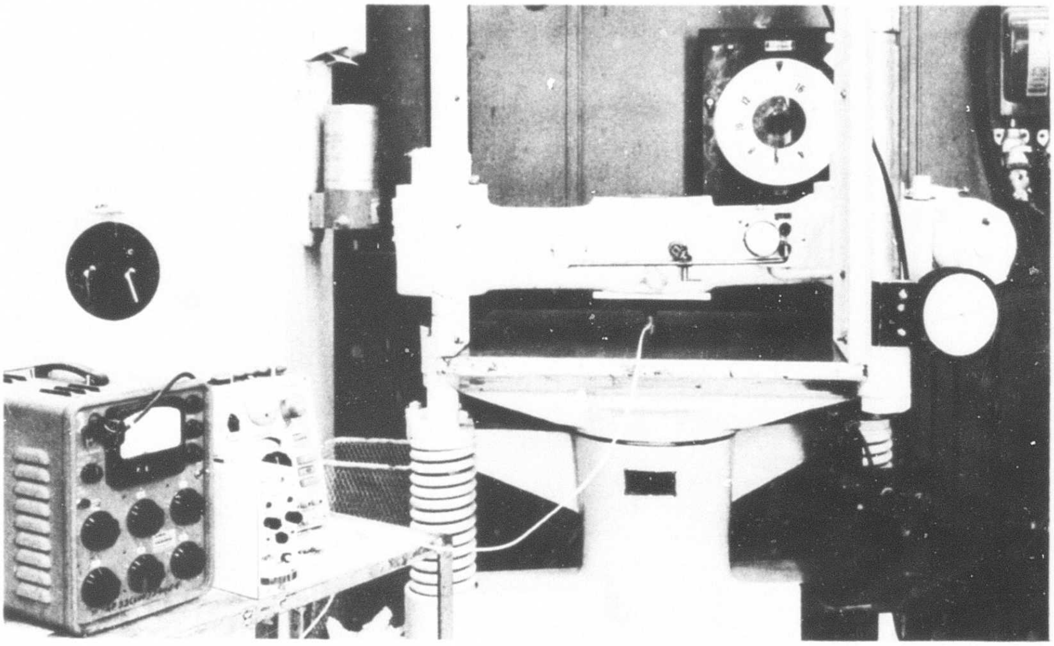

Figure 9. Overall View of Load Cell Calibration Equipment.

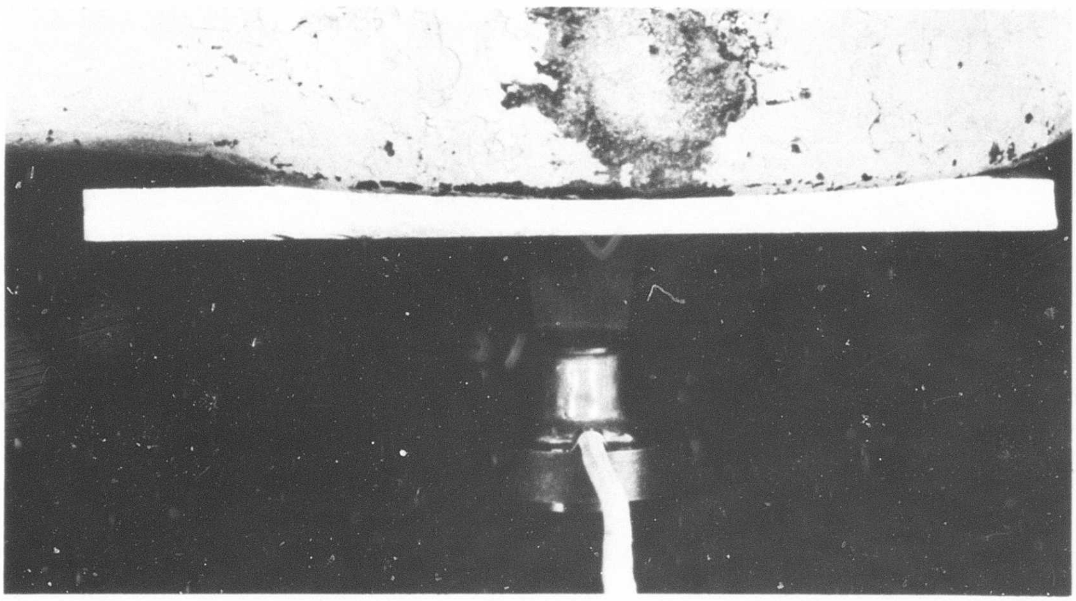

Figure 10. Close-up of Load Cell Calibration Equipment.

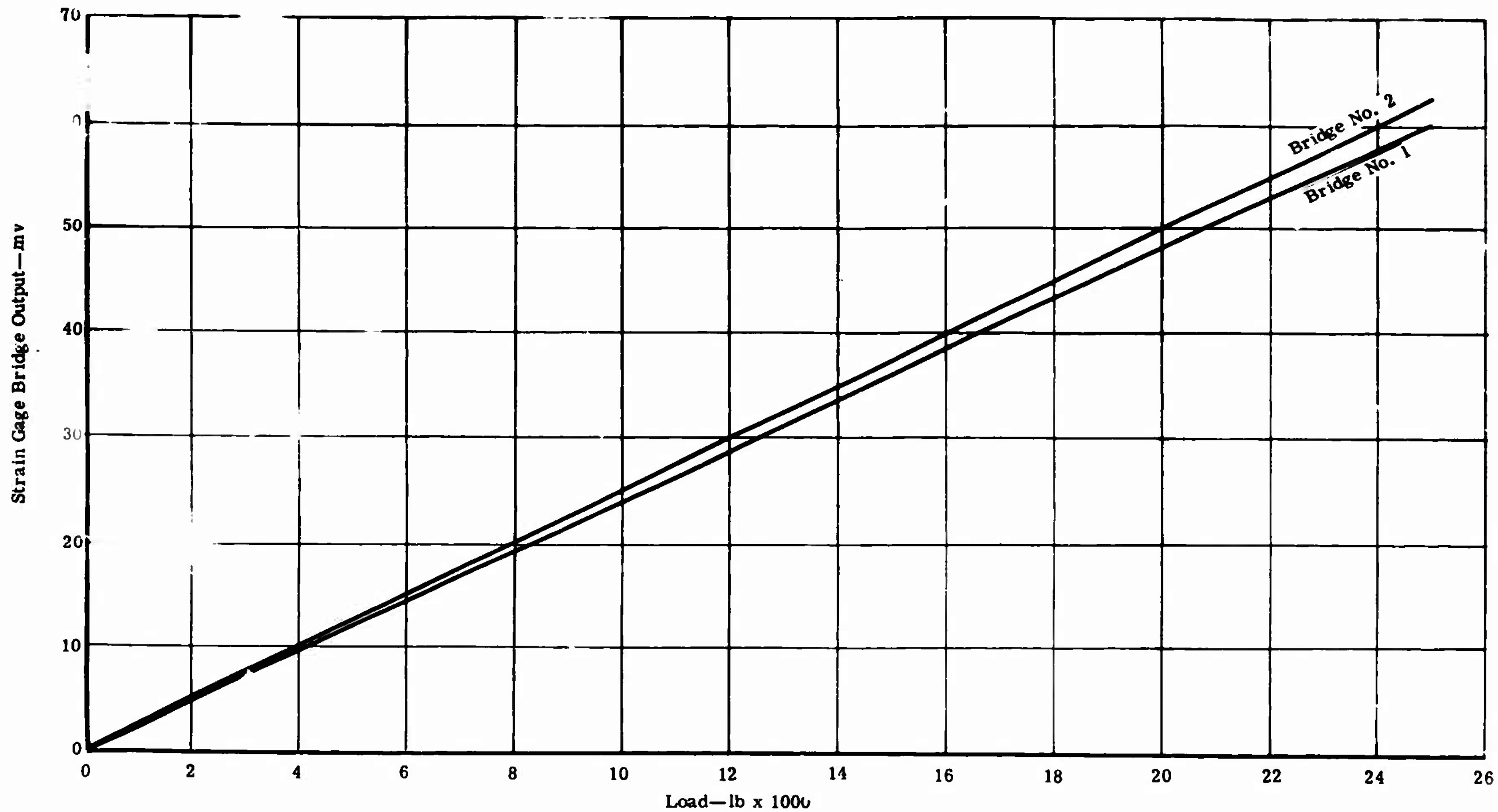

Figure 11. Typical Load Cell Calibration Curve.

Tooth Load Distribution

Correlation of fatigue test results dictated that all gears be loaded in the same manner; i.e., equal load distribution along the load contact line. The inclination of the load contact line caused nonuniform tooth deflection, and the primary concern was to verify equal load distribution along the inclined load line. The load member was instrumented with strain gages at the four end points—two on each side of the load member—as shown in Figure 12. The semiconductor strain gaged load members were calibrated on the Baldwin press to verify equal gage outputs under conditions of uniform load. The outputs were equal.

The instrumented load member was installed in the rig. Using gear EX-84117, Serial Number CXD-592, tooth No. 6, static loads were applied with the rig bias spring. Measurements of the tooth rout strain distribution and strain at both ends of the load member were taken. The data indicated that the applied load was concentrated toward the lower point of contact on the involute surface. Strain data collected from the semiconductor strain gages located on opposite ends of the load member indicate the load to be 128% higher at the lower point of contact at an applied load of 6000 pounds. Figure 13 shows the resulting tooth root strain distribution for the nonuniform loading condition.

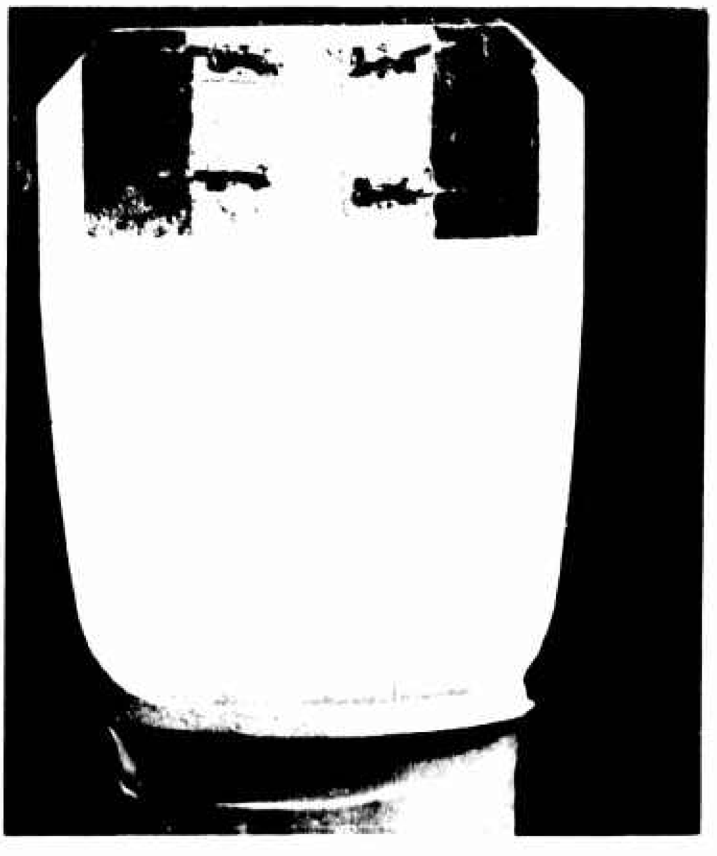

Figure 12. Load Member Tip Instrumentation Used to Determine Load Distribution.

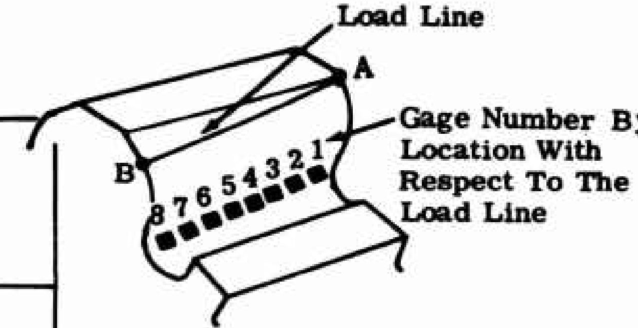

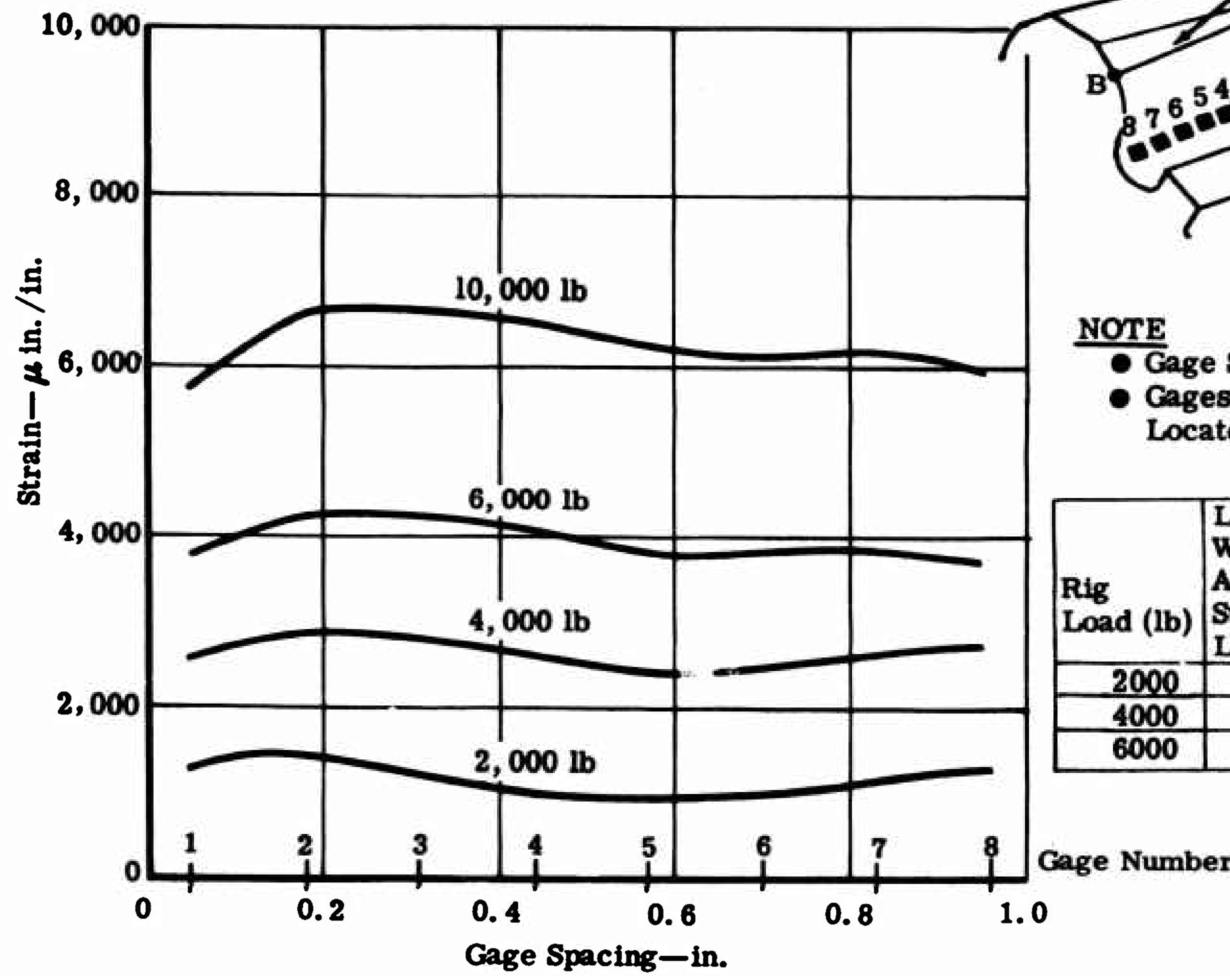

NOTE
- Gage Spacing 0.130 in. Apart
- Gages 1 And 8 Are Located 0.050 in. From Edges

Rig Load (lb)	Loss Of Load At Point A With Respect To Point B As Determined By Semiconductor Strain Gages On Tip Of Load Member (%)
2000	34
4000	64
6000	128

Figure 13. Tooth Root Strain Distribution With Nonuniform Load Distribution.

It was assumed that the nonuniform load distribution was due to the inability of the load member to follow the nonuniform deflection of the tooth resulting from the diagonal load line. To verify this assumption, a flexure was designed to allow the load member to follow the tooth deflection, and it was positioned in the rig as shown in Figure 14. A static recalibration was run using the instrumented load member with semiconductor strain gages, root instrumented gear Part Number EX-84117, Serial Number CXD 592, tooth number 6. The test results are given in Figure 15. The data show that the flexure is following the tooth deflection, and good load distribution exists.

To allow the load member to contact the gear test tooth, a number of teeth were removed as shown in Figure 16. Teeth 1, 2, 3, 4, 5, and 6 are the test teeth. The holes in the gear web are used to position the test teeth and to react the tooth load.

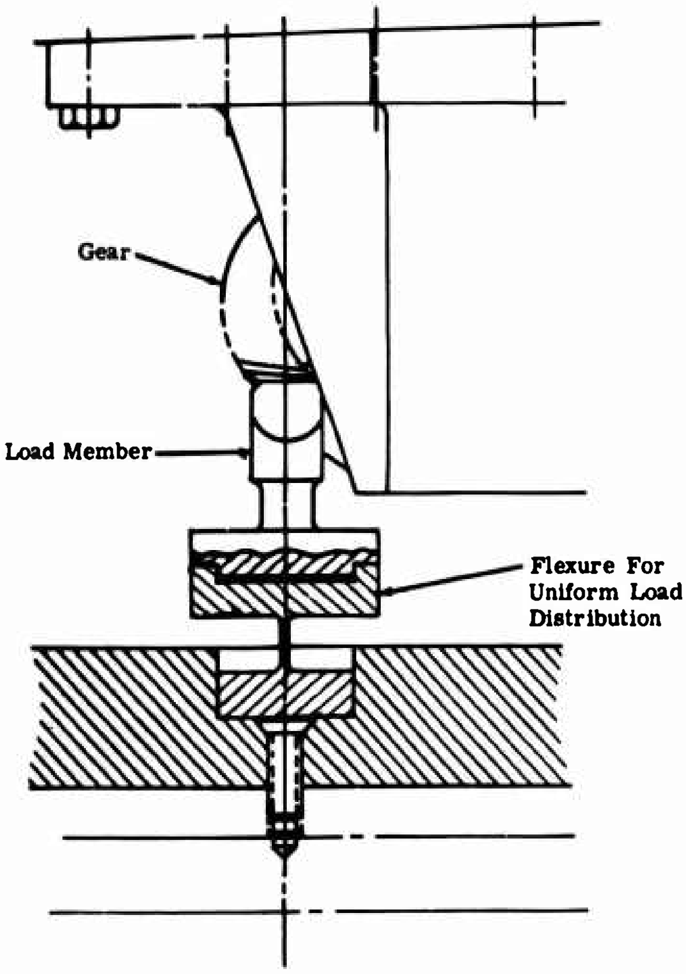

Figure 14. Test Rig Installation Showing Load Member Flexure Device.

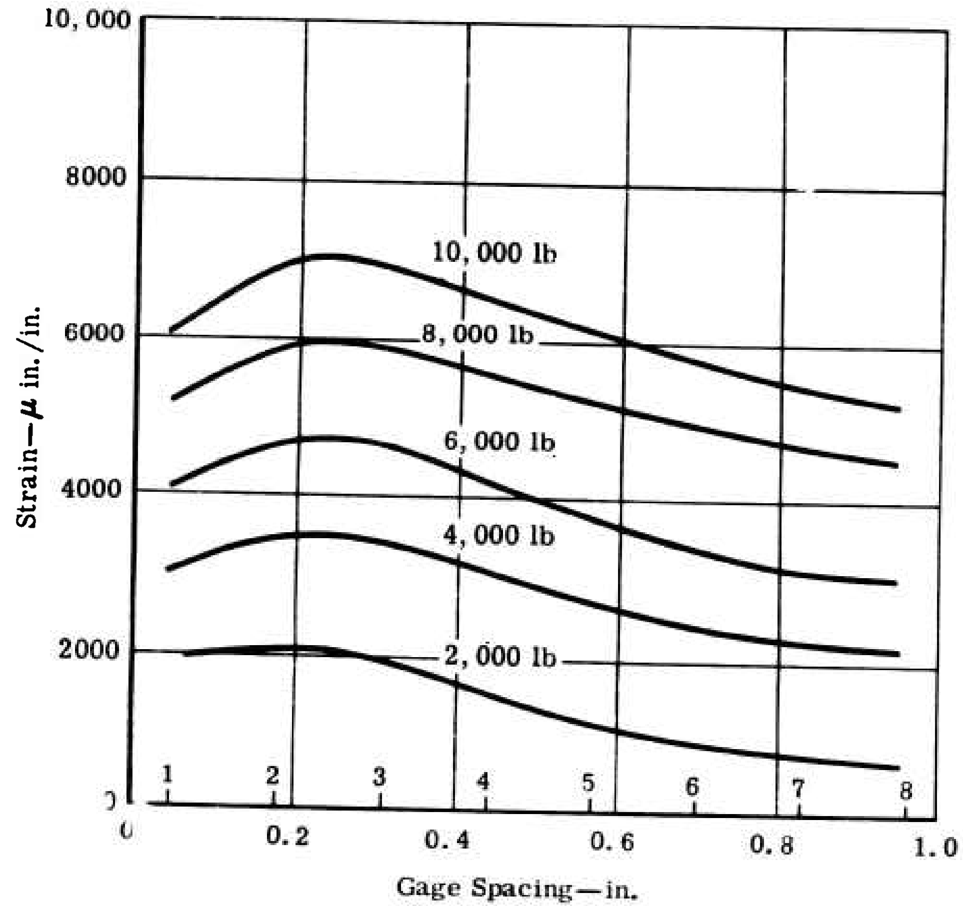

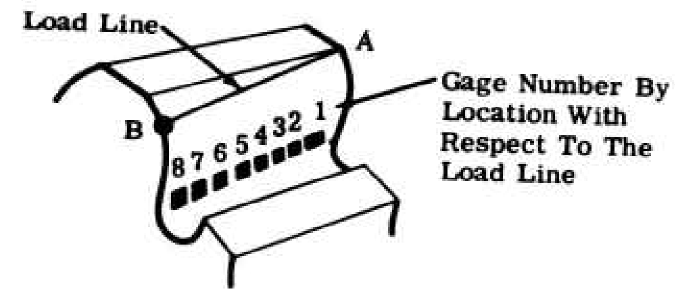

NOTE

- Gage Spacing 0.130 in. Apart
- Gages 1 and 8 Are Located 0.050 in. From Edges

Rig Load (lb)	Loss Of Load At Point A With Respect To Point B As Determined By Semiconductor Strain Gages On Tip Of Load Member (%)
2000	4
4000	10
6000	20
8000	22

Figure 15. Tooth Root Strain Distribution With Uniform Load Distribution.

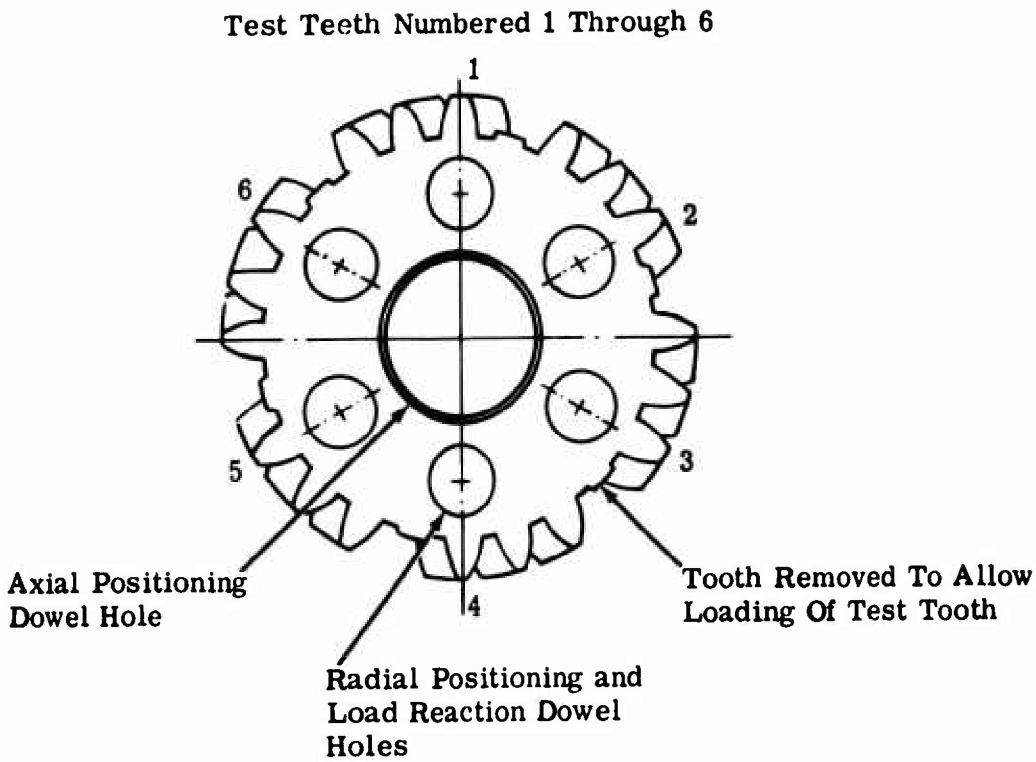

Figure 16. Typical Fatigue Test Gear.

The test procedure required that the test tooth, once positioned, be preloaded with a bias load equal to 200 pounds greater than one-half the total fatigue load. After the preload was applied and verified by the load cell, an alternating load was applied about a mean which was the preload. The tentative plan was that two gear teeth be tested at four stress levels for each combination of variables until fatigue failure occurred or 10^7 cycles were accumulated.

During testing, the dynamic load at the load cell (signal from strain gage bridge) was monitored and recorded on a strip chart recorder. A typical strip chart recording is shown in Figure 17.

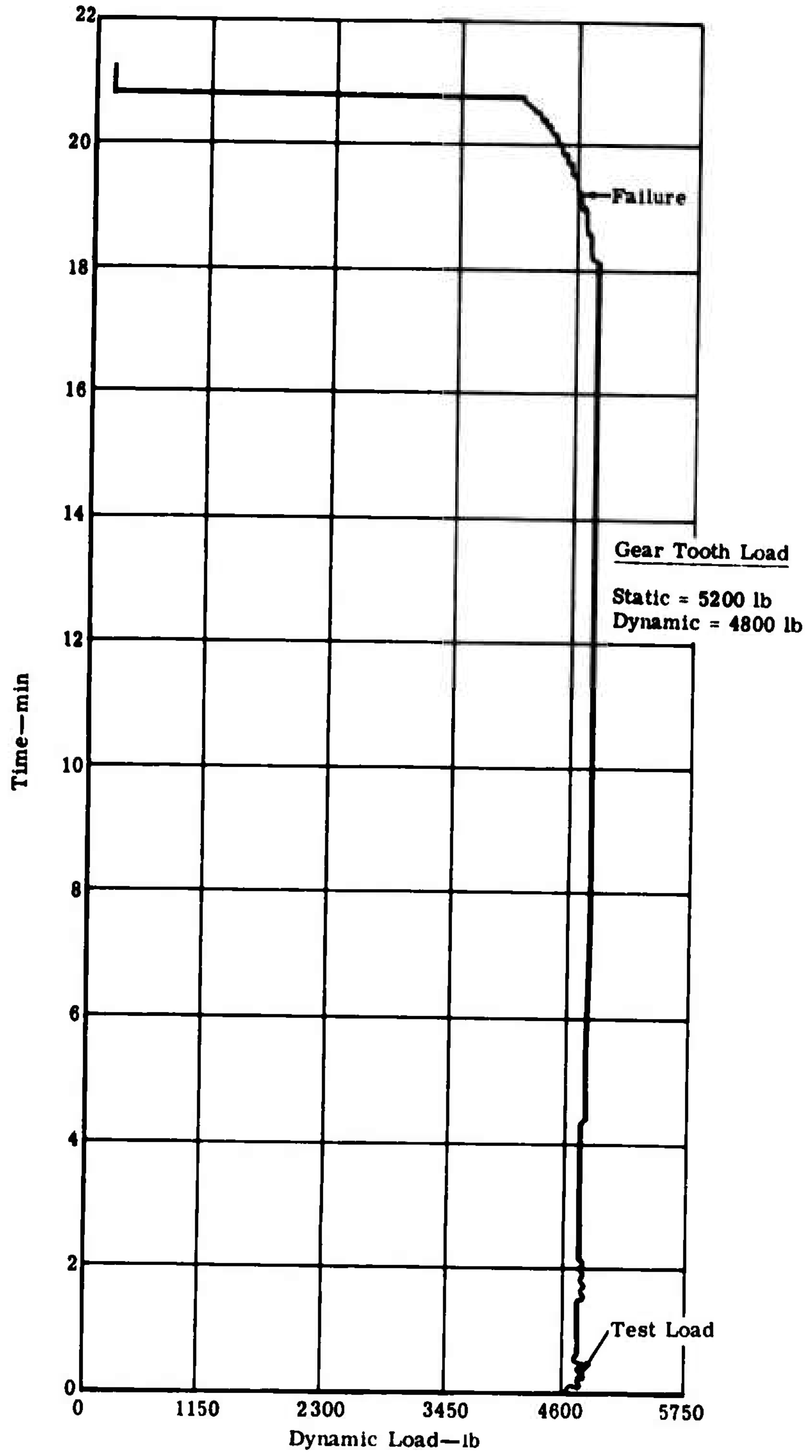

Figure 17. Typical Strip Chart Recording of Test Gear Dynamic Load.

RESULTS

FATIGUE TESTS

The fatigue test program was based on a designed experiment for evaluating two geometric variables (pressure angle and helix angle) and a load position variable (load line through the tooth tip at the edge and load line through the tooth tip 0.250 inch inboard from the edge). Two levels of each variable were employed; however, since the load position variable could be adjusted by a change in the test rig fixture, only four different gear configurations were necessary. See Table IV. Originally, two teeth from each gear configuration were to be tested at four stress levels at each load position. Failures were required to permit test evaluation on the finite portion of the S/N curve. The maximum stress was determined by the short test time (3 to 5 minutes) and the high stresses that could cause plastic yielding and, therefore, result in a failure mode other than fatigue. The minimum stress was determined by a high percentage of runouts to 2×10^6 or 10^7 cycles without tooth failure. Each gear configuration was tested at the two load conditions, yielding eight combinations. A minimum of four stress levels were tested for each configuration; however, in three of the eight combinations, only one data point was obtained for the fourth stress level.

Tables X through XVII list the gear tooth fatigue test data—load, cycles-to-failure, and configuration—for the 76 gear teeth tested. Of this total, sixty failed and the remaining gear tooth tests were terminated at 2×10^6 or 10^7 cycles.

Fatigue test data for each configuration based on applied test load are plotted in Figures 18 through 21. The mean curve drawn through the data was calculated by the procedure discussed in Appendix V. Proportionality factors can be used to relate applied load (test rig load), AMGA stress, Lewis stress, Heywood stress, Almen-Straub stress, and Cantilever Plate theory stress. Therefore, S/N curves of the test data based on any of these stress calculation methods would produce the same fit of the mean curve to the data points.

FAILED GEAR TOOTH CRACK MEASUREMENTS

A comparison was made of the calculated location of the Lewis "assumed weakest section" and the actual crack location. It was necessary to define the crack origin by metallurgical examination. The radial and axial positions were then measured within an estimated 0.002 inch. Figures 22

through 25 show the actual crack locations plotted against the Lewis "assumed weakest section" location and the actual stress distribution measured in the tooth root. The average radial actual crack location for all gears loaded through the tooth tip at the edge was 0.030 inch below the Lewis calculated maximum stress point. The average radial actual crack location for all gears loaded through the tooth tip inboard from the edge was 0.020 inch below the Lewis calculated maximum stress point.

TABLE X. GEAR TOOTH FATIGUE DATA

(Fatigue Test Gear EX-84117, -20 Degree Helix Angle, -20 Degree Pressure Angle)

Serial Number	Tooth Number	Rig Load (lb)	Cycles
CXD 586	1	6500	10^7 →
CXD 586	2	8500	9.9×10^3
CXD 566	3	6700	2.0×10^6 →
CXD 586	4	7500	2.2×10^4
CXD 586	5	7500	2.03×10^5
CXD 586	6	7500	8.4×10^5
CXD 587	1	8000	1.4×10^5
CXD 587	5	7200	10^7 →
CXD 588	1	7750	2.1×10^5
CXD 588	3	8500	4.6×10^4
CXD 589	3	7750	10^7 →
CXD 589	4	8000	8×10^4

Load Line Condition As Shown

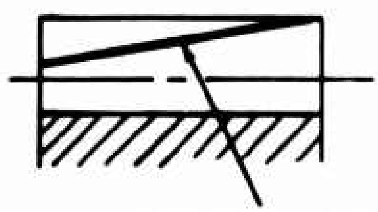

Load Line Through Corner

TABLE XI. GEAR TOOTH FATIGUE DATA

(Fatigue Test Gear EX-84117, -20 Degree Helix Angle, -20 Degree Pressure Angle)

Serial Number	Tooth Number	Rig Load (lb)	Cycles
CXD 587	2	9000	5.0×10^3
CXD 587	6	8500	1.3×10^4
CXD 588	2	8500	1.02×10^4
CXD 588	5	8000	3.73×10^4
CXD 592	1	8000	7.46×10^4
CXD 592	4	7750	2.0×10^6 →
CXD 593	2	7750	5.08×10^5
CXD 593	4	9000	9.1×10^3

Load Line Condition As Shown

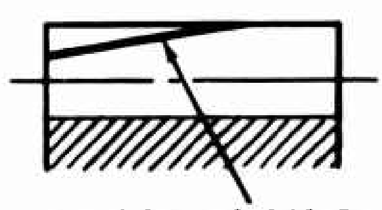

TABLE XII. GEAR TOOTH FATIGUE DATA

(Fatigue Test Gear EX-84118, -20 Degree Helix Angle, -25 Degree Pressure Angle)

Serial Number	Tooth Number	Rig Load (lb)	Cycles
CXD 596	6	11,000	2.9×10^4
CXD 597	3	11,000	2.7×10^4
CXD 597	4	8,000	2.0×10^6
CXD 599	1	10,500	3.1×10^4
CXD 601	2	9,000	1.3×10^5
CXD 601	5	9,500	1.06×10^5
CXD 602	2	10,500	2.4×10^4
CXD 602	4	9,500	4.1×10^4
CXD 603	1	10,000	4.2×10^4
CXD 603	5	10,000	4.3×10^4

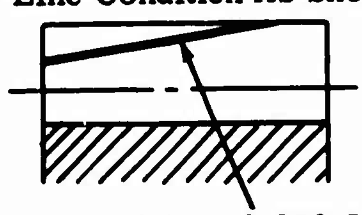

TABLE XIII. GEAR TOOTH FATIGUE DATA

(Fatigue Test Gear EX-84118, -20 Degree Helix Angle, -25 Degree Pressure Angle)

Serial Number	Tooth Number	Rig Load (lb)	Cycles
CXD 596	1	9,500	1.63×10^5
CXD 597	1	10,000	2.0×10^6 →
CXD 597	5	8,500	2.0×10^6 →
CXD 599	4	9,000	2.0×10^6 →
CXD 599	6	10,000	2.03×10^5
CXD 601	3	9,000	2.0×10^6 →
CXD 601	4	11,000	6.42×10^4
CXD 601	6	10,000	1.83×10^5
CXD 602	1	11,500	2.74×10^4
CXD 602	5	11,000	5.09×10^4
CXD 603	2	11,000	4.75×10^4

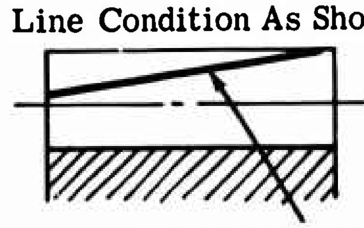

TABLE XIV. GEAR TOOTH FATIGUE DATA

(Fatigue-Test Gear EX-84119, -35 Degree Helix Angle,
-20 Degree Pressure Angle)

Serial Number	Tooth Number	Rig Load (lb)	Cycles
CXD 522	1	9,000	1.4×10^6
CXD 522	4	9,500	2.0×10^6
CXD 522	6	10,000	1.09×10^5
CXD 523	3	10,500	1.71×10^4
CXD 523	4	11,000	2.05×10^4
CXD 525	3	11,000	2.7×10^4
CXD 525	5	10,000	1.79×10^5
CXD 527	1	9,000	2.0×10^6
CXD 527	3	9,500	1.67×10^5
CXD 527	5	10,500	1.48×10^5

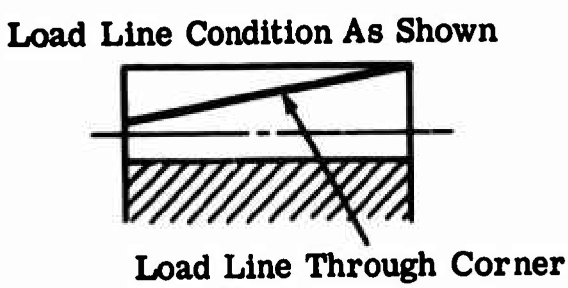

TABLE XV. GEAR TOOTH FATIGUE DATA

(Fatigue Test Gear EX-84119, -35 Degree Helix Angle, -20 Degree Pressure Angle)

Serial Number	Tooth Number	Rig Load (lb)	Cycles
CXD 522	3	10,000	4.33×10^4
CXD 522	5	10,500	1.33×10^4
CXD 523	1	9,000	1.33×10^6
CXD 523	2	10,000	1.5×10^4
CXD 523	6	9,500	1.26×10^5
CXD 524	5	9,500	1.71×10^4
CXD 525	1	8,500	2.0×10^6 →
CXD 525	2	9,500	1.8×10^5
CXD 527	2	10,500	5.38×10^4
CXD 527	6	9,000	2.02×10^4

Load Line Condition As Shown

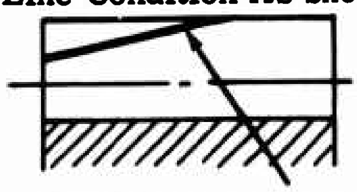

Load Line 0.250-In. Offset

TABLE XVI. GEAR TOOTH FATIGUE DATA

(Fatigue Test Gear EX-84120, -35 Degree Helix Angle, -25 Degree Pressure Angle)

Serial Number	Tooth Number	Rig Load (lb)	Cycles
CXD 546	1	10,400	2.0×10^6 →
CXD 546	5	12,000	7.15×10^4
CXD 549	1	14,000	1.33×10^4
CXD 550	4	14,000	5.79×10^4
CXD 550	6	12,000	1.68×10^5
CXD 551	2	13,000	3.0×10^4
CXD 552	3	13,000	5.83×10^4

Load Line Condition As Shown

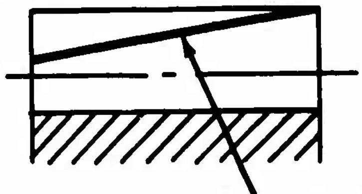

Load Line Through Corner

TABLE XVII. GEAR TOOTH FATIGUE DATA

(Fatigue Test Gear EX-84120, -35 Degree Helix Angle, -25 Degree Pressure Angle)

Serial Number	Tooth Number	Rig Load (lb)	Cycles
CXD 546	3	12,500	3.93×10^4
CXD 546	6	11,000	2.0×10^6 →
CXD 549	2	12,000	2.05×10^4
CXD 550	5	12,000	1.3×10^5
CXD 551	1	13,000	4.96×10^4
CXD 552	1	12,500	2.5×10^4
CXD 552	4	13,000	1.2×10^4
CXD 552	5	11,500	2.0×10^6 →

Load Line Condition As Shown

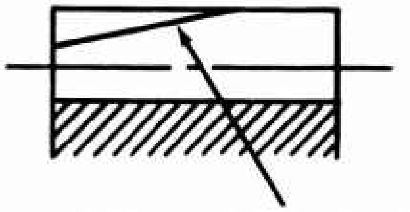

Load Line 0.250-In. Offset

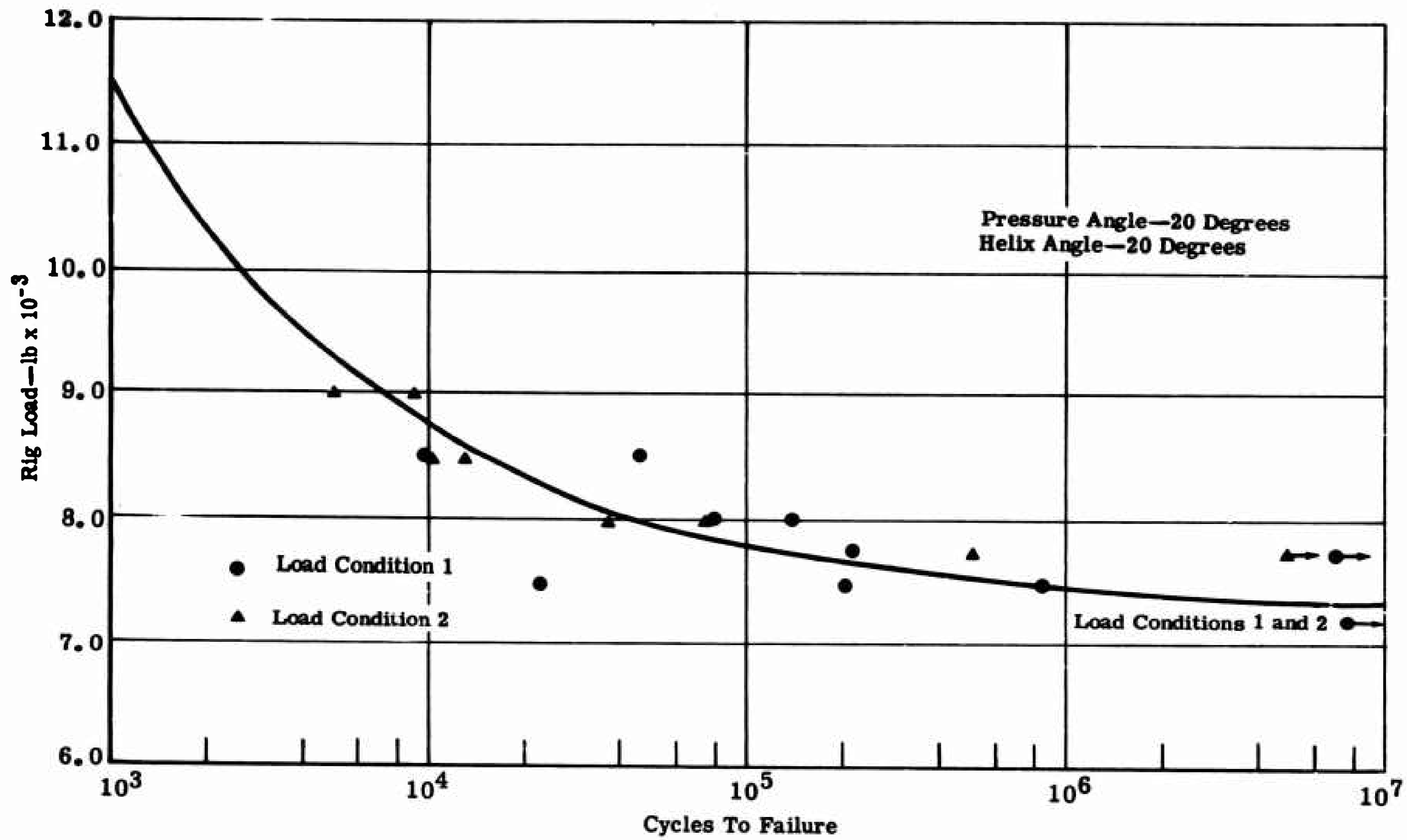

Figure 18. Fatigue Test Results—EX-84117.

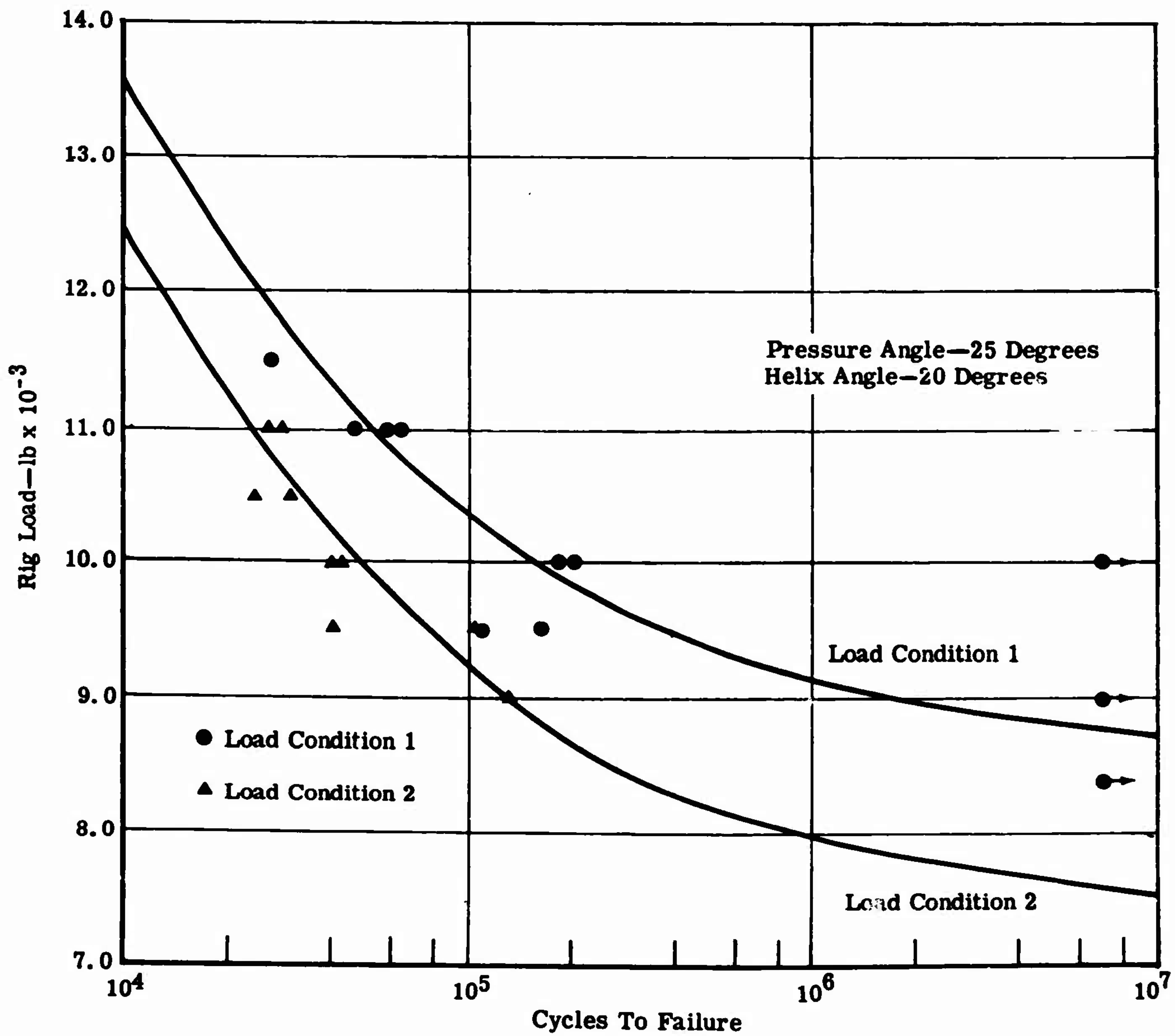

Figure 19. Fatigue Test Results—EX-84118.

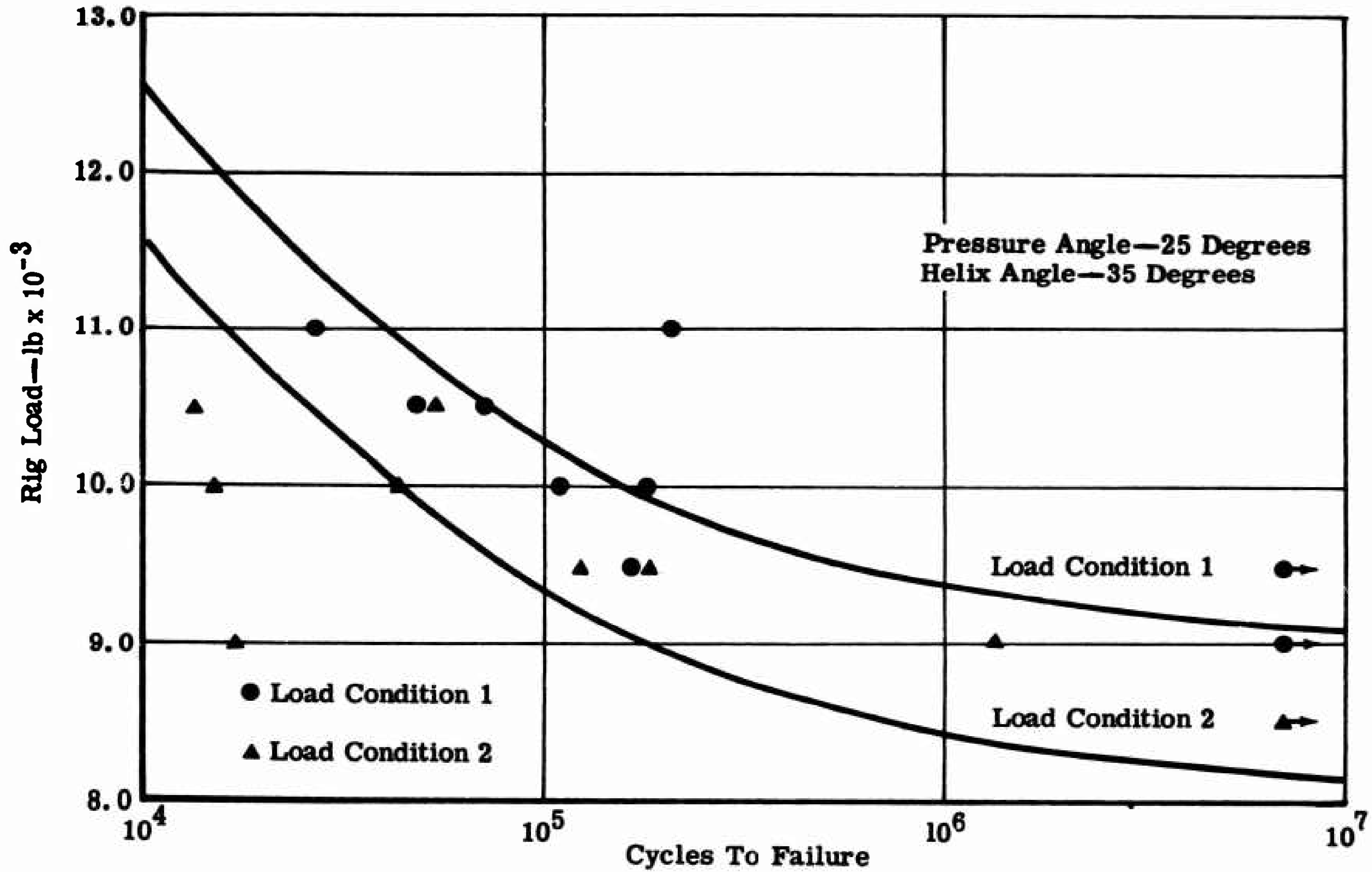

Figure 20. Fatigue Test Results—EX-84119.

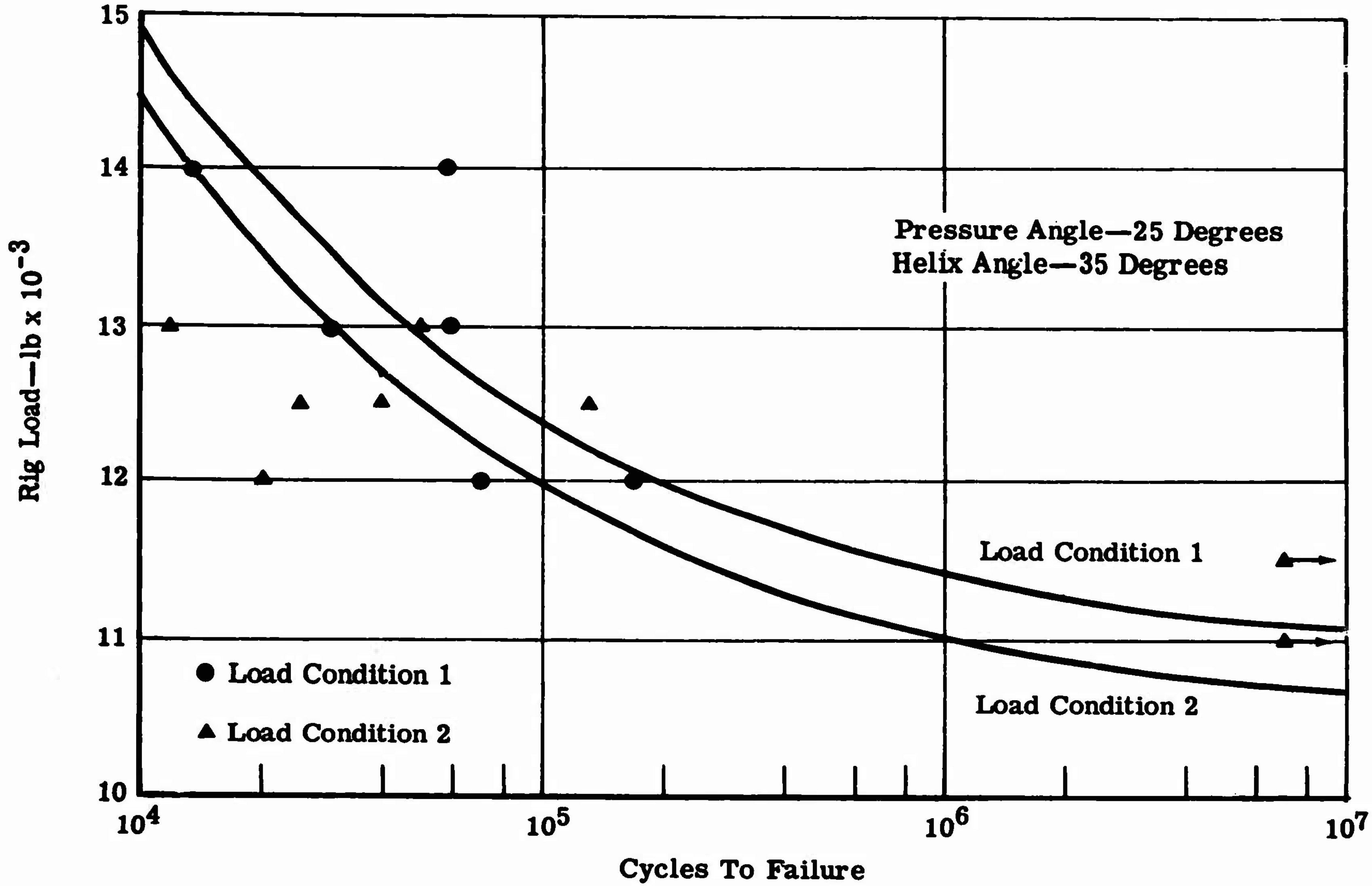

Figure 21. Fatigue Test Results—EX-84120.

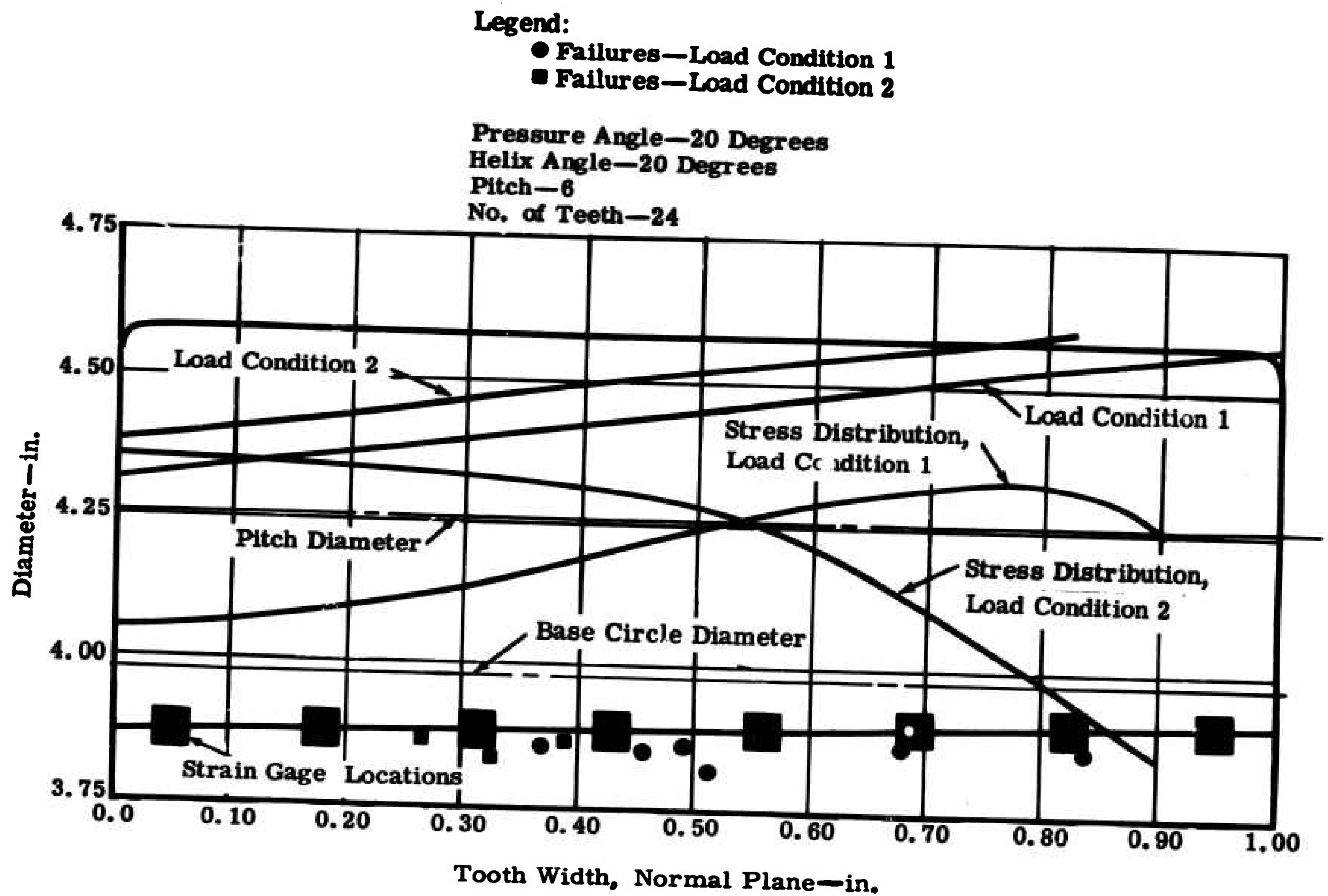

Figure 22. Failure Origin Results—EX-84117.

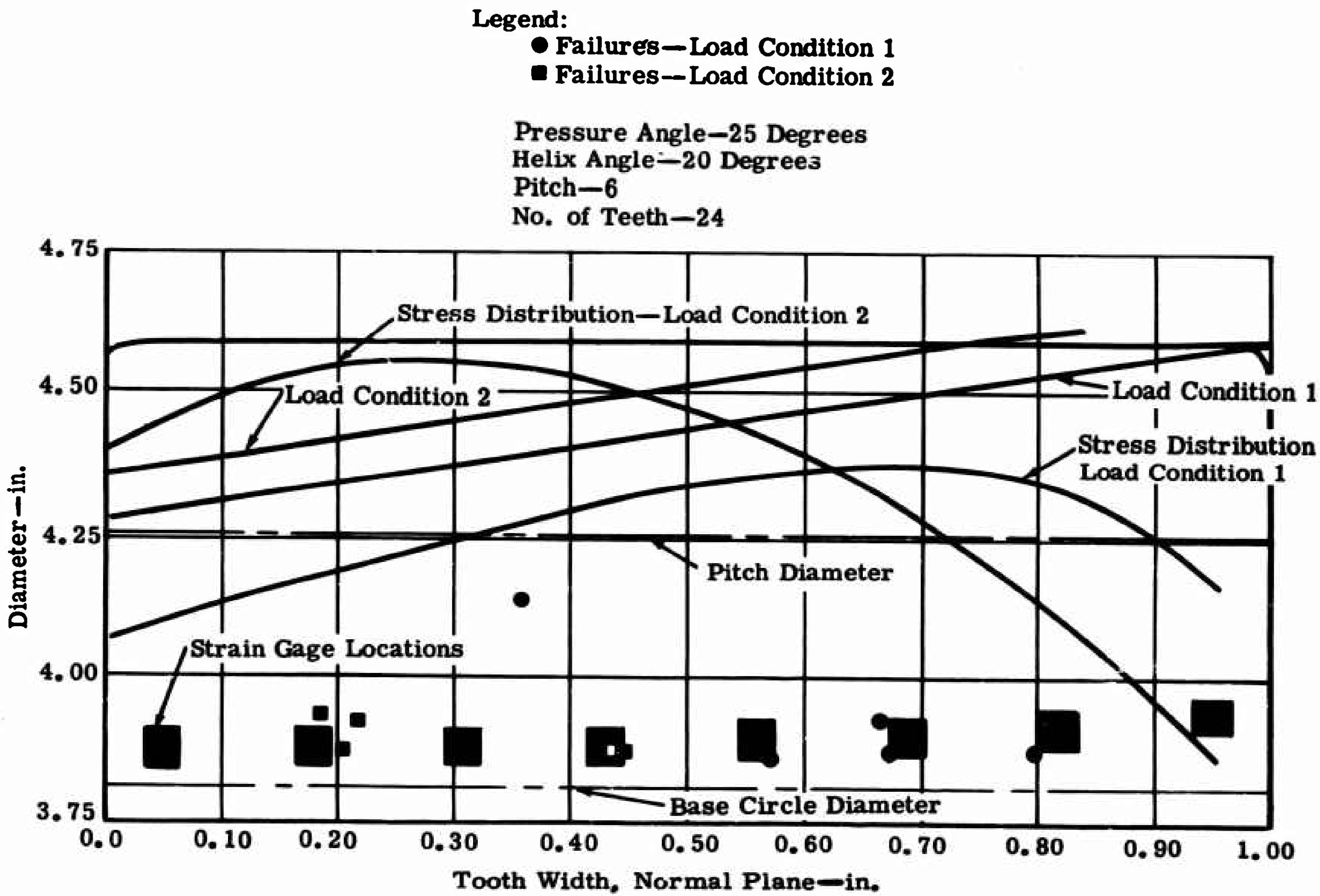

Figure 23. Failure Origin Results—EX-84118.

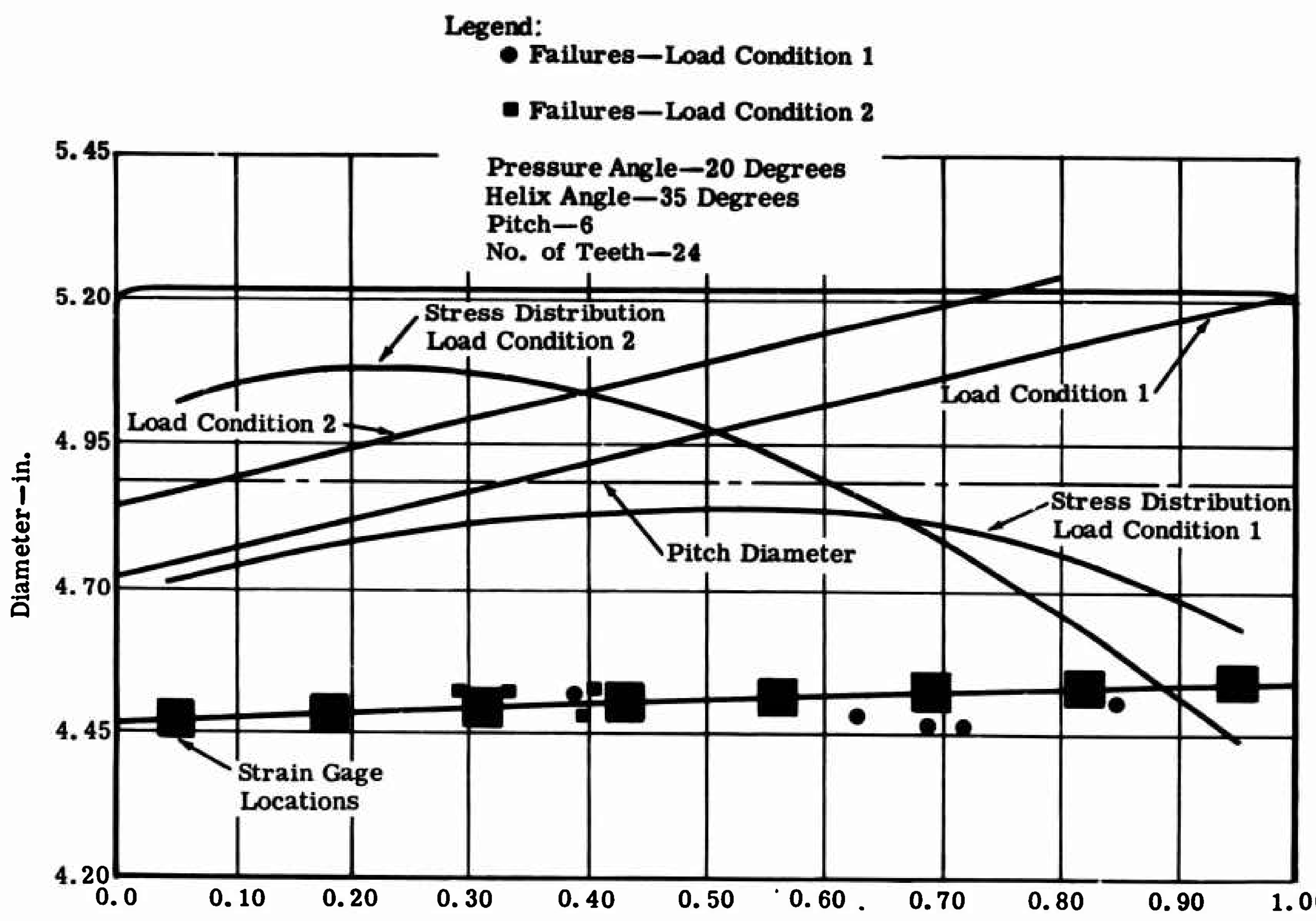

Figure 24. Failure Origin Results—EX-84119.

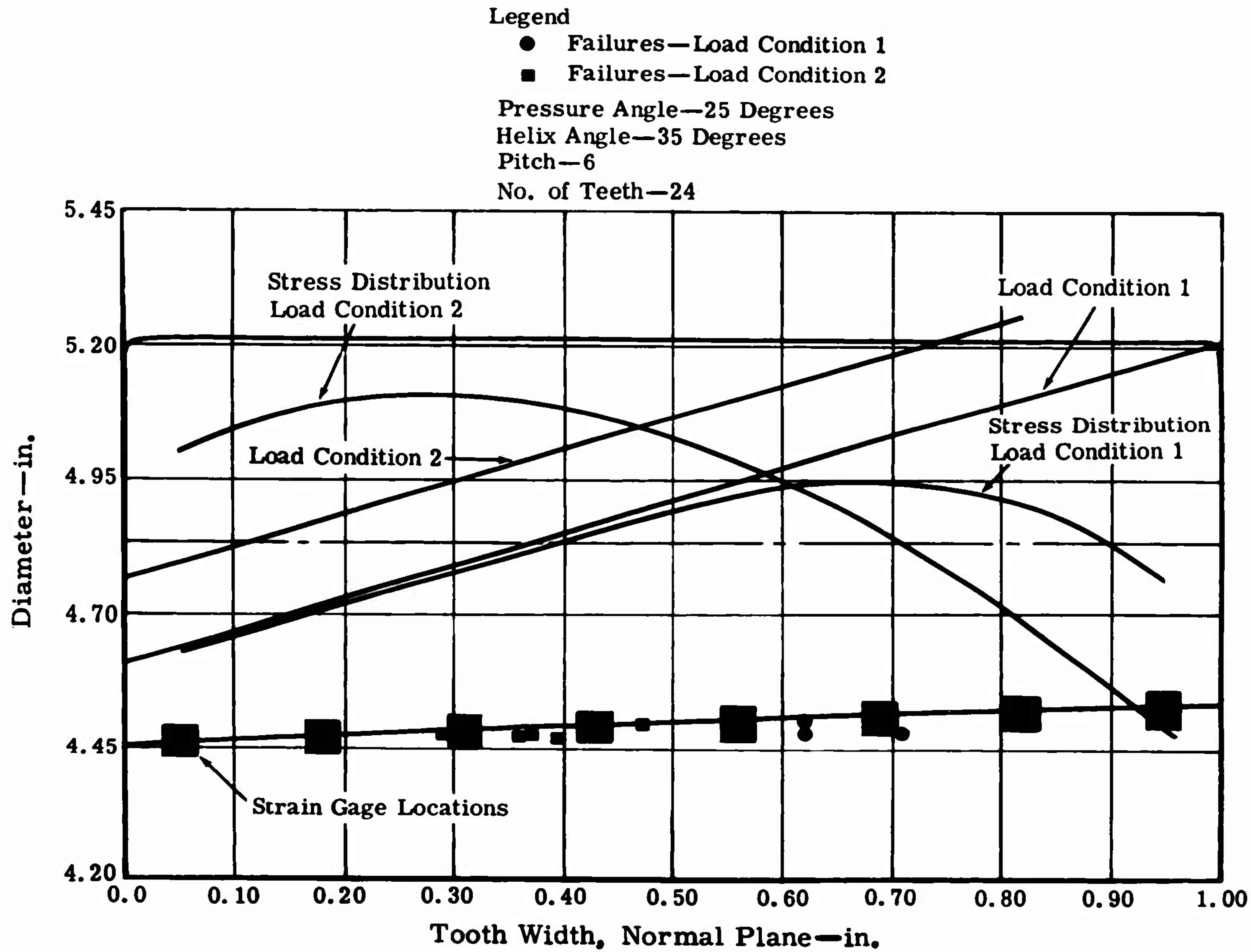

Figure 25. Failure Origin Results—EX-84120.

The fact that all crack origins were inboard of the tooth edge and in the area of actual measured maximum stress indicates the consistency of fatigue test gear manufacturing and test.

METALLURGICAL INVESTIGATIONS

Metallurgical examinations of failed test gears were conducted to determine mode of failure, origin of failure, microstructure, cas depth, hardness g. adient, and material cleanliness. The following t e gears were submitted for metallurgical investigations:

Gear Part Number	Gear Serial Number
EX-84117	CXD 586
EX-84117	CXD 592
EX-84118	CXD 599
EX-84119	CXD 522
EX-84120	CXD 551

The conclusions derived from these metallurgical investigations are as follows:

- Failure of the tested teeth occurred predominantly in fatigue.
- The failures of the tested gear teeth originated in the carburized case of the root radius below the loaded involute.
- The failure origins, as determined by electron fractography, were predominantly singular and well defined.
- The microstructure of the tested gears was typical of a rich carburized case with some noncontinuous carbide network near the surface. The core microstructures were of tempered martensite.
- The effective case depth, measured to the $R_C = 50$ level, was approximately 0.045 to 0.050 inch.
- The test gear material was free from inclusions and processing defects which could have contributed to the failures.
- The gear material conformed to the compositional requirements of AMS-6265.

Electron fractographs of the failure surfaces of two failed teeth (one from test gear EX-84117, CXD 586 and one from test gear EX-84119, CXD 522) confirmed a fatigue failure mode on each surface as shown in Figures 26 and 27. Visual examination of the failure surfaces of all test gears submitted for examination revealed a flat failure surface showing

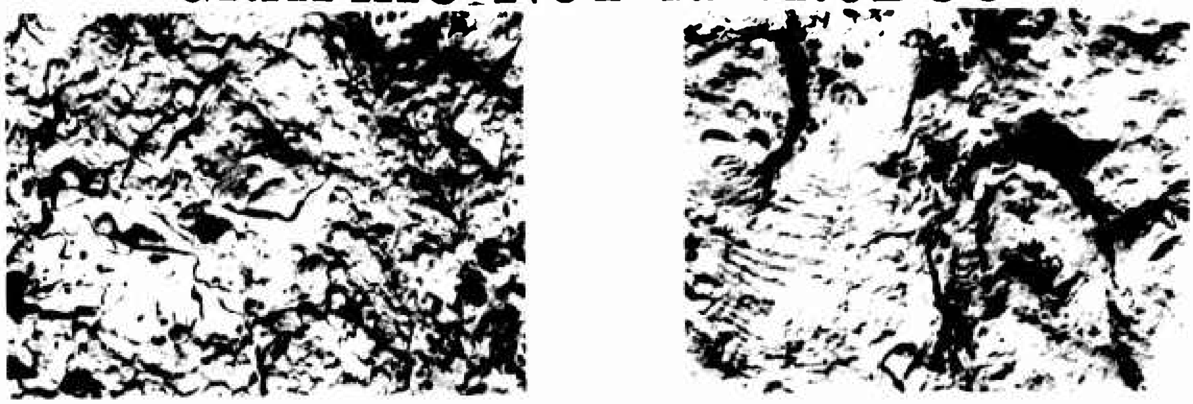

Slightly Subsurface   Subsurface

EX-84117, Serial Number CXD 586

Figure 26. Fractographs of Failure Surface of Tooth Number 6 Showing Fatigue Progressing Away from Surface (Magnification: 5000 ×).

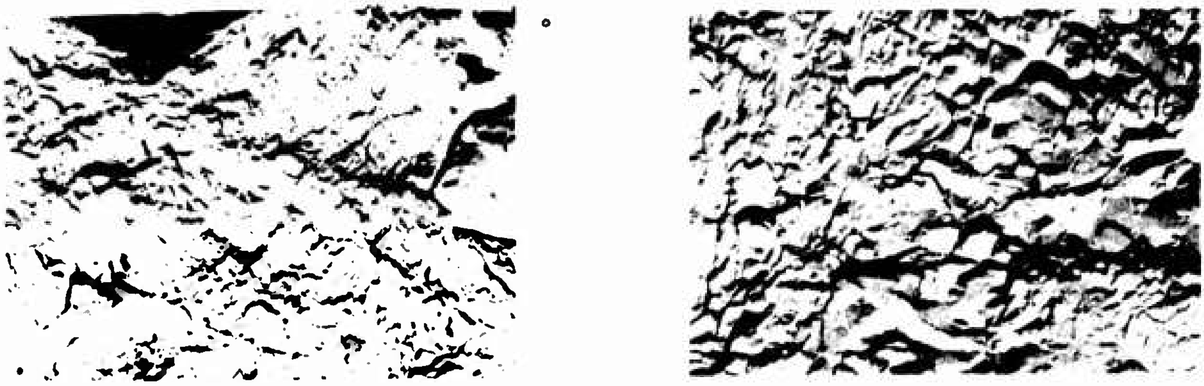

Adjacent To Surface   Slightly Subsurface

Subsurface

EX-84119, Serial Number CXD 522

Figure 27. Fractographs of Failure Surface of Tooth Number 6 Showing Fatigue Progressing Away From Loaded Surface (Magnification: 5000 ×).

progressive failure originating in the gear tooth root below the loaded involute. Figures 28 through 32 are detail views of the failure surfaces of the test gears submitted for examination. All but one of the examined failures had a single origin. Figure 29 is a detail view of the failure surface of test gear EX-84117, CXD 592 showing multiple failure origins. Although the failure had multiple origins, the origins were tightly grouped rather than randomly distributed along the tooth root. Microexamination of the transverse sections through the approximate origins of failure revealed transgranular failures typical of fatigue. These failures originated in the carburized case hardened structure in the root radius below the loaded involute, as shown in Figures 33 and 34. The failures had a single origin which coincided closely with the area of maximum stress occurring in the tooth root. Figures 35 through 40 are photomacrographs of test teeth on the gears submitted for metallurgical analysis. The sections are taken in the transverse plane of the tooth and show the general cleanliness of the material and the consistent carburized case depth around the gear teeth. Effective case depth measured to the R_C = 50 level varied from 0.044 to 0.050 inch between the five test gears examined. Case hardness of the various test gears was R_c = 65 at 0.002 inch below the surface with a diminishing gradient as given in Table XVIII. Spectrographic analysis indicated conformance of the test gear material to the compositional requirements of AMS-6265.

Fluorescent penetrant inspection of the test gears examined indicated that all failures occurred in the tooth root radii, as indicated in Figures 36 through 39.

R. R. MOORE TESTS

R. R. Moore test specimens were manufactured from the same heat of material as the test gears. The test specimens were machined so that the test section of each bar coincided with the area of the test gear tooth root after final test gear machining. Manufacturing followed heat treatment and grinding routings used for the test gears as closely as possible. The process routing for the test bar specimens is presented in Table XIX, and the test results are given in Table XX.

Figure 41 represents a typical R. R. Moore fatigue specimen showing the characteristic fatigue pattern representing the failure origin in the outer surface.

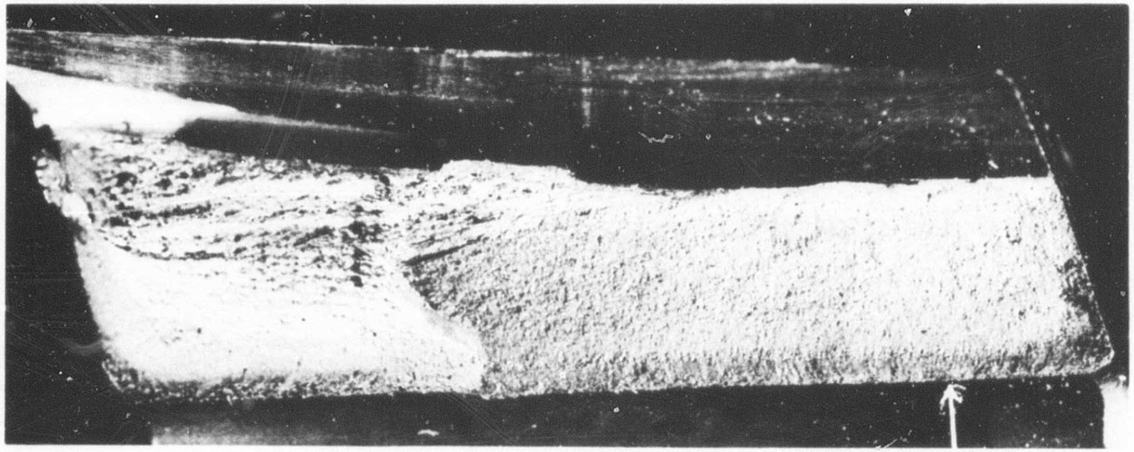

Tested Tooth No. 4

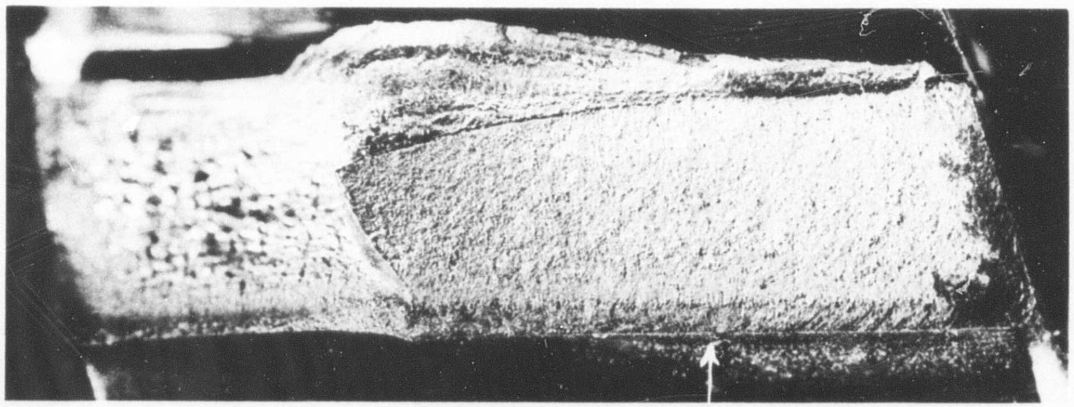

Tested Tooth No. 6
EX-84117, Serial Number CXD 586

Figure 28. Detail Views of Failure Surfaces, Showing Flat Failure Surface Typical of Fatigue (Magnification: 6×).

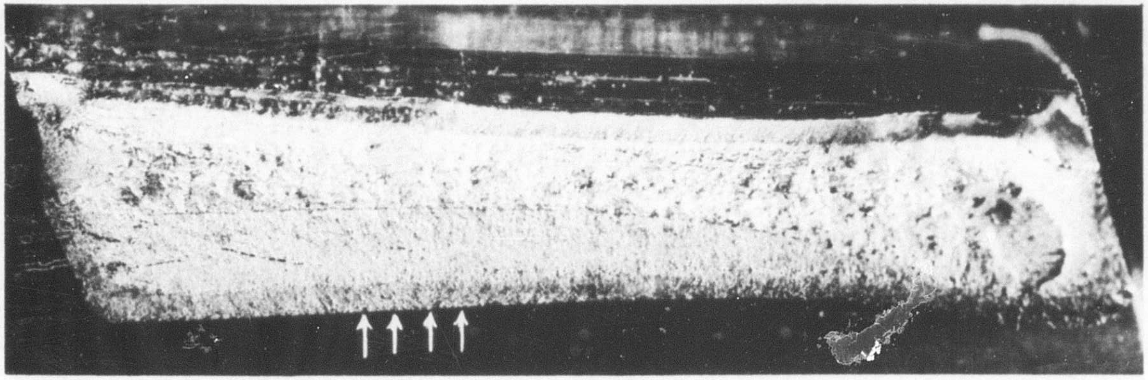

Tested Tooth Number 1 EX-84117, Serial Number CXD 592

Figure 29. Detail View of Failure Surface, Showing Progressive Failure Originating in Multiple Points Along Base of Involute.

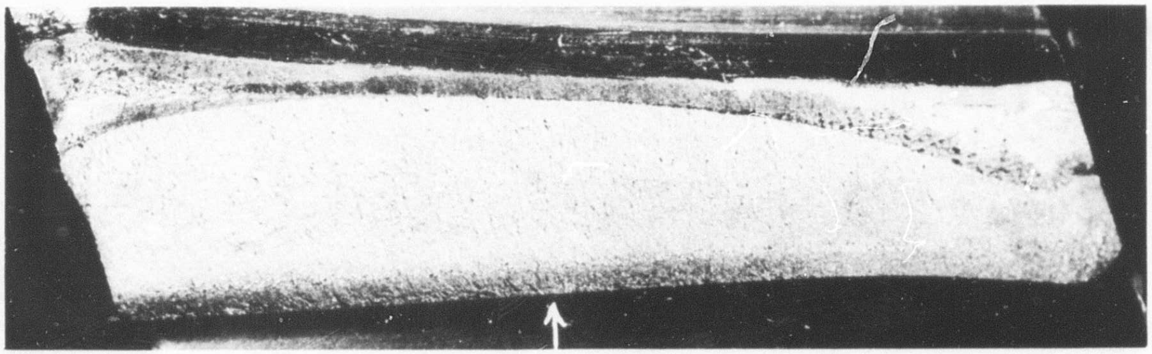

Tested Tooth Number 1 EX-84118, Serial Number CXD 599

Figure 30. Detail View of Surface Failure, Showing Progressive Failure Originating Near the Center of the Involute Base Indicated by the Arrow.

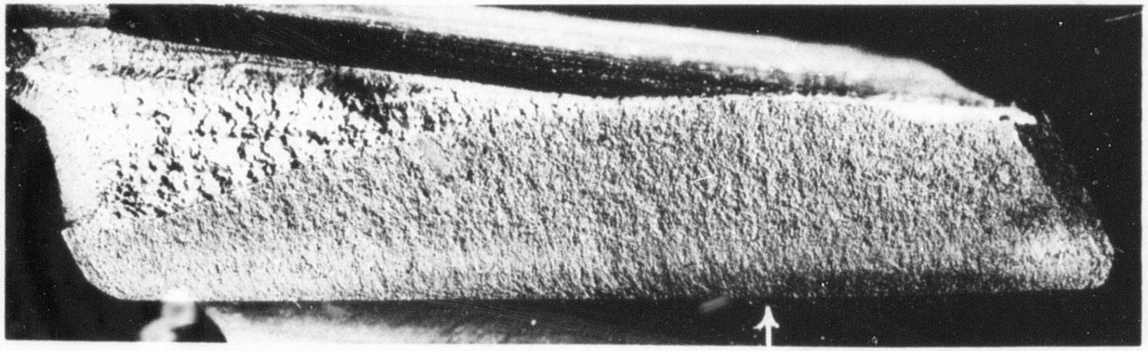

Tested Tooth Number 6 EX-84119, Serial Number CXD 522

Figure 31. Detail View of Failure Surface, Showing Progressive Failure Originating Near the Center of the Involute Base Indicated by the Arrow.

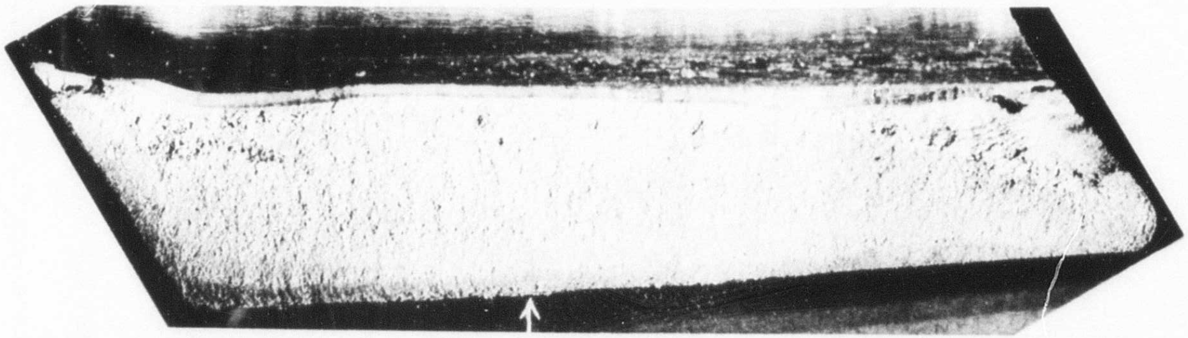

Tested Tooth Number 1 EX-84120, Serial Number CXD 551

Figure 32. Detail View of Failure Surface, Showing Progressive Failure Originating From a Single Point as Indicated by the Arrow.

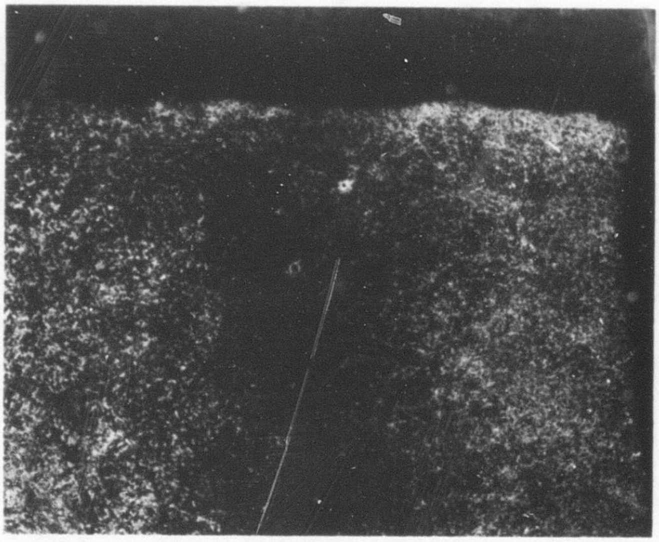

Magnification: 100X

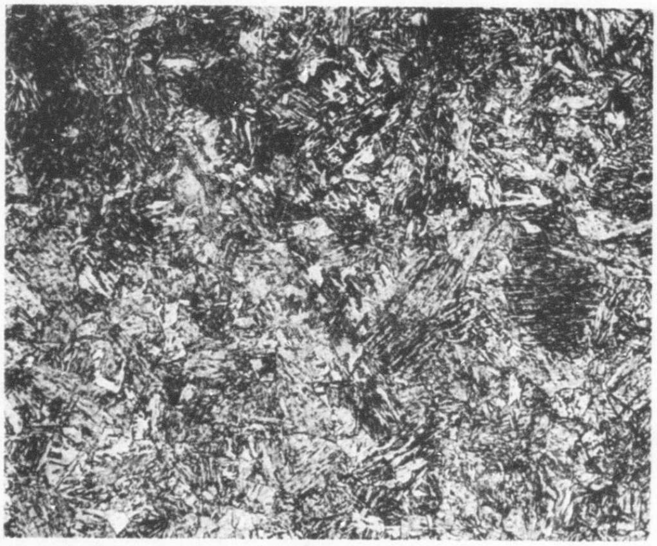

Magnification: 250X
EX-84117, Serial Number CXD 586

Figure 33. Photomicrographs of Transverse Sections Through Test Gear, Showing Typical Microstructure of the Carburized Case and the Tempered Martensitic Core at the Approximate Origin of the Fatigue Failure (Etchant: 2% Nital).

GRAPHIC NOT REPRODUCIBLE

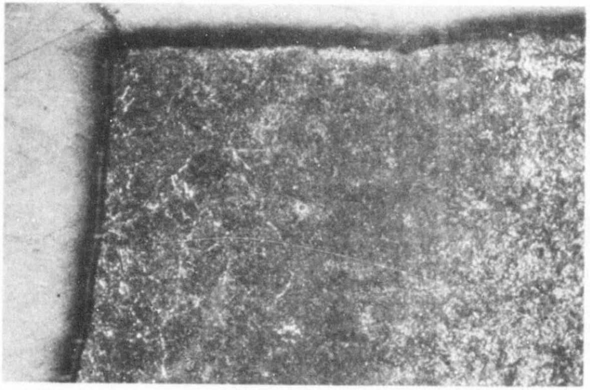

Tooth No. 1 Of Test Gear, Part No. EX-84117,
Serial No. CXD 592

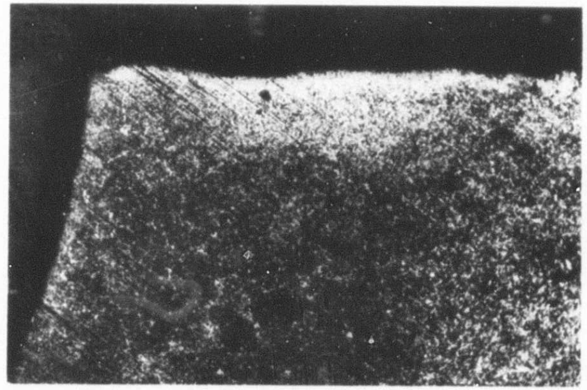

Tooth No. 1 Of Test Gear, Part No. EX-84118,
Serial No. CXD 599

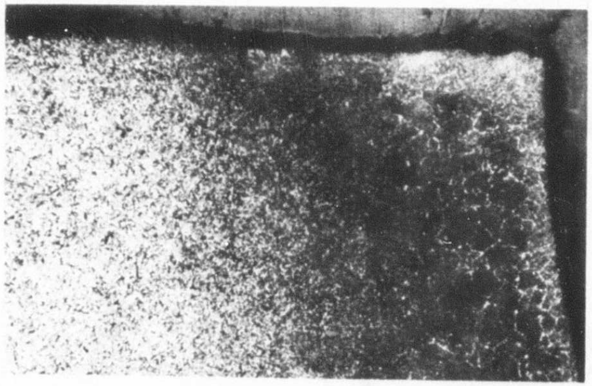

Tooth No. 6 Of Test Gear, Part No. EX-84119,
Serial No. CXD 522

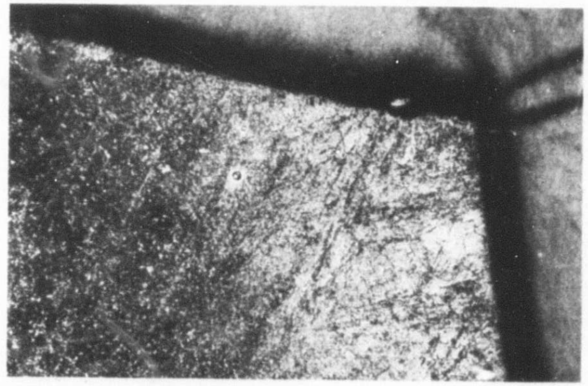

Tooth No. 1 Of Test Gear, Part No. EX-84120,
Serial No. CXD 551

Figure 34. **Photomicrographs of Transverse Sections Through the Approximate Origins of Failure, Showing Transgranular Failures Typical of Fatigue Through the Carburized Case Hardened Surfaces (Magnification: 100× and Etchant: 2% Nital).**

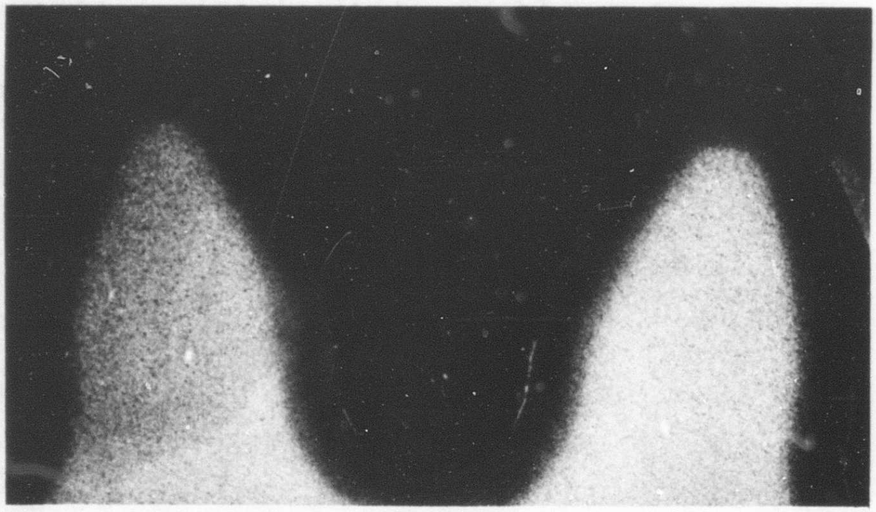

EX-84117, Serial Number CXD 586

Figure 35. Selection Through Test Gear, Showing Carburized Case Depth and Material Cleanliness (Magnification: 6× and Etchant: Nital).

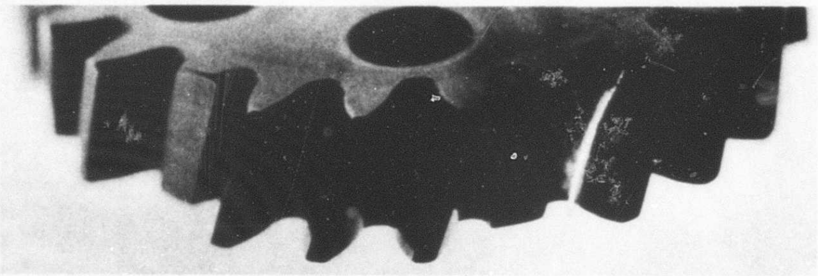

EX-84117, Serial Number CXD 586

Figure 36. Blacklight Photograph of Test Gear, Showing a Crack Indicated by Fluorescent Penetrant Inspection Across the Helical Involute Surface of a Test Tooth (Magnification: 1×).

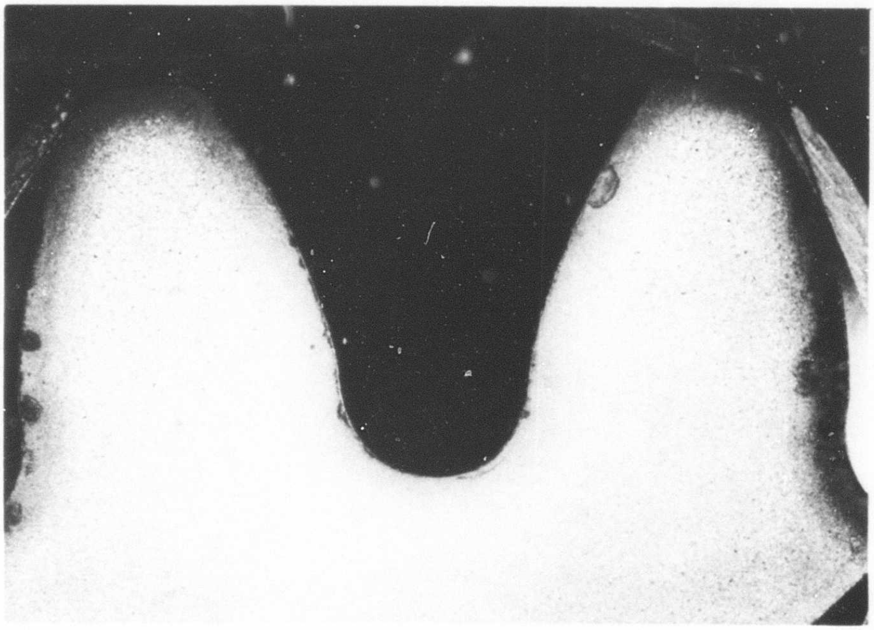

Magnification: 6X Etchant: 2% Nital

EX-84117, Serial Number CXD 592

Figure 37. Blacklight Photograph of Test Gear, Showing a Crack Across the Helical Involute and Section Through Tooth Showing Carburized Case Depth.

Magnification: 1X

Magnification: 1×

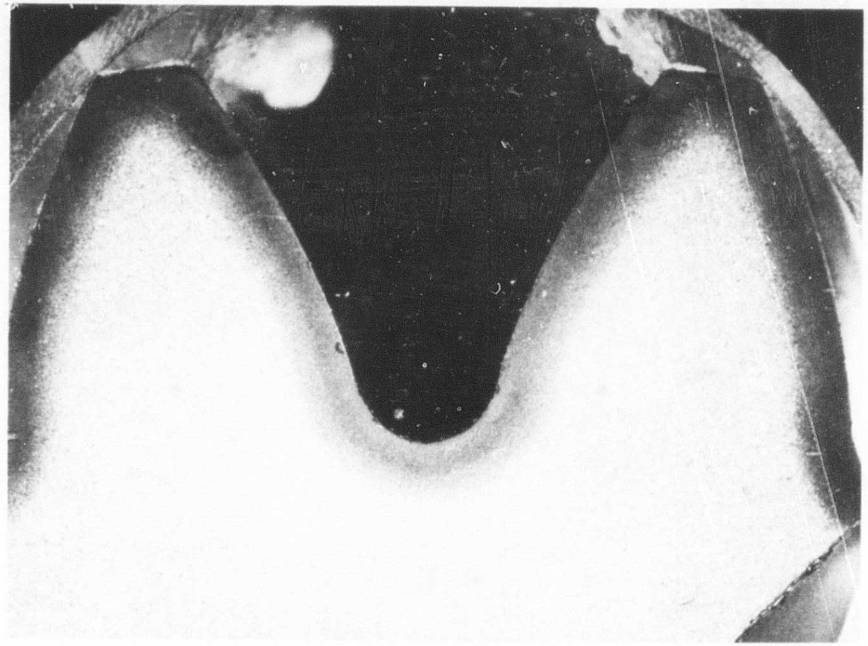

Magnification: 6×   Etchant: 2% Nital

EX-84118, Serial Number CXD 599

Figure 38. Blacklight Photograph of Test Gear, Showing a Crack Across the Helical Involute and Section Through Tooth Showing Carburized Case Depth.

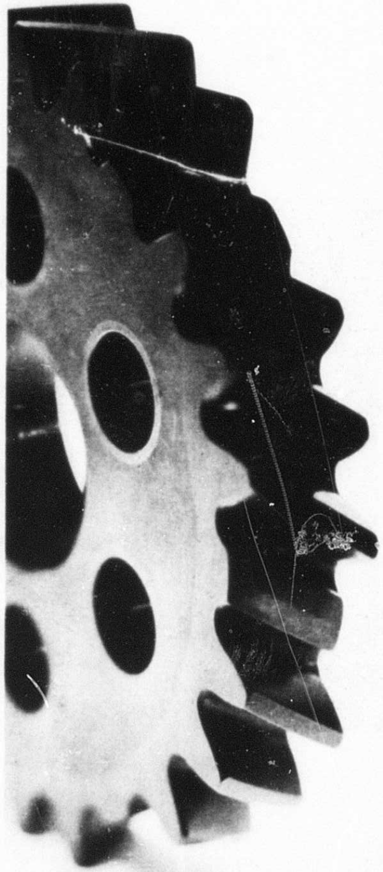

Magnification: 1×

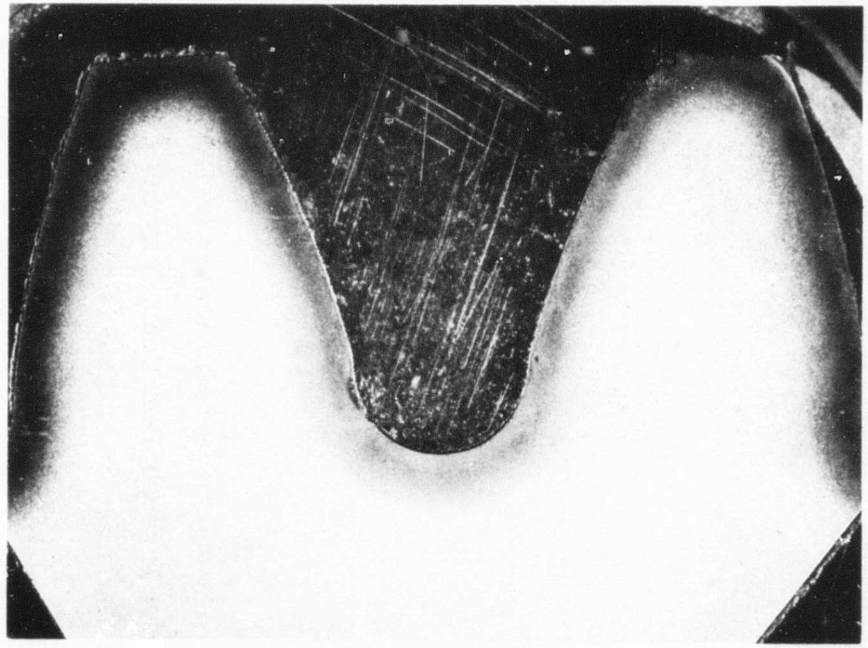

Magnification: 6×   Etchant: 2% Nital

EX-84119, Serial Number CXD 522

Figure 39. Blacklight Photograph of Test Gear, Showing a Crack Across the Helical Involute and Section Through Tooth Showing Carburized Case Depth.

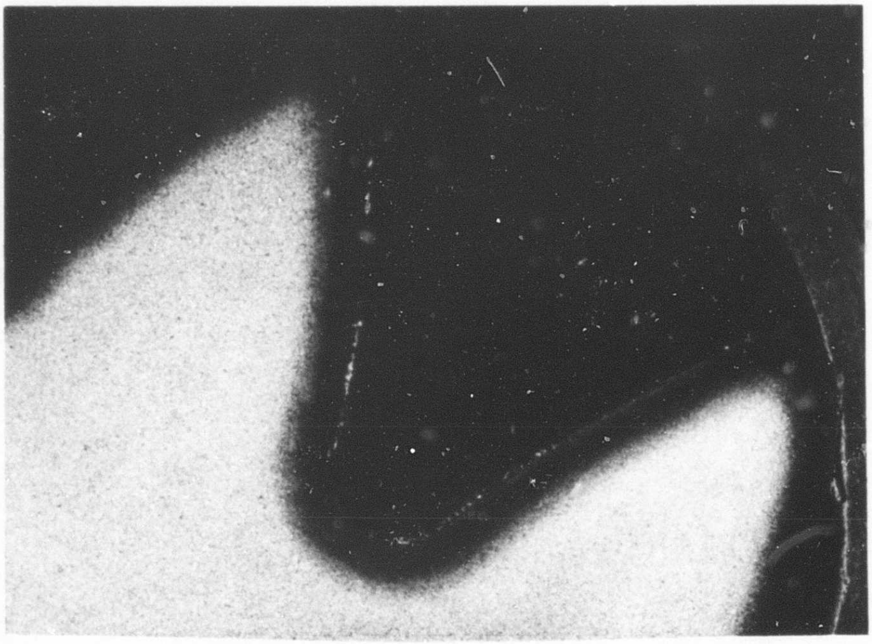

EX-84120, Serial Number CXD 551

Figure 40. Section Through Test Gear, Showing Carburized Case Depth and Material Cleanliness (Magnification: 6× and Etchant: Nital).

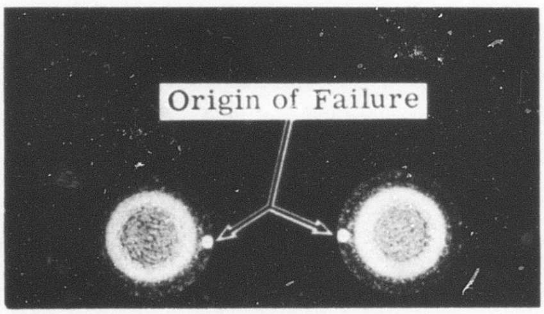

Magnification: 3×

Figure 41. A Typical R. R. Moore Fatigue Specimen From the Helical Gear Program Exposing the Carburized Case on the Fracture Surface With the Characteristic Fatigue Pattern Representing the Origin of Failure.

TABLE XVIII. RECORD OF HARDNESS GRADIENT TESTS ON HELICAL TEETH OF FATIGUE TEST GEARS FROM THE ADVANCEMENT OF GEAR TECHNOLOGY PROGRAM

Depth Below Carburized Surface (in.)	Rockwell C Hardness at the Root Radius and Tooth Involute (Durimet 100 g. ld)									
	EX-84117, CXD 586		EX-84117, CXD 592		EX-84118, CXD 599		EX-84119, CXD 522		EX-84120, CXD 551	
	Rad	In	Rad	In	Rad	In	Rad	In	Rad	In
0.001	65	65	65	64	65	65	65	65	65	67
0.002	65	65	65	64	64	66	64	64	64	66
0.005	63	64	—	—	—	—	64	65	64	64
0.010	64	64	63	64	64	66	64	64	64	64
0.020	62	62	62	62	62	64	64	61	63	63
0.030	58	59	61	60	61	60	56	59	58	60
0.040	54	54	56	55	55	55	53	53	55	55
0.044	50*	—	—	—	—	—	—	—	—	—
0.045	49	51	50*	50*	—	52	—	—	—	—
0.048	49	51*	—	—	—	50*	50*	—	51	—
0.049	—	48	—	—	—	—	—	50*	—	—
0.050	47	48	48	48	50*	49	48	49	50*	51
0.052	—	—	—	—	—	—	—	—	—	50*
0.060	41	43	44	46	49	47	43	43	48	48
0.070	40	41	40	40	40	43	42	41	40	42
0.080	37	39	37	40	37	39	39	40	37	40
0.090	39	38	40	40	42	40	39	37	40	39

Hardness—all hardness gradients were made on a plane normal to the pitch line of a tooth

Rad—root radius between two gear teeth

In—involute of a tooth

*Approximate effective case depth

TABLE XIX. SPECIMEN PROCESS ROUTING PROCEDURE	
Step	**Procedure**
1.	Carburize and anneal per EPS* 202 and EPI** 3000 to an effective case depth of 0.035 to 0.045 inch as determined by the fracture specimen
2.	Harden and temper per EPS 202 and EPI 8000 and stabilize per EPS 202: Core Hardness—R_c = 40 Case Hardness—R_{15n} - 90 (R_c = 60)
3.	Grit blast with 80-grit shot
4.	Remove 0.010 to 0.016 inch from outside diameter by grinding
5.	Stress relieve per EPS 202 and PCI 8000
6.	Nital etch per EIS† 1510
7.	Shot peen per EPS 12140 followed by EPS 12176
8.	Stress relieve per EPS 202 and PCI 8000
9.	Coat with black oxide per AMS-2485

*Allison Engineering Processing Specification
**Allison Process Control Instruction
†Allison Engineering Inspection Specification

TABLE XX. R. R. MOORE TEST RESULTS

Specimen No.	Stress (psi)	Test Cycles ($\times 10^3$)	Failure Origin
1	130,000	28,782	Surface
2	130,000	29,808	Surface
3	130,000	40,127	Surface
4	140,000	4,614	Surface
5	140,000	6,309	Surface
6	140,000	10,463	Surface
7	150,000	1,909	Surface
8	150,000	2,450	Surface
9	150,000	3,213	Surface
10	150,000	3,664	Surface
11	160,000	37	Surface
12	160,000	105	Surface
13	160,000	169	Surface
14	170,000	43	Surface
15	180,000	21	Surface
16	180,000	30	Surface

EXPERIMENTAL INVESTIGATIONS

In this phase of the program, strain gages were used to investigate the magnitude and distribution of the tooth root bending stress.

One tooth from each gear geometry configuration was instrumented with eight strain gages distributed equally along the root of the tooth. The strain gages were located at the point of maximum stress as determined by the Lewis inscribed parabola tangency point in the tooth root. Each tooth was assumed to be uniformly loaded along an inclined load line through the tip at the tooth edge. The point of maximum root stress was calculated assuming a tooth load applied at eight equally spaced points along the inclined load line. The actual gage location is shown in Figure 42. A typical strain gage installation is shown in Figure 43.

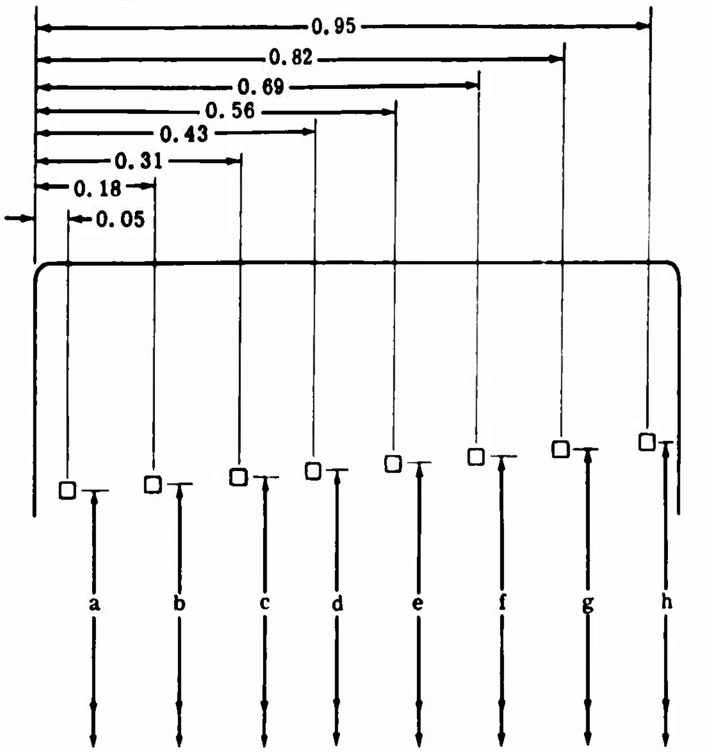

Part No.	a	b	c	d	e	f	g	h
EX-84117	3.87	3.875	3.88	3.89	3.89	3.90	3.90	3.91
EX-84118	3.865	3.874	3.882	3.89	3.897	3.90	3.91	3.92
EX-84119	4.47	4.48	4.49	4.50	4.51	4.52	4.53	4.54
EX-84120	4.46	4.47	4.48	4.49	4.50	4.51	4.52	4.54

Figure 42. Helical Gear Strain Gage Location.

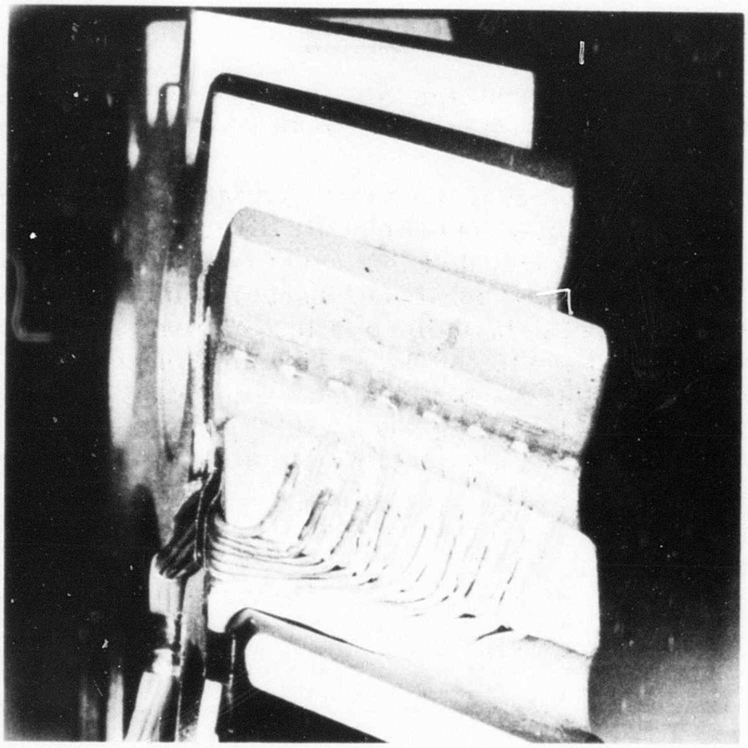

Figure 43. Typical Test Gear Strain Gage Installation.

The gears were statically loaded on the fatigue test rig using the same installation procedure used for fatigue tests. Each gear configuration was loaded along the inclined load line passing through the tip at the edge and at a point 0.250 inch inboard from the edge. The results of the data are given in Figures 44 through 49. Figures 44 and 45 show calibration curves for individual load conditions for all gears, while Figures 46 through 49 depict the load calibrations for each individual gear. Load distribution along the tooth root was measured, and the results for both load conditions are given in Figures 50 through 57.

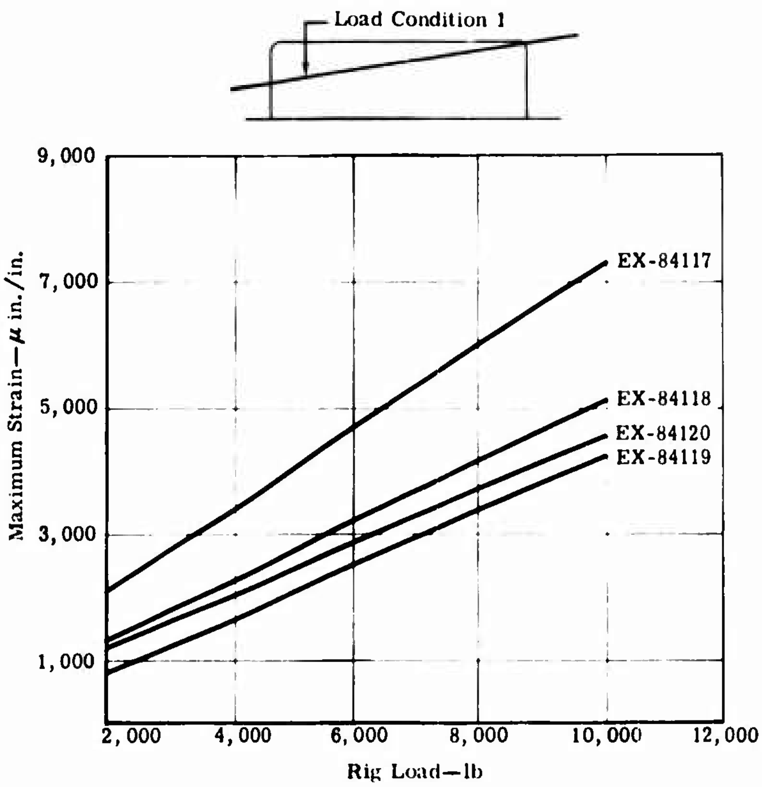

Figure 44. Calibration Curve For Load Condition 1.

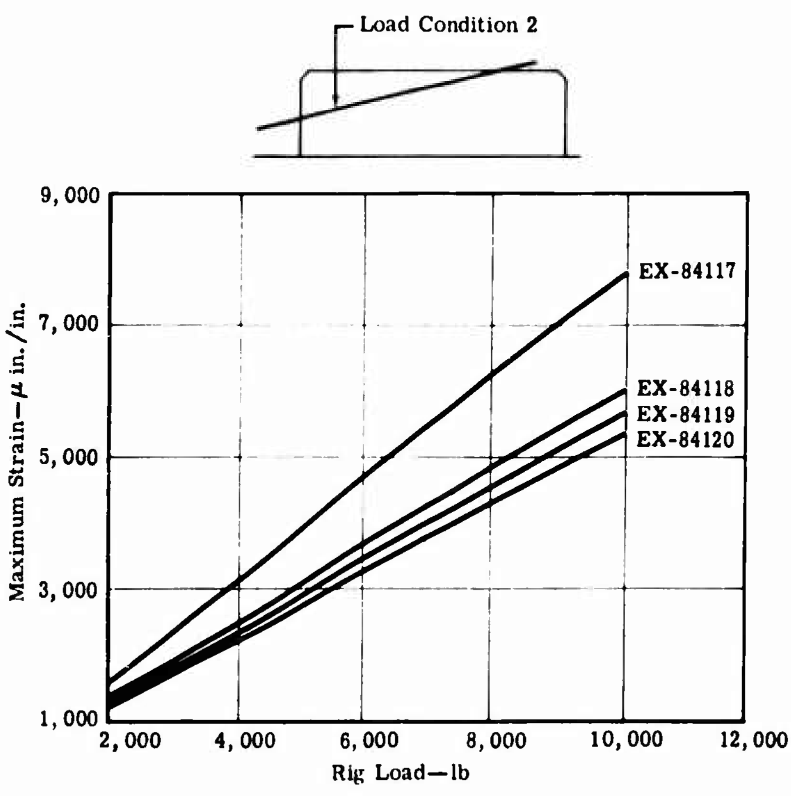

Figure 45. Calibration Curve For Load Condition 2.

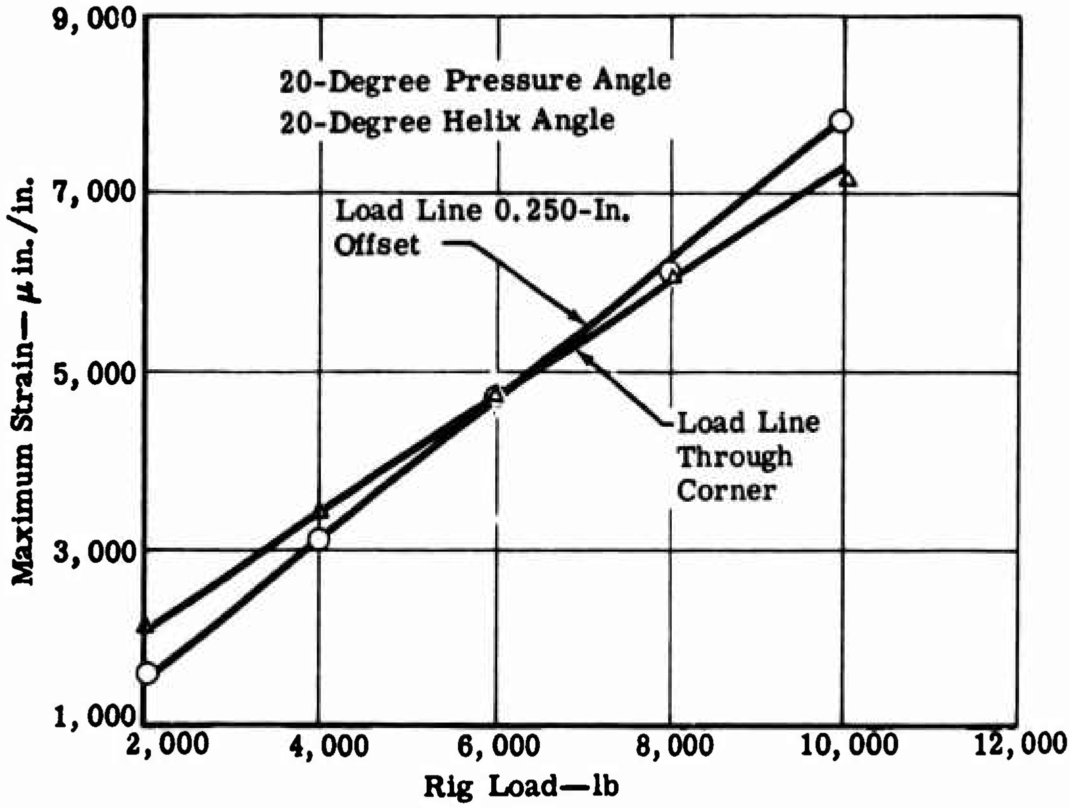

Figure 46. Calibration Curve For Test Gear EX-84117.

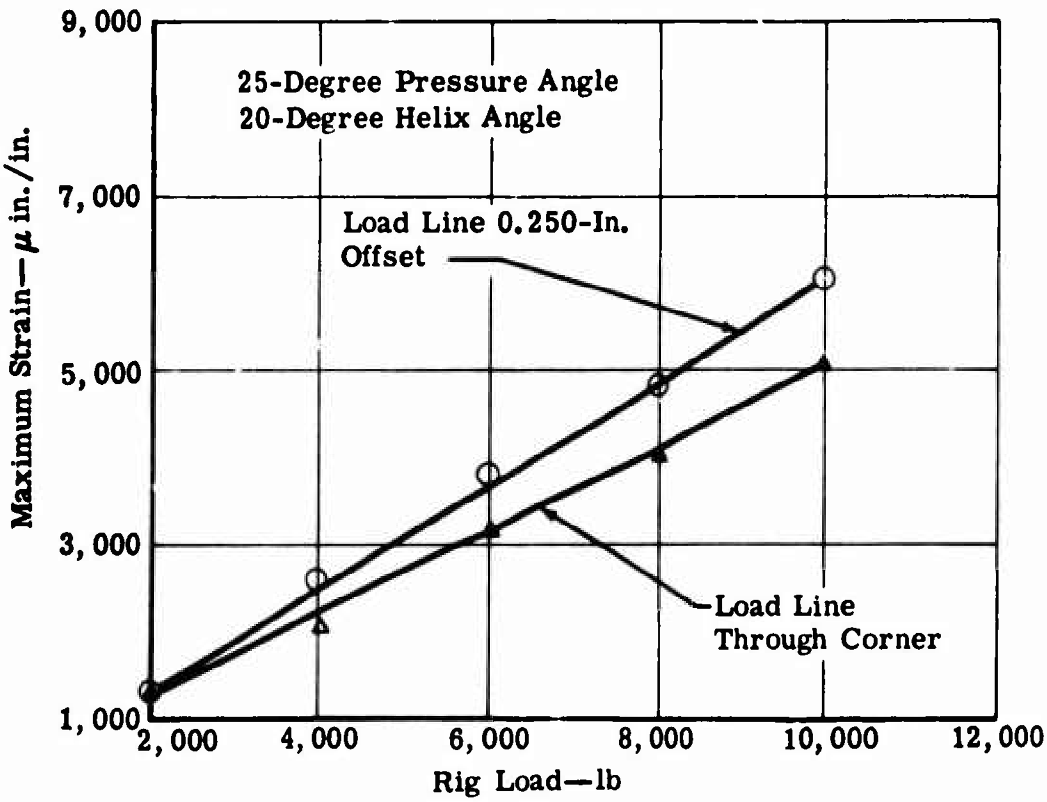

Figure 47. Calibration Curve For Test Gear EX-84118.

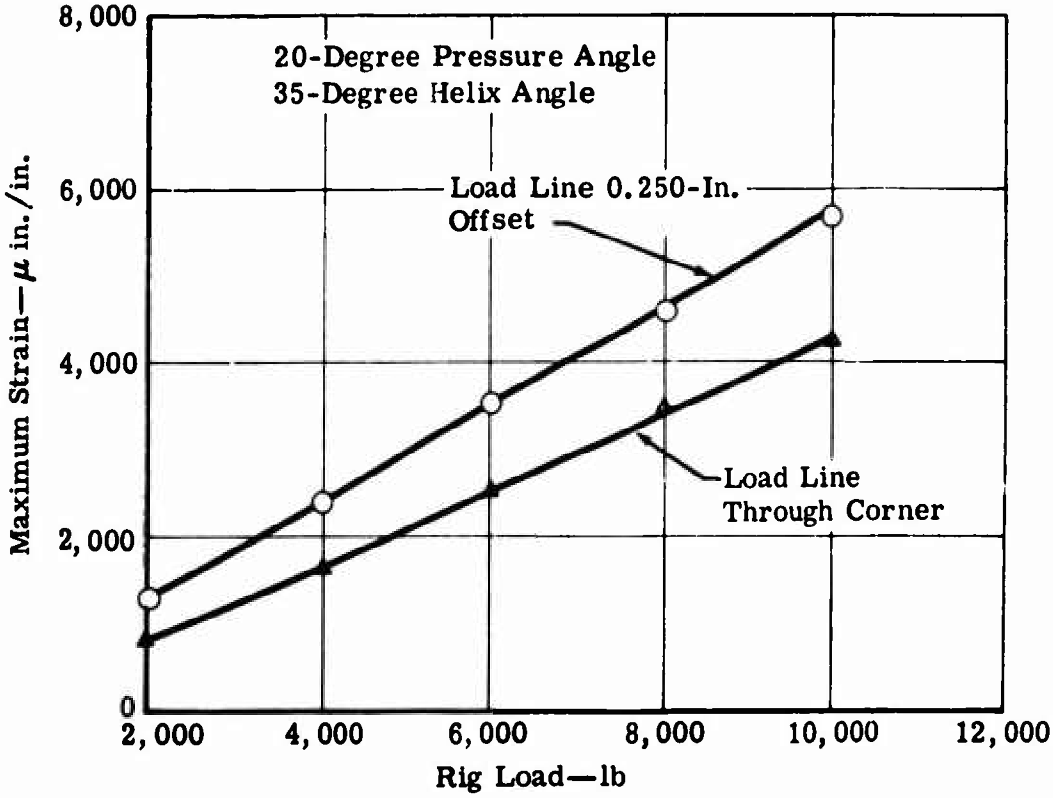

Figure 48. Calibration Curve For Test Gear EX-84119.

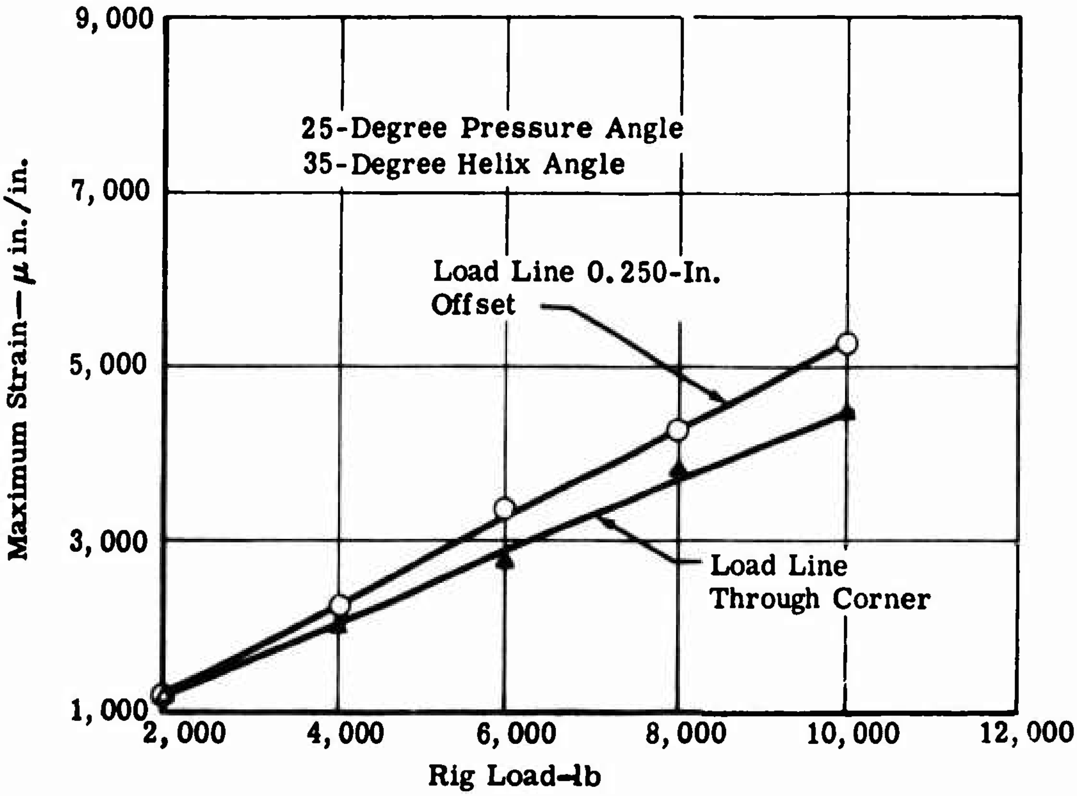

Figure 49. Calibration Curve For Test Gear EX-84120.

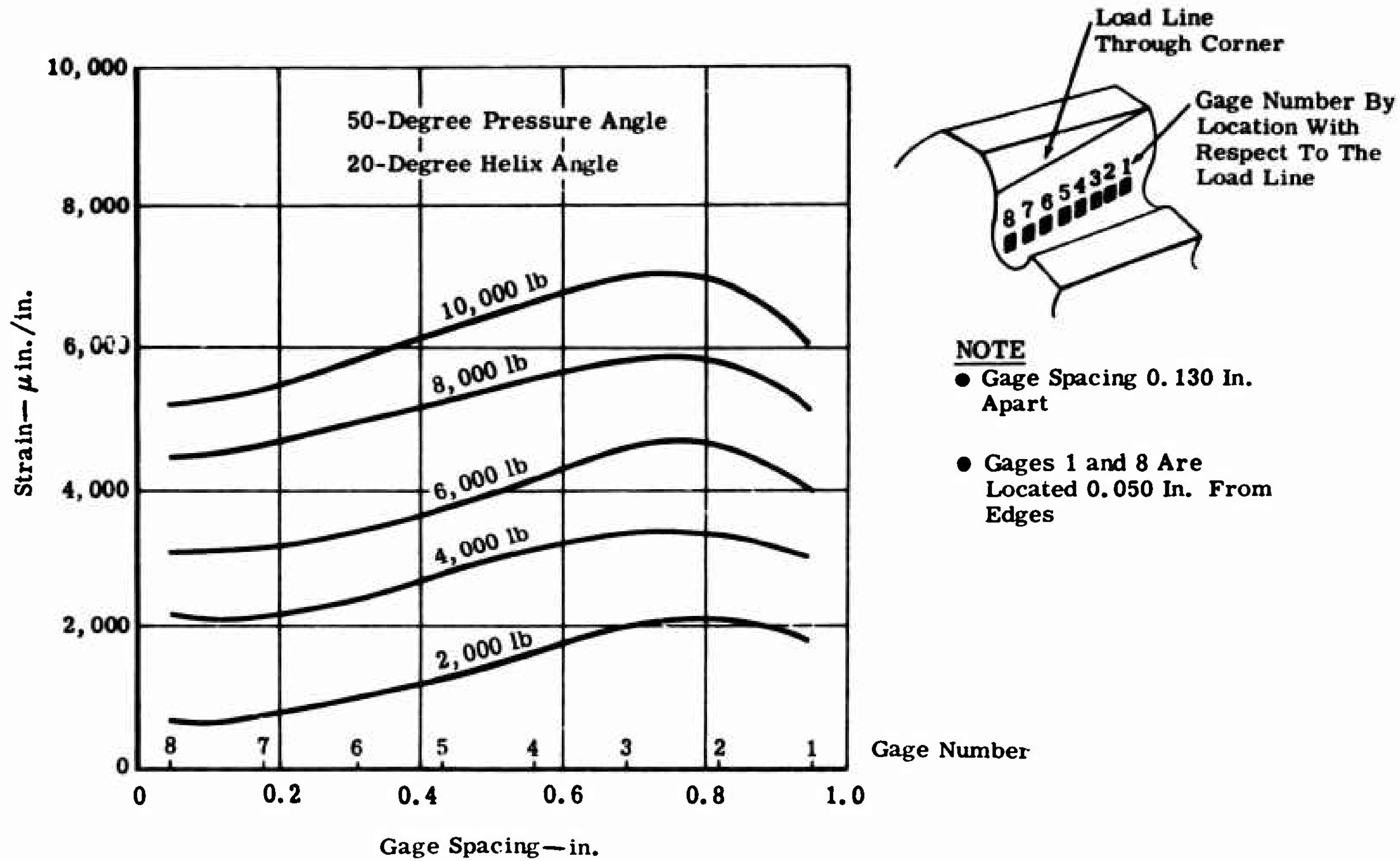

Figure 50. Tooth Root Stress Distribution—EX-84117.

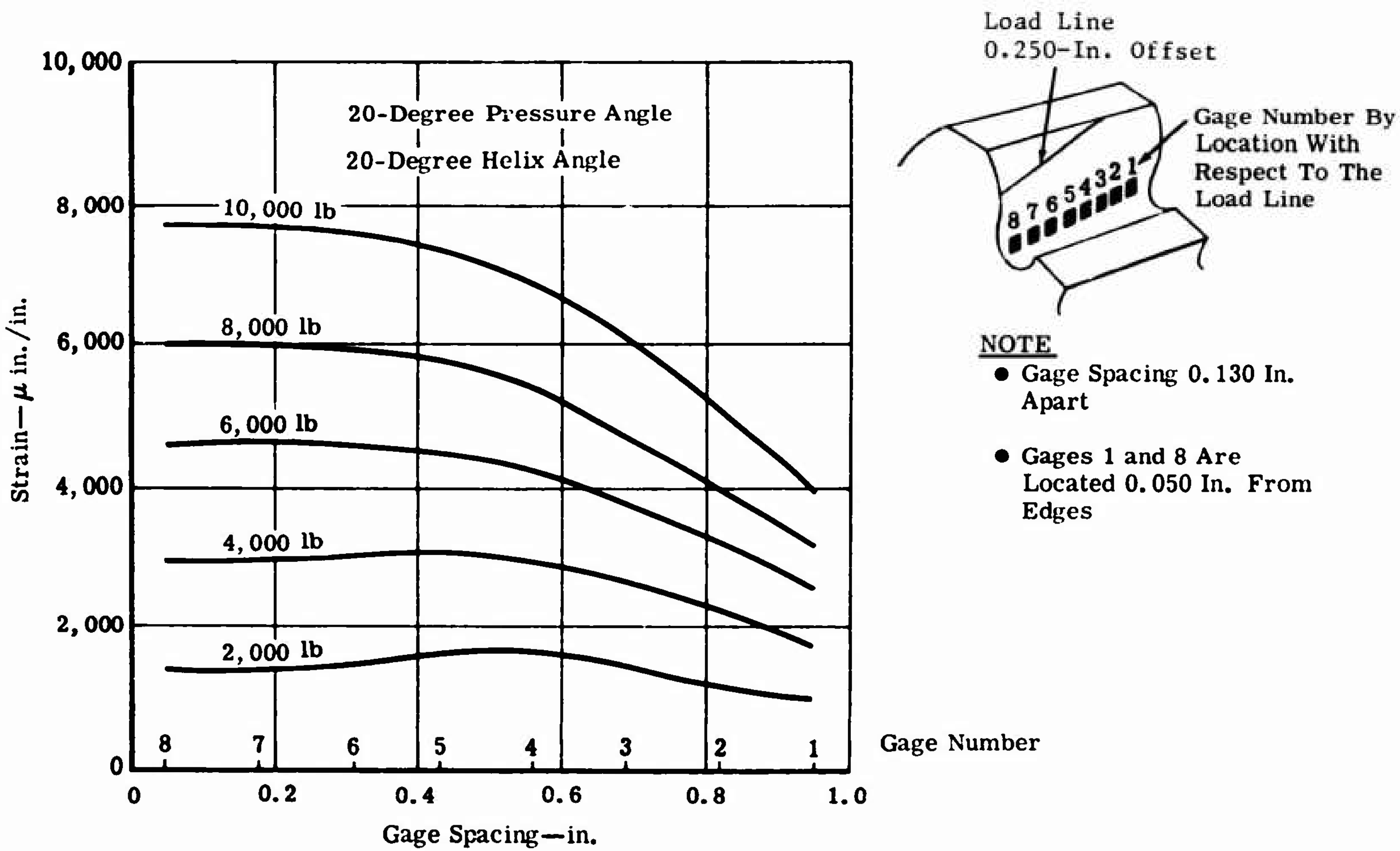

Figure 51. Tooth Root Stress Distribution—EX-84117.

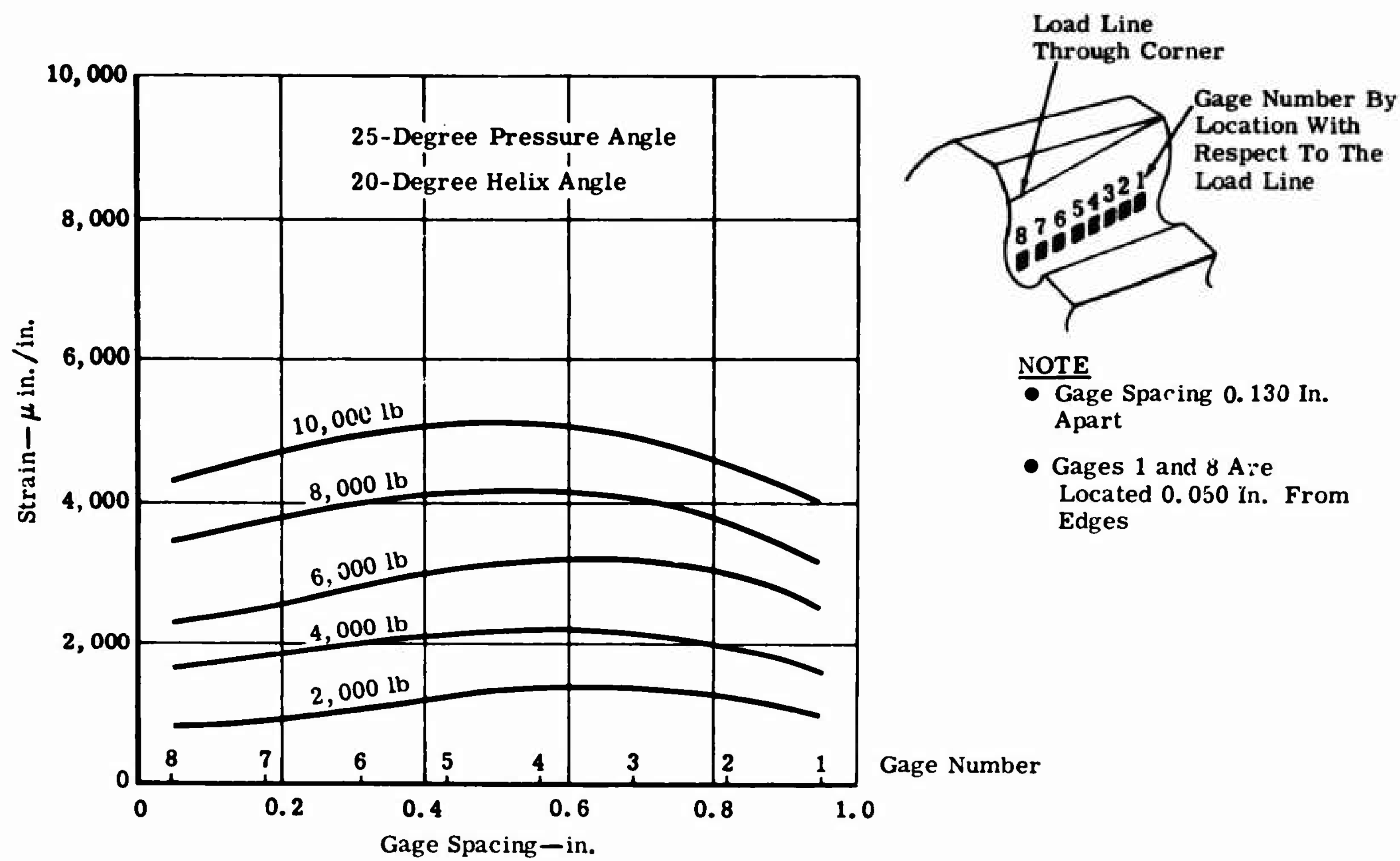

Figure 52. Tooth Root Stress Distribution—EX-84118.

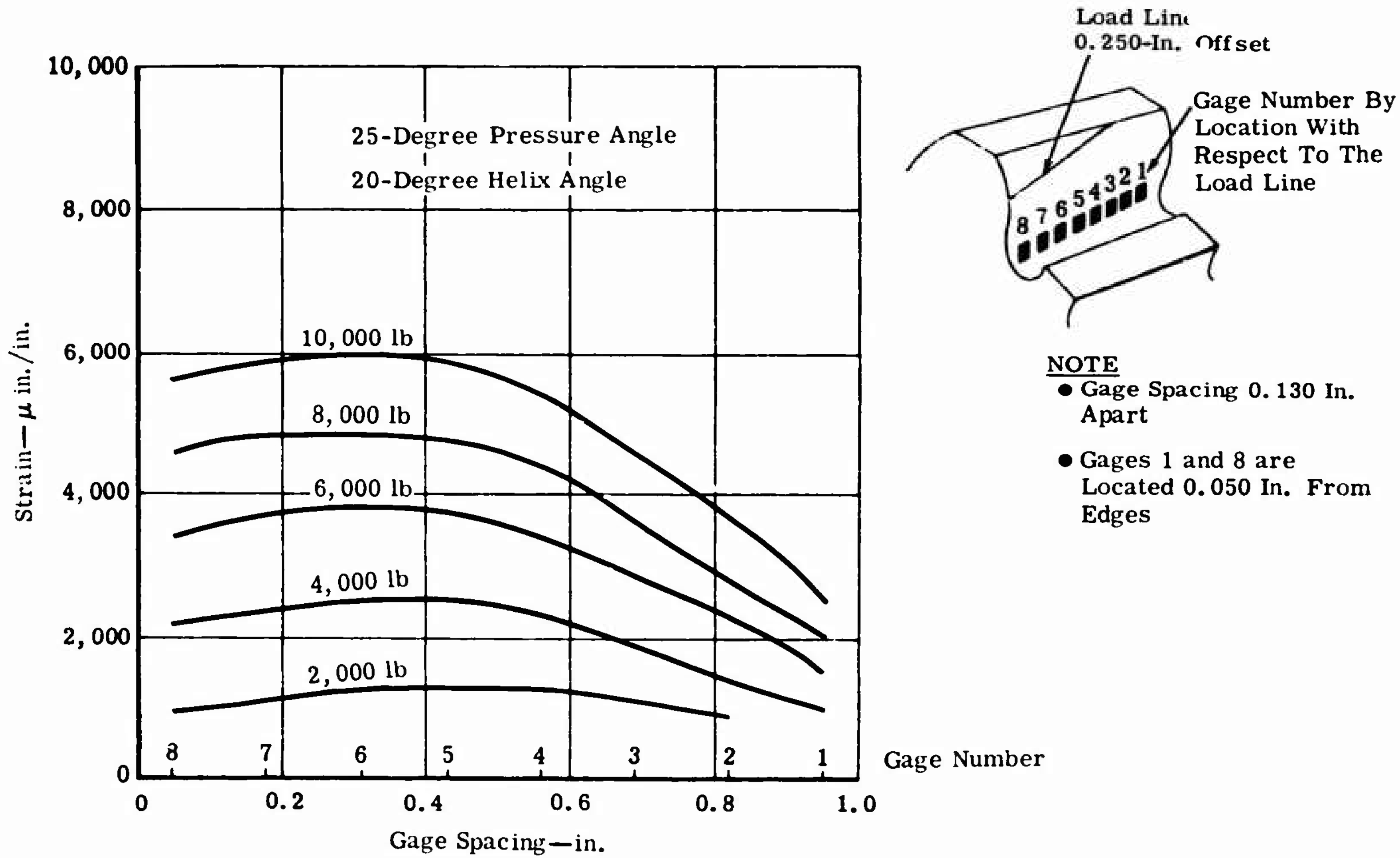

Figure 53. Tooth Root Stress Distribution—EX-84118.

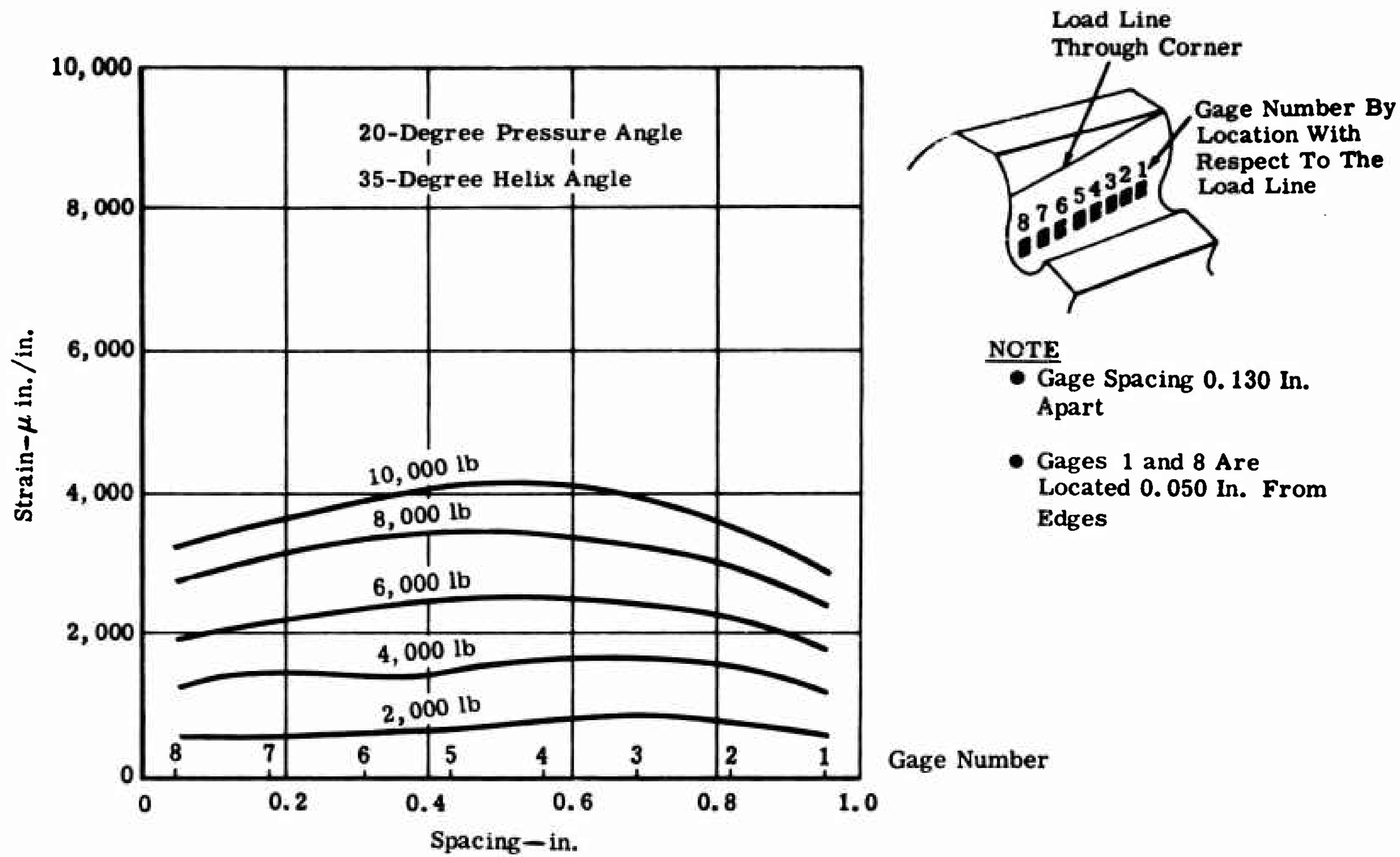

Figure 54. Tooth Root Stress Distribution—EX-84119.

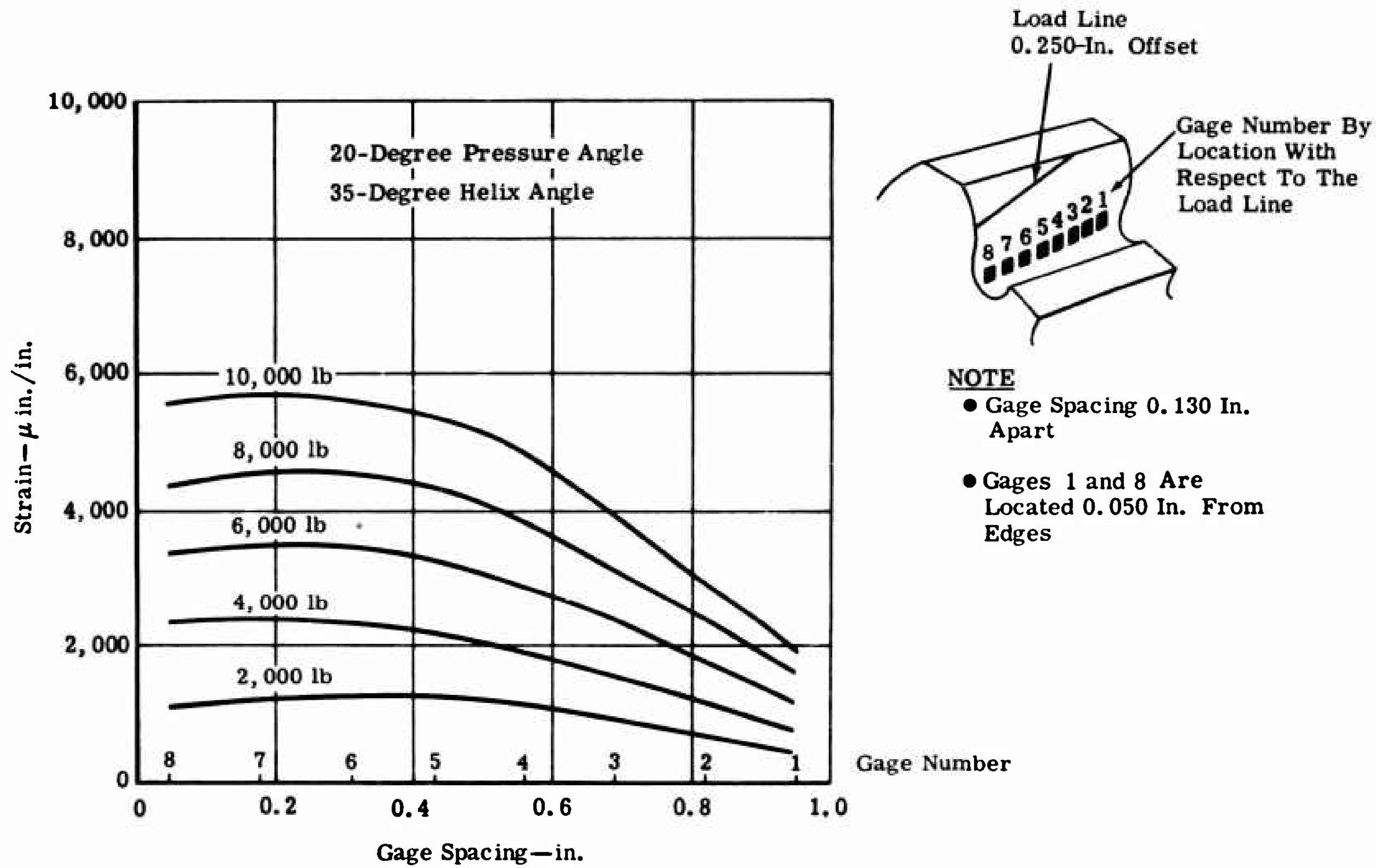

Figure 55. Tooth Root Stress Distribution—EX-84119.

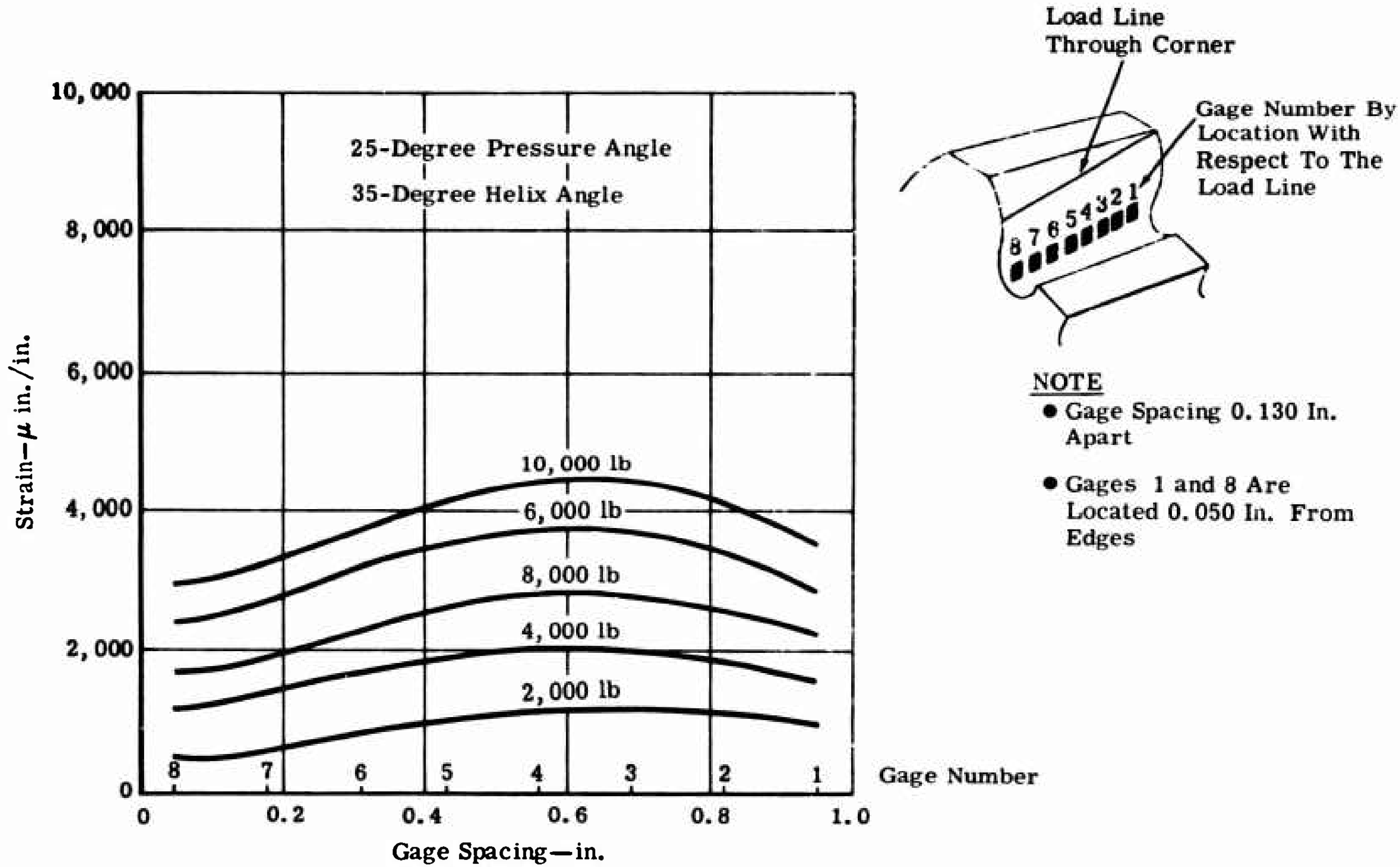

Figure 56. Tooth Root Stress Distribution—EX-84120.

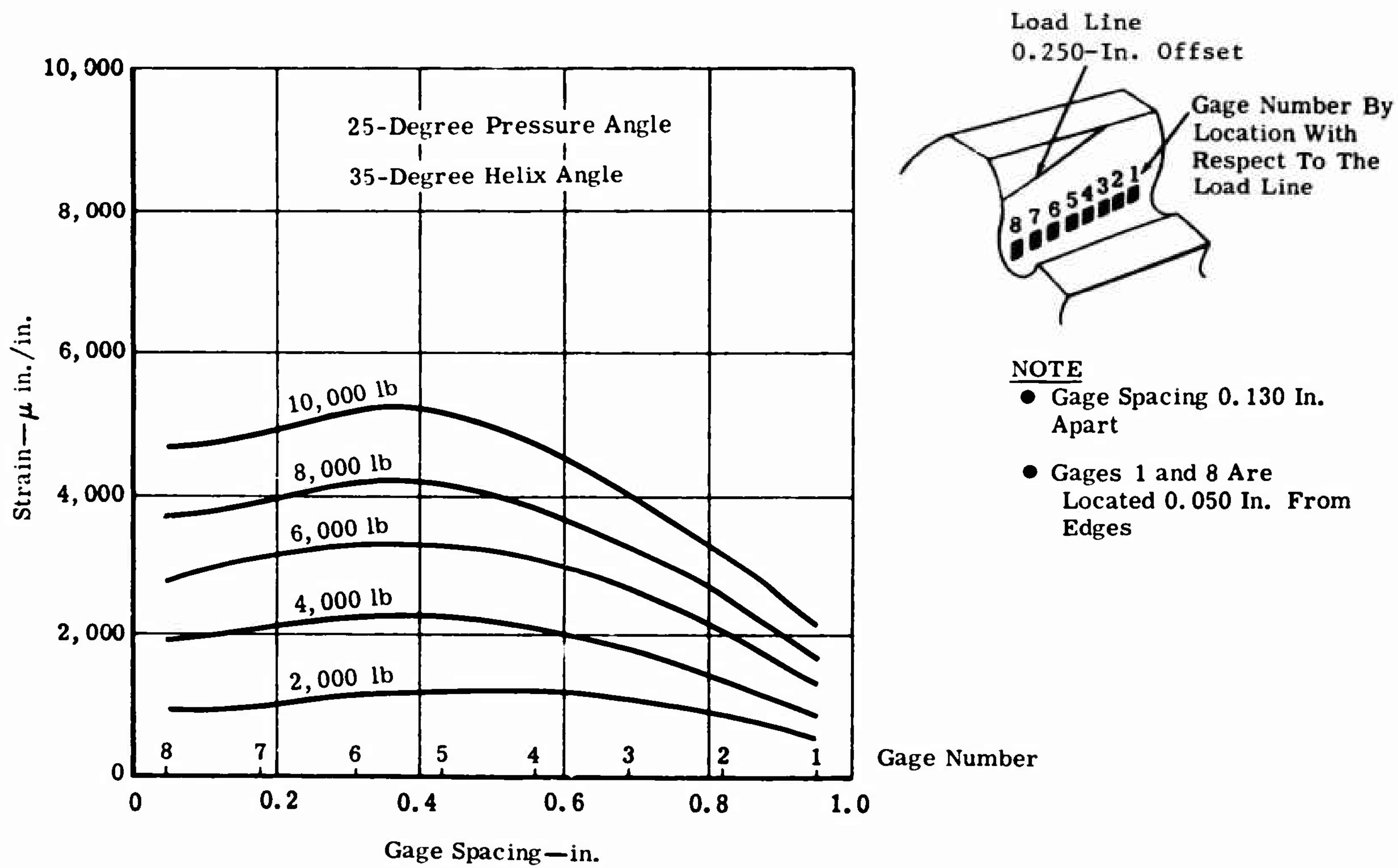

Figure 57. Tooth Root Stress Distribution—EX-84120.

DYNAMIC TESTS

The effect of speed on bending stress can be categorized as follows:

- Centrifugal stress is a steady-state stress at any particular speed caused by internal forces. Figure 58 indicates the nature of the tensile, hoop, and bending stresses.
- Dynamic stress is a cyclic stress with a constant peak magnitude at any particular speed caused by tooth load, imperfect tooth meshing, load sharing, and other geometrical and manufacturing properties of the gear. It is cyclic, since it occurs only when the tooth is under load; i. e., in mesh with a mating gear. This is shown graphically in Figure 59.

To understand the effects of speed on gear tooth bending stress, a helical gear was instrumented and strain data were recorded during actual running conditions. Data were recorded to 20, 000 feet per minute pitch-line velocity and 5000 horsepower. The gear tested was a double helical pinion gear used in a T56 development reduction gear assembly. The instrumentation consisted of strain gages located on the tooth as shown in Figures 60 and 61. The gear was inspected to determine involute and tooth spacing error. Strain gages were located on the tension side of three consecutive teeth in the area of minimum and maximum tooth spacing error on both the left and right sides of the double helical gear. Two gages were located on each tooth for a total of 24 gages.

The centrifugal and dynamic stresses were separated electronically, since centrifugal stress is manifested as a steady-state stress and dynamic stress is cyclic. Centrifugal stress was obtained by observing strain under zero load conditions at various steady-state speed points. The dynamic stress was taken under loaded conditions and was the peak strain above the centrifugal base line.

The gear train was assembled in a T56 development reduction gear case and mounted on a back-to-back gearbox test stand. Centrifugal stress was isolated by first testing at zero load conditions. Using a three-wire strain gage hookup and allowing gearbox oil temperature to stabilize, strain due to centrifugal loads was recorded. Testing was conducted at essentially zero tangential load for speeds varying from 4, 000 to 14, 300 r. p. m. Figure 62 shows the centrifugal strain on the gear tooth.

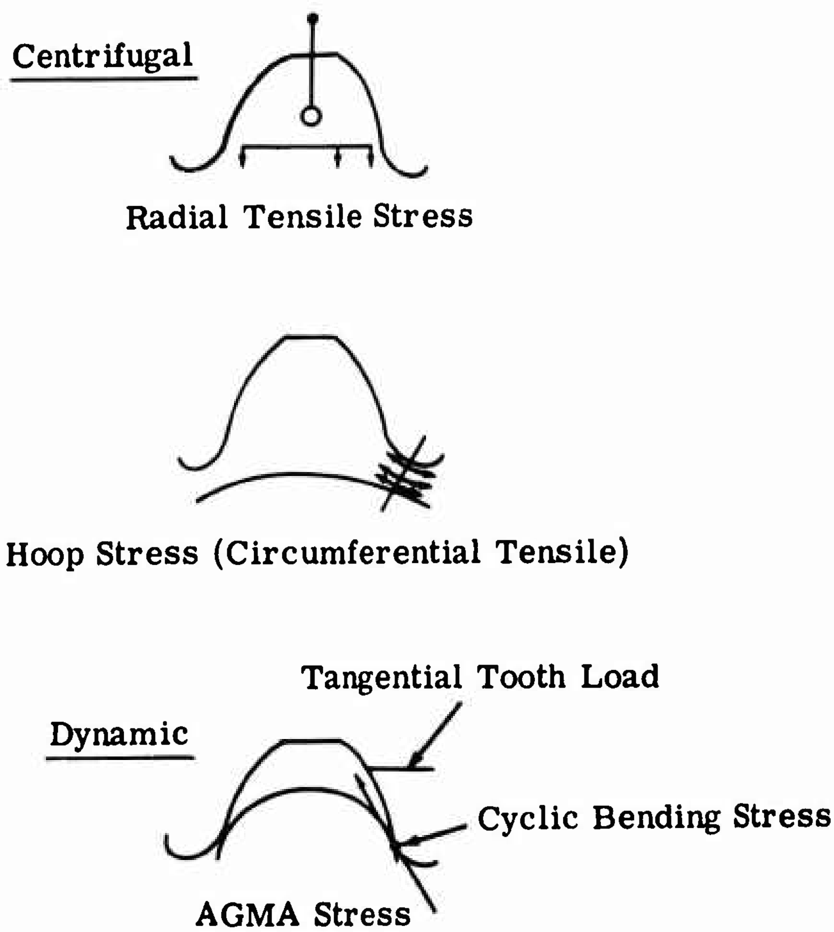

Figure 58. Gear Tooth Bending Stress Schematic.

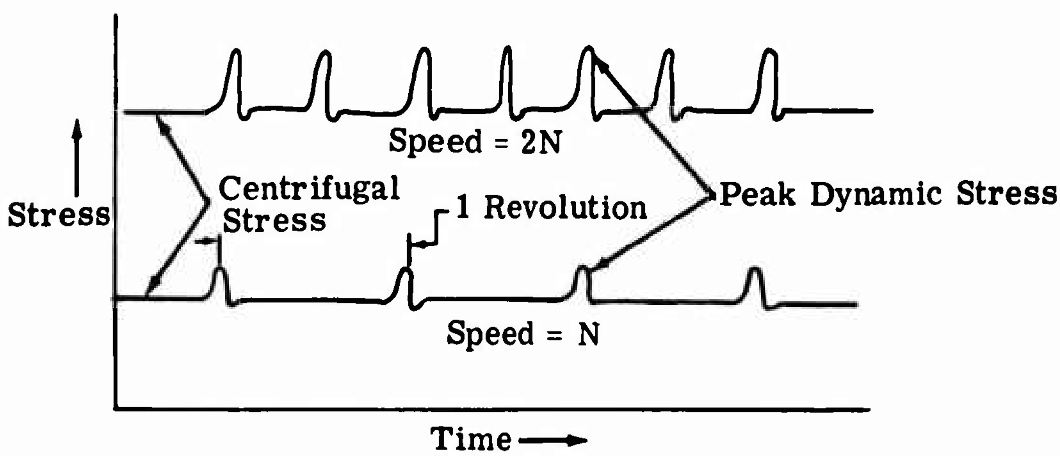

Figure 59. Diagram Showing Expected Effect of Speed on Gear Tooth Stresses.

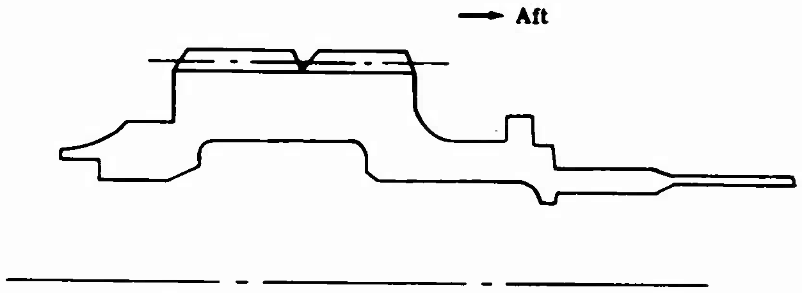

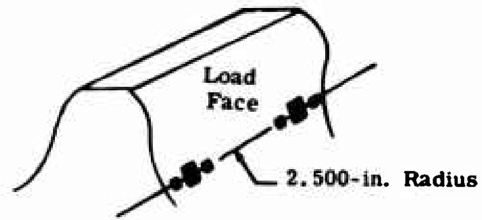

Radial Strain Gage Position

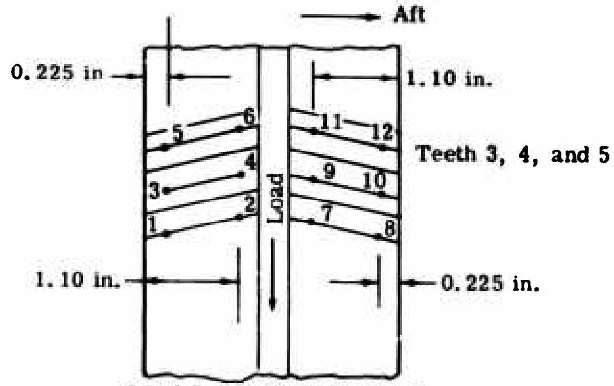

Axial Strain Gage Position

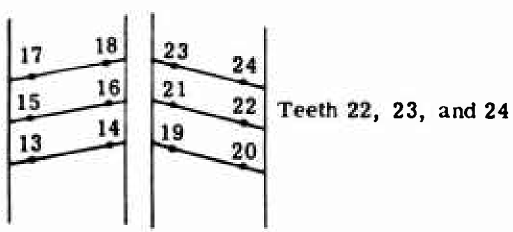

NOTES:

- 2 Strain Gages On Each Of 3 Adjacent Teeth—Both Sides On The Load Face
- Use Gages EA-06-031EC-120 Three-Wire Hookup—"Q" Lot Gages
- Instrument:
  - Teeth 3, 4, and 5 On Right Hand and Left Hand
  - Teeth 22, 23, and 24 On Right Hand and Left Hand
- Environment:
  - Gearbox Dyne Running To 14,300 r.p.m.
  - Temperatures Are 300°F
  - Oil Bath Exposure
- Lead Wires No. 30 Teflon. Routing Lead Wires Through Holes Provided On Pinion Shaft Gear. Lead Wire Length Is Approximately 10 ft.
- Surface Preparation Is Light Sand Blasting To Remove Black Oxide

Figure 60. Instrumentation of Pinion Shaft Gear.

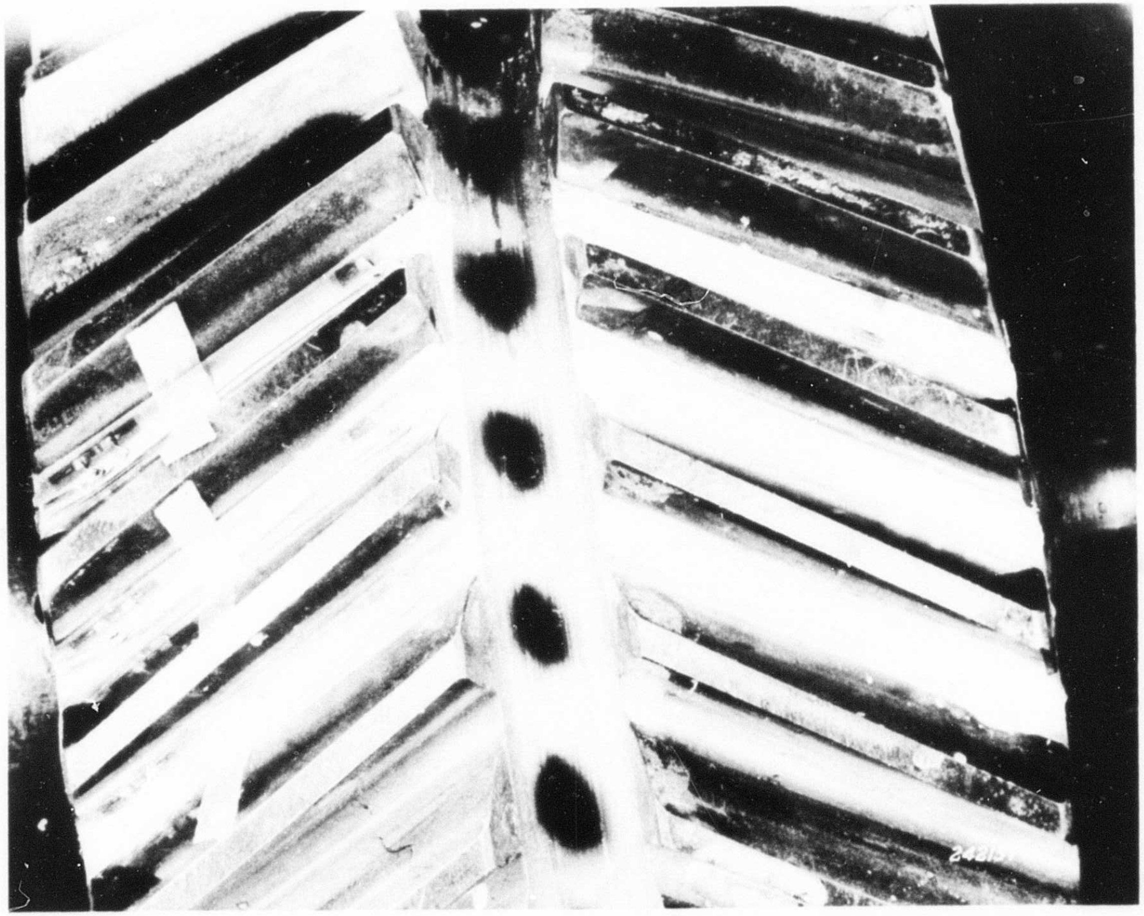

Figure 61. Strain Gages Located on Pinion Shaft Gear Tooth.

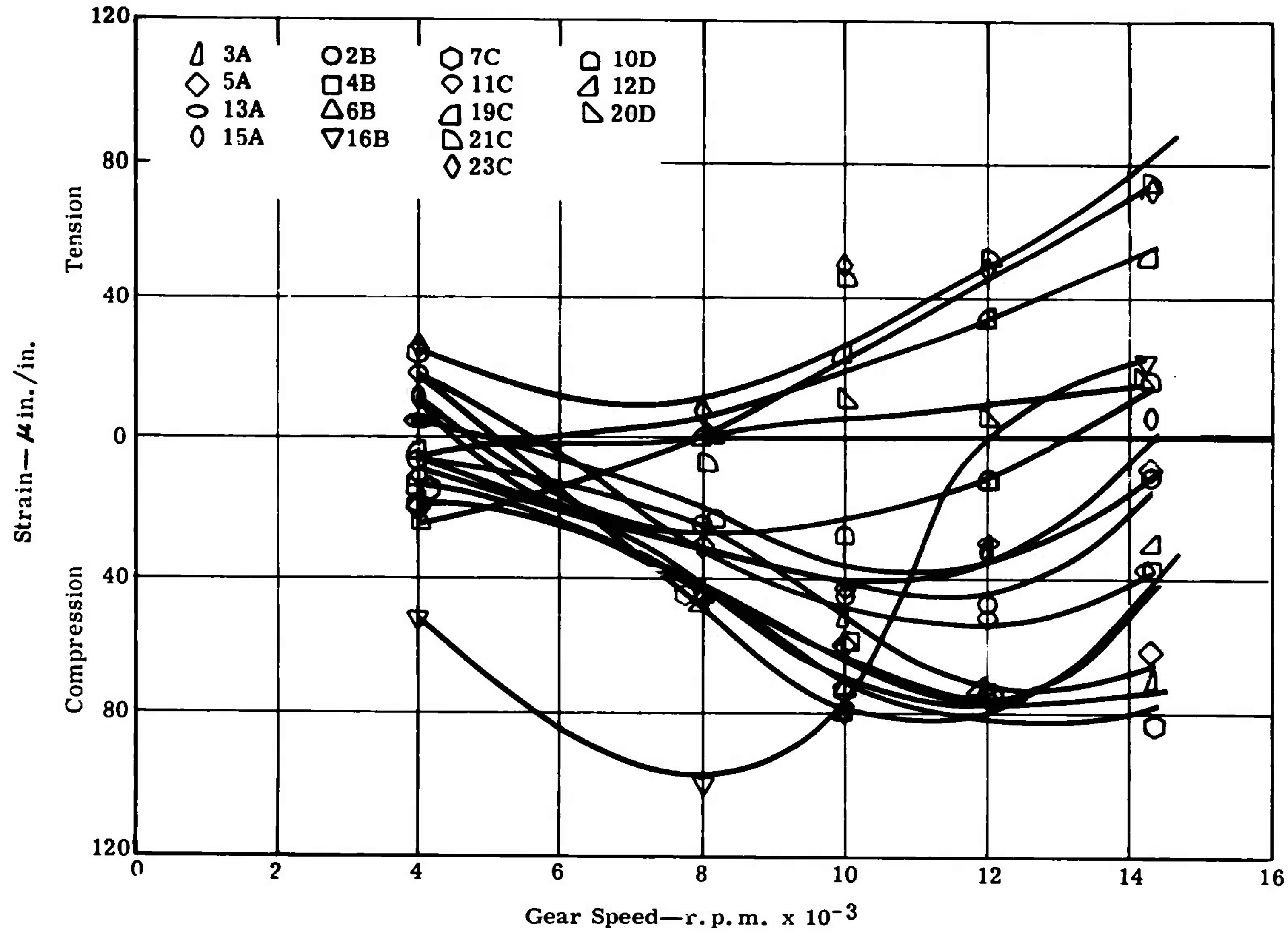

Figure 62. Effect of Speed on Gear Tooth at No-Load Condition.

The gear train was then loaded to obtain stress versus speed data. The strain gage instrumentation was routed through a slip-ring assembly, and the gage output signal was recorded by a 16-channel Miller oscillograph recorder. The gear was tested at speeds of 8,000 to 14,300 r.p.m. and at a constant torque of 24,160 inch-pounds (5000 horsepower). Figure 63 shows the data from 13 strain gages.

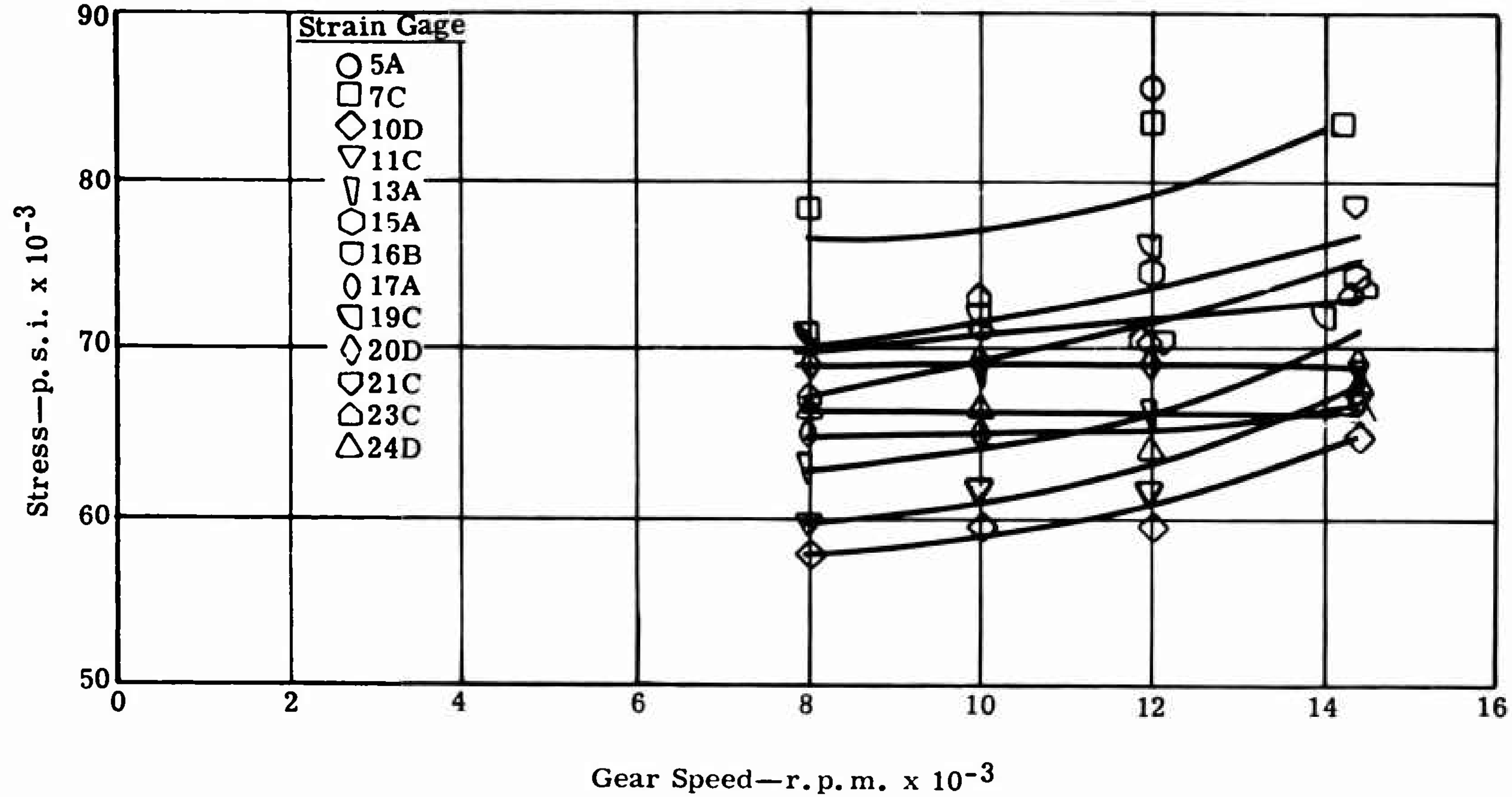

Figure 63. Effect of Speed on Loaded Gear Tooth Stress.

DISCUSSION OF RESULTS

EVALUATION PROCEDURE

The test results were evaluated by the following steps:

1. Determine the predictive ability of the five calculation methods.
2. Compare strain gage data with calculated stress.
3. Determine significance of geometric variables based on the most predictive calculation methods.
4. Determine basic material strength and design values.
5. Analyze centrifugal and dynamic load effects.
6. Establish computer program.

PREDICTIVE ABILITY OF CALCULATION METHODS

The predictive ability of the five methods studied for calculating bending stress was evaluated by use of the mean endurance limits fitted through the fatigue test gear data points. The bending stress per unit applied load was calculated for each method studied. These values were used to convert from endurance limits in terms of applied load to endurance limits in terms of calculated stress for each method studied. Figure 64 is a comparison of the calculated endurance limits for each configuration. The endurance limit values are listed in Table XXI and are ranked in descending order. Average, range, and variation in endurance strength for each calculation method are also given. The Cantilever Plate theory method—the basis for the current AGMA method—produced the smallest variation, and the average endurance limit matched the actual material strength closer than the other methods. The average endurance limit of 157,750 pounds per square inch was within 10 percent of the material endurance limit as determined by R. R. Moore bar fatigue tests. The AGMA method had a higher variation and yielded a slightly lower average endurance limit of 152,328 pounds per square inch. The Lewis method had a slightly higher variation than the Cantilever Plate method, but the average endurance limit was only 99,875 pounds per square inch compared to an actual endurance limit for the material of 175,000 pounds per square inch. The Heywood method used to calculate tooth bending stress gave fairly low variation; however, the average endurance limit produced was 32.5 percent above the actual endurance limit of the material. The Almen-Straub method produced the highest variation in the calculated endurance limit, and the average endurance limit calculated by this method was 29.5 percent below the endurance limit established for the material.

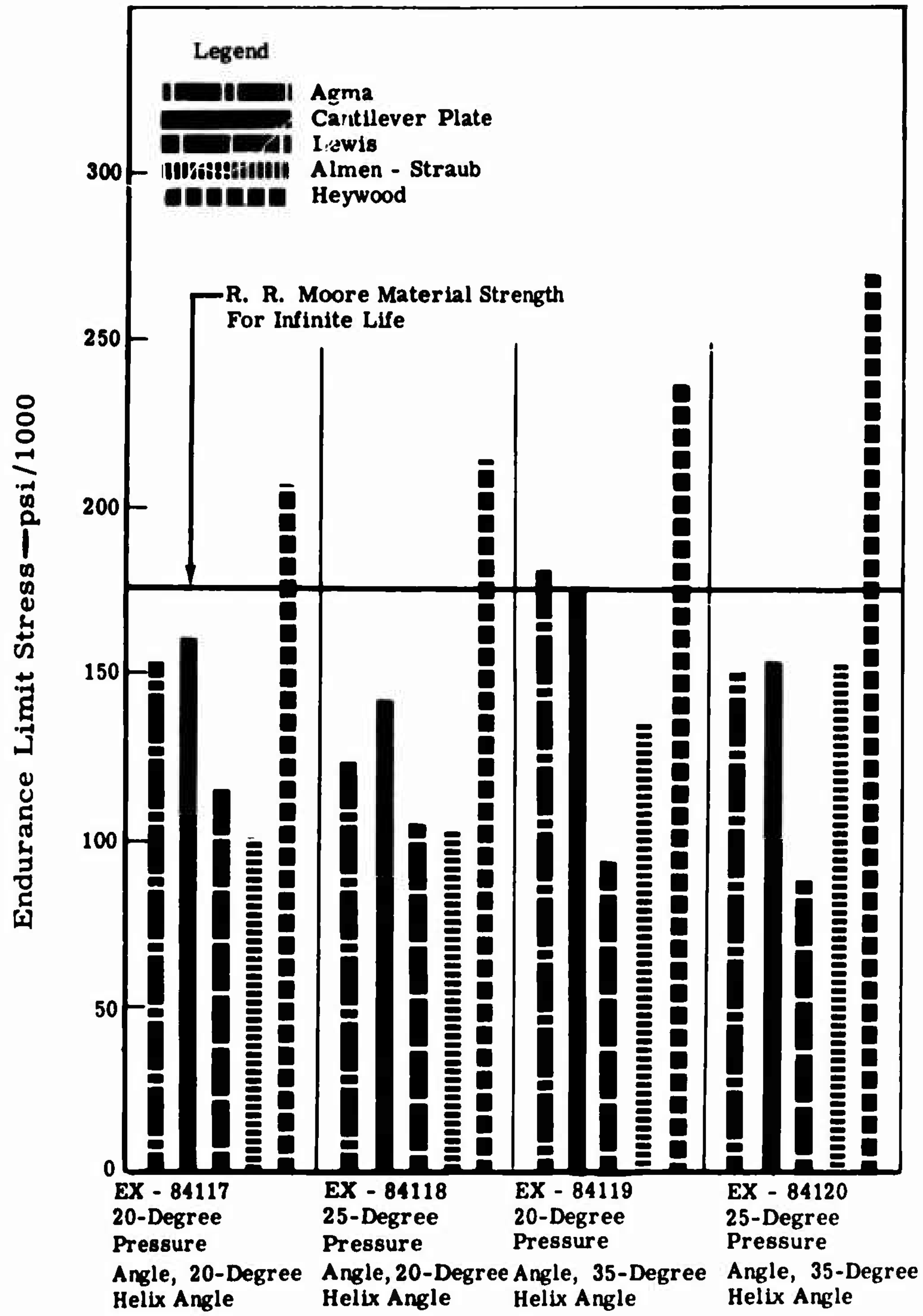

Figure 64. Calculated Endurance Limit Stress Compared With R. R. Moore Endurance.

TABLE XXI. RANKED ENDURANCE LIMITS FOR VARIOUS CALCULATION METHODS

Test Rig Load		AGMA		Cantilever Plate		
Configuration Number	Endurance Limit (lb)	Configuration Number	Endurance Limit (psi)	Configuration Number	Endurance Limit (psi)	Con Nur
4	11,100	3	182,000	3	174,665	
3	9,100	1	152,766	1	160,522	
2	8,720	4	149,850	4	152,391	
1	7,380	2	124,696	2	141,744	
Average			152,328		157,325	
Range			57,304		32,921	
Variation = $\frac{\text{Maximum}}{\text{Minimum}}$			1.46		1.23	

Legend:

Configuration Number	Test Gear	Helix Angle (Degrees)	Pressure Angle (Degrees)
1	EX-84117	20	20
2	EX-84118	20	25
3	EX-84119	35	20
4	EX-84120	35	25

A

ᶠOR
ODS

Cantilever Plate		Lewis		Almen-Straub		
Configuration Number	Endurance Limit (psi)	Configuration Number	Endurance Limit (psi)	Configuration Number	Endurance Limit (psi)	Configu Numbe
3	174,665	1	114,264	4	152,548	
1	160,522	2	104,344	3	136,827	
4	152,391	3	93,457	2	103,995	
2	141,744	4	87,435	1	99,815	
	157,325		99,875		123,296	
	32,921		26,829		52,733	
	1.23		1.3		1.53	

Pressure Angle (Degrees)
20
25
20
25

B

Lewis		Almen-Straub		Heywood	
figuration ıber	Endurance Limit (psi)	Configuration Number	Endurance Limit (psi)	Configuration Number	Endurance Limit (psi)
1	114,264	4	152,548	4	270,529
2	104,344	3	136,827	3	237,728
3	93,457	2	103,995	2	214,119
4	87,435	1	99,815	1	206,190
	99,875		123,296		232,141
	26,829		52,733		64,339
	1.3		1.53		1.31

C

BLANK PAGE

Further analyses were made by comparing the relative strength of each configuration, as predicted by each calculation method, with the relative strength determined by the fatigue tests. Table XXII lists the fatigue test gear strength, based on applied load, in descending order. A comparison is made with the relative strength of the gears as predicted by each calculation method.

TABLE XXII. GEAR CONFIGURATION RANKING COMPARISON

Test Rig Load Ranking	AGMA		Cantilever Plate	
	Rank	Difference	Rank	Difference
4	4	0	4	0
3	2	1	2	1
2	3	1	3	1
1	1	0	1	0
Correct Rankings	2	—	2	—
Prediction Accuracy	—	50%	—	50%

Lewis		Almen-Straub		Heywood	
Rank	Difference	Rank	Difference	Rank	Difference
4	0	2	2	4	0
3	0	4	1	2	1
2	0	1	1	3	1
1	0	3	2	1	0
4	—	0	—	2	—
—	100%	—	0%	—	50%

The Lewis formula predicted the rank position in every case, but was deficient in predicting the correct magnitude of endurance limit stress. The AGMA, Cantilever Plate, and Heywood formulae predicted the rank position correctly in two of the four cases. The Almen-Straub equation predicted the rank position incorrectly in every case.

STRAIN GAGE DATA

The difficulty encountered in placing strain gages in the root of helical gear teeth to accurately measure both maximum strain and strain distribution tends to limit the degree of confidence assigned to conclusions drawn from these data. Figures 65 through 68 show measured strain distribution as predicted by the Cantilever Plate theory for an 8000-pound load applied through the tip of the tooth at the unsupported edge. The theoretical and actual curve shapes are similar. The helical factor used in both the AGMA and the Cantilever Plate bending stress formulae is a proportional modifying factor and need not predict the actual level of stress or stress distribution. Only the ratio of maximum stress produced by tip loading to maximum stress produced by equal loading along the inclined helical load line is necessary.

Table XXIII lists the endurance limit in terms of strain gage data and the endurance limit stress calculated by the various methods. The percent deviation shows the magnitude of difference between the measured and calculated endurance limit stress. The AGMA method produced the lowest average deviation at 5%. The Cantilever Plate method was only slightly higher at 8.5%.

EFFECT OF VARIABLES OF GEAR FATIGUE TESTS

The following studies of the data evaluate the three variables of the gear fatigue test. Derivation of the mathematical model used to determine the S/N curves for each configuration was developed previously, but is repeated briefly in Appendix V.

This method was used to determine the characteristic and fit of the S/N curve for all the fatigue test points, stress curves, and R. R. Moore curves. S/N curves were fitted to the gear tooth fatigue data wit' respect to basic applied load, AGMA calculated stress, and Cantilever Plate calculated stress. The test rig load was used as a base line, since it is not affected by calculations. The Cantilever Plate and AGMA equations were of prime interest, since they were determined to be the best predictive calculation methods.

Pressure Angle	20 Degrees
Helix Angle	20 Degrees
Load	8000 Pounds

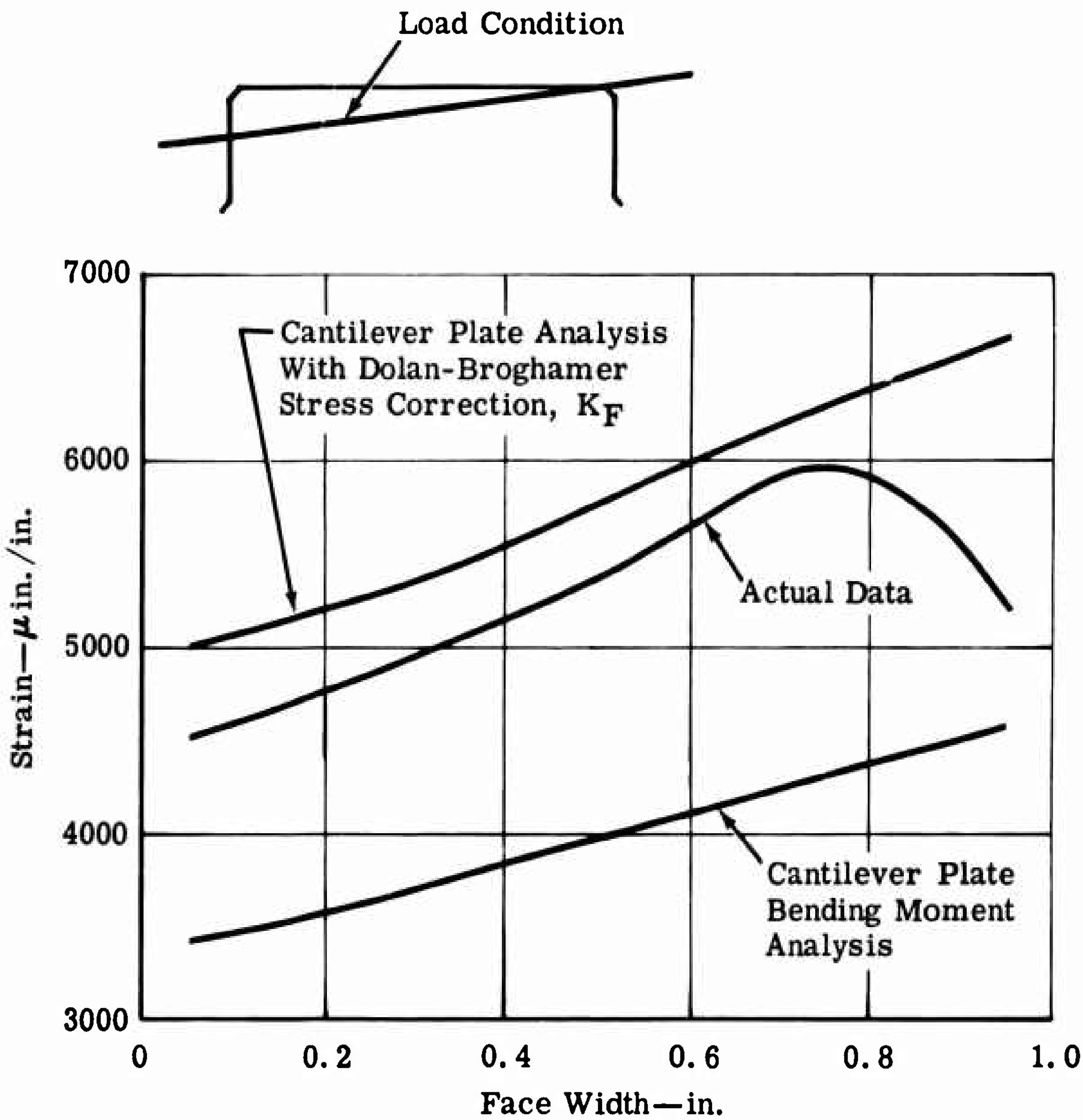

Figure 65. Strain Versus Face Width—EX-84117.

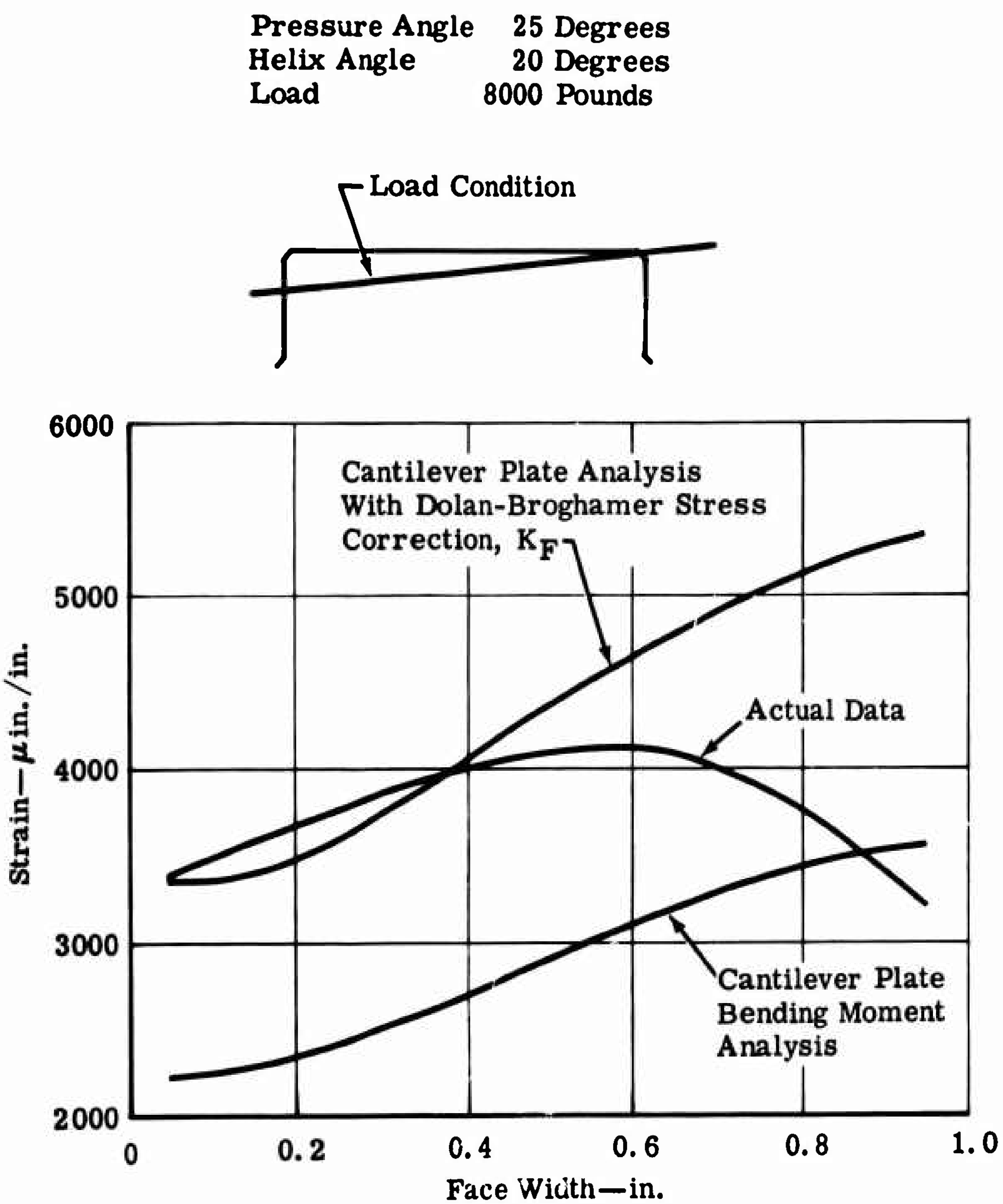

Figure 66. Strain Versus Face Width—EX-84118.

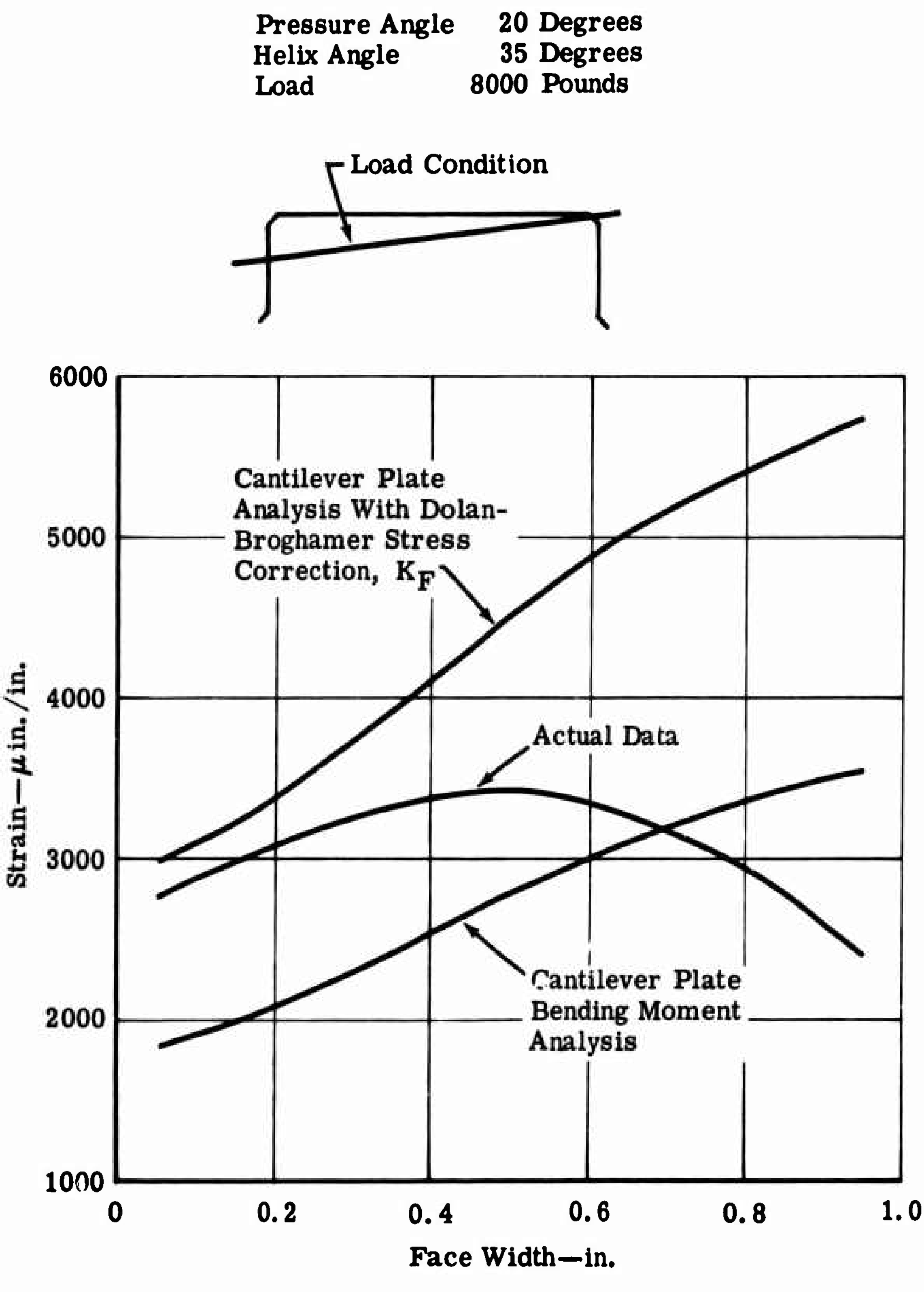

Figure 67. Strain Versus Face Width—EX-84119.

Pressure Angle	25 Degrees
Helix Angle	35 Degrees
Load	8000 Pounds

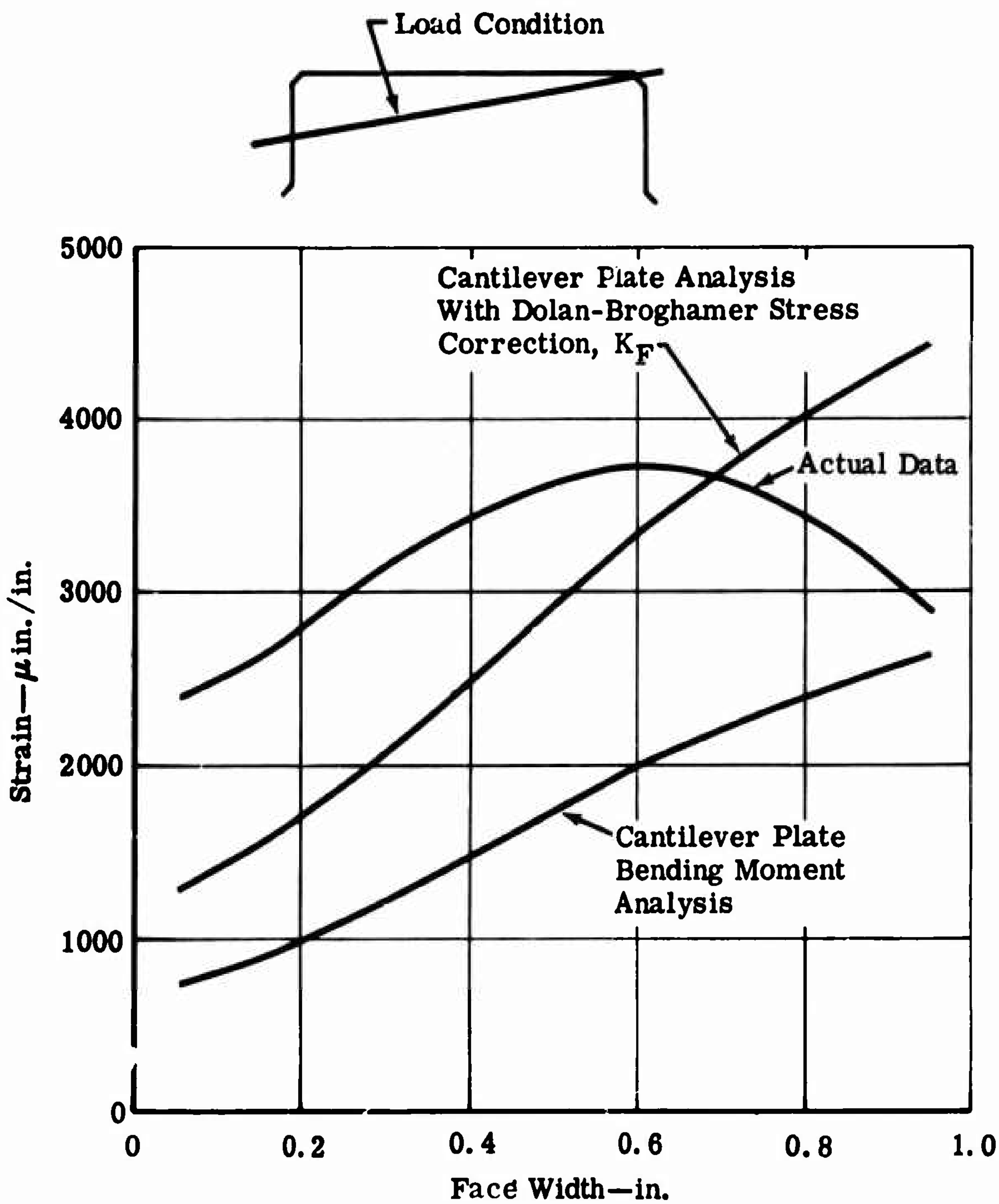

Figure 68. Strain Versus Face Width—EX-84120.

TABLE XXIII. COMPARISON OF CALCULATED AND MEASURED ENDURANCE LIMIT STRESS

		Endurance Limit Stress				
Fatigue Test Gear	Pressure/Helix Angle (Degrees)	Strain Gage	AGMA	Cantilever Plate	Lewis	Almen
EX-84117	20/20	168,000	152,500	160,500	114,264	99,
EX-84118	25/20	135,000	124,696	141,744	104,344	103,
EX-84119	20/35	130,000	182,000	174,665	93,457	136,
EX-84120	25/35	147,000	149,850	152,391	87,435	152,
		145,000	152,261	157,325	99,875	123,

A

RISON OF CALCULATED AND
RED ENDURANCE LIMIT STRESS

	Endurance Limit Stress						Per		
	Strain Gage	AGMA	Cantilever Plate	Lewis	Almen-Straub	Heywood	AGMA	Cantilever Plate	L
	168,000	152,500	160,500	114,264	99,815	206,190	-9.22	-4.5	-
	135,000	124,696	141,744	104,344	103,905	214,119	-7.6	+5	-
	130,000	182,000	174,665	93,457	136,827	237,728	+40	+34.3	-
	147,000	149,850	152,391	87,435	152,548	270,529	+1.9	+3.7	-
	145,000	152,261	157,325	99,875	123,274	232,141	+5.0	+8.5	-

B

		Percent Deviation				
Almen-Straub	Heywood	AGMA	Cantilever Plate	Lewis	Almen-Straub	Heywood
99,815	206,190	-9.22	-4.5	-32	-40.6	+22.7
103,905	214,119	-7.6	+5	-22.7	-23	+58.6
136,827	237,728	+40	+34.3	-28.1	+5.3	+82.9
152,548	270,529	+1.9	+3.7	-40.5	+3.8	+84.0
123,274	232,141	+5.0	+8.5	-31.1	-14.9	+60.1

C

BLANK PAGE

The endurance limits obtained from the S/N curves were used to evaluate each of the two geometric variables and the load position variable and related interactions. A summary of the significant test results is presented in the following paragraphs. The preselected significance level was X = 0.05, which corresponds to a statistical "t" value of 2.0. This level indicates that the result would occur 95 out of 100 times. A discussion of the statistical test of significance is presented in Appendix V.

Load Position

The effect of a change in load position was not found to be significant. None of the stress calculation methods studied consider the effect of load position directly. Stress distribution studies made by actual strain gage measurements and by the Cantilever Plate theory indicated that the area of maximum stress changes from the unsupported tooth end as the load position moves from tip loading at the end to tip loading inboard from the end. This effect was previously shown in Figures 22 through 25. Cantilever Plate theory studies made in an attempt to correlate this effect were inconclusive. Preliminary studies indicated that a change in load position changes the helical factor and the effective face width. Loading through the tooth tip inboard of the end of the tooth shifts the maximum bending moment from one end of the tooth to the other end. This appears to reduce the effectiveness of the total face width in reducing the maximum bending moment in the tooth root. Figures 69 through 72 are bending moment distribution curves showing the effect of removing the unloaded portion of the tooth while loading occurs through the tooth tip 0.250 inch inboard of the end of the tooth. The bending moment distribution curves show that approximately 20 percent of the total face width could be removed without affecting the maximum tooth root bending stress.

In actual operation, the load per unit length of contact line changes, assuming a constant transmitted load and a changing length of contact line. The distributed load (load per unit length of contact line) is maximum when the length of contact line is a minimum. The position of the tooth load line during minimum contact length is dependent on the mating gear. This test did not evaluate the effect of mating gears; however, a study was made to determine the load line position during minimum contact line length for a 1:1 ratio gear set. In every case, the contact line length was a minimum (maximum load) when the load line passed through the tooth tip at the edge of the tooth. More study is needed to accurately determine the effect of load position on gear tooth bending stress.

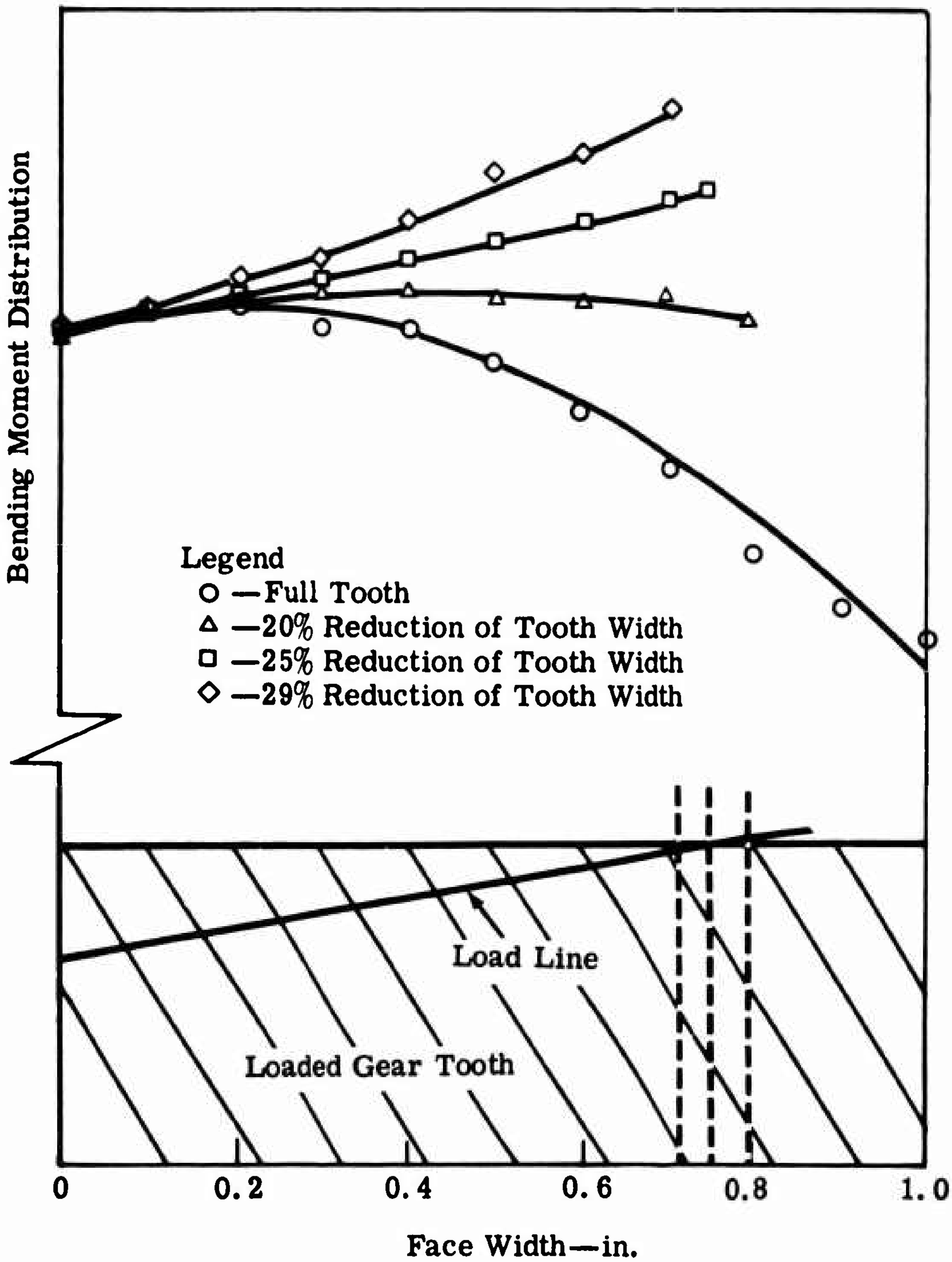

Figure 71. Effect of Face Width on Tooth Root Bending Moment Distribution—Test Gear EX-84119.

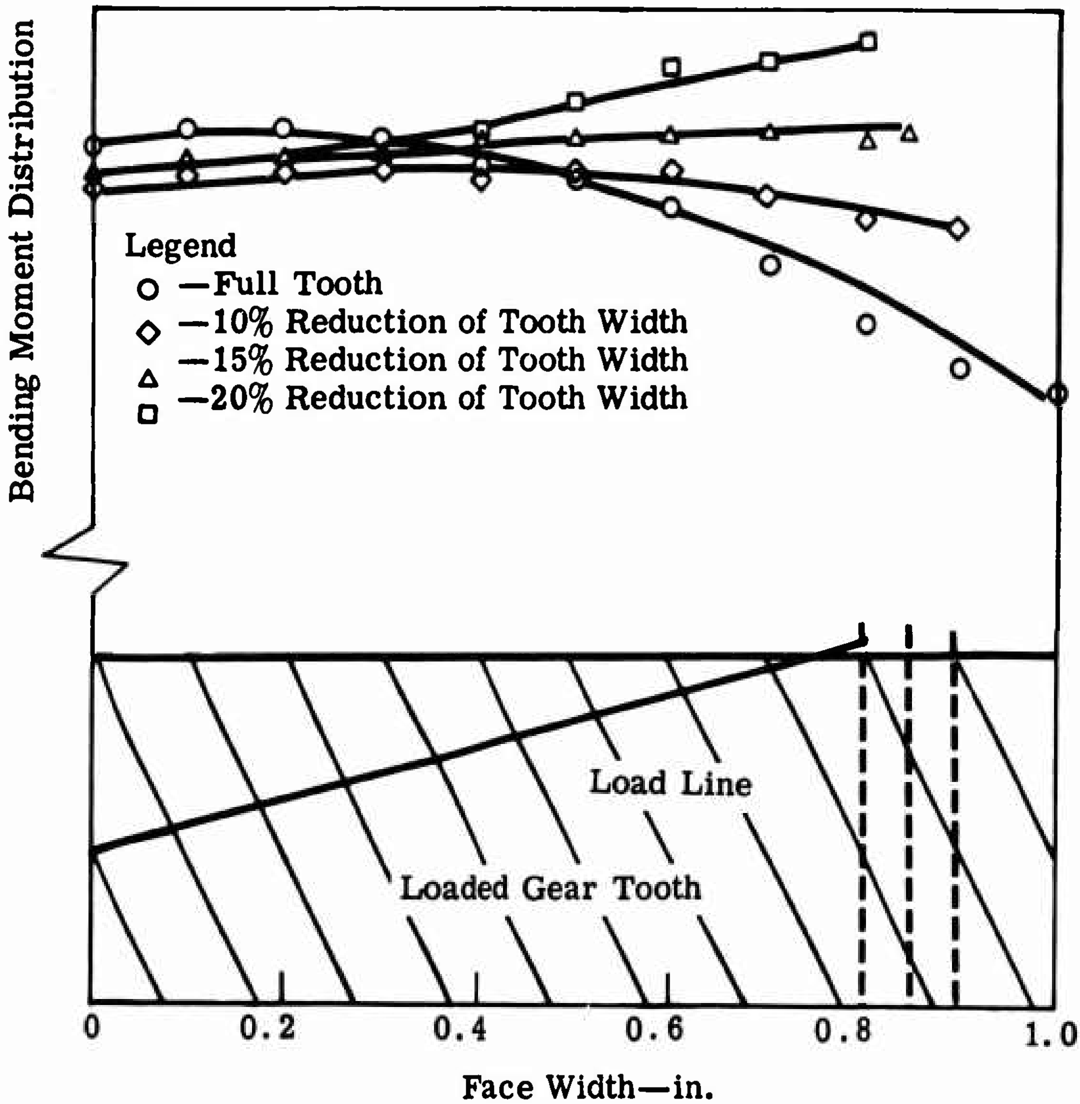

Figure 72. Effect of Face Width on Tooth Root Bending Moment Distribution—Test Gear EX-84120.

Pressure Angle

Based on applied load, a change in pressure angle was found to significantly affect the strength of gear teeth. Table XXIV lists the effect of pressure angle on fatigue strength at a constant helix angle and compares the actual results with the results predicted by the calculation methods.

TABLE XXIV. EFFECT OF PRESSURE ANGLE

Pressure Angle (degrees)	Increase of Actual Fatigue Strength (%)	Predicted Increase of Fatigue Strength (%)	
		AGMA	Cantilever Plate
From 20 to 25	16.5	31	26.5

Both methods predicted that a change in pressure angle would significantly affect the fatigue strength of the gear tooth. The Cantilever Plate theory predicted the degree of significance more accurately.

Helix Angle

Based on applied load, a change in helix angle was found to significantly affect the strength of gear teeth. Table XXV lists the effect of a change in helix angle at constant pressure angle, comparing actual results with the results predicted by the calculation methods.

TABLE XXV. EFFECT OF HELIX ANGLE

Helix Angle (degrees)	Increase of Average Fatigue Strength (%)	Predicted Increase of Fatigue Strength (%)	
		AGMA	Cantilever Plate
From 20 to 25	24.2	5	16

The AGMA method underestimated the significance of the change in helix angle on tooth strength. The Cantilever Plate method predicted the

significance with the greatest accuracy. Neither of the two factor interactions was found to be significant. The AGMA and Cantilever Plate calculation methods did not predict any significant interaction of factors.

The three-factor interaction of pressure angle, helix angle, and load position was found to be significant. This three-factor interaction is highly important in that it supersedes tests of significance for the main effects and two factor interactions. The response, or change in fatigue strength associated with any of the test variables, is dependent on specific values assigned to the other two variables. All three factors are significant, therefore, because of the interrelationships which determine fatigue strength. This load position interaction, however, is not fully understood. Continuing analytical and experimental studies are needed to clarify this relationship. The information used to determine significance is listed in Table XXVI. Table XXVI and Figures 73 and 74 are tabular and graphical representations of the test for significance of factors and interactions.

BASIC MATERIAL STRENGTH

An ideal bending stress calculation would permit direct correlation with the basic material strength. R. R. Moore rotating beam fatigue test data were compared with fatigue gear test data to determine the degree of correlation. The R. R. Moore rotating beam specimens are related to gears as described in the following paragraphs.

Type of Loading

The R. R. Moore S/N curve shown in Figure 75 presents the basic bending strength of the carburized AMS-6265 material of the test gears. The endurance limit of the R. R. Moore bars was slightly lower than the endurance limit established for spur gears during a different test . The two-directional load endurance limit was 128,000 pounds per square inch. This could represent the slight difference between different heats of the same material. The upper line in Figure 75 represents the R. R. Moore fatigue data after correction for one-direction load characteristic of the loading mode used during gear fatigue testing. The corrected endurance limit was 175,000 pounds per square inch. A modified Goodman diagram (Figure 76) was used to correct R. R. Moore fatigue data. Construction and use of the Goodman diagram were established during spur gear testing.[6]

TABLE XXVI. TABULAR PRESENTATION OF SIGNIFICANCE

Pressure Angle (degrees)

	20	25	
$\bar{X}$	7601	8858	't'* = 4.8

Helix Angle (degrees)

	20	35	
$\bar{X}$	7583	9402	't' = 5.4

Load Condition

	1	2	
$\bar{X}$	8177	7891	't' = 1.2

Pressure Angle X Helix Angle

	Pressure Angle (degrees) 20	25	
Helix Angle 20	7308	8094	't' = 1.3
Helix Angle 35	8507	10,691	

Pressure Angle X Load Condition

	Pressure Angle (degrees) 20	25	
Load Condition 1	7679	9022	't' = 1.1
Load Condition 2	7489	8608	

Helix Angle X Load Condition

	Helix Angle (degrees) 20	35	
Load Condition 1	7741	9654	't' = 0.2
Load Condition 2	7321	9132	

Pressure Angle X Helix Angle X Load Position

			Helix Angle (degrees)	Pressure Angle (degrees) 20	25	
Load Condition	1	Helix	20	7302	8,479	't' = 2.5
			35	8936	10,915	
	2	Helix	20	7316	7,329	
			35	7695	10,503	

*A 't' value larger than 2.0 is required for statistical significance.

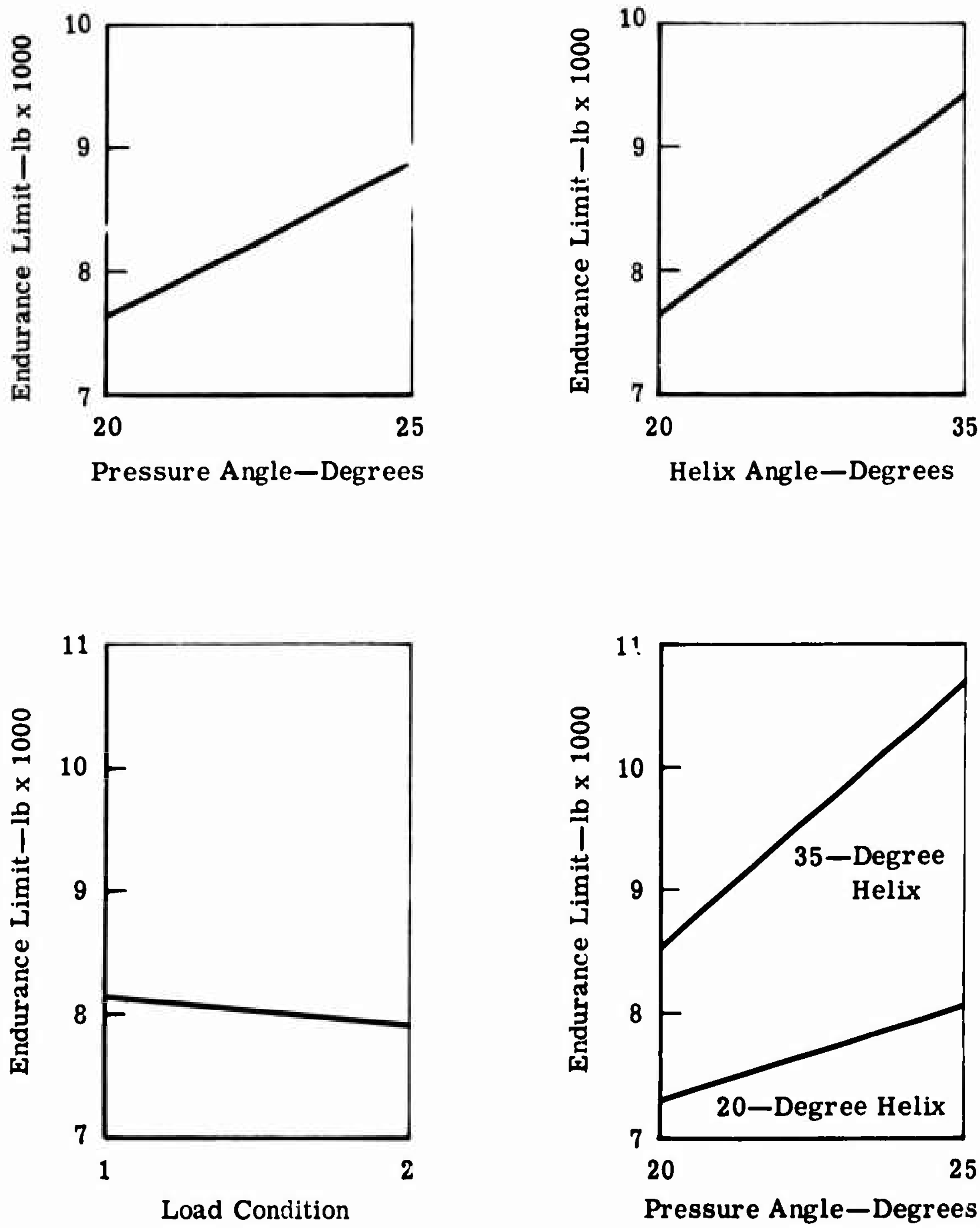

Figure 73. Effect of Test Variables on Endurance Limit.

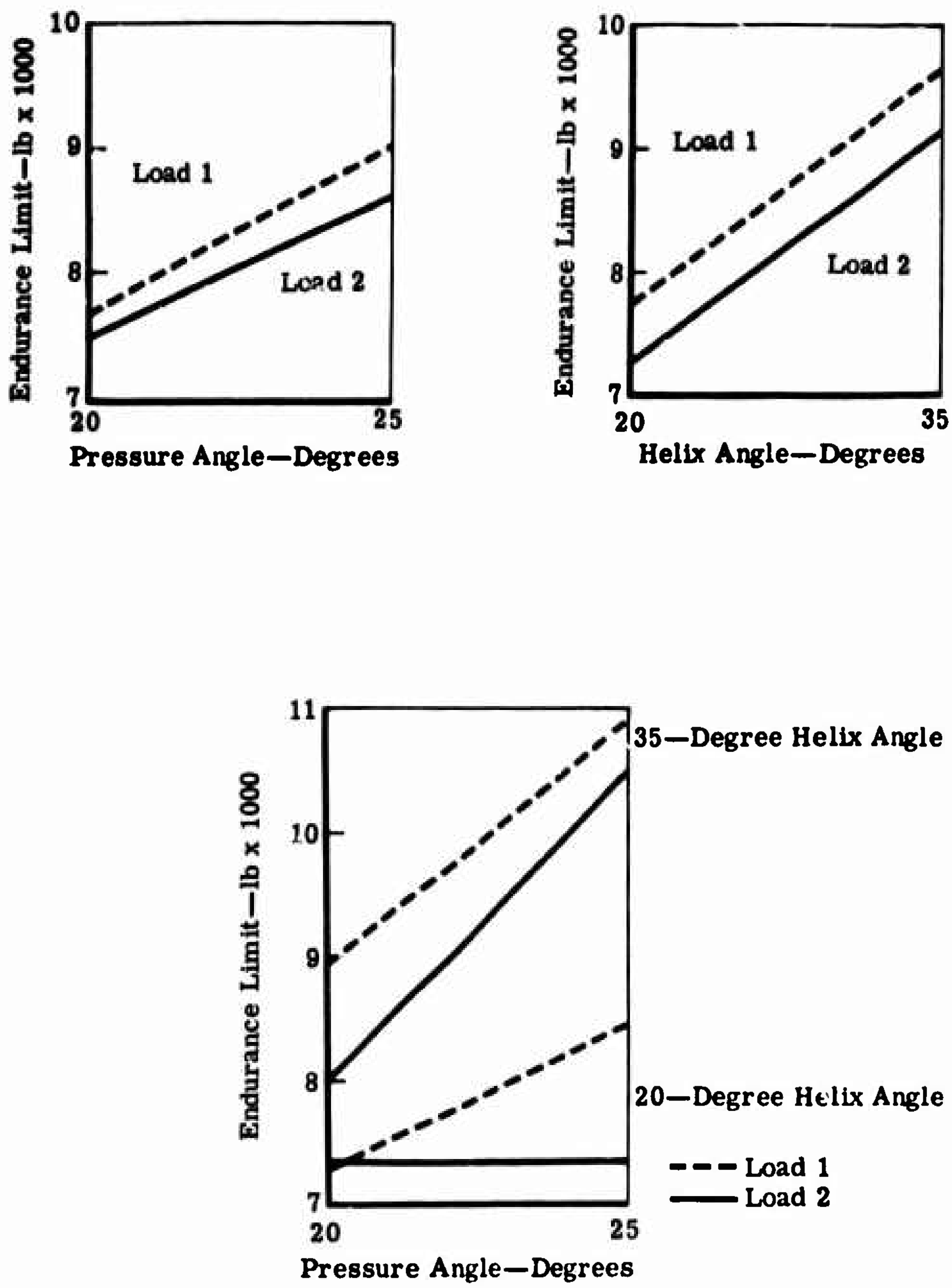

Figure 74. Effect of Test Variables on Endurance Limit.

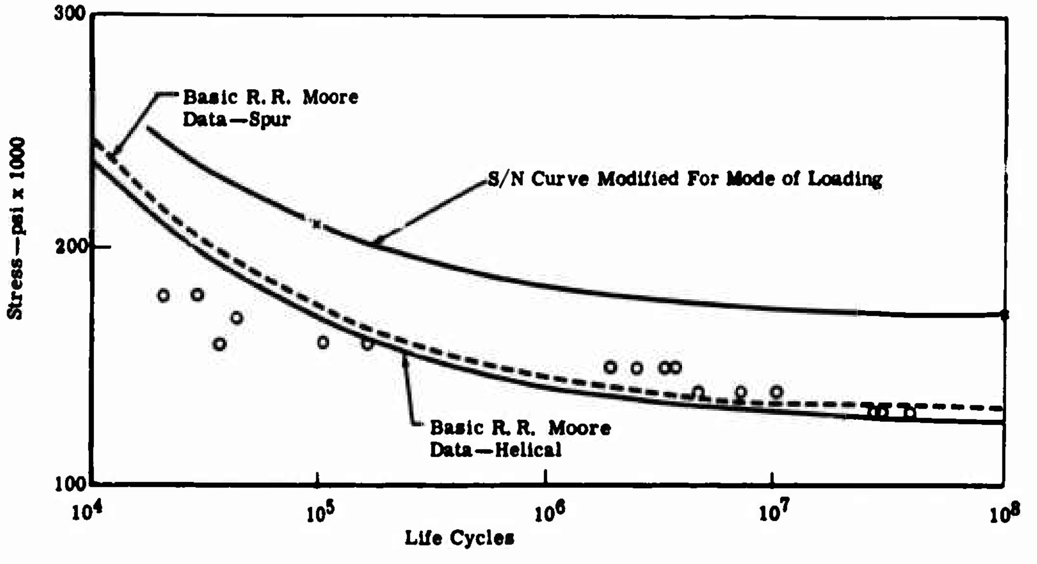

Figure 75. Basic Bending Strength of the Carburized AMS-6265 Material of the Test Gears.

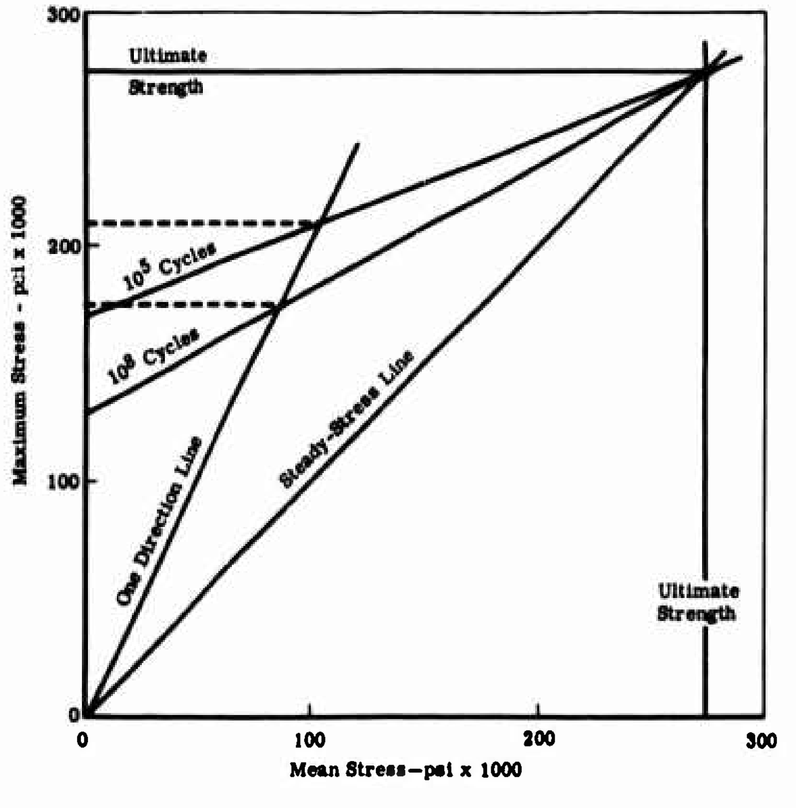

Figure 76. Modified Goodman Diagram.

Size Effect

R. R. Moore standard specimens are 0.250-inch-diameter bars. Generally, for bending, the endurance strength tends to decrease as size increases. To relate the size effect factor to carburized gears, it is recommended that the factor be "one". The literature indicates that the decrease of endurance strength for size is approximately 2 percent for carburized material; however, this effect has not been completely tested.

Surface Effect

R. R. Moore specimens are usually polished. For this analysis, however, the R. R. Moore specimens were ground to the same surface finish as the gear roots; therefore, the surface effect factor is "one". R. R. Moore data from polished samples must be reduced 10 percent.

Stress Concentration

R. R. Moore specimens are considered to have no stress concentration. Most current gear tooth bending stress calculation methods incorporate a stress concentration term based on tooth geometry. Therefore, no further consideration of stress concentration is required.

Reliability

Both R. R. Moore and fatigue test data have been analyzed based on mean endurance strength (50-percent failures) for comparison. Depending on the application, any confidence level may be selected for the gear design.

Surface Treatment

The R. R. Moore samples in this program were carburized, shot peened, and black oxided to the same specifications as the gears. The surface treatment factor, therefore, is one.

All of the previously discussed factors except stress concentration, size effect, and mode of loading are considered as one for this analysis. Therefore, the modified R. R. Moore data, as plotted on the S/N curve of Figure 75, are comparable (within 2 percent) to a calculated stress that incorporates a stress concentration factor.

Figures 77, 78, 79, and 80 show the fatigue data for each gear configuration plotted against AGMA and Cantilever Plate stress. The curves

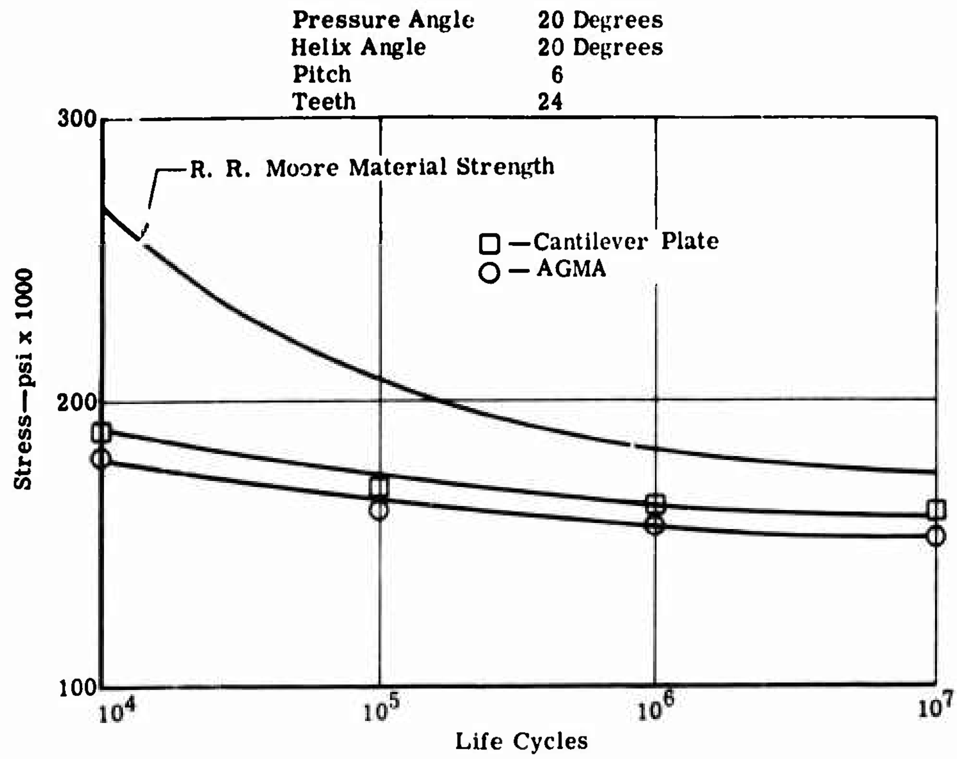

Figure 77. Fatigue Test Data As Calculated Stress—EX-84117.

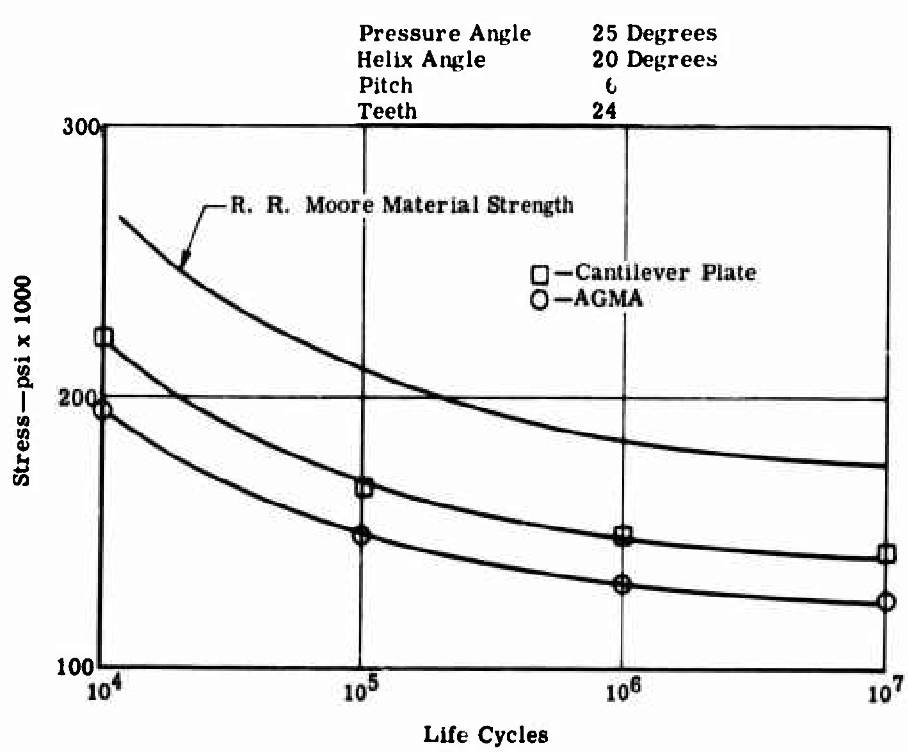

Figure 78. Fatigue Test Data As Calculated Stress—EX-84118.

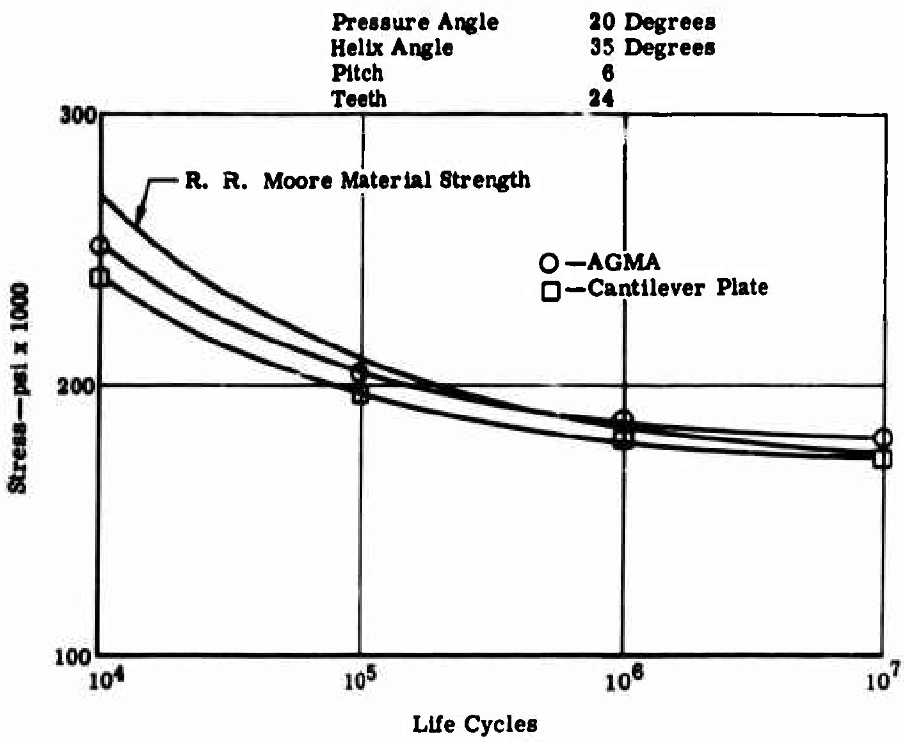

Figure 79. Fatigue Test Data As Calculated Stress—EX-84119.

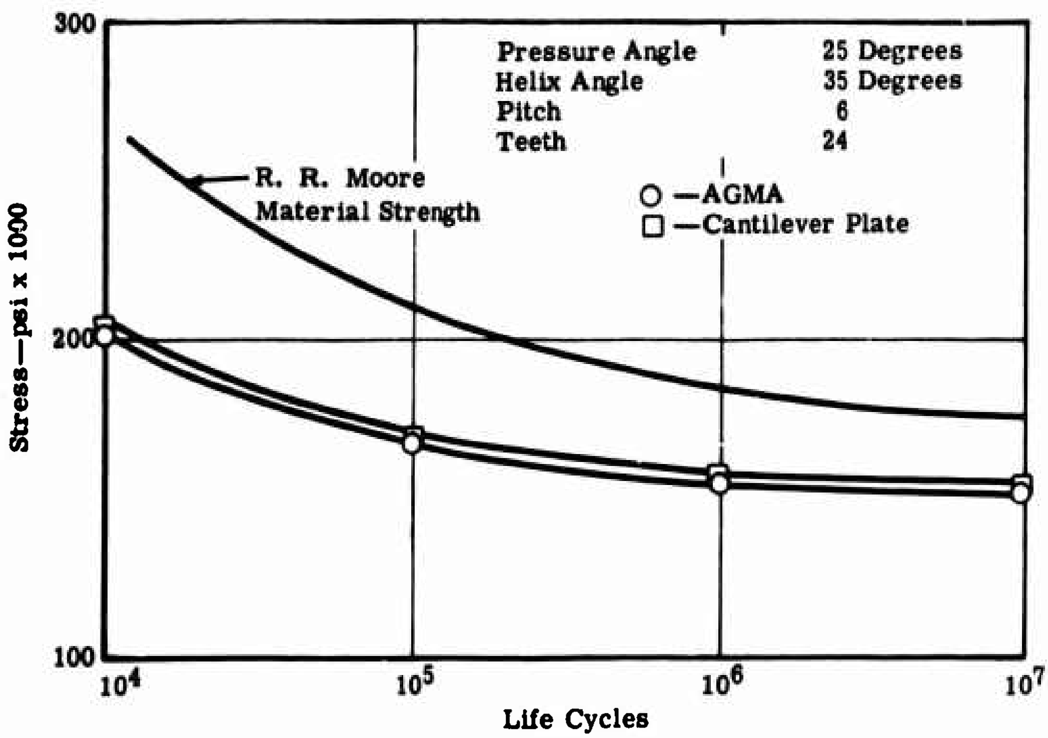

Figure 80. Fatigue Test Data As Calculated Stress—EX-84120.

presented are for the loading condition through the tooth tip at the tooth edge. Superimposed on these curves is the endurance strength line from the modified R. R. Moore data previously developed. It is considered significant that closer correlation is indicated for the Cantilever Plate stress calculation than for the AGMA calculated stress. The only difference between the calculation methods is the manner in which the helical factor, C_H, is used to modify stress. The magnitude of the factor is identical; however, the AGMA formula uses the factor to modify the Lewis tooth form factor, while the Cantilever Plate formula uses the helical factor as a direct modifier of calculated stress. The helical factor is a ratio of maximum bending moments caused by different loading modes; and, since bending moment and stress are directly proportional, it seems logical that the factor developed should be used as a direct modifying factor for stress. It is recommended, therefore, that the AGMA stress calculation method be modified to use the helical factor as a direct stress modifier. Figure 81 is a comparison of the S/N curve generated by averaging the fatigue test data and the basic material strength as determined by R. R. Moore fatigue tests. The stress calculation method used was the modified AGMA or Cantilever Plate.

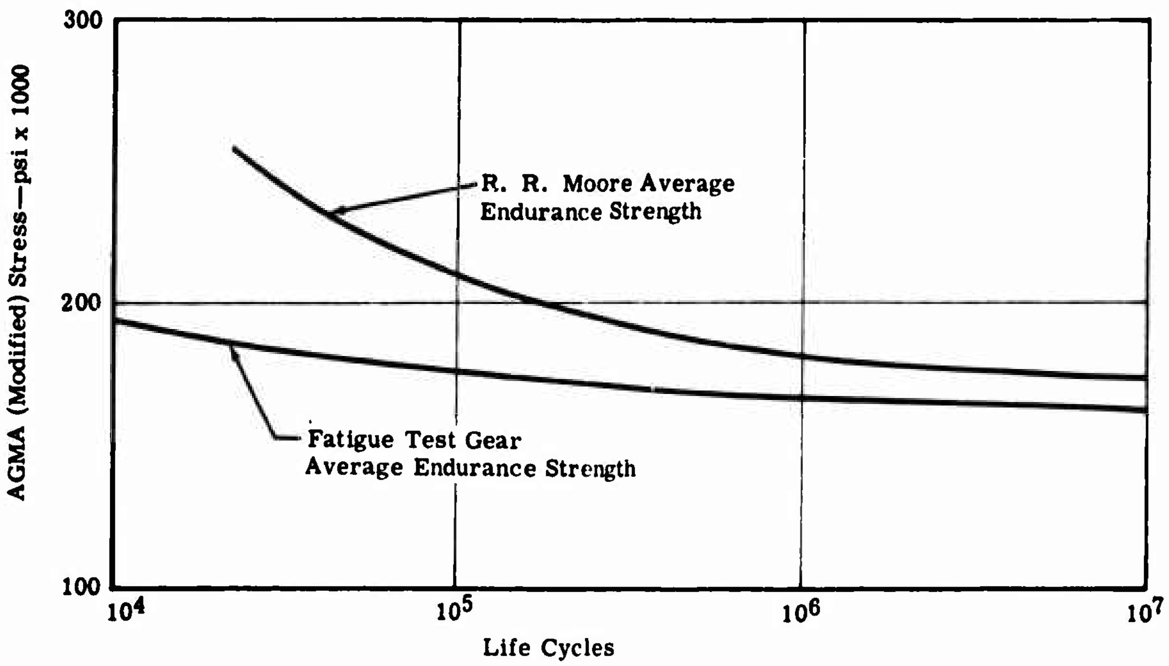

Figure 81. Average Fatigue Endurance Strength Compared With the R. R. Moore Data.

The endurance strength previously listed in Table XXI and shown in Figure 64 was compared to the basic R. R. Moore data. It is apparent that the closest correlation was demonstrated with the Cantilever Plate stress calculation for the gear fatigue tests and the basic strength as determined by the R. R. Moore data. Modification of the AGMA formula, as recommended, would provide the same correlation.

DEVELOPMENT OF DESIGN VALUE

The S/N curve in Figure 81 was obtained from all the fatigue test data taken during tooth loading through the tip at the edge of the tooth. The curve was established by computing the stress equivalent of each data point applied load and plotting against transformed cycles. See Appendix V. The anchor point of the resulting straight line was selected to be 90 percent of the ultimate strength at 1000 cycles. The line was statistically established from the point through the data. The S/N curve established by this method represents a mean or 50 percent failure estimate of the test data. For design purposes, a much lower failure probability is usually required. An endurance limit consistent with such higher reliability was obtained by statistical treatment of the aggregate data.

All data points collected during fatigue testing with the load applied through the tooth tip at the edge for all configurations were considered. The data were transformed as explained in Appendix V and plotted. Figure 82 is a plot of these transformed data. The line was computed using the equation

$$Y - Y_a = \beta (X - X_a) \tag{1}$$

where Y = transformed life cycles
Y_a = 1000 cycles transformed = 1.0
β = slope of line
X = modified AGMA calculated stress for each data point
X_a = 90% (S_u)
S_u = ultimate strength of material

The K factor for a one-sided tolerance limit at a probability P = 0.99 and a confidence of 95 percent was obtained from statistical tables. The K factor was 2.994. The 1 percent endurance limit was

$$L.\ L. = E.\ L. - K \sigma_X \tag{2}$$

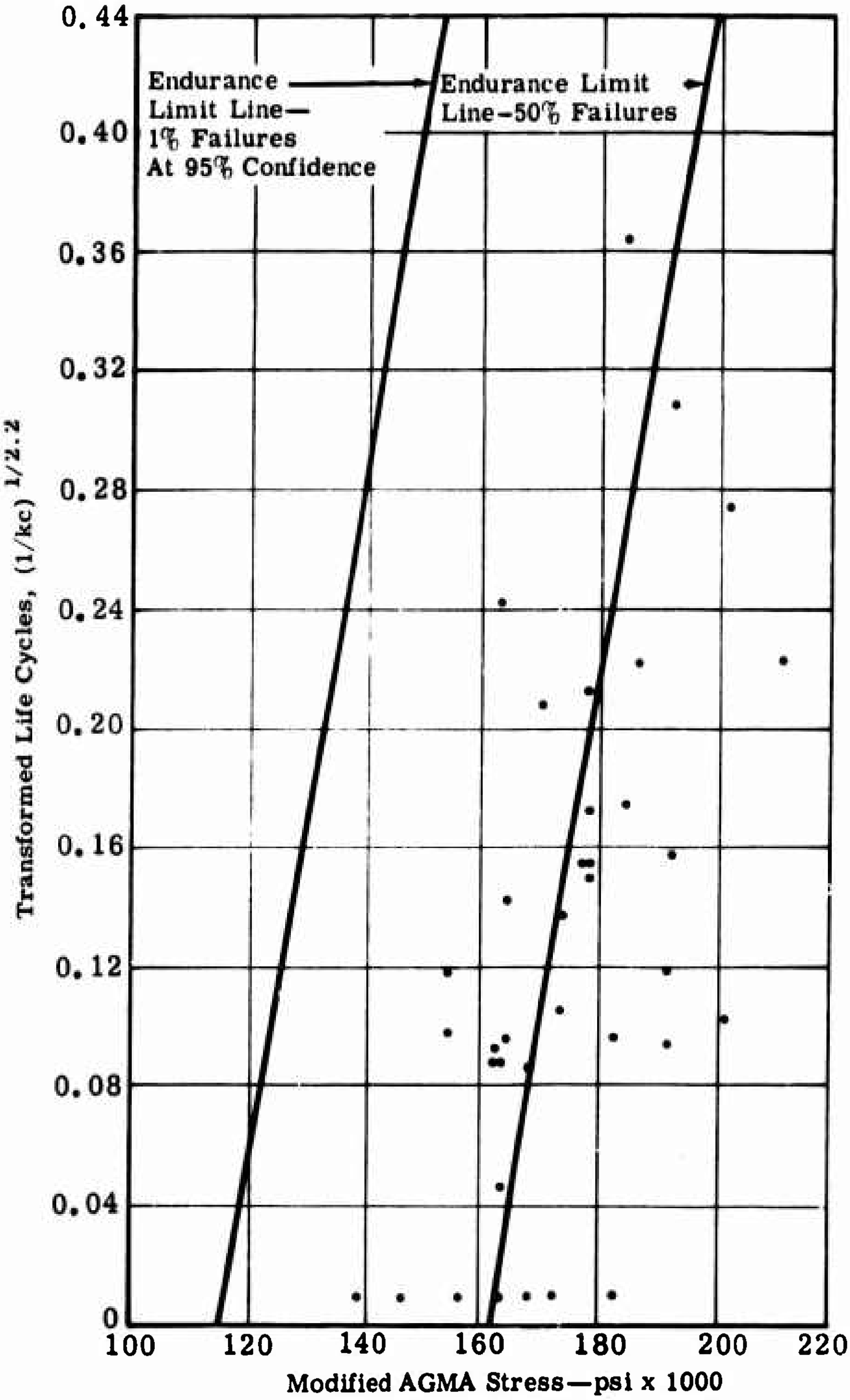

Figure 82. Transformed Fatigue Test Data—Modified AGMA Stress Versus Transformed Life.

where L. L. = 161,564 - (2.994) (15,380)
L. L. = 115,517
L. L. = lower tolerance limit
E. L. = endurance limit
K = probability factor
σ_X = standard X deviation

The probability statement can be made that there is 95 percent confidence that at least 99 percent of the endurance limits of gears will be greater than 115,500 pounds per square inch.

The S/N curves representing the overall average and a tolerance representing 1 percent failure at 95 percent confidence are shown in Figure 83. Using the 1 percent line as a design value, it is estimated that 1 percent of the gear teeth will experience failure in bending. This statement is restricted by the range of variables investigated, the significant effect of the geometric factors, and the limited knowledge relating failure of a single tooth to the probability of failure of one or more teeth on a gear.

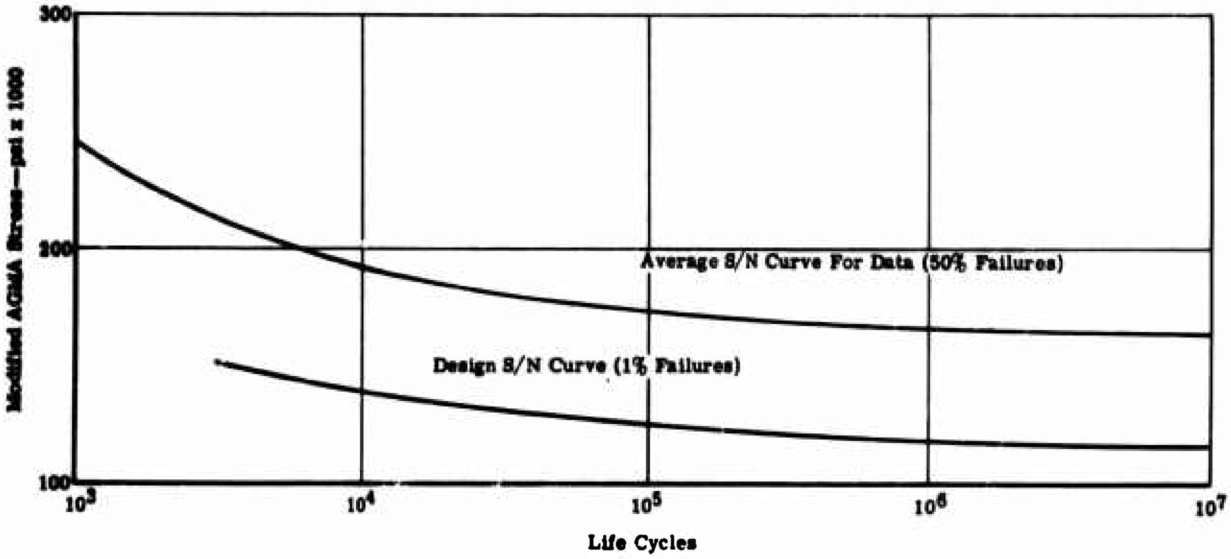

Figure 83. Modified AGMA Average S/N Curve and Design Value.

In general, the failure probability for any gear is dependent on the number of teeth on the gear in addition to strength properties and applied stress. The situation is analogous to the "weakest link" problem associated with chain strength—chain strength decreases as the number of links increase. The same phenomenological considerations apply to gears. With acknowledgement that the same problem exists with gears, it is recommended that additional theoretical research be undertaken in the field of applied order statistics to estimate gear failure probabilities based on the data existing for single tooth fatigue failures. The results of this program would be directly applicable to spur and helical gears.

EVALUATION OF DYNAMIC EFFECTS

Centrifugal Stress

Centrifugal stress consists of two major components: hoop stress and radial stress due to the centrifugal force on the gear tooth. The hoop stress is a circumferential (tangential) tensile stress at the root diameter caused by the tendency of the gear ring to expand under the influence of centrifugal force. The radial stress is caused by centrifugal force acting on each individual tooth.

Hoop stress was calculated for both a uniform circular ring and a hollow cylinder using the following equations:

- Uniform Circular Ring

$$S_h = \frac{\rho V^2}{g} \tag{3}$$

where ρ = material density, pound per cubic inch
V = rim velocity, inch per second
g = gravitational constant, 386.4 inches per square second

- Hollow Cylinder

$$S_h = \frac{\rho R_R^4 V^2}{4\,g}\left[(1-\mu) + \left(\frac{R_i}{R_R}\right)^2 (3+\mu)\right] \tag{4}$$

where ρ = material density, pound per cubic inch
R_R = gear root radius, inch
R_i = radius of gear bore
V = velocity at the root radius, inch per second
g = gravitational constant, 386.4 inches per square second
μ = Poisson's constant

The hoop stress calculated for a circular ring was approximately 10 percent higher than the stress calculated for a hollow cylinder. The gear used approximates a hollow cylinder much more closely than a circular ring. However, the circular ring hoop stress calculation was used to calculate hoop stress in the computer program for two reasons. First, the gear used for the dynamic test had a face width-to-pitch diameter ratio of approximately one. Most gears have a much lower ratio and, consequently, more closely approach a circular ring in proportion. Second, use of the circular ring formula for hoop stress is conservative.

The maximum measured centrifugal stress was found to be only slightly higher than the calculated centrifugal force stress. This suggests that the hoop stress calculated did not significantly affect the stress level measured in the tooth flank at the assumed weakest section. Figure 84 shows a comparison of calculated centrifugal force stress, calculated hoop stress, and measured maximum centrifugal stress.

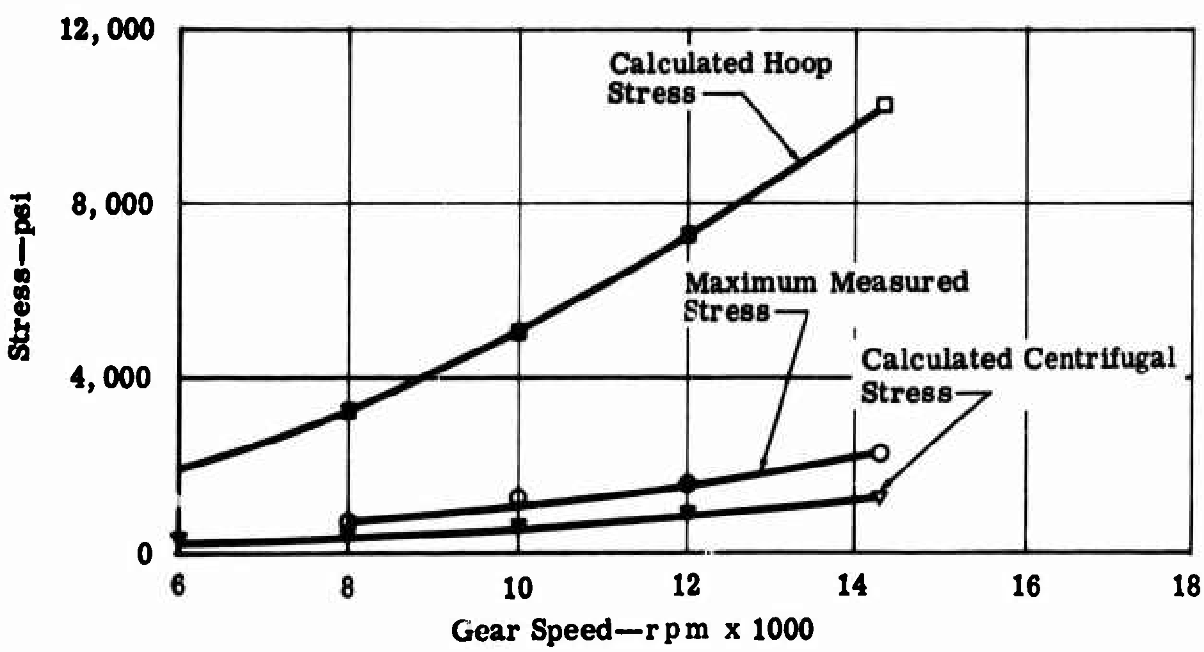

Figure 84. Comparison of Calculated and Measured Gear Stresses.

A detailed study of all the possible effects of gear tooth geometries and/or proportions on centrifugal stress was not made. The similarity of the hoop stress and centrifugal force formulae, both of which vary with the square of the speed, and the similarity of normal gear tooth geometry (unit diametral pitch rule) suggest that the observed proportional values should remain essentially constant. Design use of the calculated hoop stress should be conservative.

A modified Goodman diagram was used to combine the steady-state centrifugal stress (at constant speed) with the alternating bending stress (Figure 76). The S/N curve developed from the R. R. Moore fatigue test program was used at the zero centrifugal stress ordinate to construct the modified Goodman diagram. The Goodman diagram may be used to determine the endurance strength required for the bending stress calculation given a desired life, speed, and gear size.

For example, the dynamic test gear when operating at 14,300 r.p.m. has a calculated hoop stress of 10,100 pounds per square inch. For 10^7 cycle life, a bending stress of 170,000 pounds per square inch would be permitted based on a modified Goodman diagram. Based on direct addition of the centrifugal and bending stress, the S/N curve would permit only 165,000 pounds per square inch bending stress. To calculate a more comprehensive gear tooth bending stress under high speed operating conditions, the centrifugal hoop stress must be combined with bending stress by using a modified Goodman diagram.

Dynamic Stress

Figure 85 is a plot of the average dynamic stress versus speed. The strain readings were converted to stress and plotted against speed at constant torque loading. The measured dynamic stress does not include any centrifugal stress. Figure 86 shows a dynamic stress correction factor derived from the curve in Figure 87. The dynamic factor plotted is a ratio of gear tooth bending stress at zero speed to the gear tooth bending stress during rotation at constant torque.

Figure 88 is a comparison of the previously discussed dynamic factor with the AGMA dynamic factor (Appendix IV) for grade one gears and the dynamic factor developed during spur gear testing.[6] It can be seen that the dynamic factor developed during this test is in agreement with the value given in Appendix V up to 8000 feet per minute pitch line velocity. This test extends the factor to 20,000 feet per minute pitch line velocity.

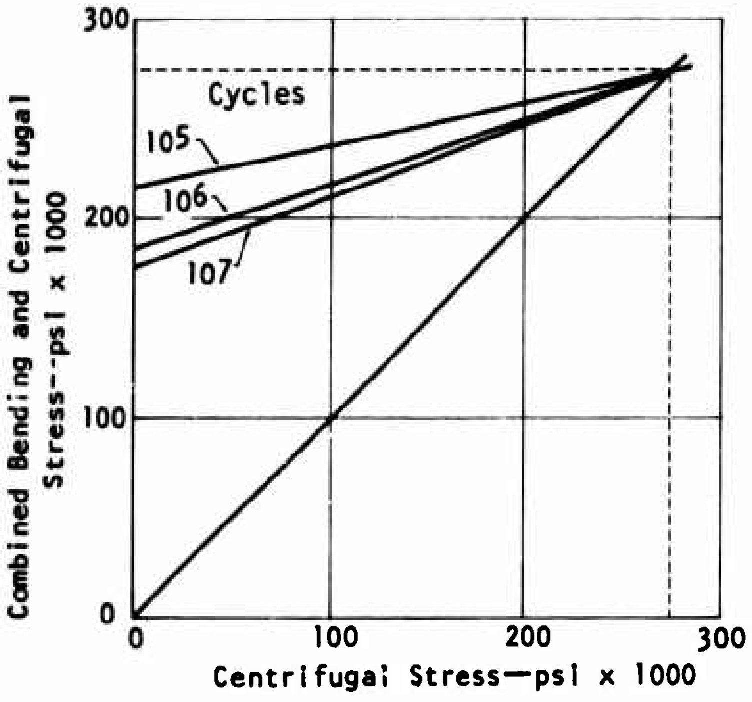

Figure 85. Average Dynamic Stress Versus Speed.

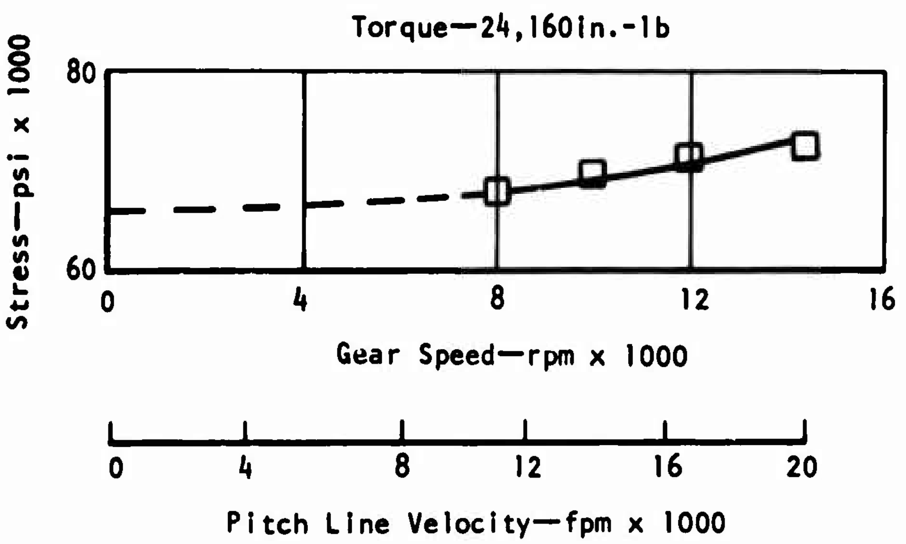

Figure 86. Average Bending Stress Versus Gear Speed at Constant Load.

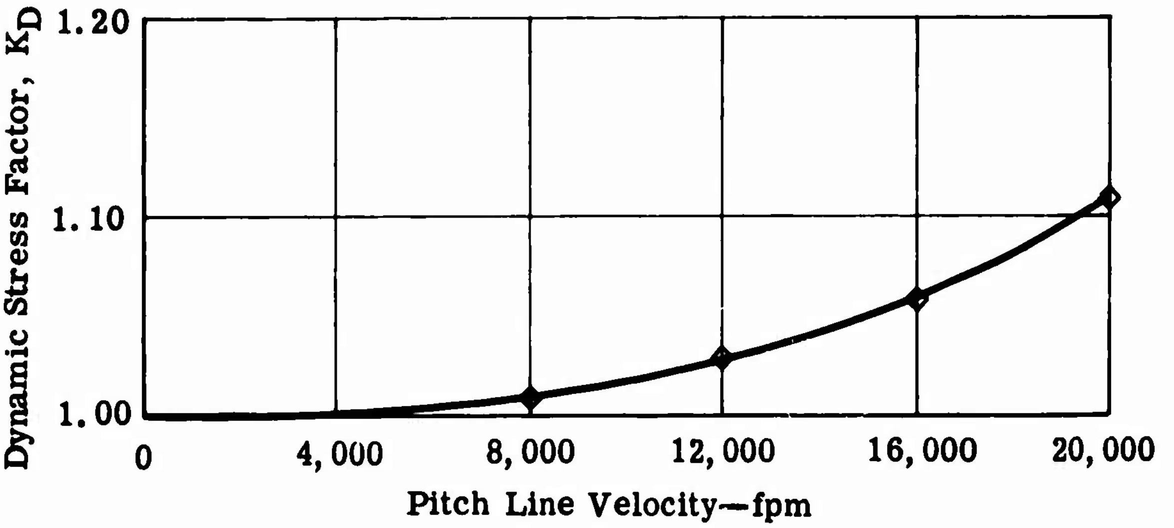

Figure 87. Dynamic Stress Factor As a Function of Pitch Line Velocity.

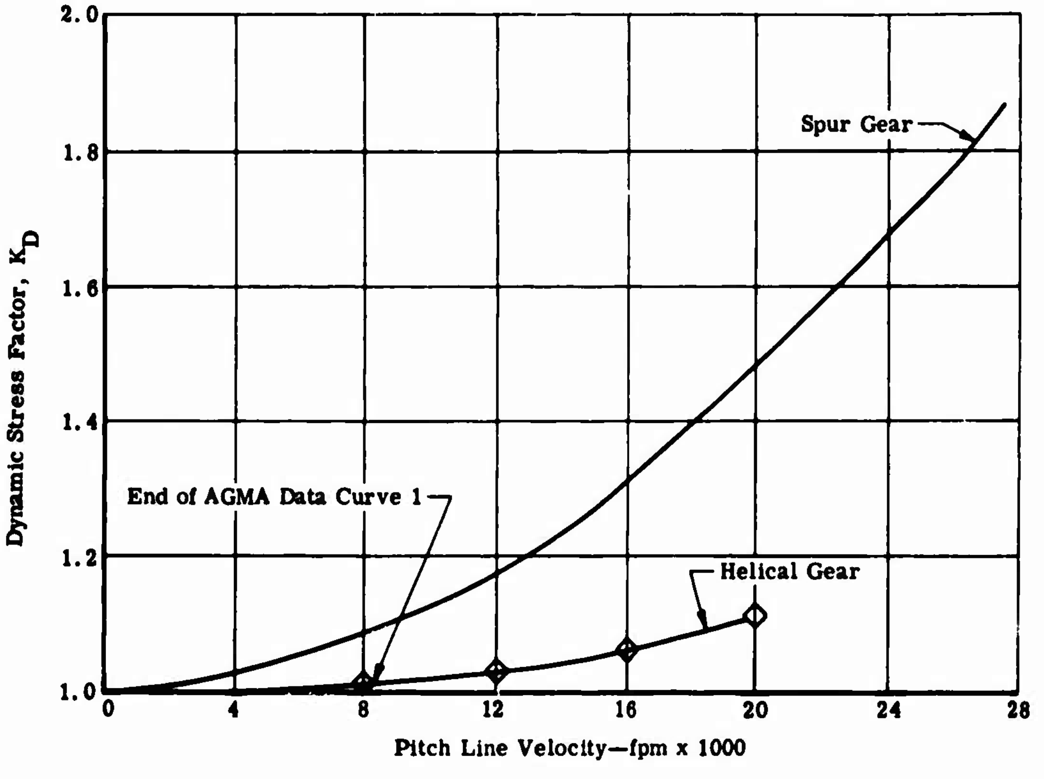

Figure 88. Comparison of Dynamic Stress Factors.

The magnitude of the dynamic factor developed for helical gears is significantly different from that developed for spur gears. The spur gear used to develop the dynamic factor was a thin webbed gear operating in a multiple gear, gear train. Therefore, it would be more subject to torsional vibrations and resonances. The helical gear used was a short, heavy, webbed gear operating in a single-stage reduction unit. This shape, in conjunction with the inherently higher overlap ratio (load sharing) available with helical gearing, should combine to reduce the dynamic effect on bending stress considerably. The dynamic factor curve (Figure 88) shown may represent the design limits that should be observed. Further definition of the dynamic factor will require an extensive program to define the effect of overlap ratio, gear geometry, rim-web proportions, etc. Although the dynamic data presented are limited, they do indicate trends for high speed helical gearing. It is recommended, therefore, that Figure 88 be used to extend the AGMA dynamic factor curve from 8000 to 20, 000 feet per minute.

ESTABLISHMENT OF COMPUTER PROGRAM

Analysis of the fatigue test data indicates that the Cantilever Plate formula produces the least variation in calculated endurance limits, reasonably predicts the actual tooth root stress, and accommodates the effect of the geometric variables with reasonable accuracy. Analysis of the AGMA and Cantilever Plate calculation methods showed that the only difference between the two methods was in the use of the helical modifying factor; however, the absolute value of the factor is the same in both formulae. It is therefore recommended that the AGMA formula be modified so that the helical factor is used to modify stress directly rather than used to modify the magnitude of the tooth form factor. The form of the modified AGMA formula would be

$$S_b = \frac{1}{C_H} \frac{W_t}{F} \frac{P_{DX}}{J} \tag{5}$$

where S_b = bending stress
C_H = helical factor—ratio of the maximum bending moment caused by tip loading to the maximum bending moment produced by equal intensity loading along the inclined load line
W_t = transmitted tangential load
P_{DX} = transverse diametral pitch
F = net face width
J = geometry factor

$$J = \frac{Y \cos^2\psi}{K_f\ m_n} \tag{6}$$

where Y = tooth form factor = $\dfrac{1.0}{\dfrac{\cos \phi_{Ln}}{\cos \phi_n}\left[\dfrac{1.5}{X} - \dfrac{\tan \theta_{Ln}}{t}\right]}$

(See Appendix V for definition of terms)

The geometry factor is established in the transverse plane for the specific tooth geometry under consideration. The computer program does not require a consideration of a virtual equivalent spur gear at one diametral pitch to establish the geometry factor. The Lewis inscribed parabola for tip loading is used to establish the location of the weakest section of the actual tooth. Computer calculation of the geometry factor should be more accurate than the values obtained from graphical layouts.

Inclusion of the helical factor in the AGMA formula requires accurate determination of the helical factor to produce an accurate calculated stress. The helical factor for the narrow face width gears used in this test varied from the value given in Figure A-3 of AGMA 221.02 (Appendix V) by as much as 12 percent. Accordingly, the computer program incorporates a subroutine to calculate the helical factor. The subroutine calculates the helical factor by the principle of superposition of the moment-image Cantilever Plate bending moment distribution curves as proposed by Wellauer and Seirig.[1] Use of the subroutine to calculate the helical factor eliminates the need for total reliance on the AGMA helical factor graph, and also eliminates the need for a time-consuming graphical analysis to determine the helical factor.

A dynamic factor is an input item of the computer program. The dynamic factor for a given application may be obtained from existing AGMA curves, the curve presented in Figure 88, literature sources, or from direct "in-house" measurements.

Hoop stress is calculated in the program and combined with the AGMA calculated bending stress based on the modified Goodman diagram. A mathematical expression for the combined stress is

$$S_c = US - \frac{US\left[US - (S_h - S_t)\right]}{US - S_h} \tag{7}$$

where S_c = combined stress, psi
S_h = hoop stress, psi (Equation 3)
S_t = tensile stress (AGMA), psi (Table II)
US = ultimate strength of the material, psi

Life cycles are then determined from the combined stress and the S/N curve based on R. R. Moore rotating beam tests of the gear material. The life may be modified further by the AGMA temperature factor and reliability factor (factor of safety) as indicated by the expression

$$L = f\,(S_c\, K_T\, K_R)$$

where L = life, cycles
S_c = combined stress, psi
K_T = AGMA temperature factor (Table II)
K_R = AGMA factor of safety (Table II)

Both AGMA bending stress and the combined bending and hoop stresses are printed out. Life is printed out if it is in the finite life area of the modified Goodman diagram; otherwise, an infinite life or an excessive stress note is printed.

CONCLUSIONS

The following conclusions are made from this study:

- A modified form of AGMA Standard 221.02 was found to provide accurate correlation with the actual material strength. The modification consisted of utilizing the helical factor, C_H, as a direct stress modifier rather than as a tooth form factor operator.
- A basic material strength curve for carburized AMS-6265 was established by R. R. Moore specimens. This strength curve correlated with the stress which was calculated by the modified AGMA bending stress formula.
- A design S/N curve was established. For design purposes, a 1-percent failure endurance strength of 115,000 pounds per square inch was statistically established.
- A curve of dynamic factor versus pitch line velocity was developed for applications to 20,000 feet per minute pitch line velocity.
- A centrifugal speed factor is necessary for high pitch line velocity applications and is included in the final computer program (Appendix III).
- The investigation of two geometric variables and tooth load positions indicated that the endurance strength was significantly affected by changes in pressure and helix angles. These changes were accurately predicated by the AGMA formula.
- The AGMA formula modified to use the helical factor as a direct stress modifier, to incorporate a centrifugal speed effect, to incorporate a dynamic factor for high speed applications, and to use established R. R. Moore fatigue strength data will produce an accurate estimate of gear tooth bending stress and life. The dynamic fluctuating stress calculated by the modified AGMA formula,

$$S_t = \frac{1}{C_H} \frac{W_t K_o}{K_v} \frac{P_a}{F} \frac{K_s K_m K_f M_n}{Y \cos^2 \psi},$$

is combined with the steady centrifugal hoop stress formula, $S_h = \rho \frac{V^2}{g}$, to produce a combined stress, S_c,

$$S_c = US - \frac{US \left[US - (S_h + S_t) \right]}{US - S_h} \tag{8}$$

The terms are defined in Equation 7. Life cycles may then be determined from an S/N curve based on R. R. Moore rotating beam fatigue tests of the gear material. The life may be modified by the AGMA temperature and reliability factors as

$$L = f\,(S_c\;K_t\;K_r) \qquad (9)$$

LITERATURE CITED

1. Wellauer, E. J., and Seireg, A., BENDING STRENGTH OF GEAR TEETH BY CANTILEVER PLATE THEORY, Journal of Engineering for Industry, Vol 82, Series B, No. 3, Transaction of the ASME, August 1960, pp 213-221.

2. MacGregor, C. W., DEFLECTION OF A LONG HELICAL GEAR TOOTH, Mechanical Engineering, Vol 57, 1935, pp 225-227.

3. Holl, D. L., CANTILEVER PLATE WITH CONCENTRATED EDGE LOAD, Journal of Applied Mechanics, Vol 4, No. 1, Transactions of the ASME, 1937, pp A-8-10.

4. Jaramillo, T. J., DEFLECTIONS AND MOMENTS DUE TO A CONCENTRATED LOAD ON A CANTILEVER PLATE OF INFINITE LENGTH, Journal of Applied Mechanics, Vol 17, No. 1, Transactions of the ASME, March 1950, pp 67-72.

5. Almen, J. O., and Straub, J. C., FACTORS INFLUENCING THE DURABILITY OF AUTOMOBILE TRANSMISSION GEARS—PART 2, Automotive Industries, 9 October 1937, pp 488-493.

6. McIntire, W. L., and Malott, R. C., ADVANCEMENT OF SPUR GEAR DESIGN TECHNOLOGY, Allison Division, General Motors, USAAVLABS Technical Report 66-85, U. S. Army Aviation Materiel Laboratories, Fort Eustis, Virginia, December 1966, AD 646648.

7. Dolan, T. J., and Broghamer, E. L., A PHOTOELASTIC STUDY OF STRESSES IN GEAR TOOTH FILLETS, Bulletin Series Number 335, University of Illinois Engineering Experiment Station, Urbana, Illinois, 1942.

8. Cummins, H. N., Stulen, F. B., and Schulte, W. C., INVESTIGATION OF MATERIALS FATIGUE PROBLEMS APPLICABLE TO PROPELLER DESIGN, WADC Technical Report 54-531, Wright-Patterson Air Force Base, Dayton, Ohio, 1954, p 29.

9. Davies, O. L., et al, STATISTICAL METHODS IN RESEARCH AND PRODUCTION, Third Edition, New York, Hafner Publishing Company, 1958.

SELECTED BIBLIOGRAPHY

1. Bennett, C. A., and Franklin, N. L., STATISTICAL ANALYSIS IN CHEMISTRY AND THE CHEMICAL INDUSTRY, First Edition, New York, John Wiley and Sons, Incorporated, 1954.

2. Buckingham, E., ANALYTICAL MECHANICS OF GEARS, First Edition, Second Impression, New York, McGraw-Hill Book Company, Incorporated, 1949.

3. Buckingham, E., MANUAL OF GEAR DESIGN, Volumes 1, 2, and 3, New York, Industrial Press, 1955.

4. Buckingham, E., SPUR GEARS—DESIGN, OPERATION, AND PRODUCTION, First Edition, Ninth Impression, New York, McGraw-Hill Book Company, Incorporated, 1928.

5. Cochram, W. G., and Cox, G. M., EXPERIMENTAL DESIGNS, Second Edition, New York, John Wiley and Son, Incorporated, 1960.

6. Dudley, D. W., GEAR HANDBOOK, First Edition, New York, McGraw-Hill Book Company, Incorporated, 1962.

7. Dudley, D. W., PRACTICAL GEAR DESIGN, First Edition, New York, McGraw-Hill Book Company, Incorporated, 1954.

8. Hald, A., STATISTICAL THEORY WITH ENGINEERING APPLICATIONS, First Edition, New York, John Wiley and Sons, Incorporated, 1957.

9. Lewis, W., INVESTIGATION OF THE STRENGTH OF GEAR TEETH, Proceedings of the Engineering Club of Philadelphia, 1893, X, 1.

10. Ostle, B., STATISTICS IN RESEARCH, First Edition, Ames, Iowa, Iowa State University Press, 1956.

11. Thoma, F. A., THE LOAD DISTRIBUTION FACTOR AS APPLIED TO HIGH SPEED AND WIDE FACE HELICAL GEARS, American Gear Manufacturers Association Paper 229.10, October 1965.

12. Wellauer, E. J., AN ANALYSIS OF FACTORS USED FOR STRENGTH RATING HELICAL GEARS, Journal of Engineering for Industry, August 1960, pp 205-212.

13. Wellauer, E. J., THE NATURE OF THE HELICAL GEAR OBLIQUE CONTACT LINE, Reprint from Industrial Mathematics, Volume II, Part 2.

14. Wellauer, E. J., HELICAL AND HERRINGBONE GEAR TOOTH DURABILITY—DERIVATION OF CAPACITY AND RATING FORMULAS, American Gear Manufacturers Association Paper 229.06, June 1962.

APPENDIX I

FATIGUE TEST GEAR DRAWINGS

This appendix consists of the fatigue test gear drawings for the four configurations tested. These drawings are shown in Figures 89 through 92. The helical gear propeller reduction drive pinion and propeller drive gear are shown in Figures 93 and 94, respectively.

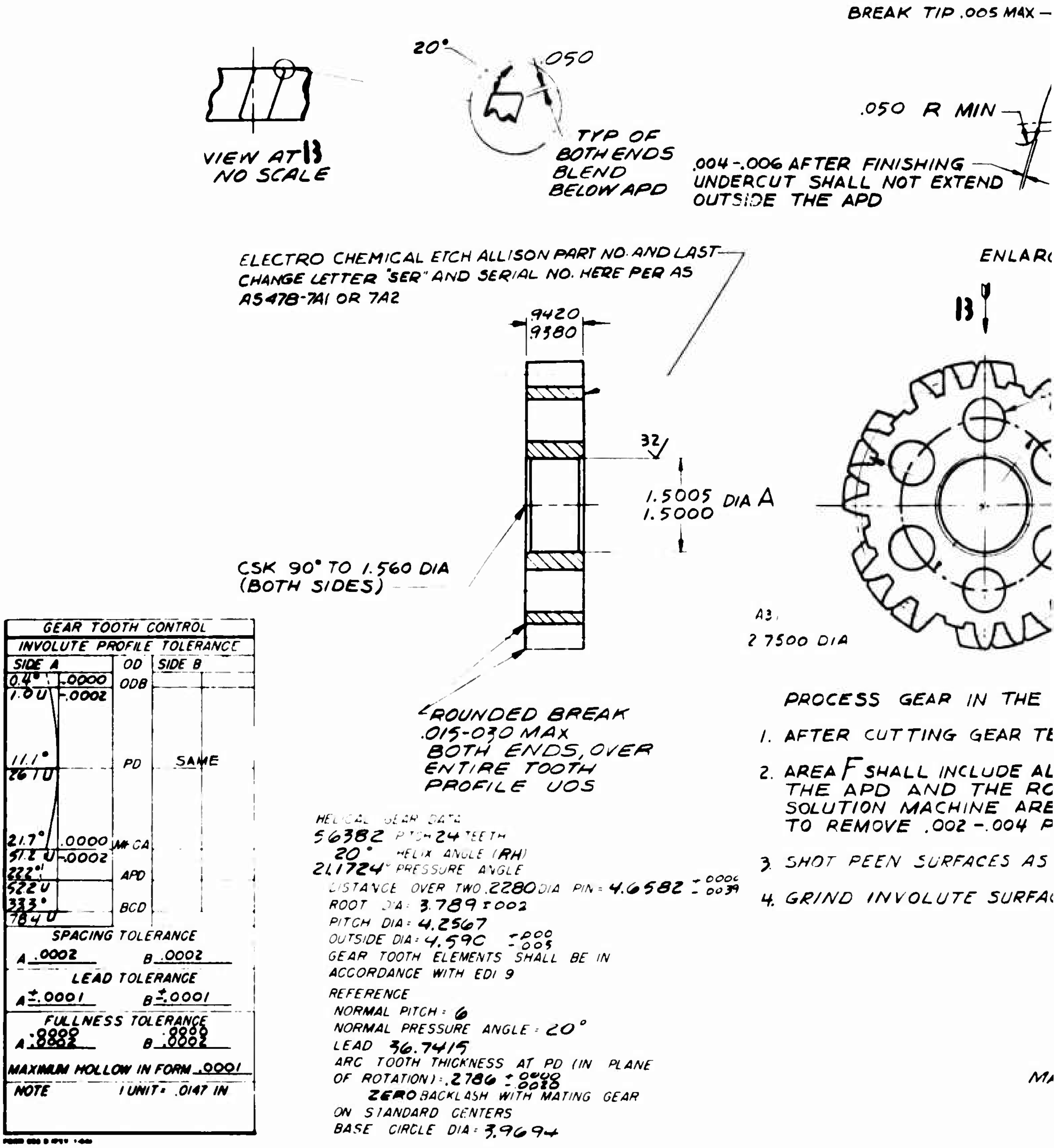

Figure 89. Fatigue Test Gear Configuration 1—EX-84117.

A

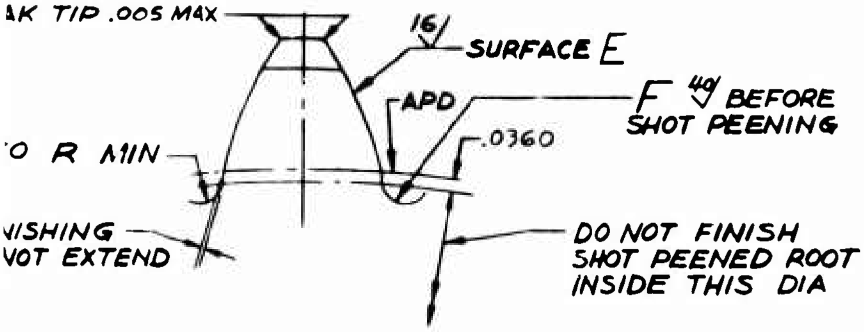

ENLARGED VIEW OF GEAR PROFILE
SCALE NONE

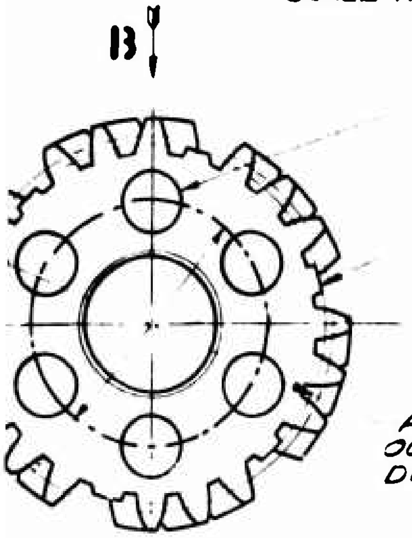

A1 .6885-.6890 REAM THRU
6 HOLES EQUALLY SPACED WITHIN .0005 R OTP
INITIAL HOLE MUST BE LOCATED CIRC WITHIN ±.0005 OF TOOTH CENTERLINE

A2 REMOVE 6 TEETH EQUALLY SPACED DOWN TO THE ACTIVE PROFILE DIA WITHIN ±.005.
INITIAL TOOTH MUST BE LOCATED AS FIRST TOOTH CW FROM TOOTH LOCATING THE .6885 DIA HOLES

ACTIVE PROFILE OUTSIDE 4.0433 DIA

GEAR IN THE FOLLOWING SEQUENCE

JTTING GEAR TEETH, CARBURIZE AND HARDEN

HALL INCLUDE ALL SURFACES BETWEEN
D AND THE ROOT DIA
I MACHINE AREA F PER EPS 13066
VE .002-.004 PER SURFACE

EN SURFACES AS REQUIRED

NVOLUTE SURFACE E TO FINISH SIZE

MATERIAL-AMS 6265 STEEL
FORGED BARS

DIA A SHALL BE CONCENTRIC WITH PD WITHIN .002 TIR

BREAK SHARP EDGES .010 UOS

MACHINE ALL OVER. PEEN GEAR TEETH PER EPS 12140 FOLLOWED BY EPS 12176
REMAINING SURFACES MAY BE PEENED PER EPS12140 UNLESS SPECIFICALLY CONTROLLED BY A √ SYMBOL

SURFACE CHARACTERISTICS NOT OTHERWISE CONTROLLED SHALL BE COMMENSURATE WITH GOOD MANUFACTURING PRACTICES WHICH PRODUCE ACCEPTABLE QUALITY LEVELS

HEAT TREAT PER EPS 202

CASE HARDEN GEAR TEETH OUTSIDE 3.340 DIA (OPTIONAL TO CASE HARDEN ALL OVER) EFFECTIVE CASE DEPTHS AS FOLLOWS:
.035-.045 BEFORE FINISHING
.030-.045 AFTER FINISHING
ROCKWELL HARDNESS - CASE C58 MIN
CORE C34 MIN

INSPECT PER EIS 985 (MAGNETIC)

BLACK OXIDE PER AMS 2485

FORGING SHALL CONFORM TO EDI138-1 AND EIS 502

B

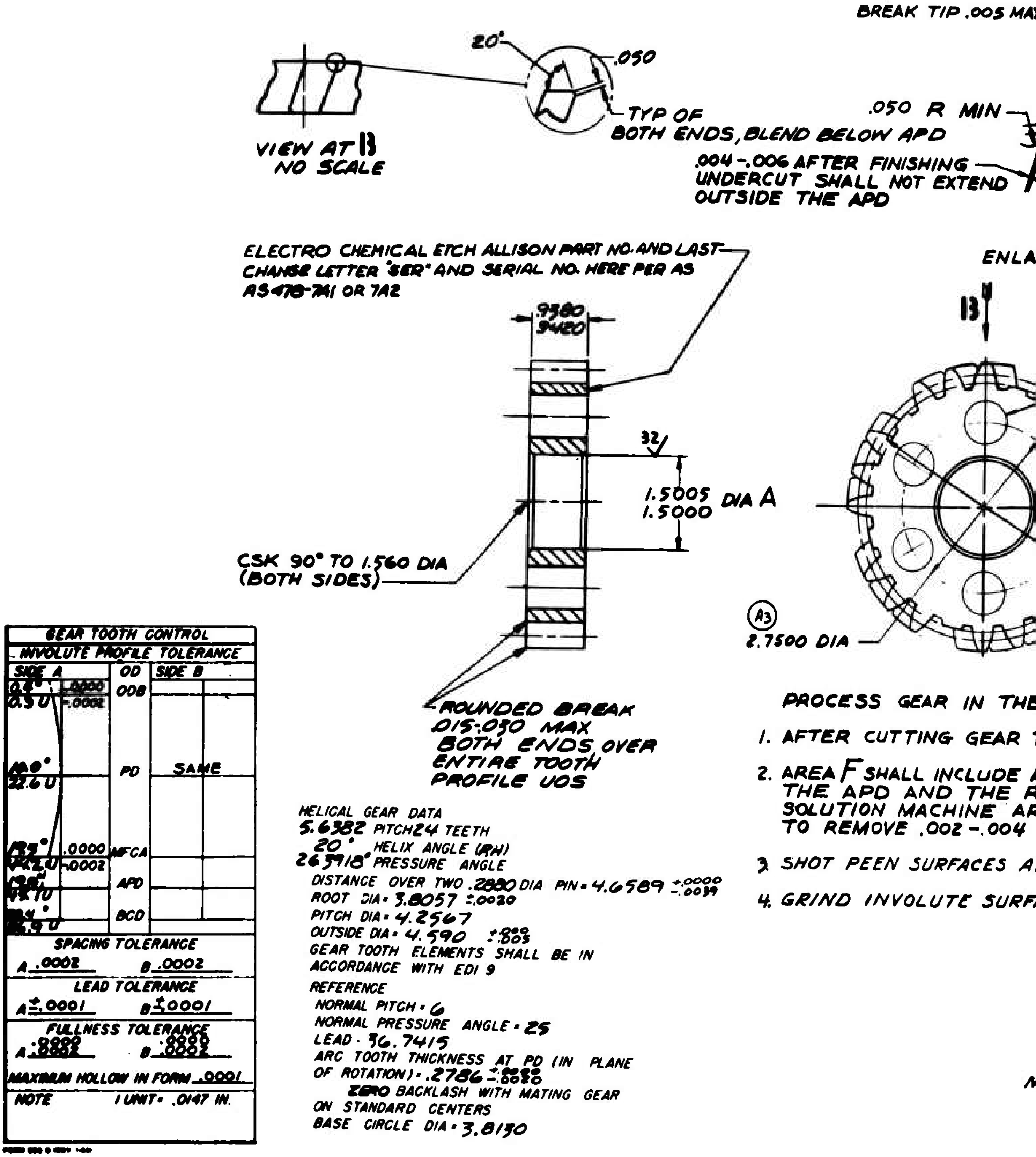

Figure 90. Fatigue Test Gear Configuration 2—EX-84118.

A

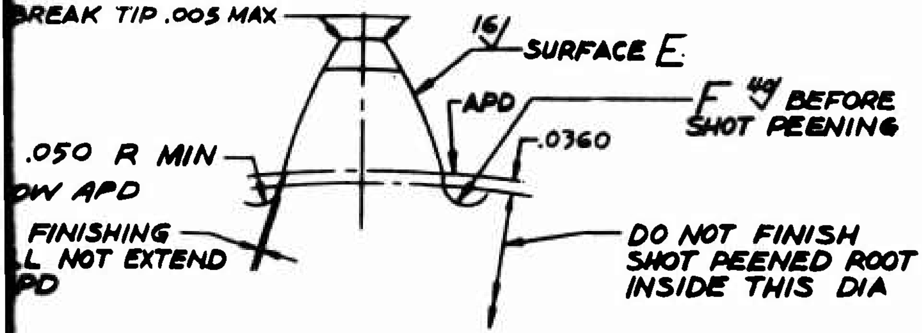

ENLARGED VIEW OF GEAR PROFILE
SCALE NONE

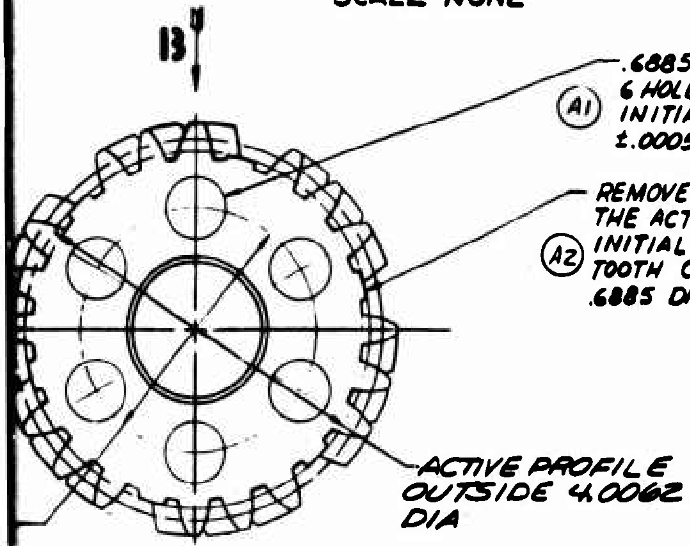

S GEAR IN THE FOLLOWING SEQUENCE

CUTTING GEAR TEETH, CARBURIZE AND HARDEN

SHALL INCLUDE ALL SURFACES BETWEEN
PD AND THE ROOT DIA
N MACHINE AREA F PER EPS 13066
OVE .002-.004 PER SURFACE

EEN SURFACES AS REQUIRED

INVOLUTE SURFACE E TO FINISH SIZE

DIA A SHALL BE CONCENTRIC WITH PD WITHIN .002 TIR

BREAK SHARP EDGES .010 UOS

MACHINE ALL OVER. PEEN GEAR TEETH PER EPS 12140
FOLLOWED BY EPS 12176
REMAINING SURFACES MAY BE PEENED PER EPS12140
UNLESS SPECIFICALLY CONTROLLED BY A √ SYMBOL

SURFACE CHARACTERISTICS NOT OTHERWISE CONTROLLED SHALL BE COMMENSURATE WITH GOOD MANUFACTURING PRACTICES WHICH PRODUCE ACCEPTABLE QUALITY LEVELS.

HEAT TREAT PER EPS 202

CASE HARDEN GEAR TEETH OUTSIDE 3.340 DIA
(OPTIONAL TO CASE HARDEN ALL OVER) EFFECTIVE CASE
DEPTHS AS FOLLOWS:
.035-.045 BEFORE FINISHING
.030-.045 AFTER FINISHING
ROCKWELL HARDNESS - CASE C58 MIN
CORE C34 MIN

INSPECT PER EIS 985 (MAGNETIC)

BLACK OXIDE PER AMS 2485

MATERIAL-AMS 6265 STEEL
FORGED BARS

FORGING SHALL CONFORM TO ED11581 ~~AND EIS 502~~

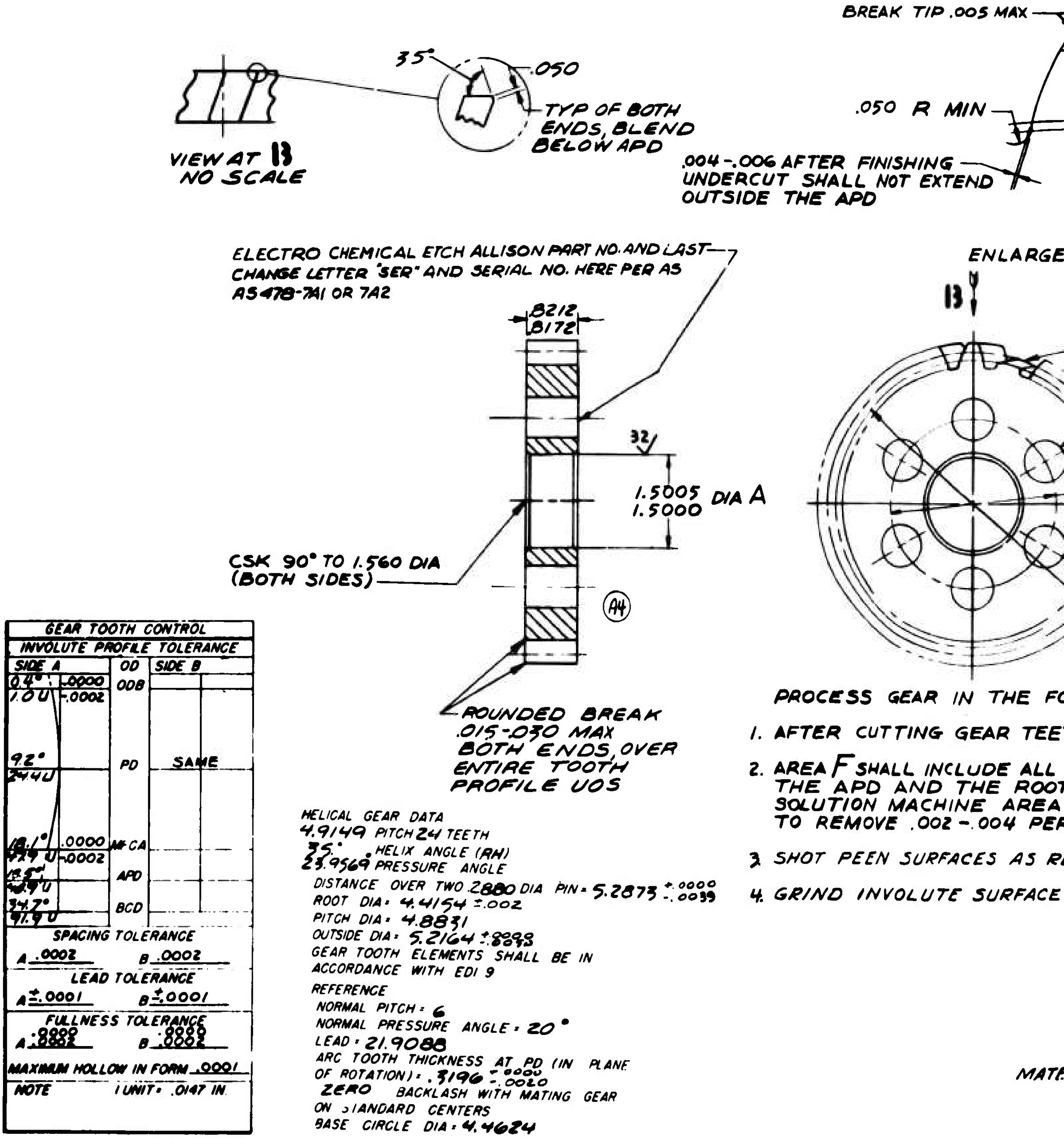

Figure 91. Fatigue Test Gear Configuration 3—EX-84119.

A

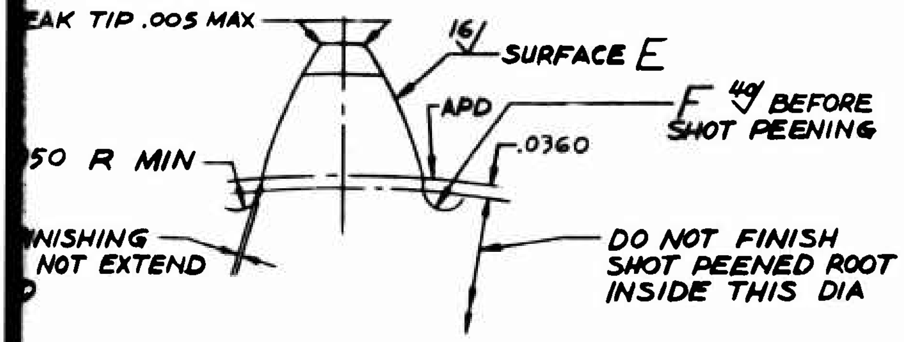

ENLARGED VIEW OF GEAR PROFILE
SCALE NONE

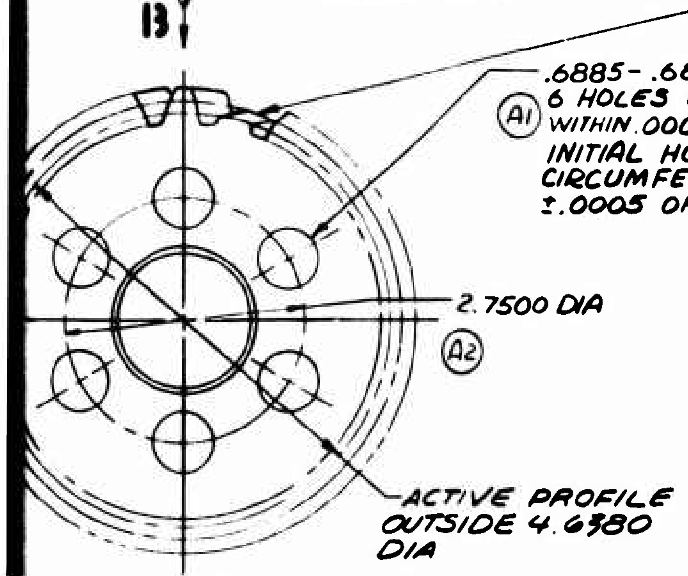

S GEAR IN THE FOLLOWING SEQUENCE

UTTING GEAR TEETH, CARBURIZE AND HARDEN

HALL INCLUDE ALL SURFACES BETWEEN
D AND THE ROOT DIA
N MACHINE AREA F PER EPS 13066
OVE .002-.004 PER SURFACE

EN SURFACES AS REQUIRED

INVOLUTE SURFACE E TO FINISH SIZE

MATERIAL-AMS 6265 STEEL
FORGED BARS

DIA A SHALL BE CONCENTRIC WITH PD WITHIN .002 TIR

BREAK SHARP EDGES .010 UOS

MACHINE ALL OVER. PEEN GEAR TEETH PER EPS 12140
FOLLOWED BY EPS 12176
REMAINING SURFACES MAY BE PEENED PER EPS12140
UNLESS SPECIFICALLY CONTROLLED BY A √ SYMBOL

SURFACE CHARACTERISTICS NOT OTHERWISE CONTROLLED SHALL BE COMMENSURATE WITH GOOD MANUFACTURING PRACTICES WHICH PRODUCE ACCEPTABLE QUALITY LEVELS.

HEAT TREAT PER EPS 202

CASE HARDEN GEAR TEETH OUTSIDE 3.340 DIA
(OPTIONAL TO CASE HARDEN ALL OVER) EFFECTIVE CASE
DEPTHS AS FOLLOWS:
.035-.045 BEFORE FINISHING
.030-.045 AFTER FINISHING
ROCKWELL HARDNESS - CASE C58 MIN
CORE C34 MIN

INSPECT PER EIS 985 (MAGNETIC)

BLACK OXIDE PER AMS 2485

FORGING SHALL CONFORM TO ED11784 AND EIS 502

B

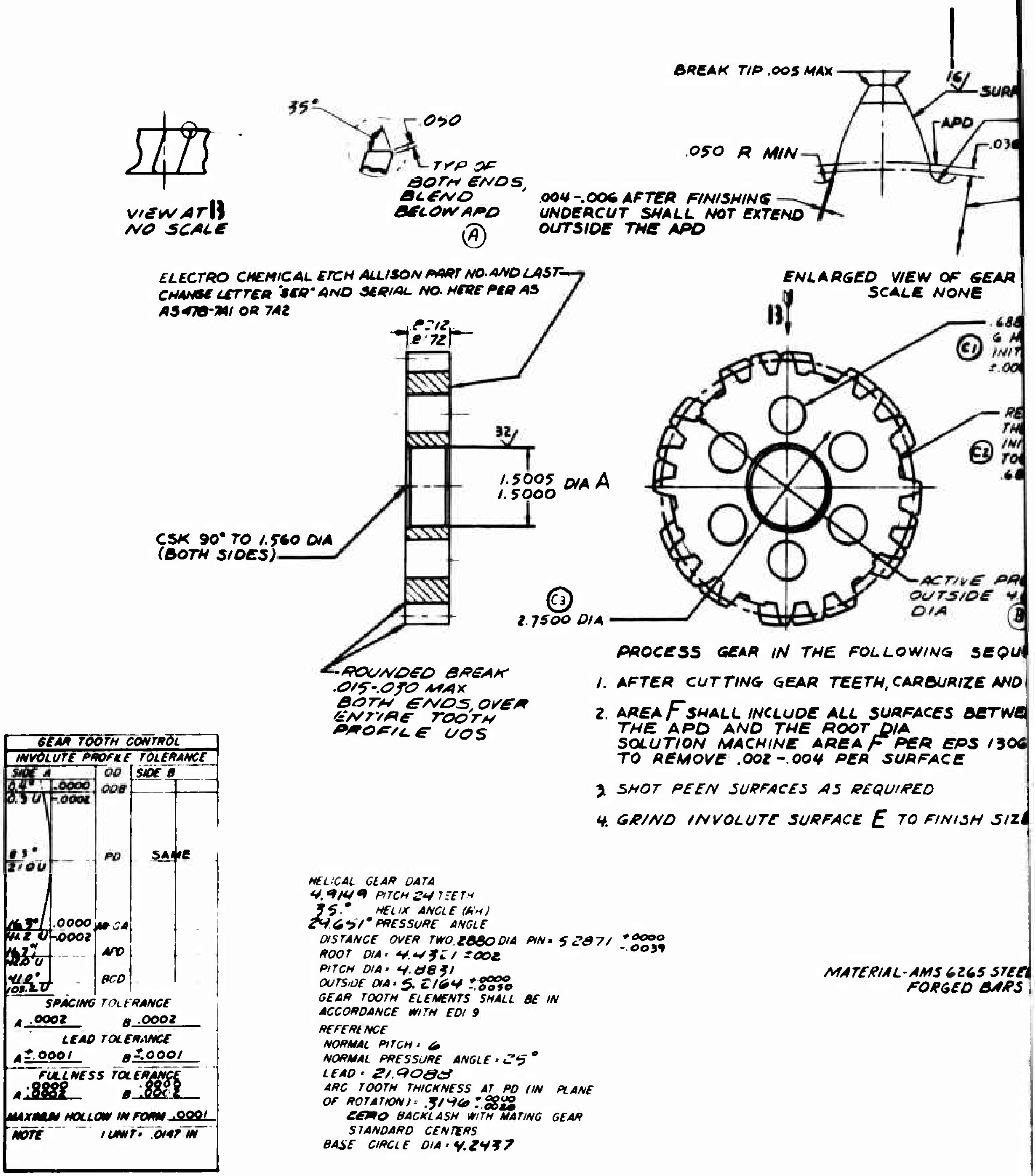

Figure 92. Fatigue Test Gear Configuration 4—EX-84120.

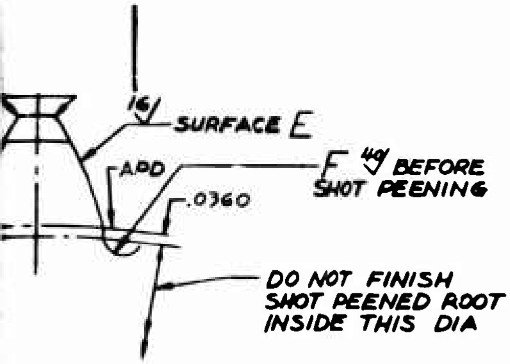

ED VIEW OF GEAR PROFILE
SCALE NONE

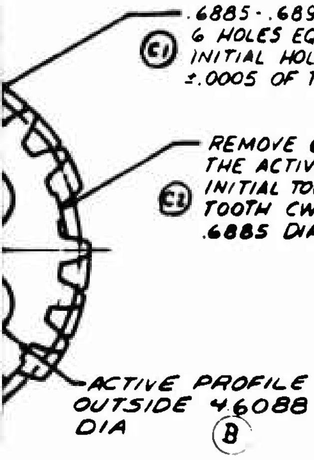

C1 .6885-.6890 DIA REAM THRU 6 HOLES EQUALLY SPACED WITHIN .0005R OTP INITIAL HOLE MUST BE LOCATED CIRC WITHIN ±.0005 OF TOOTH CENTERLINE

C2 REMOVE 6 TEETH EQUALLY SPACED DOWN TO THE ACTIVE PROFILE DIA WITHIN ±.005. INITIAL TOOTH MUST BE LOCATED AS FIRST TOOTH CW FROM TOOTH LOCATING THE .6885 DIA HOLES

OLLOWING SEQUENCE

TH, CARBURIZE AND HARDEN

SURFACES BETWEEN
T DIA
F PER EPS 13066
R SURFACE

EQUIRED

E TO FINISH SIZE

TRIAL-AMS 6265 STEEL
FORGED BARS

DIA A SHALL BE CONCENTRIC WITH PD WITHIN .002 TIR

BREAK SHARP EDGES .010 UOS

MACHINE ALL OVER. PEEN GEAR TEETH PER EPS 12140 FOLLOWED BY EPS 12176
REMAINING SURFACES MAY BE PEENED PER EPS12140 UNLESS SPECIFICALLY CONTROLLED BY A √ SYMBOL

SURFACE CHARACTERISTICS NOT OTHERWISE CONTROLLED SHALL BE COMMENSURATE WITH GOOD MANUFACTURING PRACTICES WHICH PRODUCE ACCEPTABLE QUALITY LEVELS

HEAT TREAT PER EPS 202

CASE HARDEN GEAR TEETH OUTSIDE 3.340 DIA (OPTIONAL TO CASE HARDEN ALL OVER) EFFECTIVE CASE DEPTHS AS FOLLOWS:
.035-.045 BEFORE FINISHING
.030-.045 AFTER FINISHING
ROCKWELL HARDNESS - CASE C58 MIN
CORE C34 MIN

EX84120
C

INSPECT PER EIS 985 (MAGNETIC)

BLACK OXIDE PER AMS 2485

FORGING SHALL CONFORM TO ED11381 AND EIS 502

B

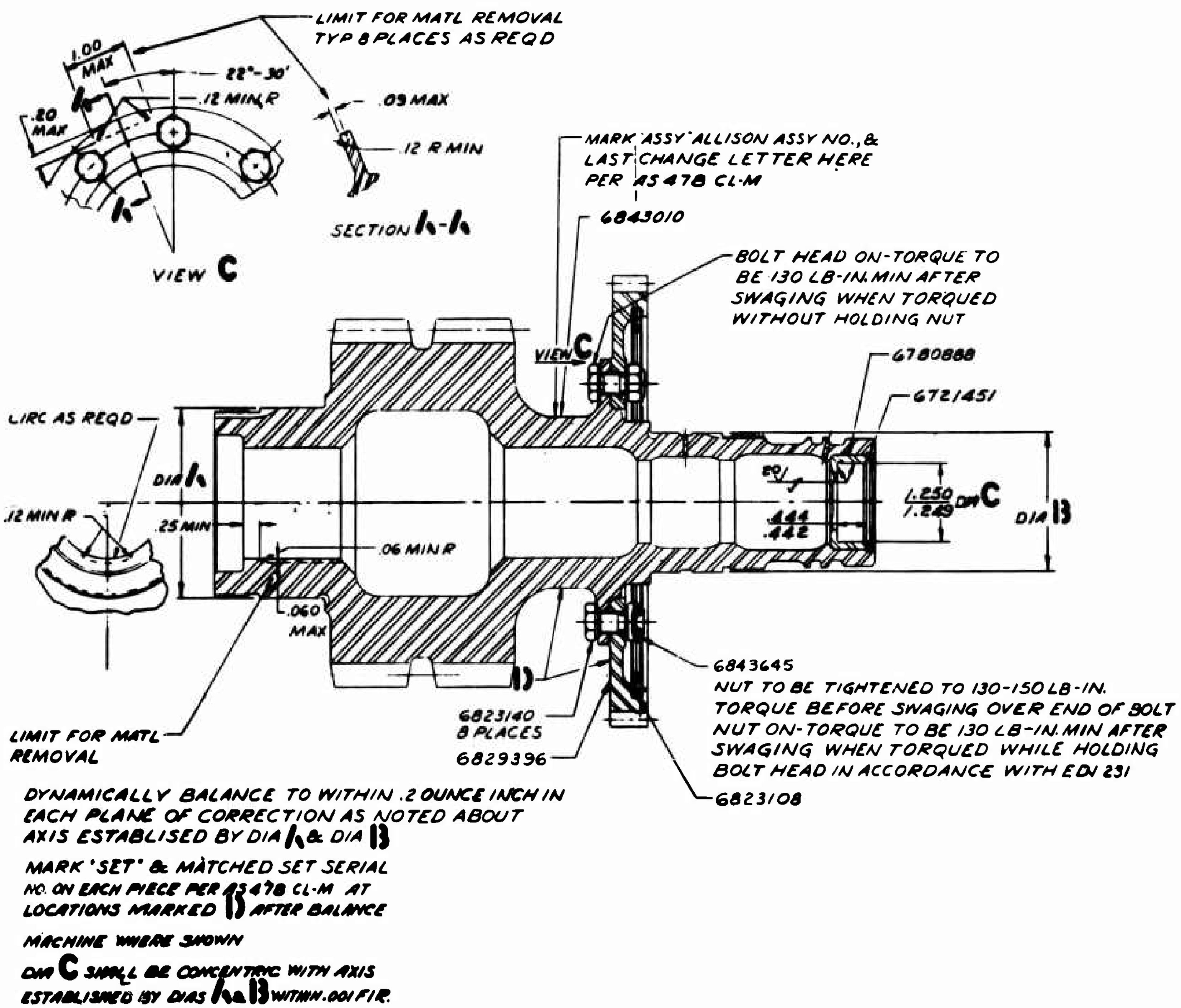

Figure 93. Pinion and Accessory Drive Shaftgear Assembly.

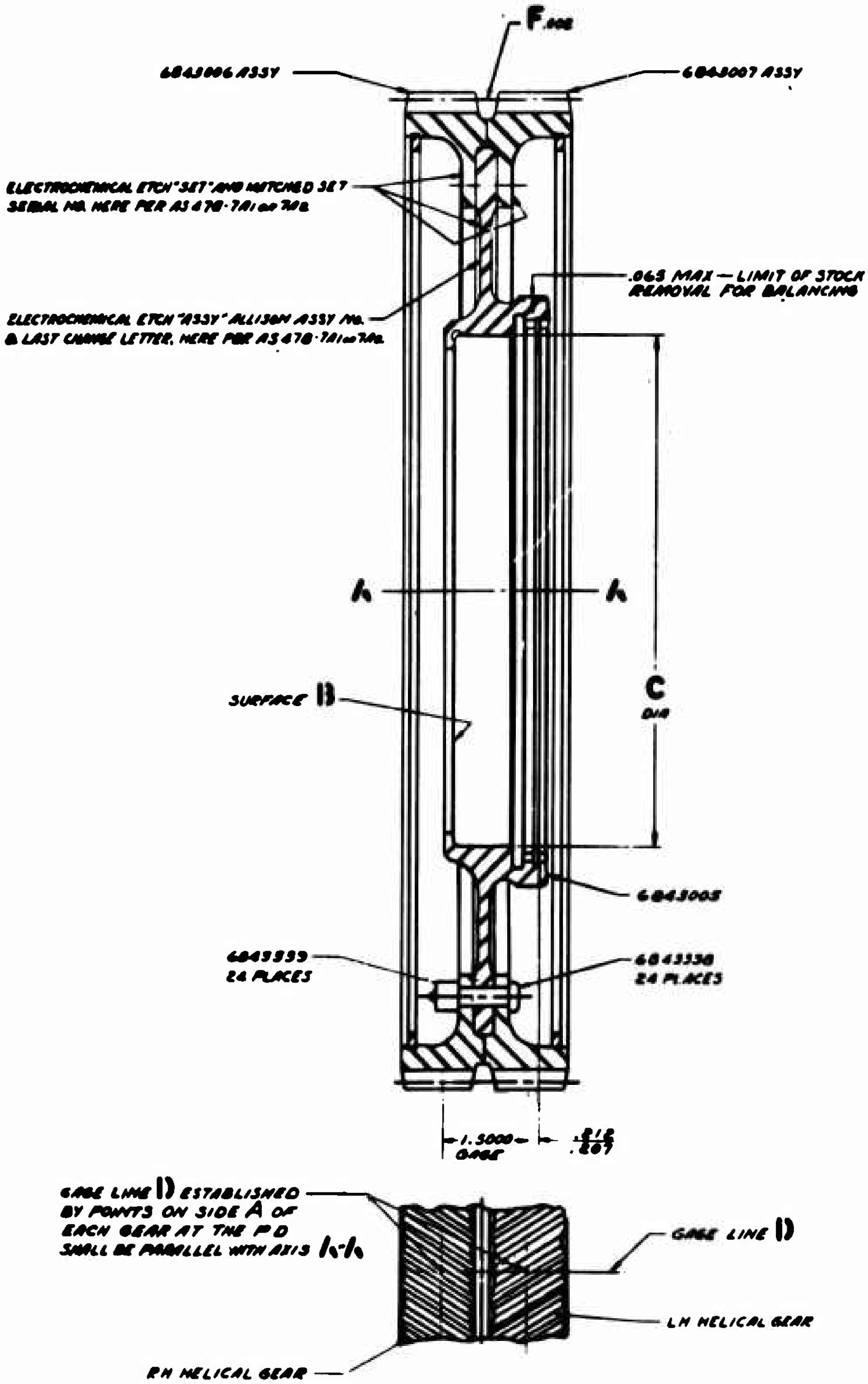

Figure 94. Herringbone Main Drive Gear Assembly.

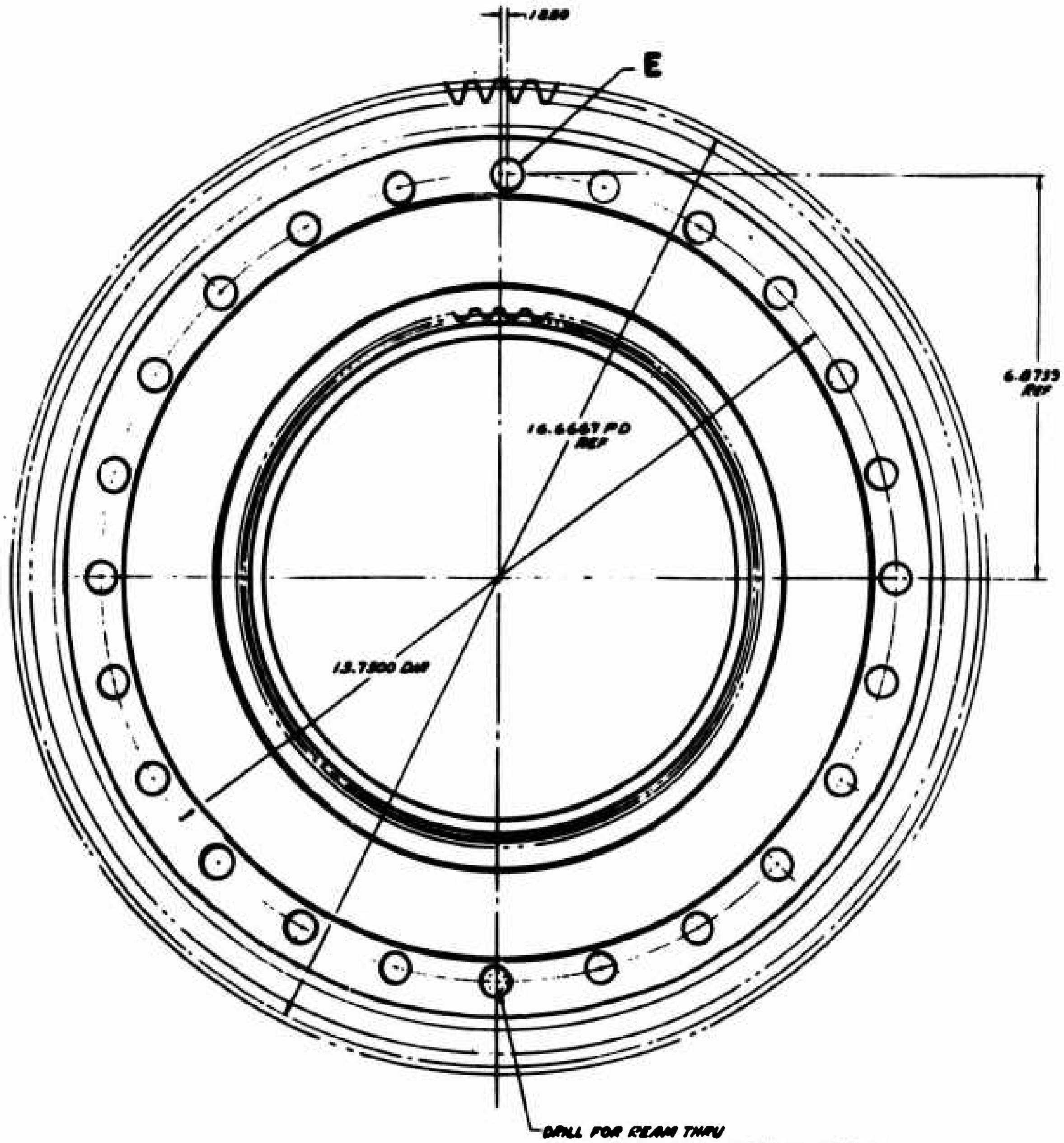

DRILL FOR REAM THRU
REAM .3035-.3100 DIA, CBORE .316-.326 DIA ×
.030-.050 DEEP WITH .030-.050 R IN CORNER
AT ASSEMBLY
24 HOLES EQUALLY SPACED EXCEPT
ONE HOLE MARKED E OFFSET AND
LOCATED WITHIN .005 OTP

AXIS K-K ESTABLISHED BY DIA C & SURFACE B
FEATURES SHALL BE CONCENTRIC ABOUT AXIS K-K
WITHIN THE FIR. SPECIFIED BY F

STATIC BALANCE ABOUT AXIS K-K WITHIN 1 OZ. INCHES

ANGULAR RELATION OF SPLINE TEETH
MAY VARY FREELY

REF INFORMATION
THIS PART AT NO REV IS SIMILAR TO
PART 602S075 REV F

B

APPENDIX II

SAMPLE PROCESS ROUTING SHEETS

This appendix consists of sample process routing sheets for test gear EX-84117 (Figure 95). The processing routings for all four fatigue test gears were identical.

ROUTE SHEET

SHEET 1 OF			
LINE 01	REVISION:	PART NAME: FATIGUE TEST GEAR	PROCESS ENGR: Phillips
LINE 02	MATERIAL SPEC & SIZE: AMS 6265 5 1/2" DIAMETER X 1 1/2" LONG FORGED BAR	PROD CODE:	NEXT ASSY NO:
LINE 03	MATERIAL SUBSTITUTION: AMS 6265 6" DIA BAR REF HEAT #513C	DRAWING PART NO: EX-84117	DRWG/CHG/LTR:

PART NO	PROC DATE	STDS INTL	STD DATE
EX-84117	9-13-66		

OPER	LINE COUNT	DEPT	MACH CODE	TOOL NO / TOOL CODE / OPERATION DESCRIPTION	SET-UP TIME	ESTIMATED HOURS
10		0856 B	100	Machine per sketch oper. 10 and break edges		
20		0819	933	Inspect and attach serial numbers. Start a log of required information. Forward to Dept. 0846		
30		0846		Hold until EX-84120, EX-84118, and EX-84119 and Moore test bars are ready for this oper.		
40		862 F	600	Harden at 1750° and temper per ERS 202 and PCl 8000. C34 - C38 Heat treat EX-84120, EX-84118, EX-84119 and Moore bars at the same time.		
50		0859	832	Grit blast		
60		0819	857	Rockwell		
70		0819	670	Magnaflux		
80		0856 S	100	Machine per sketch oper, 80 and break edges. Trans tag.		
90		0858	430	Grind per sketch oper. 90 and break edges. Trans. tag.		

Figure 95. Typical Routing Sheet for Test Gear EX-84117 (Sheet 1 of 9).

ROUTE SHEET

SHEET 2 OF		PART NO EX-84117		
LINE 01	REVISION	PART NAME FATIGUE TEST GEAR	PROCESS ENGR Phillips	PROC DATE 9-13-66 / STDS INTL / STD DATE
LINE 02	MATERIAL SPEC & SIZE	AMS 6265 5 1/2" DIAMETER X 1 1/2" LONG FORGED BAR	PROD CODE	NEXT ASSY NO
LINE 03	MATERIAL SUBSTITUTION	AMS 6265 6" DIAMETER BAR REF HEAT #513C	DRAWING PART NO EX-84117	DRWG/CHG/LTR

OPER	LINE COUNT	DEPT	MACH CODE	TOOL NO / TOOL CODE / OPERATION DESCRIPTION	SET-UP TIME	ESTIMATED HOURS
100		0858	400	Grind per sketch oper 90 and break edges trans tag		
110		0854	375	8-17429 Hob bushing SPT 2605 Gear Hob Rough hob gear to 4.690 + 000 - 004 over 2 .288 dia. pins.		
				Hob 4 pieces at a time trans tag		
120		0851	320	Mill .050 X 35° angle break on acute angle both ends of gear tooth trans tag.		
130		0854	900	Round break remaining edges of gear teeth .035 - .045		
140		0819	933	Inspect and forward to dept. 0846. Etch S/N on each part for heat treat Operations.		
150		0846		Hold until EX-84120, EX-84118, EX-84119 and Moore bars are ready for carburizing		
152		0851	320	Remove 6 gear teeth equally spaced down to active profile dia. break edges.		
157		0826 C	987	Mask gear teeth and copper plate all remaining surfaces per PCl 8000 and P61 2001. Remove mask from gear teeth. Copper plate EX-84117, EX-84118, EX-84119, EX-84120 and Moore bars at the same time.		

149

Figure 95. Continued (Sheet 2 of 9).

ROUTE SHEET

SHEET 3 OF				PART NO EX-84117	
LINE 01	REVISION	PART NAME FATIGUE TEST GEAR	PROCESS ENGR Phillips	PROC DATE 9-13-66	STDS INTL / STD DATE
LINE 02	MATERIAL SPEC & SIZE AMS 6265 5 1/2" DIAMETER X 1 1/2" LONG FORGED GAR			PROD CODE	NEXT ASSY NO
LINE 03	MATERIAL SUBSTITUTION AMS 6265 6" DIA BAR REF HEAT #513C			DRAWING PART NO EX-84117	DRWG/CHG/LTR

OPER	LINE COUNT	DEPT	MACH CODE	TOOL NO / TOOL CODE / OPERATION DESCRIPTION	SET-UP TIME	ESTIMATED HOURS
160		0862 F	600	Carburize and anneal per EPS 202 and PC1 8000 .035 - .045 effective case depth. Caution: Carburize EX-84120, EX-84118, EX-84119, and Moore bars at the same time.		
170		0862 C	987	Strip Plating Copper plate all over per PC1 8000 and PC1 2001. Caution: Copper plate EX-84120, EX-84118, EX-84119 and Moore bars at the same time.		
180		0862 F	600	Harden and temper per EPS 202 and PC1 8000, as follows: A. Harden B. Temper C. Stabilize D. Re-temper Caution: Harden and temper EX-84120, EX-84118, EX-84119 and Moore bars at the same time.		
190		0859	832	Light grit blast to clean for stripping copper plating.		
200		0862 C	987	Strip copper plating per PC1 8000 and PC1 2001 Caution: Strip EX-84120, EX-84118, EX-84119 and Moore bars at the same time.		
210		0859	832	Mask and shotblast gear teeth with 80 grit chilled shot		
220		0819	857	Rockwell		
230		0819	670	Magnaflux		

Figure 95. Continued (Sheet 3 of 9).

ROUTE SHEET

SHEET 4 OF			PART NO EX-84117
LINE 01	REVISION	PART NAME FATIGUE TEST GEAR	PROCESS ENGR Phillips	PROC DATE 9-13-66	STDS INTL	STD DATE
LINE 02	MATERIAL SPEC & SIZE AMS 6265 5 1/2" DIAMETER X 1 1/2" LONG FORGED BAR	PROD CODE	NEXT ASSY NO
LINE 03	MATERIAL SUBSTITUTION AMS 6265 6" DIA BAR REF HEAT #513C	DRAWING PART NO EX-84117	DRWG/CHG/LTR

OPER	LINE COUNT	DEPT	MACH CODE	TOOL NO / TOOL CODE / OPERATION DESCRIPTION	SET-UP TIME	ESTIMATED HOURS
240		0819	933	Inspect gear and record information. Check P/N size and root dia.		
250		0862 C	630	Solution machine gear teeth per EPS 13066. Remove 002 stock max. solution mach. .003 from Moore test bars.		
260		0819	933	Inspect solution machining. Check pin size and root dia and record.		
270		0859	833	Shot peen gear teeth per EPS 12140 followed by EPS 12176. Caution: Shot peen EX-84120, EX-84118, EX-84119 at same time. Shot peen Moore Bars.		
280		0858	430	Grind per sketch oper. 280 and break edges. Trans tag.		
290		0858	400	Grind per sketch oper. 280 and break edges. Tran tag.		
300		0819	933	Remove metal tag and etch S/N on web.		
310		0862 E	600	Moore test bars must accompany part stress believe per EPS 202 and PC1 8000		
320		0819	933	Inspect pin size, root dia. and root radius. Record information.		
330		0854	388	8-17428 8-19199 Finish grind gear. Grind as many as possible at one time. Trans. tag.		
340		0819	933	Stress relieve per EPS 202 and PC1 8000. Moore test bars must accompany part.		

Figure 95. Continued (Sheet 4 of 9).

ROUTE SHEET

SHEET 5 OF			PART NO EX-84117
LINE 01	REVISION	PART NAME: FATIGUE TEST GEAR	PROCESS ENGR: Phillips
	PROC DATE: 9-13-66	STDS INTL	STD DATE
LINE 02	MATERIAL SPEC & SIZE: AMS 6265 5 1/2" DIAMETER X 1 1/2" LONG FORGED BAR	PROD CODE	NEXT ASSY NO
LINE 03	MATERIAL SUBSTITUTION: AMS 6265 6" DIA BAR REF HEAT #513C	DRAWING PART NO. EX-84117	DRWG/CHG/LTR

OPER	LINE COUNT	DEPT	MACH CODE	TOOL NO / TOOL CODE / OPERATION DESCRIPTION	SET-UP TIME	ESTIMATED HOURS
360		0862 C	959	Nital etch per EIS 1510		
370		0854	900	Break edges of gear teeth per B/P		
375		0852 S	550	Drill and ream (6) .6885 - .6890 dia. holes. Note location.		
380		0819	670	Magnaflux		
385		0819	933	Etch number on teeth, inspect per ETX 2189		
390		0819	933	Inspect for black oxide		
400		1805		Black oxide per AMS 2485		
410		0819	934	Inspect and identify		

Figure 95. Continued (Sheet 5 of 9).

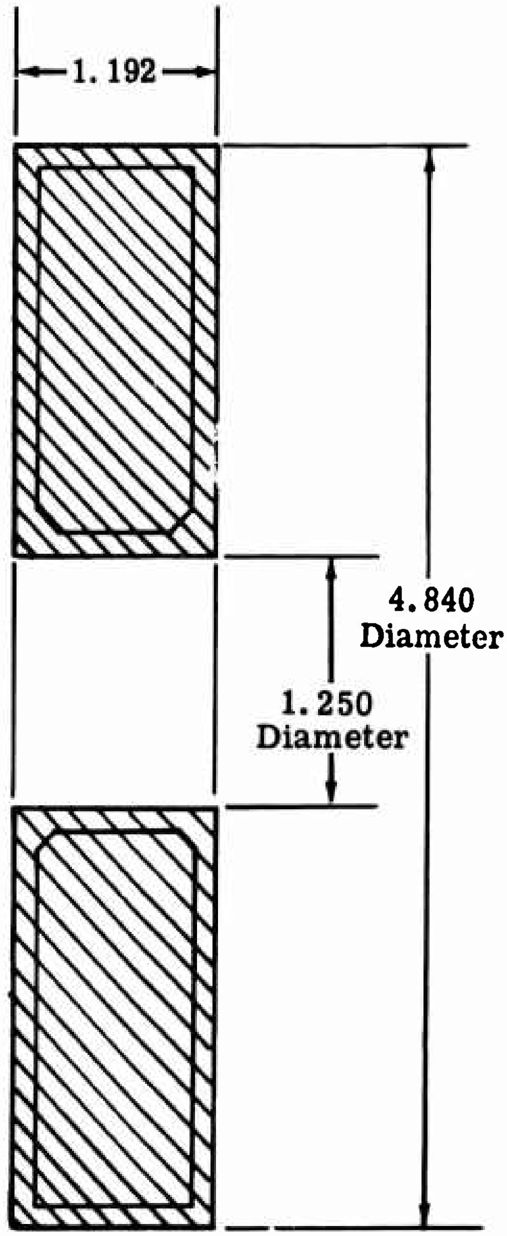

Dimensions In Inches
ALL THREE PLACE DECIMALS ARE ± 0.010
UNLESS OTHERWISE SPECIFIED

Figure 95. Continued (Sheet 6 of 9).

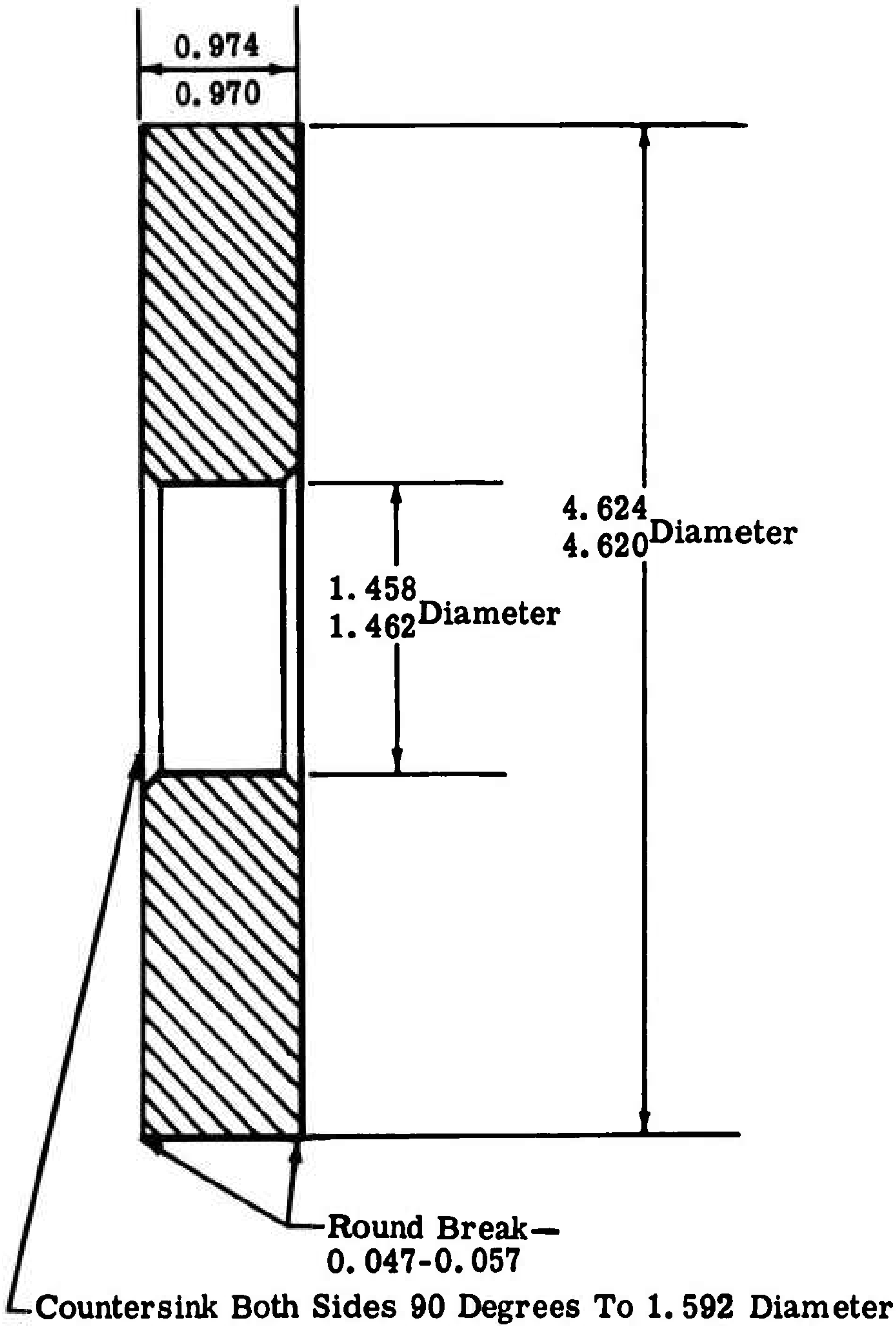

Dimensions In Inches

ALL THREE PLACE DECIMALS ARE ± 0.010
UNLESS OTHERWISE SPECIFIED

Figure 95. Continued (Sheet 7 of 9).

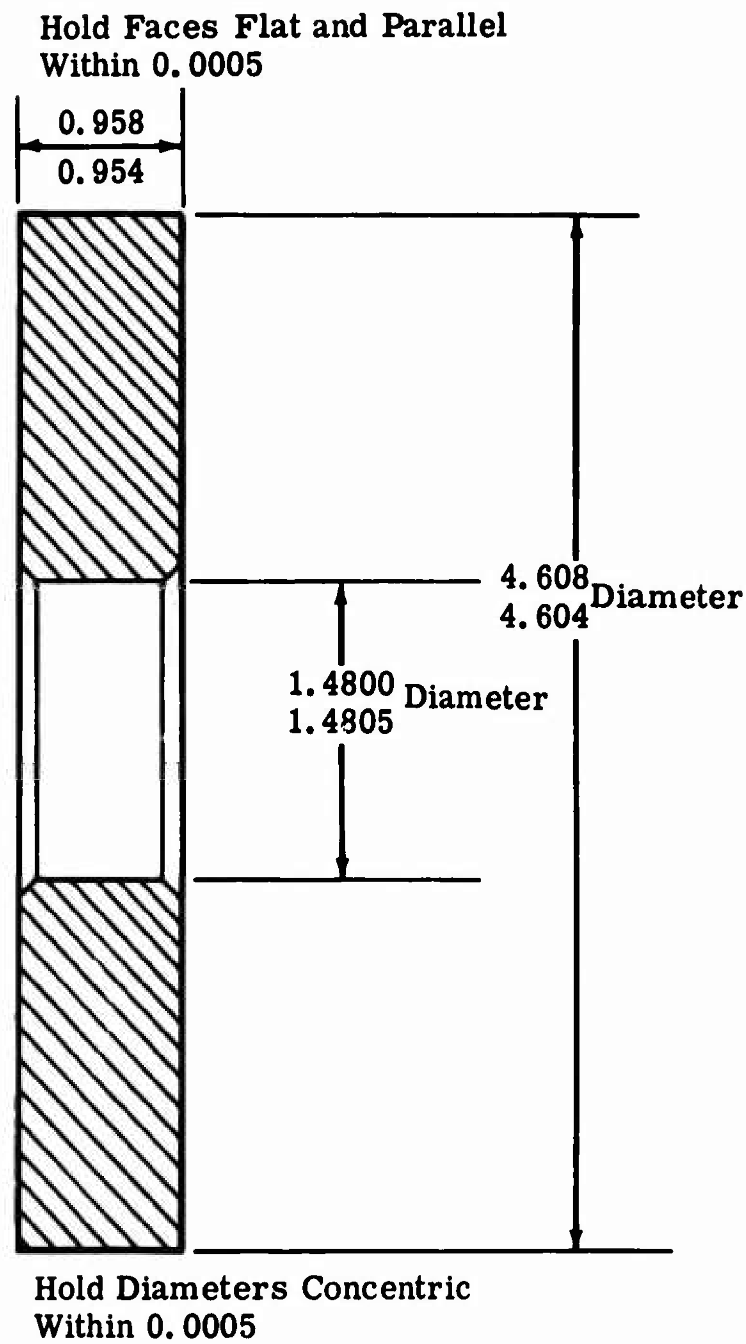

Dimensions In Inches

ALL THREE PLACE DECIMALS ARE ± 0.010
UNLESS OTHERWISE SPECIFIED

Figure 95. Continued (Sheet 8 of 9).

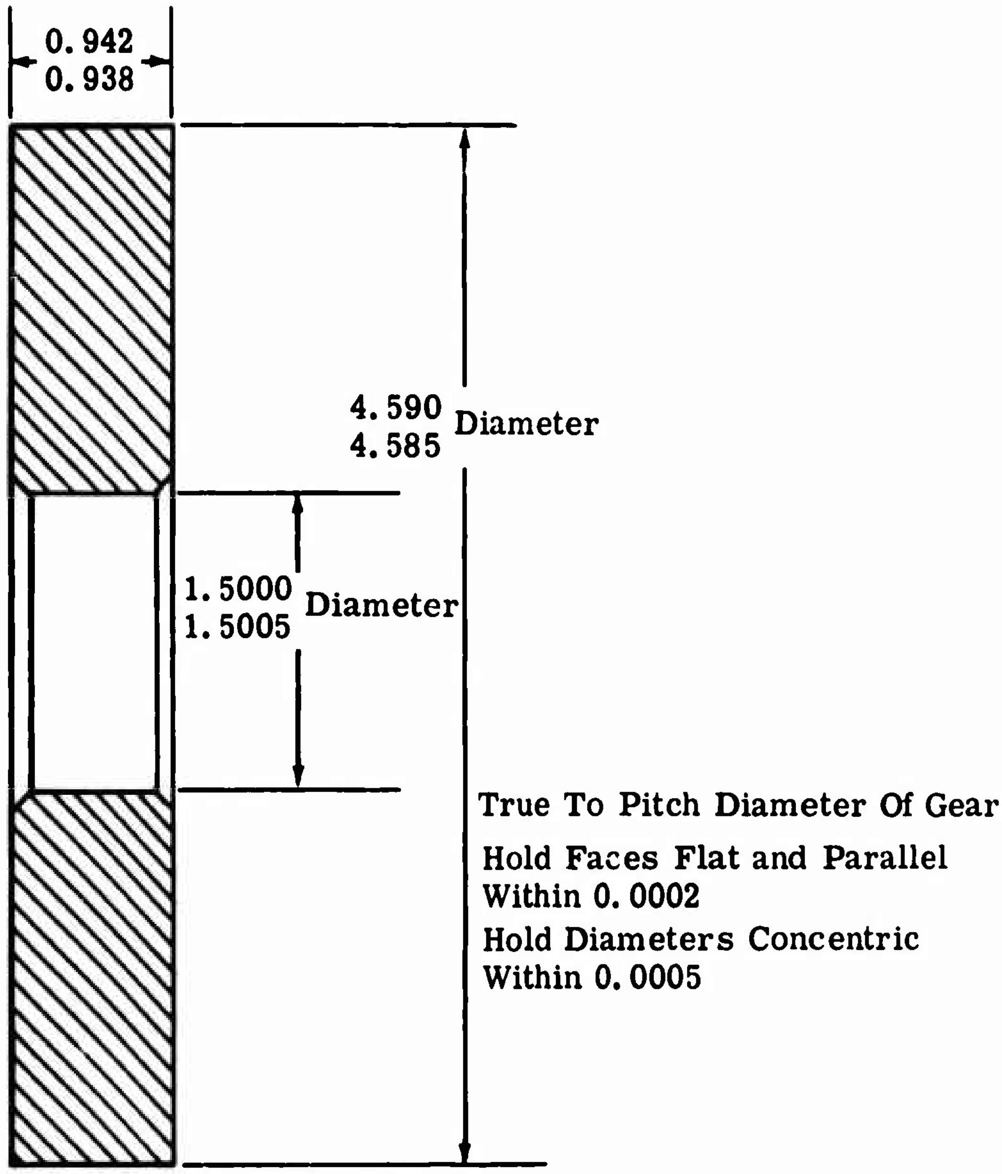

Dimensions In Inches

ALL THREE PLACE DECIMALS ARE ± 0.010
UNLESS OTHERWISE SPECIFIED

Figure 95. Continued (Sheet 9 of 9).

APPENDIX III

DESCRIPTION OF COMPUTER PROGRAM

This appendix consists of a complete description of the computer program and includes the program equations, input data sheet, source program print-out, and a sample problem. The equations are given in both engineering and computer program terms.

DESCRIPTION OF PROBLEM

Gear tooth bending strength is one of the major criteria in gear design. Gear tooth loading is cyclic in nature, subjecting the material to fatigue. The critical section is close to the root diameter. Failure usually results in fracture of an entire tooth from the gear rim.

Calculation of gear tooth bending stress requires geometrically precise description of the root fillet contour and location of the critical section. The point of the involute tooth profile at which the transmitted load produces the maximum bending stress is also required. Knowledge of the mounting and operating conditions of the unit in which the gear is assembled is required to assess the increase in bending stress caused by misalignment, overloads, system dynamics, and centrifugal forces. Gear material ultimate strength and fatigue data must be known to convert the calculated stress to anticipated gear life.

The purpose of this program is to calculate gear tooth bending stress considering these factors.

METHOD OF SOLUTION

The gear tooth geometry has been developed using basic formulae available in the literature. The hob dimensions have been used in the program to generate the trochoidal fillet contour resulting on a finished gear from some gear processing procedures. A true radius fillet is used when a shaped contour is specified in the program input. The program uses an iteration routine to inscribe a parabola (per Lewis construction) and to locate its tangency point with the root fillet contour. The program also uses an iteration process to establish the helical factor by computing and comparing the maximum bending moment for total tip loading and equal intensity loading along the inclined load line through the tooth tip edge. The calculated parameters are then used in the AGMA formula given in Appendix V to calculate a bending stress. The AGMA temperature, safety, and load distribution factors are applied to the bending stress.

COMPUTER TYPE AND PROGRAM LANGUAGE

The subject program is written in FORTRAN IV language for use on an IBM 360/44 computer. There must be four, five, or six cards per data set depending on the data input for words 1 and 2 on Card 4. Data sets may be stacked. Computer running time will be approximately 0.2 minute per data set.

INPUT DATA

A sample input data form is shown in Figure 96. Each set of data requires four, five, or six cards. A description of the cards follows:

Input Card 1

Word	Column	Description
1	1-5	Number of teeth—pinion.
2	6-10	Number of teeth—gear.
3	11-20	Standard center distance.
4	21-30	Nonstandard center distance 1 (same as standard, if standard).
5	31-40	Horsepower.
6	41-50	R.P.M.—pinion.
7	51-55	Overload factor.
8	56-60	Dynamic factor.
9	61-65	Size factor.
10	66-70	Load distribution factor.

Input Card 2

Word	Column	Description
1	1-10	Pressure angle at the standard pitch diameter—degrees.
2	11-20	Diametral pitch at the standard pitch diameter P_{ND} normal plane.
3	21-30	Helix angle at operating pitch diameter.
4	31-35	Backlash—minimum.
5	36-40	Backlash—maximum.
6	41-50	Face width—minimum (pinion).
7	51-60	Face width—minimum (gear).
8	61-65	Tip break—maximum (pinion).
9	66-70	Tip break—maximum (gear).

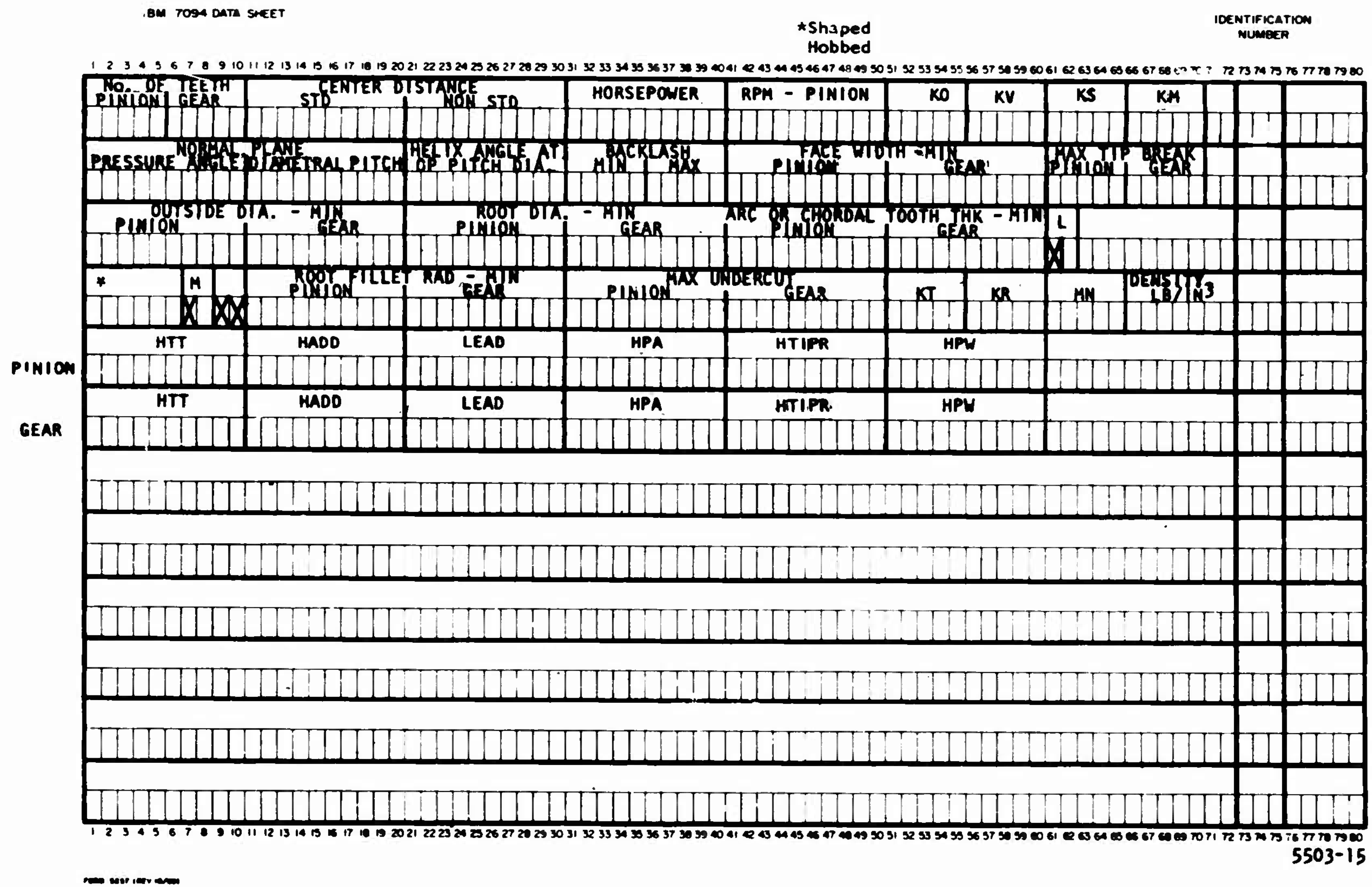
IBM 7094 DATA SHEET

*Shaped
Hobbed

IDENTIFICATION NUMBER

No. OF TEETH PINION | GEAR	CENTER DISTANCE STD | NON STD	HORSEPOWER	RPM - PINION	KO	KV	KS	KM		
PRESSURE ANGLE	NORMAL PLANE DIAMETRAL PITCH	HELIX ANGLE AT OP PITCH DIA.	BACKLASH MIN | MAX	FACE WIDTH - MIN PINION | GEAR		MAX TIP BREAK PINION | GEAR			
OUTSIDE DIA. - MIN PINION | GEAR	ROOT DIA. - MIN PINION | GEAR		ARC OR CHORDAL TOOTH THK - MIN PINION | GEAR		L				
*	M	ROOT FILLET RAD - MIN PINION | GEAR	MAX UNDERCUT PINION | GEAR		KT	KR	MN	DENSITY LB/IN3	
PINION	HTT	HADD	LEAD	HPA	HTIPR	HPW			
GEAR	HTT	HADD	LEAD	HPA	HTIPR	HPW			

1 2 3 4 5 6 7 8 9 10 11 12 13 14 15 16 17 18 19 20 21 22 23 24 25 26 27 28 29 30 31 32 33 34 35 36 37 38 39 40 41 42 43 44 45 46 47 48 49 50 51 52 53 54 55 56 57 58 59 60 61 62 63 64 65 66 67 68 69 70 71 72 73 74 75 76 77 78 79 80

5503-15

Figure 96. Sample Input Data Form.

Input Card 3

Word	Column	Description
1	1-10	Outside diameter—minimum (pinion).
2	11-20	Outside diameter—minimum (gear).
3	21-30	Root diameter—minimum (pinion).
4	31-40	Root diameter—minimum (gear).
5	41-50	Arc or chordal tooth thickness—minimum (pinion).
6	51-60	Arc or chordal tooth thickness—minimum (gear).
7	62	This must be one of the following in Column 62: 0—if Columns 41 through 60 are arc tooth thickness 1—if Columns 41 through 60 are chordal tooth thickness

Input Card 4

1	1-6	This must be one of the following beginning in Column 1: SHAPED HOBBED
—	7	Blank.
2	8	This must be one of the following: 0—if pinion is "HOBBED" 1—if gear is "HOBBED" 2—if pinion and gear are "HOBBED" Blank—if "SHAPED" is in Columns 1 through 6
—	9-10	Blank
3	11-20	Fillet radius (true)—minimum (pinion). Blank if pinion is "HOBBED."
4	21-30	Fillet radius (true)—minimum (gear). Blank if gear is "HOBBED."
5	31-40	Maximum undercut—pinion Blank if pinion is "HOBBED."
6	41-50	Maximum undercut—gear. Blank if gear is "HOBBED".
7	51-55	Temperature factor.
8	56-60	Safety factor.
9	61-65	Load sharing ratio.
10	66-72	Density—pounds per cubic inch.

Input Card 5

This card is needed only when words 1 and 2 of Card 4 are given as "HOBBED" and "0" or "2," respectively. This card is for pinion only. See Figure 97.

Word	Column	Description
1	1-10	Hob tooth thickness.
2	11-20	Hob addendum.
3	21-30	Hob lead.
4	31-40	Hob pressure angle—degrees.
5	41-50	Hob tip radius—in.
6	51-60	HPW (hob protuberance width). See Figure 96.

Input Card 6

This card is needed only when words 1 and 2 of Card 4 are given as "HOBBED" and "1" or "2," respectively. This card is for gear only and is the same format as Input Card 5.

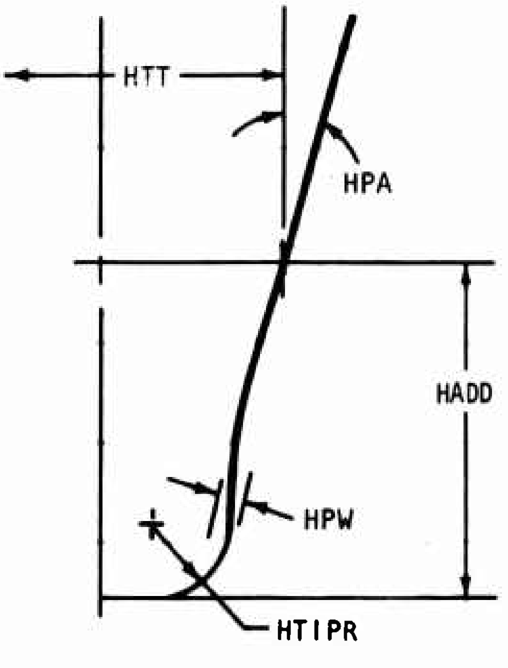

Figure 97. Standard or Protuberance Hob Form For Input.

PROGRAM EQUATIONS

Computer program input symbols in both engineering (AGMA) and program terms are listed as follows:

AGMA	Program	Definition
Np	ANP	Number of teeth—pinion.
Ng	ANG	Number of teeth—gear.
C	CSTD	Standard center distance.
C_x	CNSTD	Nonstandard center distance.
H_p	HORSES	Horsepower.
n_c	RPMP	rpm—pinion.
K_o	KO	Overload factor.
K_v	KV	Dynamic factor.
K_s	KS	Safety factor.
K_m	KM	Load distribution factor.
M_n	MN	Load sharing factor.
ϕ_n	PHIN	Pressure angle—normal plane.
Pnd	PND	Diametral pitch—normal plane.
ψ	PSI	Helix angle.
B_{mi}	BMIN	Backlash—minimum.
B_{ma}	BMAX	Backlash—maximum.
F_{pmi}	FMINP	Face width—minimum (pinion).
F_{gmi}	FMING	Face width—minimum (gear).
—	BRKP	Max tip break—pinion.
—	BRKG	Max tip break—gear.
domi	DOPMI	Outside diameter—minimum (pinion).
Domi	DOGMI	Outside diameter—minimum (gear).
drmi	DRPMI	Root diameter—minimum (pinion).
Drmi	DRGMI	Root diameter—minimum (gear).
T_{pmi} or Tcpmi	TPMIS	Arc or chordal tooth thickness—minimum (pinion).
T_{gmi} or Tcgmi	TGMIS	Arc or chordal tooth thickness—minimum (gear).
rfpmi	RFMIP	True root fillet radius—pinion.
rfgmi	RFMIG	True root fillet radius—gear.
—	UCP	Max undercut—pinion.
—	UCG	Max undercut—gear.
a_c	HADD	Hob addendum.
L_c	HLEAD	Hob lead.
ϕ_c	HPA	Hob pressure angle.
—	HPW	Hob protuberance width.
r_t	HTIPR	Hob tip radius.
t_c	HTT	Hob tooth thickness.

The computer program equations in both engineering (AGMA) and program terms follow. The basic geometric equations for gear teeth can be obtained or developed from the literature.

AGMA	Program
$Pd_x = \dfrac{NP + NG}{2 \times C_x}$	$PDX = \dfrac{ANP + ANG}{2 \times CNSTD}$
$\phi_{std} = \dfrac{Pd_x}{Pnd} \cdot \tan(\psi_x)$	$SI = \left(\dfrac{PDX}{PND} \times STA\right)^{-1}$
$Pd = Pnd \times \cos(\psi_{sta})$	$PD = PND \times COS\ (SI)$
$\phi = \text{arc tan}\ \dfrac{\tan(\phi n)}{\cos(\psi_{std})}$	$FRA = ATAN \left(\dfrac{FNTA}{COS\ (SI)}\right)$
$\phi_x = \text{arc tan} \left(\dfrac{C \times \cos(\phi)}{C_x}\right)$	$PHIX = ATAN \left(\dfrac{CSTD \times COS\ (FRA)}{CNSTD}\right)$
$mg = \dfrac{N_G}{N_P}$	$MG = \dfrac{ANG}{ANP}$
$Rmg = \dfrac{N_P}{N_G}$	$RMG = \dfrac{ANP}{ANG}$
$dp = \dfrac{NP}{Pnd}$	$DP = \dfrac{ANP}{PND}$
$db = dp \times \cos(\phi_n)$	$DBP = DP \times FNCO$
$d_x = \dfrac{NP}{Pd_x}$	$DXP = \dfrac{ANP}{PDX}$
$\epsilon_{ECP} = \left[\left(\dfrac{domi - 2 \times BRKP}{db}\right)^2 - 1\right]^{1/2}$	$EECP = \left[\left(\dfrac{DOPMI - 2 \times BRKP}{DBP}\right)^2 - 1\right]^{1/2}$
$\epsilon_{BCG} = \left[\left(\dfrac{domi - 2 \times BRKG}{Db}\right)^2 - 1\right]^{1/2}$	$EBCG = \left[\left(\dfrac{DOGMI - 2 \times BRKG}{DBG}\right)^2 - 1\right]^{1/2}$
$\epsilon_{BCP} = \tan \phi_x \times (mg + 1) - \epsilon_{BCG} \times mg$	$EBCP = F \times TA \times (MG + 1) - EBCG \times MG$
$\epsilon_{ECG} = \tan \phi_x \times (Rmg + 1) - \epsilon_{ECP} \times Rmg$	$EECG = F \times TA \times (RMG + 1) - EECP \times RMG$
$d_{BC} = \left[\epsilon_{BCP}^2 + 1\right]^{1/2} \times db$	$DBCP = \left[EBCP^2 + 1\right]^{1/2} \times DBP$
$D_{BC} = \left[\epsilon_{BCG}^2 + 1\right]^{1/2} \times Db$	$DBGG = \left[EBCG^2 + 1\right]^{1/2} \times DBG$
$d_{EC} = \left[\epsilon_{ECP}^2 + 1\right]^{1/2} \times db$	$DECP = \left[EECP^2 + 1\right]^{1/2} \times DBP$

AGMA	Program
$D_{EC} = \left[\epsilon_{ECG}^{2} + 1\right]^{1/2} \times Db$	$DECG = \left[EECG^{2} + 1\right]^{1/2} \times DBG$
See Figure 98.	
$SIN\ (AN) = \dfrac{0.5\ t_c}{0.5\ D}$	$AN = \dfrac{0.5 \times TPMIS}{0.5 \times DP}$
$\widehat{AN} = ARC\ TAN\left(\dfrac{AN}{\sqrt{1 - AN^2}}\right)$	$AN = ATAN\left(\dfrac{AN}{\sqrt{1 - AN^2}}\right)$
$t = \widehat{AN} \times D$	$TPMIS = AN \times DP$
$t_x = D_x\left[\left(\left(\dfrac{t}{D}\right) + INV\phi\right) - INV\ \phi_x\right]$	$TPMIN = D \times P\left[\left(\left(\dfrac{TPMIS}{DP}\right) + ZF\right) - ZFX\right]$
$K = \dfrac{t}{D_x} + INV\ \phi_x$	$K = \dfrac{TPMIN}{DXP} + ZFX$
$\cos \phi_x = \dfrac{D_b}{D_x}$	$F = \dfrac{DB}{DX}$
	where DX = DECP or DBCG
$\phi_x = \text{arc tan}\left(\dfrac{\sqrt{1 - \phi_x^{\ 2}}}{x}\right)$	$FRA = ATAN\left(\dfrac{\sqrt{1 - F^2}}{F}\right)$
$F = \tan\ (\phi_x) - K$	$F = TAN\ (FRA) - K$
$D_V = \dfrac{D_b}{\cos\ (F)}$	$DV = \dfrac{DB}{COS\ (F)}$

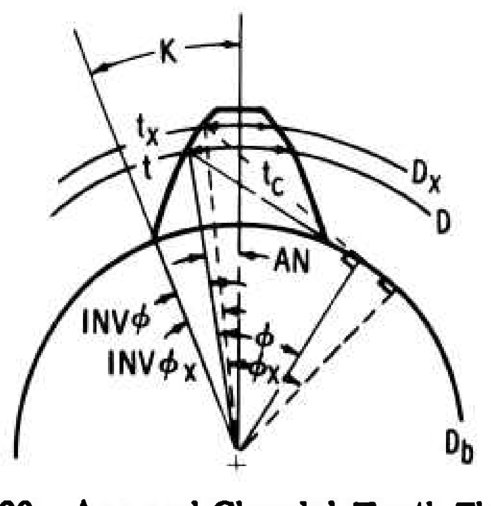

Figure 98. Arc and Chordal Tooth Thickness.

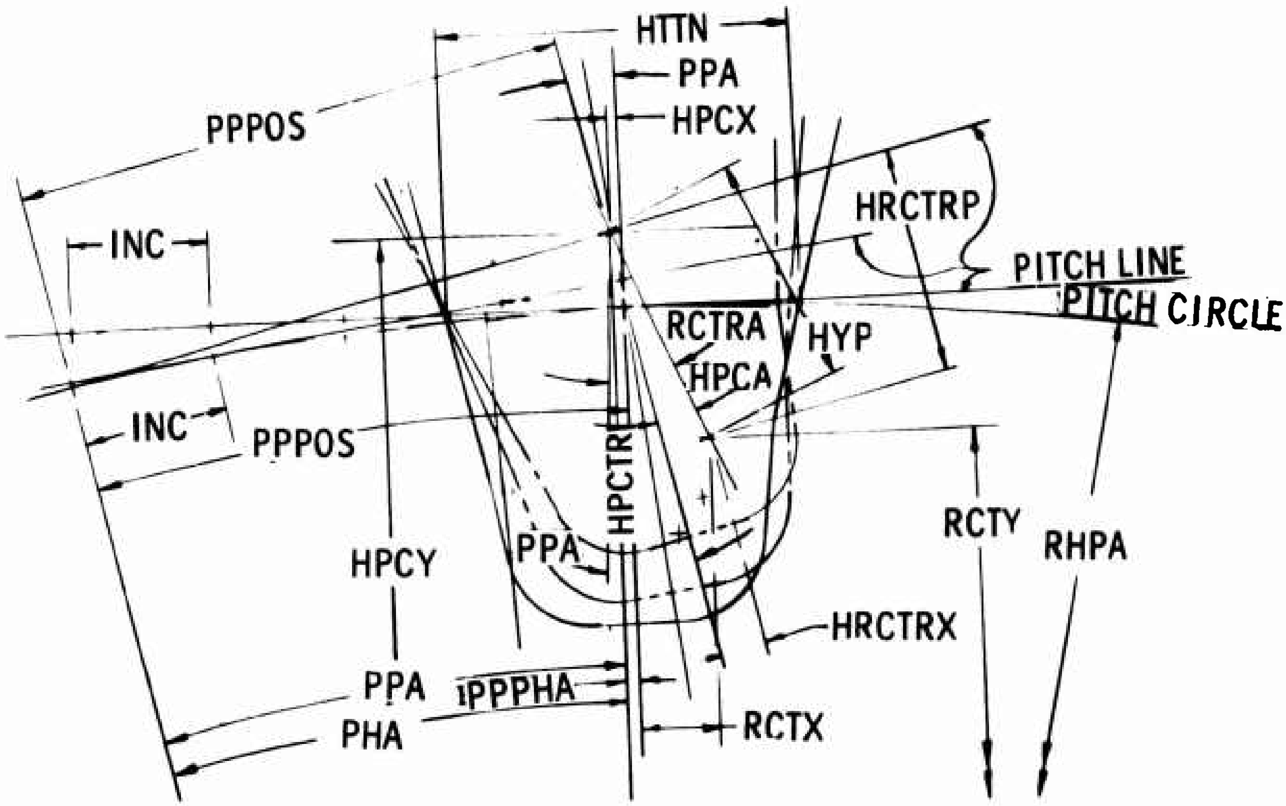

Figure 99. Standard or Protuberance Hob Form For Calculation.

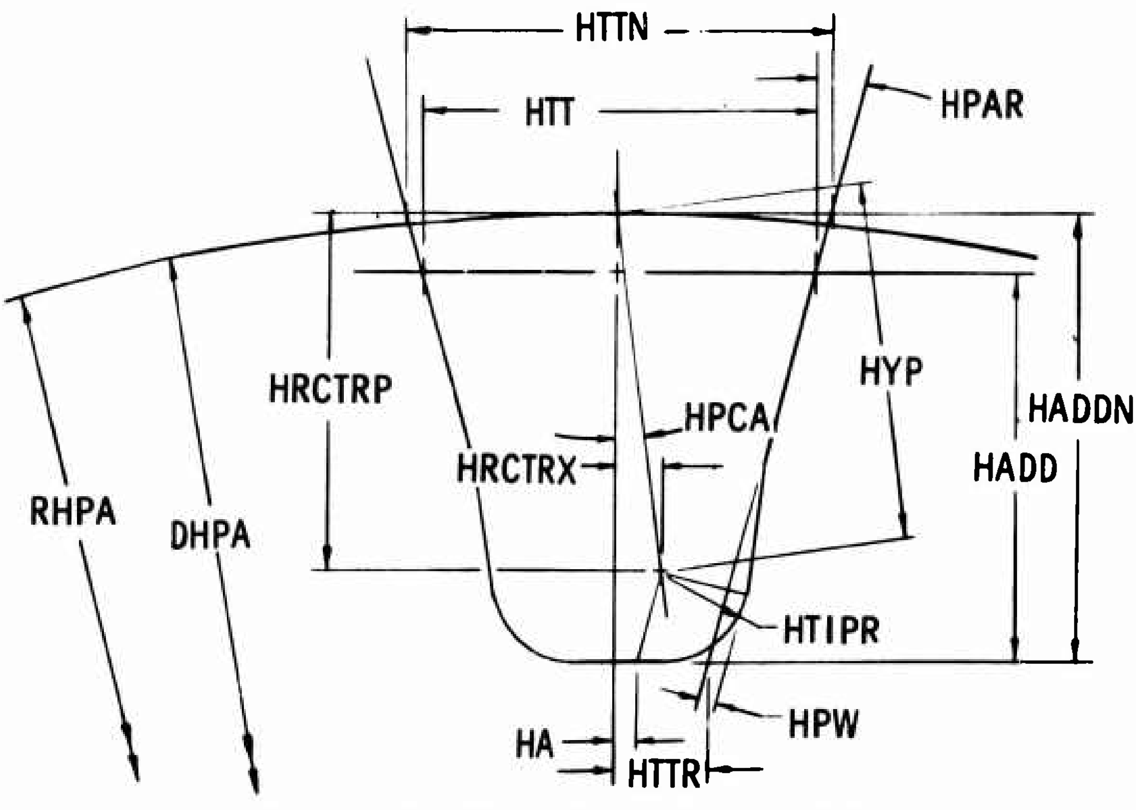

Figure 100. Tooth Generation By Hob.

BLANK PAGE

Program

INC = 0.1 × HTTN (increment of change)

PPPOS = 0 (pitch point position—first time through increase PPPOS by increments each time)

$$\text{PPA} = \frac{\text{PPPOS}}{\text{RHPA}}$$

$$\text{HPCTR} = \sqrt{\text{PPPOS}^2 + \text{RHPA}^2}$$

$$\widehat{\text{PHA}} = \text{ARC TAN}\left(\frac{\text{PPPOS}}{\text{RHPA}}\right)$$

PPPHA = PPA - PHA

HPCX = HPCTR × SIN (PPPHA)

HPCY = HPCTR × COS (PPPHA)

RCTRA = HPCA + PPA

RCTX = HYP × SIN (RCTRA) - HPCX

RCTY = HPCY - HYP × COS (RCTRA)

Calculate points where hot tip radius is making final cut in fillet of gear. See Figure 101.

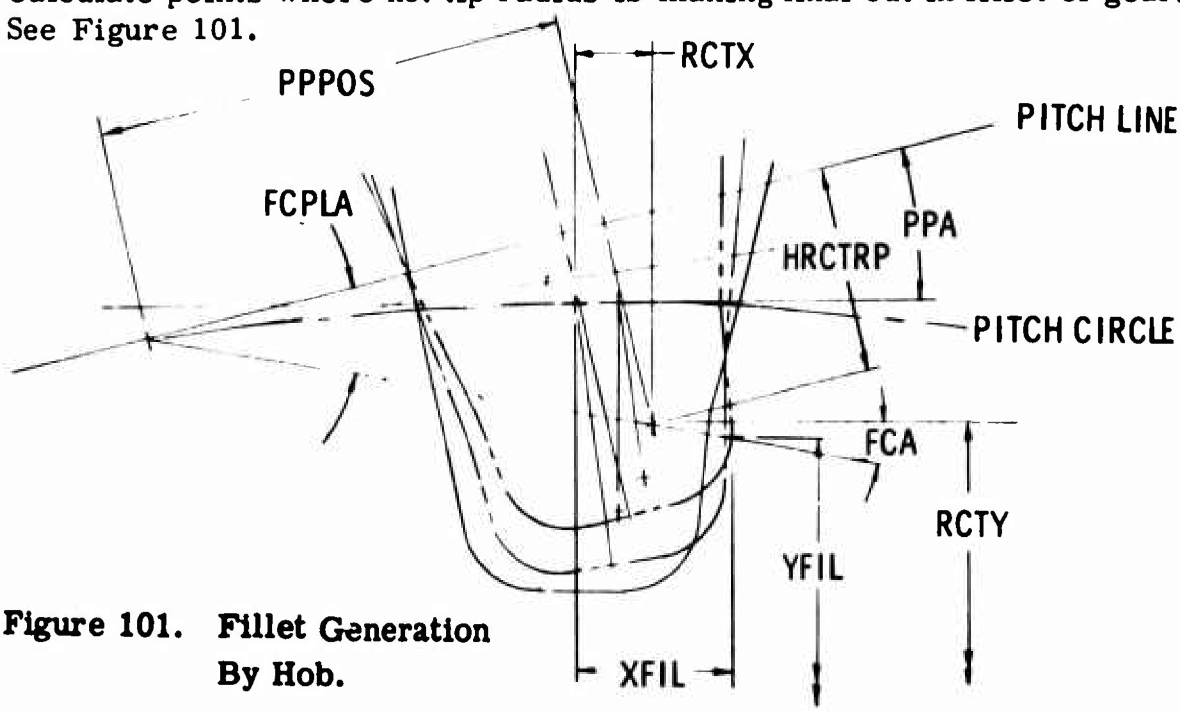

Figure 101. Fillet Generation By Hob.

<u>Program</u>

$$\widehat{FCPLA} = ARC\ TAN\left(\frac{HRCTRP}{PPPOS}\right)$$

$$FCA = FCPLA - PPA$$

$$XFIL = RCTX + HTIPR \times COS\ (FCA)$$

$$YFIL = RCTY - HTIPR \times SIN\ (FCA)$$

Convert location of fillet points from center of tooth space to center of gear tooth. See Figure 102.

$$\widehat{FSA} = ARC\ TAN\left(\frac{XFIL}{YFIL}\right)$$

$$FTA = TSA - \widehat{FSA}$$

$$RFIL = \sqrt{XFIL^2 + YFIL^2}$$

$$XTFIL = RFIL \times SIN\ (FTA)$$

$$YTFIL = RFIL \times COS\ (FTA)$$

Find parabola for evaluating bending stress. See Figure 103.

$$FTCA = \frac{\pi}{2} - TSA$$

$$FTPA = \pi - (FTCA + FCA)$$

$$FPARA = \frac{\pi}{2} - FTPA$$

$$AB = T/TAN\ (FPARA)$$

$$H = 0.5\ DV - YTFIL$$

Reiterate for new T, H, and YTFIL values until AB = 2H is satisfied.

Find the radius of curvature of generated fillet tangent to parabola. See Figure 104.

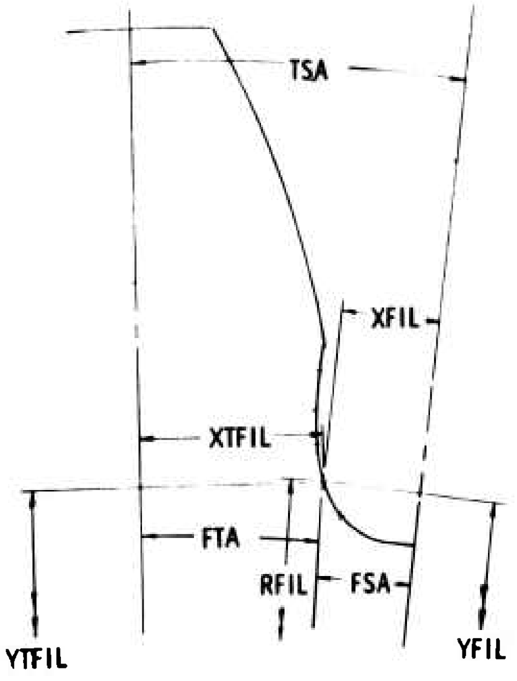

Figure 102. Generated Tooth Fillet.

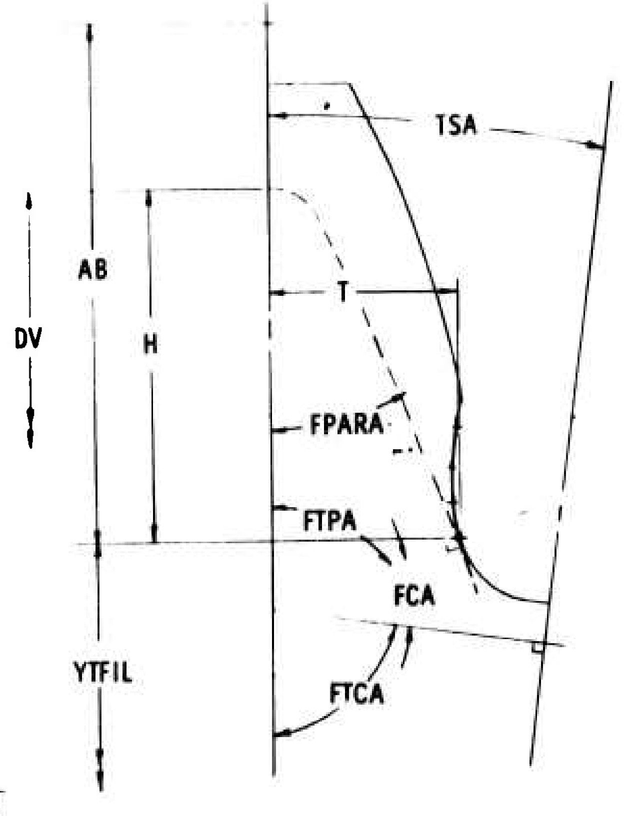

Figure 103. Trochoidal Fillet Inscribed Lewis Parabola.

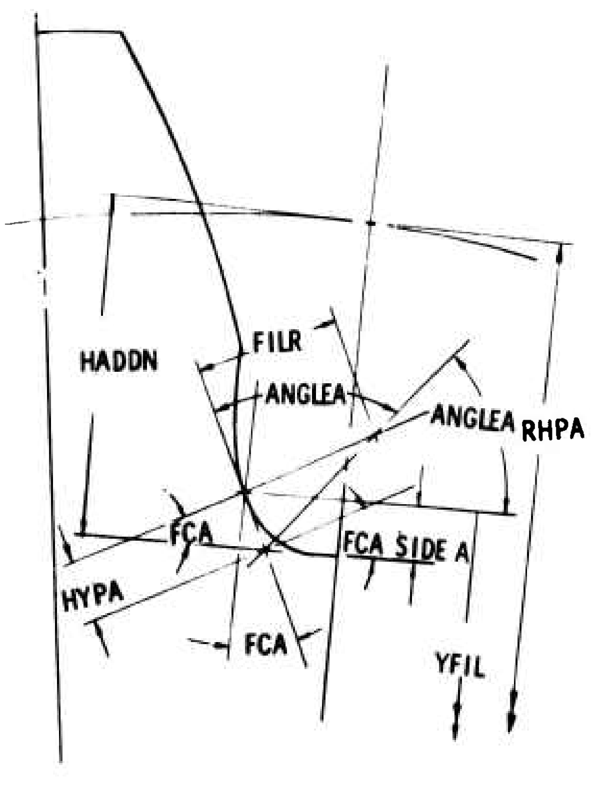

Figure 104. Radius of Curvature at Weakest Section.

Program

SIDEA = YFIL - (RHPA - HADDN)

$$HYPA = \frac{SIDEA}{COS\ (FCA)}$$

$$ANGLEA = 0.5\left(\left(\frac{\pi}{2}\right) + FCA\right)$$

FILR = HYPA × TAN (ANGLEA)

Find X value from parabola and diameter of the weakest section of tooth. See Figure 105.

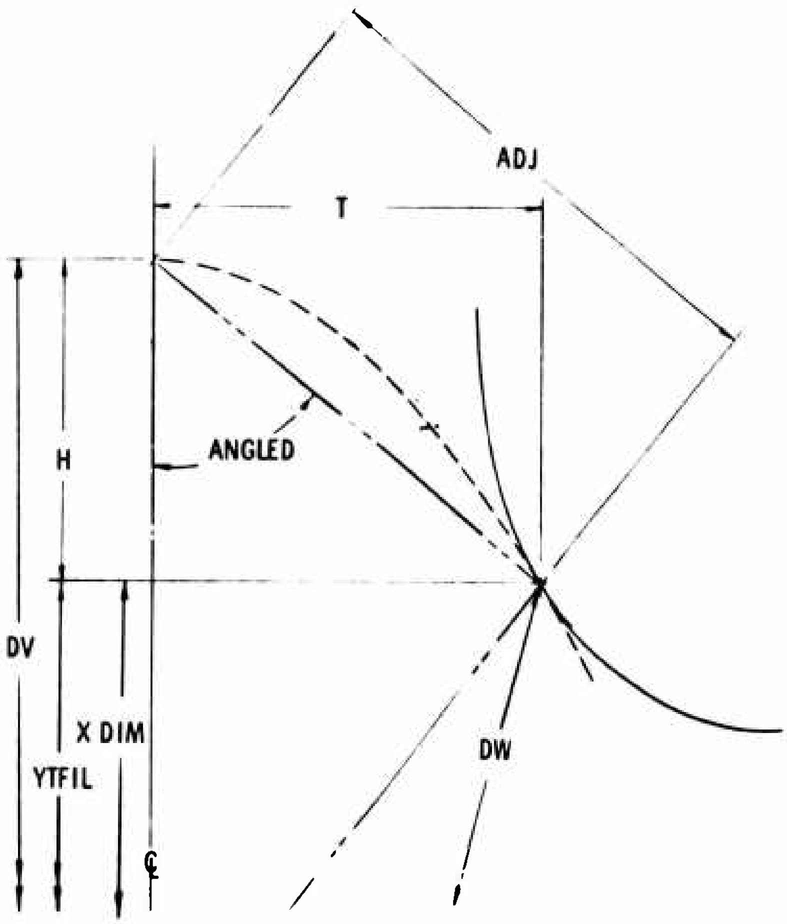

Figure 105. Diameter of Weakest Section and Lewis X Value.

Program

$$ANGLED = ARC\ TAN \left(\frac{T}{H}\right)$$

$$ADJ = \frac{T}{SIN\ (ANGLED)}$$

$$XDIM = \frac{ADJ}{COS\ (ANGLED)} - H$$

$$DW = 2\sqrt{T^2 + YTFIL^2}$$

Find coordinates to center of true fillet radius. See Figures 106 and 107.

$$H = \frac{DR}{2} + RF$$

When $\frac{DB}{2} \leq H$, then (Figure 106):

$$CPR = \frac{0.5\ DB}{H}$$

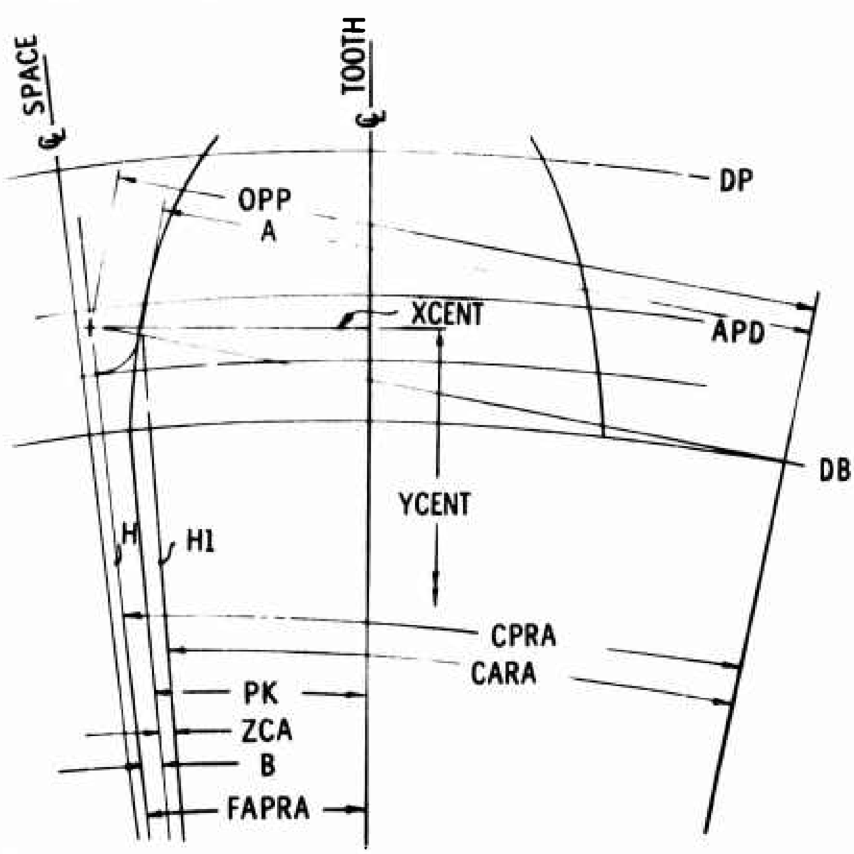

Figure 106. Coordinates at Center of True Fillet Radius—Base Circle Below Root Diameter.

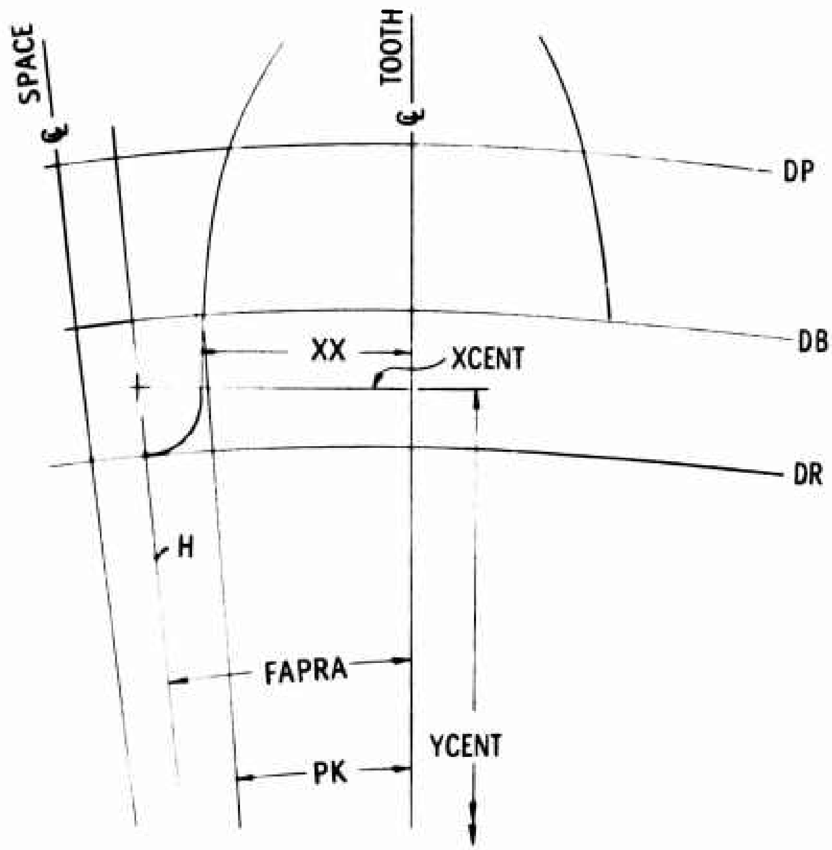

Figure 107. Coordinates at Center of True Fillet Radius—Base Circle Above Root Diameter.

<u>Program</u>

$$CPRA = ARC\ TAN \left(\frac{\sqrt{1 - CPR^2}}{CPR} \right)$$

$$OPP = \sqrt{H^2 - (0.5\ DB)^2}$$

$$A = OPP - RF$$

$$H1 = \sqrt{A^2 + (0.5\ DB)^2}$$

$$CA = \frac{0.5\ DB}{H1}$$

$$CARA = ARC\ TAN \left(\frac{\sqrt{1 - CA^2}}{CA} \right)$$

Program

$$ZCA = TAN\ (CARA) - \widehat{CARA}$$

$$B = CPRA - CARA - ZCA$$

$$FAPRA = PK + B$$

$$XCENT = SIN\ (FAPRA) \times H$$

$$YCENT = COS\ (FAPRA) \times H$$

When $\frac{DB}{2} > H$, then (Figure 107):

$$XX = \left(\frac{DB}{2}\right) SIN\ (PK)$$

$$FAPSI = \frac{XX + RF}{H}$$

$$FAPRA = ARC\ TAN\left(\frac{FAPSI}{\sqrt{1 - FAPSI^2}}\right)$$

$$XCENT = SIN\ (FAPRA) \times H$$

$$YCENT = COS\ (FAPRA) \times H$$

Find parabola for evaluating bending stress. Also, find X value and diameter of weakest section. See Figure 108.

$ALPHA = 0.1$ (First time only)

$$V = SIN\ (ALPHA) \times RF$$

$$VI = \sqrt{RF^2 - V^2}$$

$$T = XCENT - VI$$

$$YA = \frac{T}{TAN\ (ALPHA)}$$

$$H = (RV - YCENT) + V$$

Reiterate for new value of ALPHA until YA = 2H is satisfied.

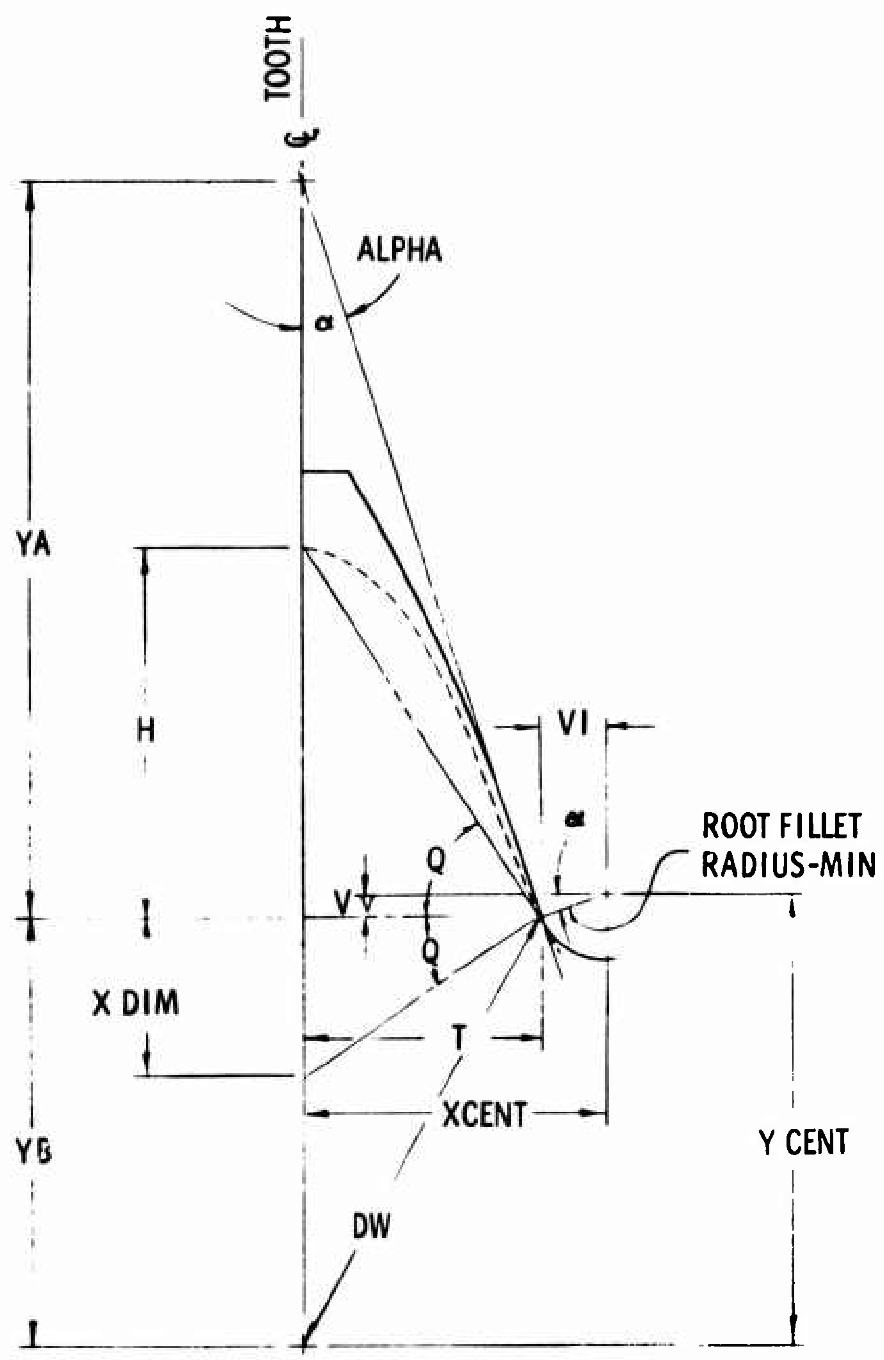

Figure 108. True Fillet Radius Inscribed Lewis Parabola.

<u>Program</u>

$$YB = YCENT - V$$

$$DW = \sqrt{YB^2 + T^2} \times 2$$

Program

$$Q = \text{ARC TAN}\left(\frac{H}{T}\right)$$

$$Q = \frac{\pi}{2} - Q$$

$$\text{XDIM} = T \times \text{TAN}(Q)$$

AGMA	Program
$T = \dfrac{63025 \times HP}{\eta_p}$	$TQ = \dfrac{63025 \times HORSES}{RPMP}$
$Wt = \dfrac{2 \times T}{\eta_p}$	$WT = \dfrac{2 \times TQ}{RPMP}$
$G = \eta_p \times R\, mg$	$RPMG = RPMP \times RMG$
$S_h = \dfrac{\rho V^2}{g}$	$SHOOP = RHO\ \dfrac{V^2}{386.064}$
$b_1 = b - r_T$	$B1 = HADD - HTIPR$
$r_1 = \dfrac{b_1^2}{Rp + b_1}$	$R1 = \dfrac{B1^2}{RP + B1}$
$r_f = r_1 + r_T$	$RFMI = R1 + HTIPR$
$K_f = 0.22 + \left(\dfrac{T}{r_f}\right)^{0.20} \left(\dfrac{T}{h}\right)^{0.40}$	$KF = 0.22 + \left(\dfrac{T}{RFMI}\right)^{0.20} \left(\dfrac{T}{H}\right)^{0.40}$
$K_f = 0.18 + \left(\dfrac{T}{r_f}\right)^{0.15} \left(\dfrac{T}{h}\right)^{0.45}$	$KF = 0.18 + \left(\dfrac{T}{RFMI}\right)^{0.15} \left(\dfrac{T}{H}\right)^{0.45}$
$K_f = 0.14 + \left(\dfrac{I}{r_f}\right)^{0.11} \left(\dfrac{T}{h}\right)^{0.50}$	$KF = 0.14 + \left(\dfrac{T}{RFMI}\right)^{0.11} \left(\dfrac{T}{H}\right)^{0.50}$
$Y = \dfrac{PDX}{\dfrac{\cos \phi_{Ln}}{\cos \phi_n}\left[\dfrac{1.5}{X} - \dfrac{\tan \phi_{Ln}}{Tw}\right]}$	$Y = \dfrac{PDX}{\dfrac{COS\,\phi L}{COS\,\phi N}\left[\dfrac{1.5}{XDIM} - \dfrac{TAN\,\phi L}{TW}\right]}$
$J = \dfrac{Y \cos^2 \psi}{K_f \times m_n}$	$J = \dfrac{Y\, COS^2\, (\psi)}{KF \times MN}$
$S_t = \dfrac{1}{C_H}\ \dfrac{Wt\ Ko}{Kv}\ \dfrac{PD}{F}\ \dfrac{KS\ KM}{J}$	$SB = \dfrac{1}{CH}\ \dfrac{WT \times KO}{[illegible]}\ \dfrac{PD}{FMINP}\ \dfrac{KS \times KM}{J}$

C_H = a factor calculated by the principle of superposition of the moment image Cantilever Plate bending moment distribution curves as proposed by Wellauer and Seireg.[1] This procedure is based on the work done by Jaramillo[4] to determine bending moment distribution in a loaded Cantilever Plate. See Figure 109.

SOURCE PROGRAM LISTING

The source program is listed on the following pages. Comment cards have been used to define generated symbols within the program. Several subroutines are used and are also listed.

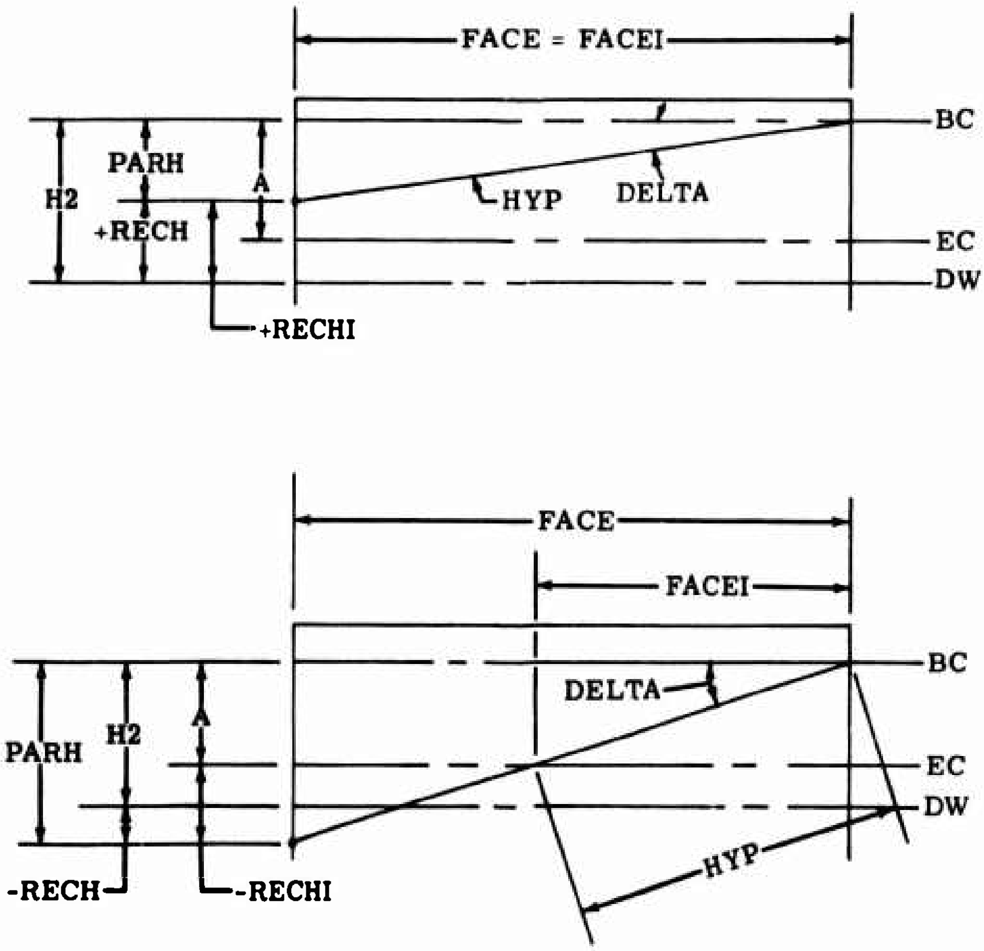

DELTA = ATAN (TAN (ψ) x SIN (ϕ_n))
H2 = (DBC - DW) x 0.5
HYP = FACE/COS (DELTA)
PARH = HYP x SIN (DELTA)

RECH = H2 - PARH
A = (DBC - DEC) x 0.5
RECH1 = A - PARH

When A is larger than RECH1, FACE1 = FACE
When A is less than RECH1, FACE1 = A x TAN (DELTA), and
HYP = FACE1/COS (DELTA)

Figure 109. Determination of Maximum Bending Moment.

SOURCE PROGRAM PRINT-OUT

```
                C             * * * * * * * * * * * * * * * *
                C             * BENDING STRESS FOR HELICAL    *
                C             * GEARS                         *
                C             *                               *
                C             * PROGRAM BY M.R. CHAPLIN       *
                C             * ALLISON,DIV. GMC.             *
                C             * * * * * * * * * * * * * * * *
                C
0001                  DIMENSION XDIMP(6),DWP(6),TWP(6),HP(6),ALPHP(6),
                     *XDIMG(6),DWG(6),TWG(6),HG(6),ALPHG(6)
0002                  DIMENSION XCYC(4),YPSI(4),DVP(6),RVP(6),DVG(6),RVG(6)
0003                  REAL JP,JG,MG,KO,KV,KS,NP,NG,KFP,KFG,KM,MN,KT,KR
0004                  COMMON RHPA,HPCA,HYP,HRCTRP,TSA,FCA,YFIL,STA,FNSI
0005                  DATA PIN,ION,GE,AR /3HPIN,3HION,3HGEA,3HR   /
0006                  DATA SHA,PED,HOB,BED /3HSHA,3HPED,3HHOB,3HBED/
0007                  DATA XCYC /4.,5.,6.,7./
0008                  DATA YPSI /193000.,175000.,165000.,162000./
0009                  LIN=5
0010                  LOU=6
0011                1 READ (LIN,2) ANP,ANG,CSTD,CNSTD,HORSES,RPMP,KO,KV,KS,KM,
                     *PHIN,PND,PSI,BMIN,BMAX,FMINP,FMING,BRKP,BRKG,
                     *DOPMI,DOGMI,DRPMI,DRGMI,TPMIS,TGMIS,L,
                     *CUT,TER,M,RFMIP,RFMIG,UCP,UCG,KT,KR,MN,RHO
                C
0012                  IF (CUT.EQ.SHA)           GO TO 16
0013                  IF (M - 1)                10,12,14
0014               10 READ (LIN,4) HTTP,HADDP,HLFADP,HPAP,HTIPRP,PROTP
0015                  GO TO 16
0016               12 READ (LIN,4) HTTG,HADDG,HLEADG,HPAG,HTIPRG,PROTG
0017                  GO TO 16
0018               14 READ (LIN,4) HTTP,HADDP,HLEADP,HPAP,HTIPRP,PROTP
0019                  READ (LIN,4) HTTG,HADDG,HLEADG,HPAG,HTIPRG,PROTG
0020                2 FORMAT (2F5.0,4F10.0,4F5.0/3F10.0,2F5.0,2F10.0,2F5.0/
                     *6F10.0,I2/A3,A3,I2,2X,4F10.0,3F5.0,F7.0)
0021                4 FORMAT (6F10.0)
```

```
C
   16 PI=3.1415926536
      RN=PI/180.
      DEGR=180./PI
      FNRA=PHIN*RN
      SRA=PSI*RN
      FNSI=SIN(FNRA)
      FNCO=COS(FNRA)
      FNTA=FNSI/FNCO
      ZFN=FNTA-FNRA
      SSI=SIN(SRA)
      SCO=COS(SRA)
      STA=SSI/SCO
      NP=ANP
      NG=ANG
      NPA=NP
      NGA=NG
      IF(CUT.EQ.SHA) GO TO 601
      RFMIP=0.
      RFMIG=0.
  601 WRITE (LOU,1000) NPA,NGA,CSTD,CNSTD,HORSES,RPMP,KO,KV,KS,KM,
     *PHIN,PND,PSI,BMIN,BMAX,FMINP,FMING,BRKP,BRKG
      IF (L)   602,600,602
  600 WRITE (LOU,1002)
      GO TO 604
  602 WRITE (LOU,1003)
  604 CONTINUE
      WRITE (LOU,1004) DOPMI,DOGMI,DRPMI,DRGMI,TPMIS,TGMIS,L,
     *CUT,TER,M,RFMIP,RFMIG,UCP,UCG,KT,KR,MN,RHO
      IF (CUT.EQ.SHA)       GO TO 650
      WRITE (LOU,1006)
      IF (M - 1)            606,608,610
  606 WRITE (LOU,1008) PIN,ION,HTTP,HADDP,HLEADP,HPAP,HTIPRP,PROTP
      GO TO 650
  608 WRITE (LOU,1008) GE,AR,HTTG,HADDG,HLEADG,HPAG,HTIPRG,PROTG
      GO TO 650
  610 WRITE (LOU,1008) PIN,ION,HTTP,HADDP,HLEADP,HPAP,HTIPRP,PROTP
```

```
      WRITE (LOU,1008) GE,AR,HTTG,HADDG,HLEADG,HPAG,HTIPRG,PROTG
  650 CONTINUE
C
      PDX=(NP&NG)/(2.*CNSTD)
      SI=(PDX/PND)*STA
      SI=ATAN(SI/(SQRT(1.-SI**2)))
      PD=PND*COS(SI)
      FRA=ATAN(FNTA/COS(SI))
      ZF=TAN(FRA)-FRA
      PHI=FRA*DEGR
      FX=(CSTD*COS(FRA))/CNSTD
      FXRA=ATAN(SURT(1.-FX**2)/FX)
      FXSI=SIN(FXRA)
      FXCO=COS(FXRA)
      FXTA=FXSI/FXCO
      PHIX=FXRA*DEGR
      ZFX=FXTA-FXRA
      PN=PI/PND
      P=PI/PD
      PX=PI/PDX
      PBN=(PI*FNCO)/PND
      PB= (PI*COS(FRA))/PD
      PBX=(PI*FXCO)/PDX
C
      DP=NP/PD
      DBP=DP*COS(FRA)
      DXP=NP/PDX
      DG=NG/PD
      DBG=DG*COS(FRA)
      DXG=NG/PDX
C
C        EPSILON ANGLFS AT THE ENGAGEMENT CONDITIONS
C
      EECP=SQRT(((DOPMI-2.*BRKP)/DBP)**2-1.)
      EBCG=SQRT(((DOGMI-2.*BRKG)/DBG)**2-1.)
      MG=ANG/ANP
      RMG=ANP/ANG
      EBCP=(FXTA*(MG&1.))-(EBCG*MG)
```

```
      EECG=(FXTA*(RMG&1.))-(EECP*RMG)
      DBCP=SQRT(EBCP**2&1.)*DBP
      DBCG=SQRT(EBCG**2&1.)*DBG
      DECP=SQRT(EECP**2&1.)*DBP
      DECG=SQRT(EECG**2&1.)*DBG
C
      IF (L)               80,82,80
C
C       CALCULATE ARC TOOTH THK FROM CHORDAL THK  (IF L = 1)
C
   80 AN=(.5*TPMIS)/(.5*DP)
      AN=ATAN(AN/(SQRT(1.-AN**2)))
      TPMIS=AN*DP
      AN=(.5*TGMIS)/(.5*DG)
      AN=ATAN(AN/(SQRT(1.-AN**2)))
      TGMIS=AN*DG
C
C       CALCULATE ARC TOOTH THK AT THE OPERATING PITCH DIA  --DX
C
   82 TPMIN=DXP*(((TPMIS/DP)&ZF )-ZFX)
      TGMIN=DXG*(((TGMIS/DG)&ZF )-ZFX)
      PK=(TPMIN/DXP)&ZFX
      GK=(TGMIN/DXG)&ZFX
C
      F=DBP/DECP
      FPRA=ATAN(SQRT(1.-F**2)/F)
      F=DBG/DBCG
      FGRA=ATAN(SQRT(1.-F**2)/F)
      F=TAN(FPRA)-PK
      DVP(1)=DBP/COS(F)
      RVP(1)=DVP(1)*.5
      F=TAN(FGRA)-GK
      DVG(1)=DBG/COS(F)
      RVG(1)=DVG(1)*.5
      FPDE=FPRA*DEGR
      FGDE=FGRA*DEGR
      IF (CUT.EQ.SHA)          GO TO 50
```

```
0118           IF (M - 1)              40,42,44
0119        40 CALL HOBB(DRPMI,ANP,DVP(1),HTTP,HADDP,HLEADP,HPAP,HTIPRP,PROTP,
              *XDIMP,DWP,TWP,HP,PI,RN,1,ALPHP,SCO)
0120           GO TO 46
0121        42 CALL HOBB(DRGMI,ANG,DVG(1),HTTG,HADDG,HLEADG,HPAG,HTIPRG,PROTG,
              *XDIMG,DWG,TWG,HG,PI,RN,1,ALPHG,SCO)
0122           GO TO 48
0123        44 CALL HOBB(DRPMI,ANP,DVP(1),HTTP,HADDP,HLEADP,HPAP,HTIPRP,PROTP,
              *XDIMP,DWP,TWP,HP,PI,RN,1,ALPHP,SCO)
0124           CALL HOBB(DRGMI,ANG,DVG(1),HTTG,HADDG,HLEADG,HPAG,HTIPRG,PROTG,
              *XDIMG,DWG,TWG,HG,PI,RN,1,ALPHG,SCO)
0125           GO TO 52
0126        46 CALL XY (DBG,DRGMI,RFMIG,GK,XCENG,YCENG,0)
0127           RFMG=RFMIG&UCG
0128           CALL WEAK (RVG,XCENG,YCENG,RFMG,DBG,GK,TWG,HG,DWG,XDIMG,
              *ALPHG,1,0)
0129           GO TO 52
0130        48 CALL XY (DBP,DRPMI,RFMIP,PK,XCENP,YCENP,0)
0131           RFMP=RFMIP&UCP
0132           CALL WEAK (RVP,XCENP,YCENP,RFMP,DBP,PK,TWP,HP,DWP,XDIMP,
              *ALPHP,1,0)
0133           GO TO 52
0134        50 CALL XY (DBP,DRPMI,RFMIP,PK,XCENP,YCENP,0)
0135           CALL XY (DBG,DRGMI,RFMIG,GK,XCENG,YCENG,0)
0136           RFMP=RFMIP&UCP
0137           RFMG=RFMIG&UCG
0138           CALL WEAK (RVP,XCENP,YCENP,RFMP,DBP,PK,TWP,HP,DWP,XDIMP,
              *ALPHP,1,0)
0139           CALL WEAK (RVG,XCENG,YCENG,RFMG,DBG,GK,TWG,HG,DWG,XDIMG,
              *ALPHG,1,0)
0140        52 CONTINUE
         C
0141           CORDP=SIN(PK-(TAN(FPRA)-FPRA))*DBCP
0142           CORDG=SIN(GK-(TAN(FGRA)-FGRA))*DBCG
0143           CALL FACTOR (DECP,DBCP,DWP(1),FMINP,CHP)
0144           CALL FACTOR (DBCG,DECG,DWG(1),FMING,CHG)
0145           IPHI=PHIN
```

```
0146          FLN=TAN(FPRA)-PK
0147          A=COS(FLN)/FNCO
0148          B=1.5/XDIMP(1)
0149          C=TAN(FLN)/(TWP(1)*2.0)
        C
0150          YCP=PDX/(A*(B-C))
        C
0151          FLNG=TAN(FGRA)-GK
0152          A=COS(FLNG)/FNCO
0153          B=1.5/XDIMG(1)
0154          C=TAN(FLNG)/(TWG(1)*2.0)
        C
0155          YCG=PDX/(A*(B-C))
        C
0156          IF (CUT.EQ.SHA)      GO TO 406
0157          IF (M - 1)            402,404,400
0158      400 B1=HADDP-HTIPRP
0159          R1=B1**2/((DP*.5)&B1)
0160          RFMIP=R1&HTIPRP
0161      404 B1=HADDG-HTIPRG
0162          R1=B1**2/((DG*.5)&B1)
0163          RFMIG=R1&HTIPRG
0164          GO TO 406
0165      402 B1=HADDP-HTIPRP
0166          R1=B1**2/((DP*.5)&B1)
0167          RFMIP=R1&HTIPRP
0168      406 IF (IPHI-20)          408,412,416
0169      408 KFP=.22&(((TWP(1)*2.)/RFMIP)**.20*((TWP(1)*2.)/HP(1))**.40)
0170          KFG=.22&(((TWG(1)*2.)/RFMIG)**.20*((TWG(1)*2.)/HG(1))**.40)
0171          GO TO 420
0172      412 KFP=.18&(((TWP(1)*2.)/RFMIP)**.15*((TWP(1)*2.)/HP(1))**.45)
0173          KFG=.18&(((TWG(1)*2.)/RFMIG)**.15*((TWG(1)*2.)/HG(1))**.45)
0174          GO TO 420
0175      416 KFP=.14&(((TWP(1)*2.)/RFMIP)**.11*((TWP(1)*2.)/HP(1))**.50)
0176          KFG=.14&(((TWG(1)*2.)/RFMIG)**.11*((TWG(1)*2.)/HG(1))**.50)
        C
0177      420 JP=YCP*SCO**2/(KFP*MN)
```

```
0178          JG=YCG*SCO**2/(KFG*MN)
           C
0179          TQP=(63025.*HORSES)/RPMP
0180          RPMG=RPMP*RMG
0181          TQG=(63025.*HORSES)/RPMG
0182          WTP=(2.*TQP)/DXP
0183          WTG=(2.*TQG)/DXG
           C
0184          SBP=(WTP*KO/KV) * (PDX/FMINP) * ((KS*KM)/JP) *(1.0/CHP)
0185          SBG=(WTG*KO/KV) * (PDX/FMING) * ((KS*KM)/JG) * (1.0/CHG)
0186     1000 FORMAT (1H123X32HSTD AND NON STD EXTERNAL HELICAL/24X26HGEARS - MA
             *X BENDING STRESS///19X35HI N P U T   D A T A   S E C T I O N//
             *5X12HNO. OF TEETH5X15HCENTER DISTANCE5X10HHORSEPOWER3X10HRPM-PINIO
             *N5X2HKO9X2HKV9X2HKS9X2HKM/5X12HPINION  GEAR5X3HSTD6X7HNON STD/
             *5XI4,3XI4,F12.6,F11.6,F13.6,F11.2,F12.6,3F11.6,//8X12HNORMAL PLANE
             *9X5HHELIX8X8HBACKLASH8X16HFACE WIDTH - MIN6X13HMAX TIP BREAK/
             *7X5HPHI N6X3HPND8X5HANGLE6X3HMIN6X3HMAX6X6HPINION6X4HGEAR5X6HPINIO
             *N6X4HGEAR/F14.6,F10.6,F12.6,2F9.4,F11.6,F12.6,F11.6,F10.6)
0187     1002 FORMAT (/5X17HOUTSIDE DIA - MIN8X14HROOT DIA - MIN9X13HARC TOOTH T
             *HK9X1HL)
0188     1003 FORMAT (/5X17HOUTSIDE DIA - MIN8X14HROOT DIA - MIN7X17HCHORDAL TOO
             *TH THK7X1HL)
0189     1004 FORMAT (6X6HPINION6X4HGEAR6X6HPINION7X4HGEAR6X6HPINION7X4HGEAR/
             *F14.6,F10.6,F12.6,F11.6,F12.6,F11.6,4XI2//5X15HSHAPED OR     M8X19
             *HROOT FILLET RAD-MIN7X12HMAX UNDERCUT9X2HKT8X2HKR8X2HMN6X7HDENSITY
             */5X6HHOBBED17X6HPINION7X4HGEAR6X6HPINION7X4HGEAR35X9HLB/CU.IN./
             *5X2A3,7XI2,F15.5,F12.5,F12.6,F11.6,4F10.5)
0190     1006 FORMAT (//5X16H--- HOB DATA ---)
0191     1008 FORMAT (/14X2A3//8X3HHTT7X4HHADD9X4HLEAD6X3HHPA8X5HHTIPR7X3HHPW/
             *F13.5,F11.5,F12.5,F11.4,F11.5,F11.5)
0192          WRITE (LOU,1010) PHIX,P,PDX,DXP,DXG,DBP,DBG,DBCP,DBCG,
             *DECP,DECG,DWP(1),DWG(1),TPMIN,TGMIN,CHP,CHG,YCP,YCG,KFP,KFG,
             *JP,JG,SBP,SBG
0193          VP=PI*DRPMI*(RPMP/60.)
0194          SHOOPP=RHO*(VP**2/386.064)
0195          VG=PI*DRGMI*(RPMG/60.)
0196          SHOOPG=RHO*(VG**2/386.064)
```

```
      SBPHO =SBP&SHOOPP
      SBGHO =SBG&SHOOPG
      HOOPMA=274000.0
      DIFFP=HOOPMA-SBPHO
      DIFFG=HOOPMA-SBGHO
      EP=HOOPMA-SHOOPP
      EG=HOOPMA-SHOOPG
      AP=(HOOPMA*DIFFP)/EP
      AG=(HOOPMA*DIFFG)/EG
      SBPHOP=(HOOPMA-AP)*KT*KR
      SBGHOG=(HOOPMA-AG)*KT*KR
C
      IF (SBPHOP-274000.)     526,526,524
  524 WRITE (LOU,2003) PIN,ION
  526 IF (SBGHOG-274000.)     530,530,528
  528 WRITE (LOU,2003) GE,AR
  530 IF (SBPHOP-175000.)     624,624,626
  624 WRITE (LOU,2008) PIN,ION
      GO TO 628
  626 CALL DISCOT (SBPHOP,DUMA,YPSI,XCYC,DUMB,-31,4,0,EXP)
  628 IF (SBGHOG-175000.)     630,630,632
  630 WRITE (LOU,2008) GE,AR
      GO TO 609
  632 CALL DISCOT (SBGHOG,DUMA,YPSI,XCYC,DUMB,-31,4,0,EXG)
  609 CONTINUE
C
 2003 FORMAT (///5X15HBENDING STRESS ,2A3, 9H AT HPC  /4X31HFXCEEDS ULTI
     *MATE OF 274000. PSI)
 2008 FORMAT (///5X15HBENDING STRESS ,2A3,16H-AT HPC IS LESS /4X
     *56HTHAN THE ENDURANCE LIMIT OF 175000. PŠI - INFINITE LIFE.)
C
C
      WRITE (LOU,2009) SBPHOP,SBGHOG
C
 2009 FORMAT (//12X25HBENDING STRESS (COMBINED)//23X8HBC (HPC)F14.2,
     *F13.2)
```

```
0225      1010 FORMAT (1H118X35H*----  O U T P U T   D A T A  ----*///9X
               *14HTOOTH GEOMETRY//12X19HPHI  (PRESSURE ANGLE/17X21HTRANSVERSE PLAN
               *E)   =F10.5/ 12X14HCIRCULAR PITCH11X1H=F10.5/ 12X15HDIAMETRAL PITC
               *H10X1H=F10.5//41X6HPINION8X4HGEAR/12X9HPITCH DIAF27.5,F13.5/
               *12X15HBASE CIRCLE DIAF21.5,F13.5/12X17HBEGIN CONTACT DIAF19.5,
               *F13.5/12X17HEND   CONTACT DIAF19.5,F13.5/12X
               *19HWEAKEST SECTION DIAF17.5,F13.5//12X16HARC TOOTH THK AT/12X
               *12HOPERATING DPF24.5,F13.5/12X2HCHF34.5,F13.5/12X
               *2HYCF34.5,F13.5/12X2HKFF34.5,F13.5/12X1HJF35.5,F13.5///12X
               *14HBENDING STRESS//23X8HBC (HPC)F14.2,F13.2)
0226            GO TO 1
0227            END
0001            SUBROUTINE FACTOR (DIAH,DIAL,DW,FACE,CH)
0002            DIMENSION Z(11),XARG(20)
0003            DIMENSION X(6),ELL(5),Y(30)
0004            DIMENSION YANS1(10),YANS2(10),YANS3(10),YANS4(10),YANS5(10),
               *YANS6(10),YANS7(10),YANS8(10),YANS9(10),YANS10(10),YANSS(10)
0005            DATA  X / 0.,.25,.5,1.,1.5,2./
0006            DATA ELL/ 0.,.25,.5,.75,1./
0007            DATA  Y / 0.,0.,0.,0.,0.,0.,
               *.325,.174,.074,.022,.0075,.0026,
               *.370,.302,.196,.076,.0290,.0108,
               *.428,.385,.298,.140,.0590,.0230,
               *.509,.474,.390,.205,.0910,.0370/
0008            COMMON RHPA,HPCA,HYP,HRCTRP,TSA,FCA,YFIL,STA,FNSI
          C
0009            DELTA=ATAN(STA*FNSI)
0010            H2=DIAH*.5-DW*.5
0011            HYP=FACE/COS(DELTA)
0012            PARH=HYP*SIN(DELTA)
0013            RECH=H2-PARH
0014            A=(DIAH-DIAL)*.5
0015            RECH1=A-PARH
0016            IF (A-RECH1)          40,30,30
0017        30  FACE1=FACE
0018            GO TO 50
0019        40  FACE1=A*TAN(DELTA)
```

```
      IF(H2-RECH)              45,50,50
   45 RECH=0.
   50 HYP=FACE1/COS(DELTA)
      ENDD=.05*HYP
      DEC=(HYP-(2.*ENDD))/9.
      SIDE=ENDD
      DO 54 I=1,10
      C=RECH&(SIDE*SIN(DELTA))
      Z(I)=C/H2
   54 SIDE=SIDE&DEC
      XARG(1)=0.
      DO 100 I=1,9
      CALL DISCOT (XARG(I),Z(1),X,Y,ELL,&33,30,5,YANS1(I))
  100 XARG(I&1)=XARG(I)&DEC
      XARG(1)=0.
      DO 105 I=1,9
      CALL DISCOT (XARG(I),Z(2),X,Y,ELL,&33,30,5,YANS2(I))
  105 XARG(I&1)=XARG(I)&DEC
      XARG(1)=0.
      DO 110 I=1,9
      CALL DISCOT (XARG(I),Z(3),X,Y,ELL,&33,30,5,YANS3(I))
  110 XARG(I&1)=XARG(I)&DEC
      XARG(1)=0.
      DO 115 I=1,9
      CALL DISCOT (XARG(I),Z(4),X,Y,ELL,&33,30,5,YANS4(I))
  115 XARG(I&1)=XARG(I)&DEC
      XARG(1)=0.
      DO 120 I=1,9
      CALL DISCOT (XARG(I),Z(5),X,Y,ELL,&33,30,5,YANS5(I))
  120 XARG(I&1)=XARG(I)&DEC
      XARG(1)=0.
      DO 125 I=1,9
```

```
      CALL DISCOT (XARG(I),Z(6),X,Y,ELL,&33,30,5,YANS6(I))
  125 XARG(I&1)=XARG(I)&DEC
      XARG(1)=0.
      DO 130 I=1,9
      CALL DISCOT (XARG(I),Z(7),X,Y,ELL,&33,30,5,YANS7(I))
  130 XARG(I&1)=XARG(I)&DEC
      XARG(1)=0.
      DO 135 I=1,9
      CALL DISCOT (XARG(I),Z(8),X,Y,ELL,&33,30,5,YANS8(I))
  135 XARG(I&1)=XARG(I)&DEC
      XARG(1)=0.
      DO 140 I=1,9
      CALL DISCOT (XARG(I),Z(9),X,Y,ELL,&33,30,5,YANS9(I))
  140 XARG(I&1)=XARG(I)&DEC
      XARG(1)=0.
      DO 145 I=1,9
      CALL DISCOT (XARG(I),Z(10),X,Y,ELL,&33,30,5,YANS10(1..
  145 XARG(I&1)=XARG(I)&DEC
      TOT1=(YANS1(1)&YANS2(2)&YANS3(3)&YANS4(4)&YANS5(5)
     *&YANS6(6)&YANS7(7)&YANS8(8)&YANS9(9)&YANS10(10))*2.
      XARG(1)=0.
      DO 200 I=1,9
      CALL DISCOT (XARG(I),1.0,X,Y,ELL,&33,30,5,YANSS(I))
  200 XARG(I&1)=XARG(I)&DEC
      TOT2=0.
      DO 20 I=1,10
      SUM=TOT2&YANSS(I)
   20 TOT2=SUM
      TOT2=TOT2*2.
      CH=TOT2/TOT1
      RETURN
      END
```

```
C
C        SUBROUTINE XY -- CALCULATES (X , Y) COORDINATES FROM THE
C        CENTER LINE OF TOOTH AS REF.
C
C        NNN=0  - EXTERNAL
C        NNN=1  - INTERNAL
C
      SUBROUTINE XY (DB,DR,RF,K,XCENT,YCENT,NNN)
      REAL K
C
C        WHERE -
C          DB     = BASE CIRCLE DIA.
C          DR     = ROOT DIA.
C          RF     = FILLET RADIUS (TRUE)
C          K      = ANGLE FROM ORIGIN OF INVOLUTE TO CENTER LINE OF TOOTH
C          XCENT  = X COORDINATE TO CENTER OF RF
C          YCENT  = Y COORDINATE TO CENTER OF RF
C          NNN    = CODE FOR EXTERNAL OR INTERNAL (SEE ABOVE)
C
      IF (NNN)       8,8,6
    6 H=(DR*.5)-RF
      CPR=(DB*.5)/H
      CPRA=ATAN(SQRT(1.-CPR**2)/CPR)
      A=SQRT(H**2-(DB*.5)**2)
      OPP=A&RF
      H1=SQRT(OPP**2&(DB*.5)**2)
      CA=(DB*.5)/H1
      CARA=ATAN(SQRT(1.-CA**2)/CA)
      ZCA=(SIN(CARA)/COS(CARA))-CARA
      B=(CARA-CPRA)&ZCA
    7 FAPRA=K&B
      GO TO 11
    8 H=(DR/2.)&RF
      IF((DB/2.)-H)          10,12,12
   10 CPR=(DB*.5)/H
      CPRA=ATAN(SQRT(1.-CPR**2)/CPR)
      OPP=SQRT(H**2-(DB*.5)**2)
      A=OPP-RF
      H1=SQRT(A**2&(DB*.5)**2)
      CA=(DB*.5)/H1
      CARA=ATAN(SQRT(1.-CA**2)/CA)
```

```
      ZCA=(SIN(CARA)/COS(CARA))-CARA                                    XY    25
      B= CPRA-CARA-ZCA                                                  XY    26
      GO TO 7                                                           XY    27
   11 XCENT=SIN(FAPRA)*H                                                XY    28
      YCENT=COS(FAPRA)*H                                                XY    29
      RETURN                                                            XY    30
   12 XX=SIN(K)*(DB*.5)
      XCENT=XX&RF
      FAPS=XCENT/H
      FAPRA=ATAN(FAPS/(SQRT(1.-FAPS**2)))
      YCENT=XCENT/TAN(FAPRA)
      RETURN
      END                                                               XY    34
C
C         INVOLUTOMETRY WEAKEST SECTION  (SUBROUTINE WEAK)
C         NOD=  NO. OF DIA. AT WHICH THE LOAD IS CALC. (MAX 6)
C         NNN=0 EXTERNAL
C         NNN=1 INTERNAL
C
      SUBROUTINE WEAK (RV,XCENT,YCENT,RF,DB,K,T,H,DW,XDIM,ALPHA,NOD,NNN)WEAK   1
      REAL K                                                            WEAK   2
      DIMENSION RV(6),T(6),H(6),DW(6),XDIM(6),ALPHA(6)                  WEAK   3
      IF (NNN)                 140,140,152                              WEAK   4
C                                                                       WEAK   5
C         CALCULATIONS FOR EXTERNAL GEAR(S)                             WEAK   6
C                                                                       WEAK   7
  140 DO 10 I=1,NOD                                                     WEAK   8
      ALPHA(I)=.1                                                       WEAK   9
      DELTA=.1                                                          WEAK  10
  144 V=SIN(ALPHA(I))*RF                                                WEAK  11
      V1=SQRT(RF**2-V**2)                                               WEAK  12
      T(I)=XCENT-V1                                                     WEAK  13
C
C         T(I) = 1/2 CHORD AT THE WEAKEST SECTION
C
      YA=T(I)/(SIN(ALPHA(I))/COS(ALPHA(I)))                             WEAK  14
      H(I)=(RV(I)-YCENT)&V                                              WEAK  15
      YAP=YA/2.                                                         WEAK  16
      IF (YAP - H(I))          146,150,148                              WEAK  17
  146 ALPHA(I)=ALPHA(I)-DELTA                                           WEAK  18
      DELTA=.1*DELTA                                                    WEAK  19
```

```
      IF ( .0000001 - DELTA) 144,150,150                                WEAK  20
  1.8 ALPHA(I)=ALPHA(I)&DELTA                                           WEAK  21
      GO TO 144                                                         WFAK  22
  150 YB=YCENT-V                                                        WEAK  23
      DW(I)=SQRT(YB**2&T(I)**2)*2.                                      WEAK  24
      Q=ATAN(H(I)/T(I))                                                 WEAK  25
      Q=1.570796327-Q                                                   WEAK  26
      XDIM(I)=T(I)*(SIN(Q)/COS(Q))                                      WEAK  27
   10 CONTINUF                                                          WEAK  28
      RETURN                                                            WEAK  29
C
C        CALCULATIONS FOR INTERNAL GEAR(S)
C
  152 DO 20 I=1,NOD                                                     WEAK29.5
      ALPHA(I)=.1                                                       WEAK  30
      DELTA=.1                                                          WFAK  31
  154 V=SIN(ALPHA(I))*RF                                                WFAK  32
      V1=SQRT(RF**2-V**2)                                               WEAK  33
      T(I)=XCENT-V1                                                     WEAK  34
      YA=T(I)/(SIN(ALPHA(I))/COS(ALPHA(I)))                             WFAK  35
      H(I)=(YCENT-RV(I))&V                                              WEAK  36
      YAP=YA/2.                                                         WEAK  37
      IF (YAP - H(I))          156,160,158                              WEAK  38
  156 ALPHA(I)=ALPHA(I)-DELTA                                           WEAK  39
      DELTA=.1*DELTA                                                    WEAK  40
      IF ( .0000001 - DELTA) 154,160,160                                WEAK  41
  158 ALPHA(I)=ALPHA(I)&DELTA                                           WEAK  42
      GO TO 154                                                         WEAK  43
  160 YB=YCENT&V                                                        WEAK  44
      DW(I)=SQRT(YB**2&T(I)**2)*2.                                      WEAK  45
      Q=ATAN(H(I)/T(I))                                                 WFAK  46
      Q=1.570796327-Q                                                   WEAK  47
      XDIM(I)=T(I)/(SIN(Q)/COS(Q))                                      WEAK  48
   20 CONTINUF                                                          WEAK  49
      RETURN                                                            WEAK  50
      END                                                               WEAK  51
      SUBROUTINE HOBB(DR,AN,DV,HTT,HADD,HLEAD,HPA,HTIPR,PROT,           HOB    1
     *XDIM,DW,TW,H,PI,RN,NOD,ALPHA,SCO)                                 HOB    2
```

```
      DIMENSION DV(6),XDIM(6),DW(6),TW(6),YYFIL(6),H(6),ALPHA(6)        HOB    3
      COMMON RHPA,HPCA,HYP,HRCTRP,TSA,FCA,YFIL,STA,FNSI
      REAL INC                                                          HOB    5
      HPAR=HPA*RN
      HTT=HTT/SCO
      SI=SIN(HPAR)/SCO
      HPARR=ATAN(SI/(SQRT(1.-SI**2)))
      HTIPR=(HTIPR&(HTIPR/SCO))/2.
      HLEAD=HLEAD/SCO
      HPAR=HPARR
      TSA=PI/AN                                                         HOB    6
      DHPA=(AN*HLEAD)/PI                                                HOB    7
      HADDN=.5*(DHPA-DR)                                                HOB    8
      HTTN=HTT&2.*(HADDN-HADD)*TAN(HPAR)                                HOB   10
      HTTR=.5*HTT-HADD*TAN(HPAR)                                        HOB   11
      HA=HTTR-(HTIPR-PROT)/COS(HPAR)                                    HOB   12
      HRCTRX=HA&HTIPR*TAN(HPAR)                                         HOB   13
      RHPA=.5*DHPA                                                      HOB   14
      HRCTRP=HADDN-HTIPR                                                HOB   15
      HPCA=ATAN(HRCTRX/HRCTRP)                                          HOB   16
      HYP=HRCTRP/COS(HPCA)                                              HOB   17
C
C        FIND PARABOLA TANGENT TO GENERATED FILLET
C
      FTCA=(PI/2.)-TSA                                                  HOB   18
      DO 25 I=1,NOD                                                     HOB   19
      INC=.1*HTTN                                                       HOB   20
      PPPOS=0.                                                          HOB   21
    5 PPPOS=PPPOS&INC                                                   HOB   22
      CALL GENFIL (PPPOS,TW(I),YYFIL(I),DW(I),HTIPR)                    HOB   23
      FTPA=PI-(FTCA&FCA)                                                HOB   24
      ALPHA(I)=(PI/2.)-FTPA                                             HOB   25
      AB=TW(I)/TAN(ALPHA(I))                                            HOB   26
      H(I)=.5*DV(I)-YYFIL(I)                                            HOB   27
      IF (AB-(2.*H(I)))       5,15,10
   10 PPPOS=PPPOS-INC                                                   HOB   30
      INC=.1*INC                                                        HOB   31
```

```
      IF (.000001-INC)        5,15,15
   15 CONTINUE                                                          HOB   33
C
C        FIND --X-- VALUF FOR PARABOLA
C
      ANGLED=ATAN(TW(I)/H(I))                                           HOB   34
      ADJ=TW(I)/SIN(ANGLED)                                             HOB   36
   25 XDIM(I)=ADJ/COS(ANGLED) - H(I)                                    HOB   37
      RETURN                                                            HOB   38
      END                                                               HOB   39
      SUBROUTINE GENFIL (PPPOS,XTFIL,YTFIL,DFIL,HTIPR)                  GENFIL 1
      COMMON RHPA,HPCA,HYP,HRCTRP,TSA,FCA,YFIL,STA,FNSI
      PPA=PPPOS/RHPA                                                    GENFIL 3
      PHA=ATAN(PPA)                                                     GENFIL 4
      HPCTR=RHPA/COS(PHA)                                               GENFIL 5
      PPPHA=PPA-PHA                                                     GENFIL 6
      HPCX=HPCTR*SIN(PPPHA)                                             GENFIL 7
      HPCY=HPCTR*COS(PPPHA)                                             GENFIL 8
      RCTRA=HPCA&PPA                                                    GENFIL 9
      RCTX=HYP*SIN(RCTRA)-HPCX                                          GENFIL10
      RCTY=HPCY-HYP*COS(RCTRA)                                          GENFIL11
      IF (PPPOS)              10,10,5                                   GENFIL12
   10 XFIL=RCTX                                                         GENFIL13
      YFIL=RCTY-HTIPR                                                   GENFIL14
      GO TO 15                                                          GENFIL15
    5 FCPLA=ATAN(HRCTRP/PPPOS)                                          GENFIL16
      FCA=FCPLA-PPA                                                     GENFIL17
      XFIL=RCTX&HTIPR*COS(FCA)                                          GENFIL18
      YFIL=RCTY-HTIPR*SIN(FCA)                                          GENFIL19
   15 FSA=ATAN(XFIL/YFIL)                                               GENFIL20
      FTA=TSA-FSA                                                       GENFIL21
      RFIL=YFIL/COS(FSA)                                                GENFIL22
      XTFIL=RFIL*SIN(FTA)                                               GENFIL23
      YTFIL=RFIL*COS(FTA)                                               GENFIL24
      DFIL=2.*RFIL                                                      GENFIL25
      RETURN                                                            GENFIL26
      FND                                                               GENFIL27
```

```
                    STD AND NON STD EXTERNAL HELICAL
                    GEARS - MAX BENDING STRESS

                I N P U T   D A T A   S E C T I O N

NO. OF TEETH    CENTER DISTANCE      HORSEPOWER   RPM-PINION      KO         KV         KS         KM
PINION  GEAR      STD      NON STD
  32    100    11.0C0000 11.000000  2500.000000   13820.00    1.000000   1.000000   1.000000   1.099999

  NORMAL PLANE        HELIX       BACKLASH        FACE WIDTH - MIN      MAX TIP BREAK
 PHI N     PND        ANGLE      MIN     MAX      PINION      GEAR      PINION     GEAR
20.000000 7.000000  31.002686  0.0120  0.0180    1.219999   1.212000   0.010000  0.010000

OUTSIDE DIA - MIN       ROOT DIA - MIN         ARC TOOTH THK          L
 PINION      GEAR     PINION       GEAR      PINION      GEAR
 5.665999 16.904999  4.985000  16.223999    0.275800   0.235800      0

SHAPED OR     M       ROOT FILLET RAD-MIN      MAX UNDERCUT           KT         KR         MN        DENSITY
HOBBED                PINION       GEAR      PINION      GEAR                                         LB/CU.IN.
SHAPED        0       0.05000     0.05000    0.005000   0.005000    1.00000    1.00000    1.00000    0.28300
```

```
*----  O U T P U T   D A T A  ----*

TOOTH GEOMETRY

   PHI (PRESSURE ANGLE
        TRANSVERSE PLANE)      =  23.00758
   CIRCULAR PITCH              =   0.52360
   DIAMETRAL PITCH             =   6.00000

                                   PINION         GEAR
   PITCH DIA                       5.33333     16.66666
   BASE CIRCLE DIA                 4.90908     15.34086
   BEGIN CONTACT DIA               5.14635     16.88496
   END   CONTACT DIA               5.64599     16.40411
   WEAKEST SECTION DIA             5.04337     16.28586

   ARC TOOTH THK AT
   OPERATING DP                    0.27580      0.23580
   CH                              1.68077      1.67606
   YC                              0.53355      0.57368
   KF                              1.67296      1.72974
   J                               0.23431      0.24367

   BENDING STRESS

              BC (HPC)      58729.43     57007.02


 BENDING STRESS PINION-AT HPC IS LESS
THAN THE ENDURANCE LIMIT OF 175000. PSI - INFINITE LIFE.


 BENDING STRESS GEAR  -AT HPC IS LESS
THAN THE ENDURANCE LIMIT OF 175000. PSI - INFINITE LIFE.

   BENDING STRESS (COMBINED)

              BC (HPC)      60847.62     59243.87
```

APPENDIX IV

STATISTICAL TREATMENT OF TEST DATA

This appendix consists of a description of the mathematical model developed to linearize the test data, its substantiation, its use to determine an endurance limit, and the determination of the variability associated with this endurance limit. A description of the method used to determine the significance of main effects and interactions for the three experimental variables is included.

DERIVATION OF S/N CURVE

Linearizing Transformation

A linearizing transformation was derived to facilitate the analysis of fatigue data. In general, the requirements for a successful transformation are as follows:

- Transformed fatigue data should form a straight line graph with stress (or load) as the independent (or x) variable.
- The inherent variability, or variance, of transformed data should be equal for stress values or rig loads within the range of practical interest.

Transformed fatigue data can be used to compute S/N diagrams, endurance limits and associated variances, and standard deviations necessary for statistical tests of significance.

The transformation derived to express kilocycles to failure as a straight line function of stress is

$$(1/kc)^{1/2.2} = Y = A + BX \qquad (10)$$

where kc = kilocycles to failure
X = stress or applied load
A and B = constants to be evaluated using the least squares technique

Figures 110 and 111 show extensive fatigue data from another experiment in the transformed form and in the conventional S/N diagram. These charts provide a visual measure of the accuracy of the transformation and the derived straight line equation.

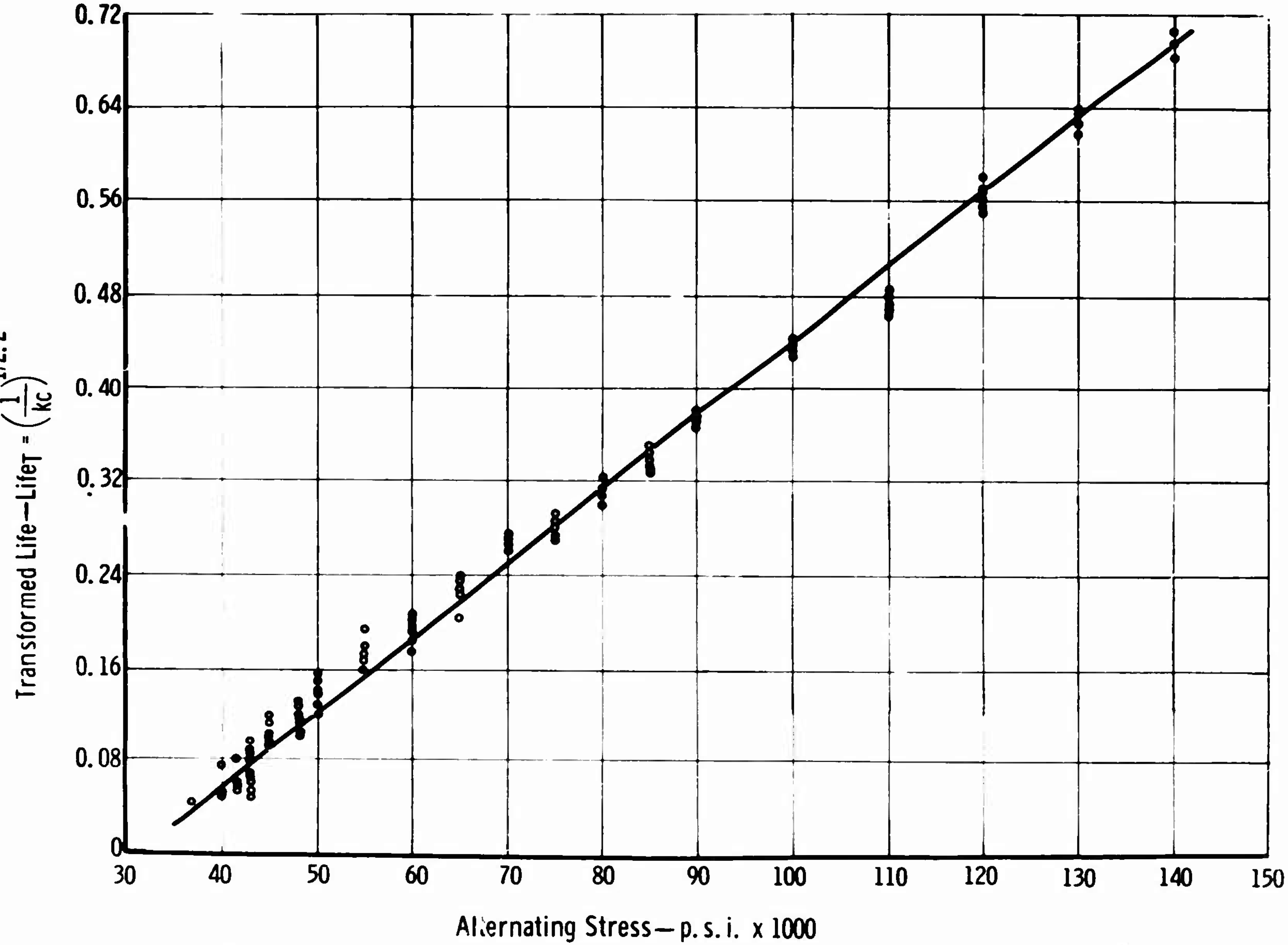

Figure 110. Results of R. R. Moore Tests on Notched 4340 Steel.[8]

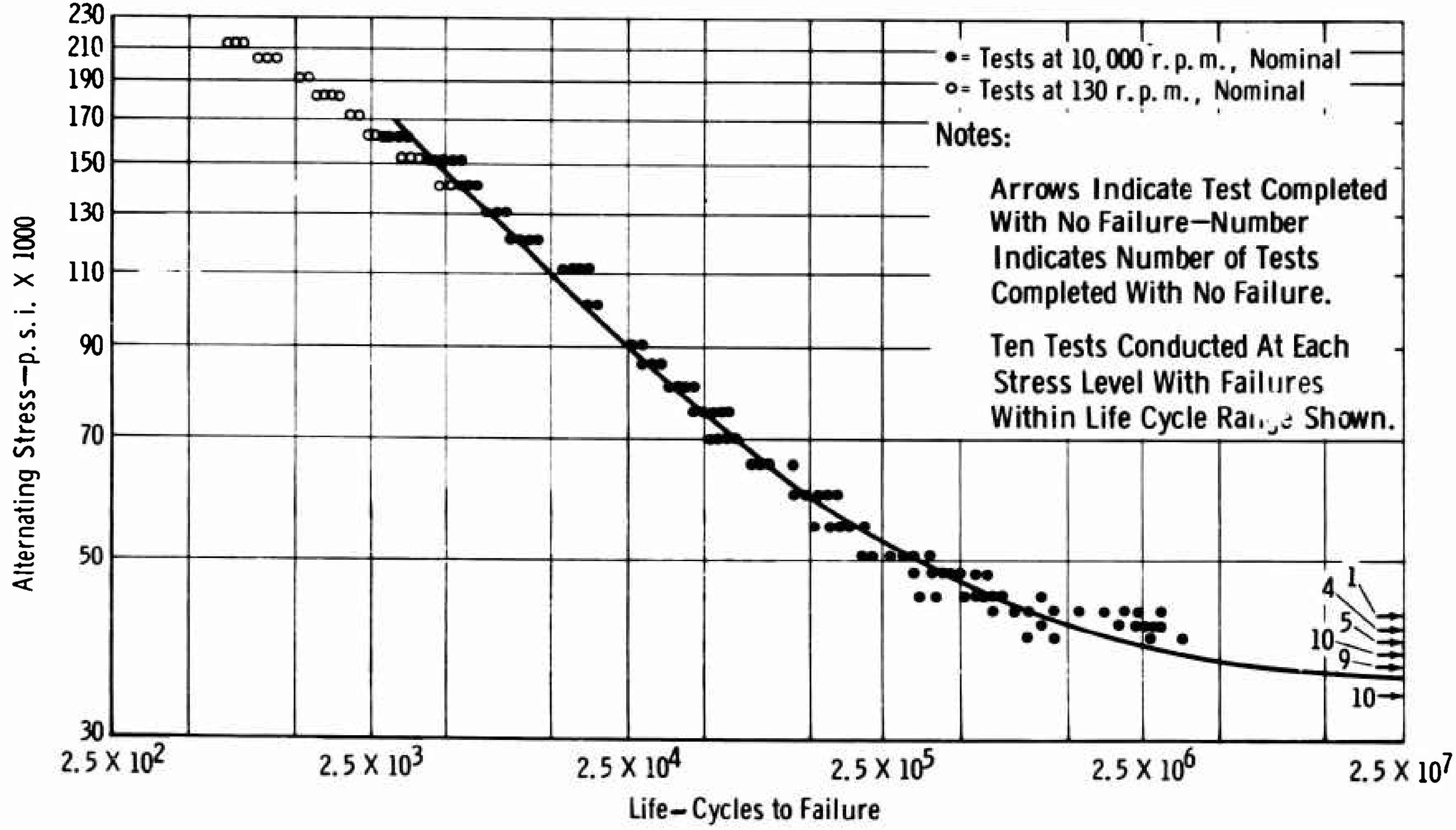

Figure 111. R. R. Moore Rotating Bending Test Data.[8]

The transformation $(1/kc)^{1/2.2}$ was originally derived to evaluate spur gear fatigue data in 1966. The form of the transformation was based on the relationship between the variance of fatigue life and stress. The exponent 1/2.2 was arrived at through trial and error methods which achieved a straight line relationship between transformed cycles and stress.

ANALYSIS OF TRANSFORMED GEAR FATIGUE DATA

Eight sets of helical gear fatigue data were analyzed using the derived linear transformation. Transformed kilocycles to failure were related to rig load by the equation

$$Y = (1/kc)^{1/2.2} = A + BX \tag{11}$$

where X = applied load

To solve for the constants, the equation $Q = \Sigma(Y - A - BX)^2$ is minimized with respect to A and B using the techniques of differential calculus,

$$\frac{\partial Q}{\partial A} = 2\ \Sigma(Y - A - BX)\ (-1) = 0 \tag{12}$$

and

$$\frac{\partial Q}{\partial B} = 2\ \Sigma(Y - A - BX)\ (-X) = 0$$

The two equations and two unknowns resulting from this system are

$$A \cdot N + B\ \Sigma X = \Sigma Y \tag{13}$$

and

$$A\ \Sigma X + B\ \Sigma X^2 = \Sigma XY$$

where N is the number of data points. Solving these equations, the expressions for A and B are

$$B = \frac{\Sigma(X - \bar{X})\ (Y - \bar{Y})}{\Sigma(X - \bar{X})^2} \tag{14}$$

and

$$A = \bar{Y} - B\bar{X} \equiv (\Sigma Y/n) - (B\Sigma X/n)$$

In considering the equation $Y = (1/kc)^{1/2.2} = A + BX$, note that Y approaches zero as kilocycles approach infinity. The endurance limit can be obtained by setting $Y = 0$ and solving for X.

Endurance limit = $-A/B$

STATISTICAL SIGNIFICANCE TESTS

In general, the 't' test for significance is computed by obtaining a difference and then dividing by the standard deviation of that difference; the computed 't' is then compared with a tabular 't' value to determine significance. The tabular 't' is determined by a preselected significance level, α, and degrees of freedom. The significance level, α, is defined as the probability of falsely concluding that a difference exists, when in fact there is no response due to changing factor levels. Degrees of freedom is the number of independent observations used to compute a standard deviation or variance.

In mathematical terms, the statistical significance test is determined by an assumption, termed the null hypothesis, which has the form $H_0: \mu_1 = \mu_2$; the null hypothesis implicitly states there is no differential response associated with factor levels. An alternate hypothesis is also established which is $H_a: \mu_1 \neq \mu_2$ for the two-tailed test. If H_0 is true and $\alpha = 0.05$, there is a 1 in 20 chance that a 't' value larger than the critical 't' will be computed; or alternately expressed, the odds are 1 to 19 that H_0 will be rejected even though it is true. Mathematically, H_0 can be rejected at any preselected value of α; the converse does not follow. H_0 cannot be mathematically proven true or accepted at any probability level. If H_0 is not rejected, judgment is reserved regarding the factor under consideration; however, the failure to reject H_0 may lead to the same course of action that would be indicated if H_0 were indeed true.

The consequence of the foregoing discussion regarding tests of significance is that, in the absence of a significant difference, no assertion is made that any given factor has no true effect on fatigue strength. In fact, large differences may exist that are not detectable because of insufficient test data or excessive variability in the data.

To perform statistical tests of significance, it is necessary to obtain the variance of the endurance limits, V(E.L.):

$$V(E.L.) = \frac{S_e^2}{B^2}\left\{\frac{1}{n} + \frac{(E.L. - \bar{X})^2}{\Sigma(X - \bar{X})^2}\right\} \tag{15}$$

where $S_e^2 = \dfrac{\Sigma(Y - A - BX)^2}{N-K}$

where K = the number of constants evaluated in the least squares system

N-K = the degrees of freedom for S_e^2

The equation for V(E.L.) is obtained through straightforward application of error propagation techniques.

A statistical significance test for any factor (or interaction) is performed by averaging the endurance limits associated with that factor, obtaining a difference associated with factor levels, and dividing this difference by the appropriate standard deviation.

The notations are defined as follows:

- A = Pressure angle (20 and 25 degrees)
- B = Helix angle (20 and 35 degrees)
- C = Load condition (1 and 2)

The eight experimental combinations can be specified by letter designation as follows, where the presence of a letter denotes the high (or second) level for that factor, while the absence of a letter denotes the low (or first) level:

(1) = 20 degrees PA 20 degrees HA Load 1	(B) = 20 degrees PA 35 degrees HA Load 1	(C) = 20 degrees PA 20 degrees HA Load 2	(BC) = 20 degrees PA 35 degrees HA Load 2
(A) = 25 degrees PA 20 degrees HA Load 1	(AB) = 25 degrees PA 35 degrees HA Load 1	(AC) = 25 degrees PA 20 degrees HA Load 2	(ABC) = 25 degrees PA 35 degrees HA Load 2

The following procedures define statistical tests of significance for the factors tested plus interactions:

- A linear combination involving all eight configurations of the experimental factors must be uniquely obtained for the factor or interaction to be tested.
- A standard deviation associated with the linear combination is then obtained using error propagation techniques.
- Degrees of freedom are estimated and a critical 't' value is established based on degrees of freedom and a preselected significance level.
- The test of significance is executed by dividing the linear combination by the standard deviation. The variable, or interaction, is significant if the computed 't' exceeds the critical 't'.

The linear combinations for all factors and interactions are as follows. The column headings designate the factor or interaction to be evaluated and the sign to be associated with each experimental configuration. To establish a linear combination, endurance limits associated with experimental factor configurations are algebraically manipulated as indicated.

A

+	-
A	(1)
AB	B
AC	C
ABC	BC

B

+	-
B	(1)
AB	A
BC	C
ABC	AC

AB

+	-
(1)	A
AB	B
C	AC
ABC	BC

C

+	-
C	(1)
AC	A
BC	B
ABC	AB

AC

+	-
(1)	A
B	C
AC	AB
ABC	BC

BC

+	-
(1)	B
A	AB
BC	C
ABC	AC

ABC

+	-
A	(1)
B	AB
C	AC
ABC	BC

In mapped-out form, the linear combination for ABC is

$$ABC = \left\{A + B + C + ABC\right\} - \left\{(1) + AB + AC + BC\right\} \qquad (16)$$

In theory, the linear combination for ABC is obtained by inserting the appropriate endurance limits represented by the letter designation. In practice, however, it was necessary to use weighted endurance limits; the

weighting factors used were reciprocals of the standard deviations of the endurance limits. Weighting factors were required because the variances associated with the eight endurances were not all equal.

An example of a test of significance is delineated for the ABC interaction as follows:*

- Linear combination:

$$ABC = \frac{\Sigma W_i X_i}{\Sigma W_i} - \frac{\Sigma W_j X_j}{\Sigma W_j} \tag{17}$$

$$ABC = \frac{(41.33)(0.8479) + (20.82)(0.8936) + (45.81)(0.7318) + (14.04)(1.0503)}{122.01}$$

$$- \frac{(69.50)(0.7302) + (11.84)(1.0915) + (20.81)(0.7329) + (16.50)(0.7965)}{118.67}$$

$$ABC = 0.8354 - 0.7760 = 0.0594$$

- Variance:

$$V(ABC) = \left(\frac{1}{\Sigma W_i}\right)^2 \left\{W_A^2 \quad S_A^2 + \ldots + W_{ABC}^2 \quad S_{ABC}^2\right\} + \left(\frac{1}{\Sigma W_j}\right)^2 \left\{W_1^2\, S_1^2 + \ldots + W_{BC}^2\, S_{BC}^2\right\} \tag{18}$$

$$V(ABC) = \left(\frac{1}{122.01}\right)^2 \Big\{(1708.3)(5.8539 \times 10^{-4}) + (433.5)$$
$$(23.0665 \times 10^{-4}) + (2099.3)(4.7634 \times 10^{-4}) + (197.2)$$
$$(50.7036 \times 10^{-4})\Big\} + \left(\frac{1}{118.67}\right)^2 \Big\{(4831.0)(2.0700 \times 10^{-4})$$
$$+ (140.4)(71.2145 \times 10^{-4}) + (432.9)(23.0986 \times 10^{-4})$$
$$+ (272.4)(36.7162 \times 10^{-4})\Big\}$$

---

*For convenience in making calculations, the numbers used are derived by multiplying endurance limits by 10^{-4}.

$V(ABC) = 5.527 \times 10^{-4}$

$$\text{Standard deviation ABC} = \sqrt{V(ABC)}$$

$$ABC = \sqrt{5.527 \times 10^{-4}} = 0.0235$$

- Degrees of freedom:
  The exact degrees of freedom is obscured by the complexity of calculations used to compute the standard deviation. Therefore, this equation was used to compute degrees of freedom:

$S_T^2 = a_1 S_1^2 + a_2 S_2^2 + \ldots + a_n S_n^2$, degrees of freedom is:

$$(df) = \frac{\left[S_T^2\right]^2}{a_1^2 \frac{\left[S_1^2\right]^2}{(df)_1} + \frac{a_2^2 \left[S_2^2\right]^2}{(df)_2} + \ldots + \frac{a_n \left[S_n^2\right]^2}{(df)_n}} \qquad (19)$$

  Using this equation, degrees of freedom for the three-factor interaction was 114. The tabular 't' for 114 degrees of freedom and $\alpha = 0.05$ is 2.0.

- T test:

  $'t' = \frac{0.0594}{0.0235} = 2.5$, which exceeds the critical value of 2.0, and the interaction is significant.

A specific example of significance testing was provided for the three-factor interaction. The other six significance tests were performed in the same manner. In all tests, degrees of freedom were estimated to be 100, $\alpha = 0.05$, and the critical 't' value remained at 2.0.

S/N DIAGRAMS

The S/N diagrams, based on applied load rather than stress, are shown in both conventional and transformed form in Figures 112 through 127. On each figure, a lower 90 percent tolerance limit is also shown.

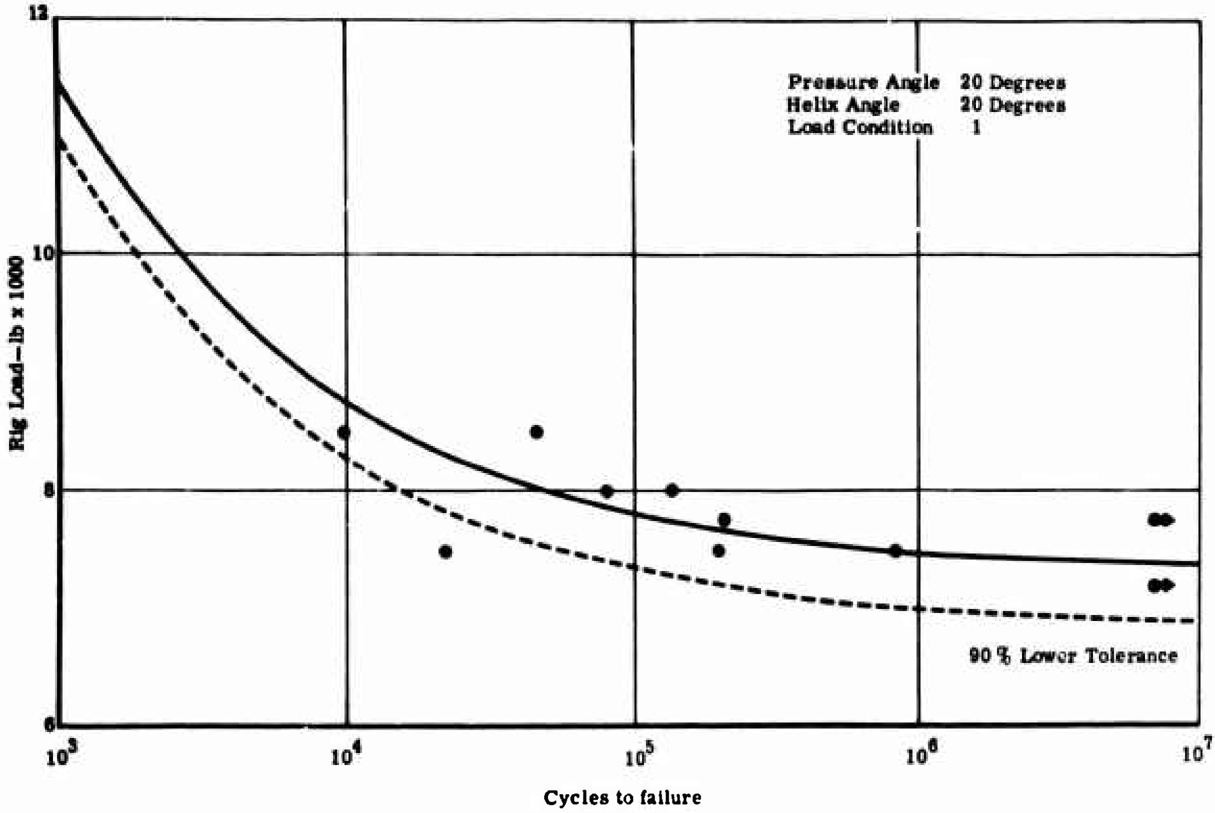

Figure 112. Fatigue Test Results—Applied Load Versus Life (EX-84117).

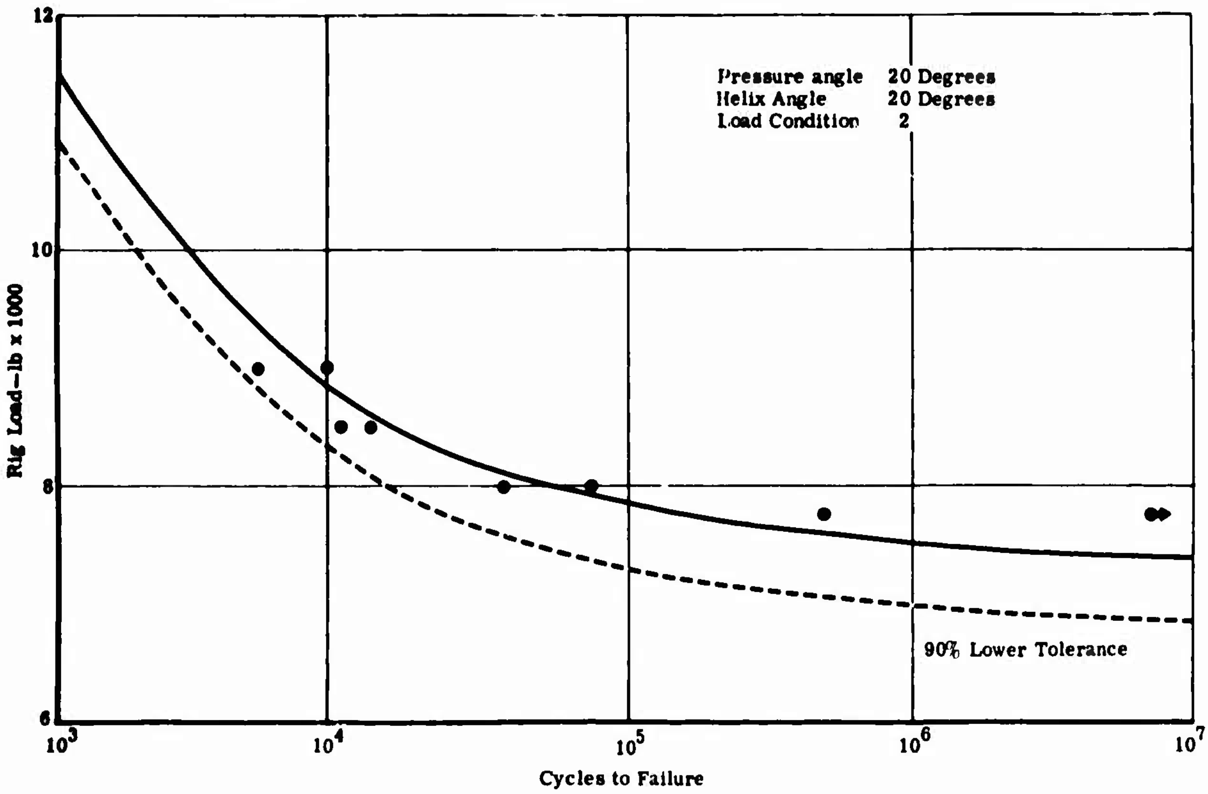

Figure 113. Fatigue Test Results—Applied Load Versus Life (EX-84117).

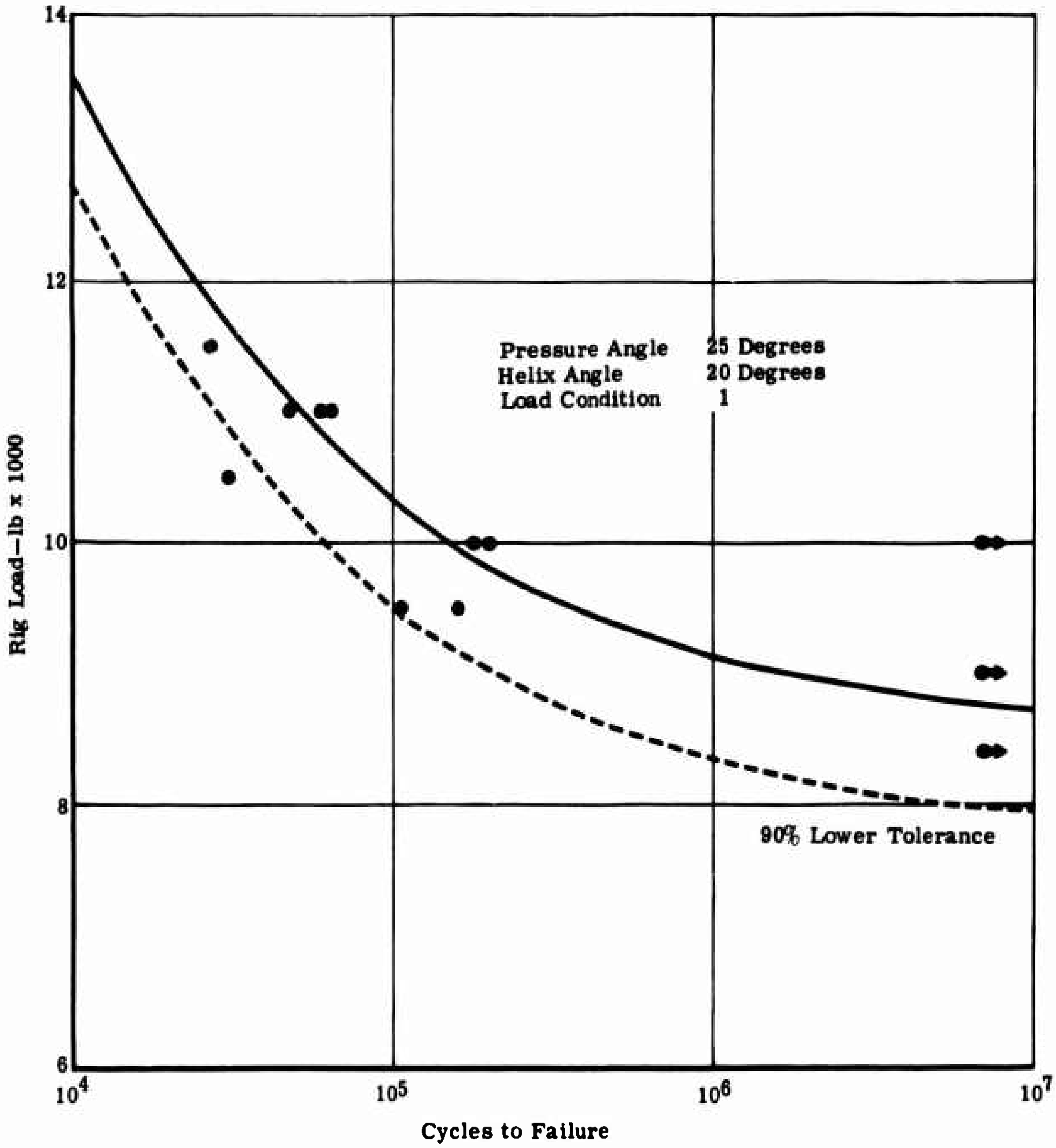

Figure 114. Fatigue Test Results—Applied Load Versus Life (EX-84118).

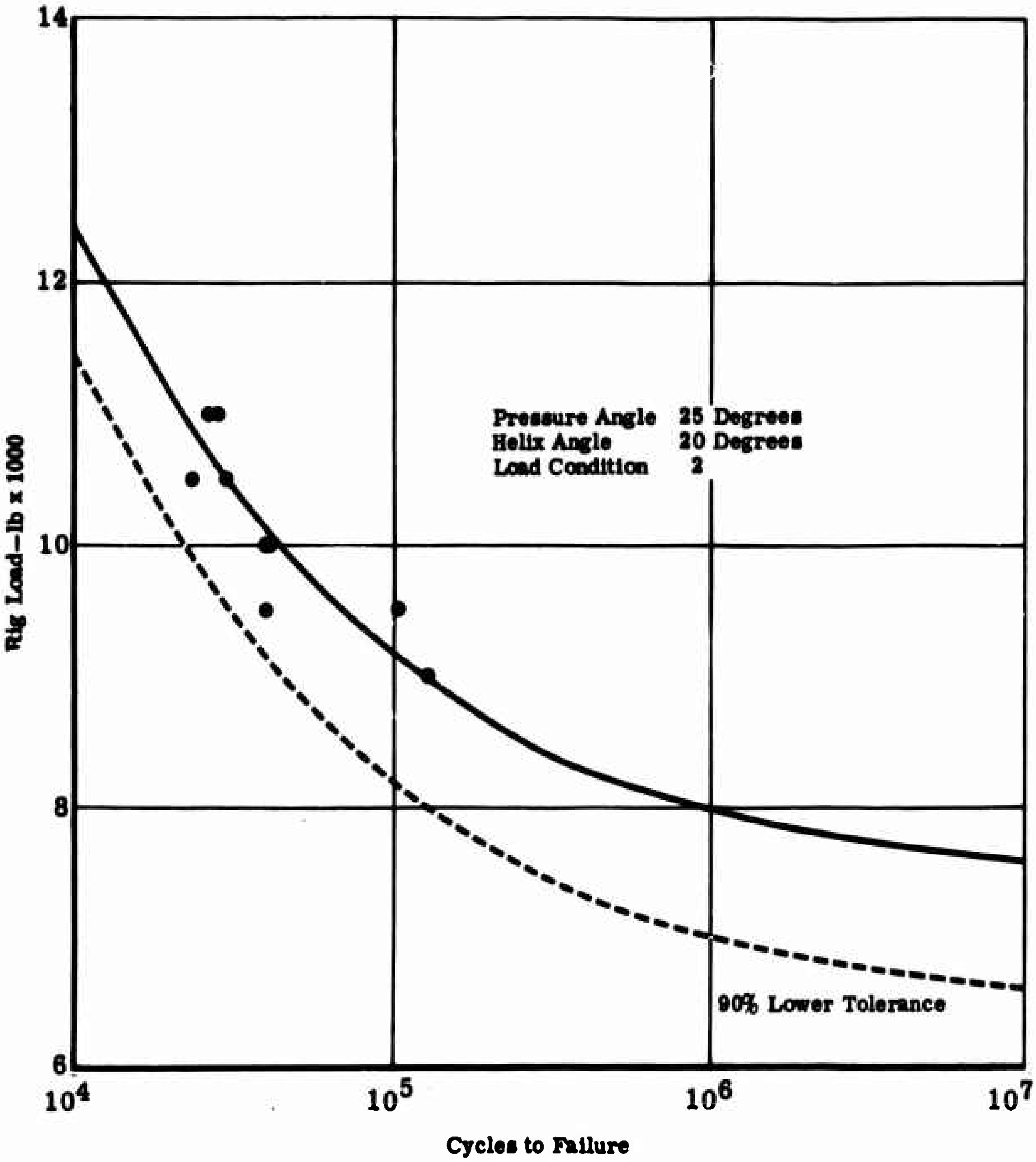

Figure 115. Fatigue Test Results—Applied Load Versus Life (EX-84118).

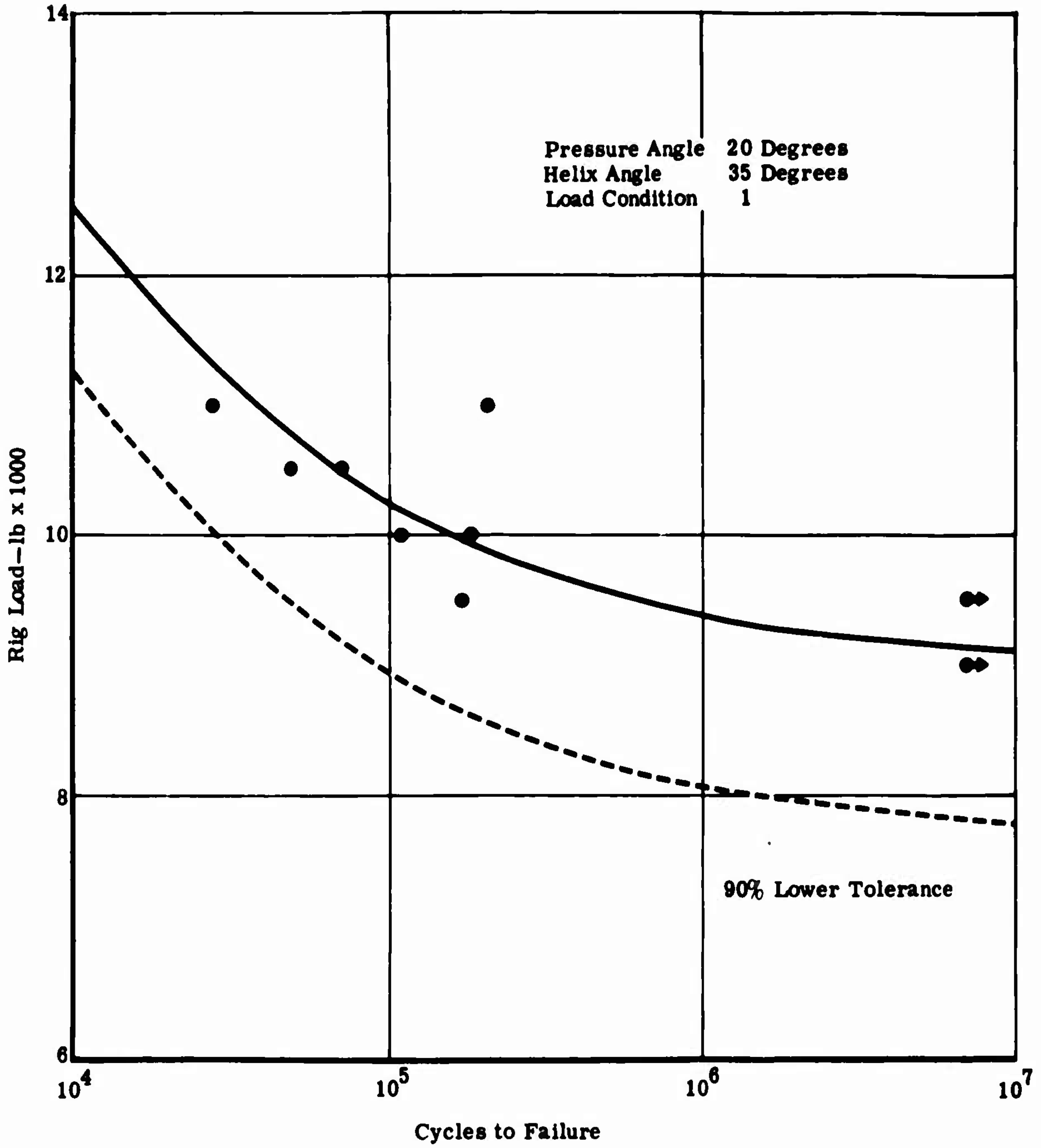

Figure 116. Fatigue Test Results—Applied Load Versus Life (EX-84119).

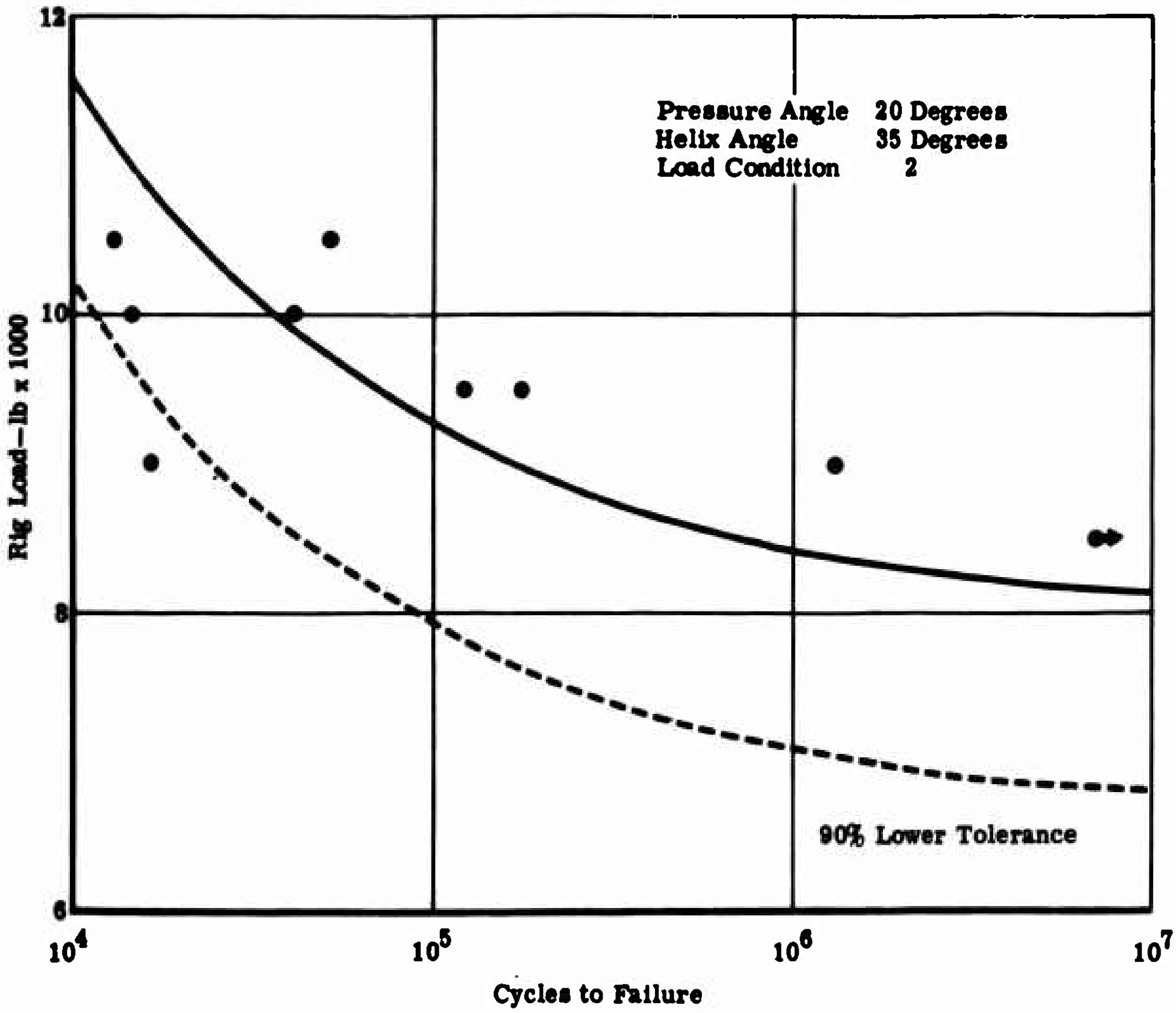

Figure 117. Fatigue Test Results—Applied Load Versus Life (EX-84119).

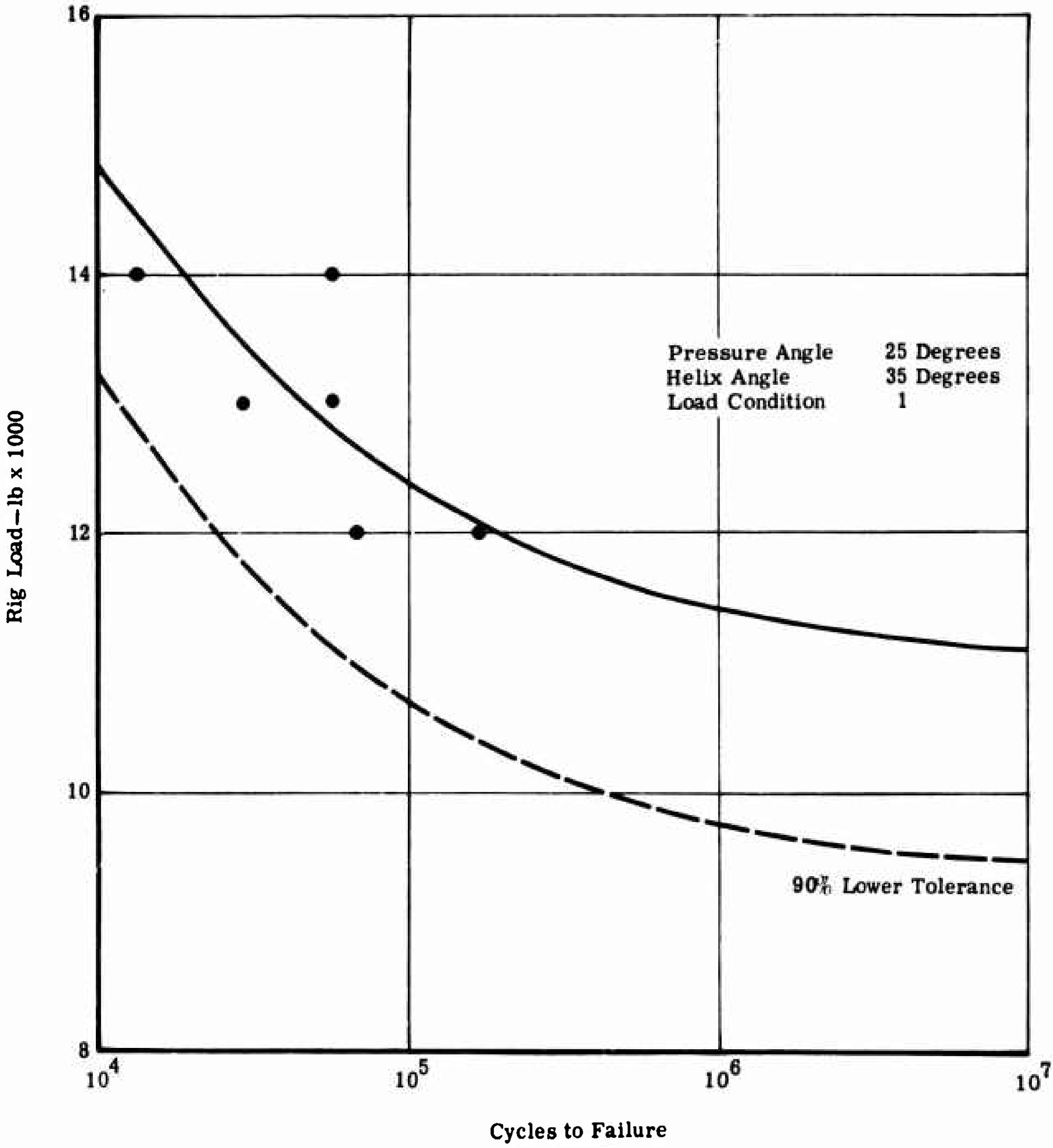

Figure 118. Fatigue Test Results—Applied Load Versus Life (EX-84120).

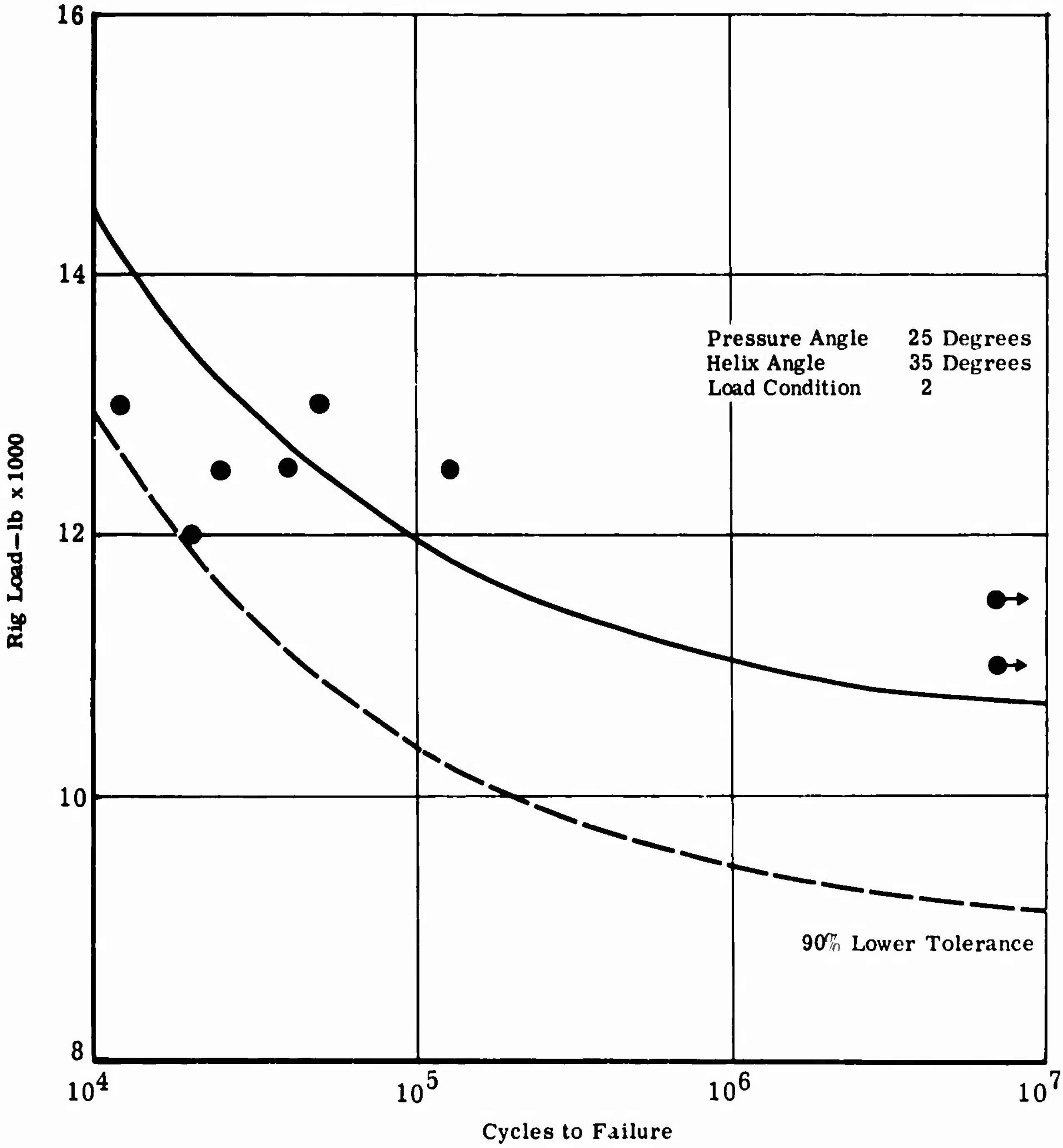

Figure 119. Fatigue Test Results—Applied Load Versus Life (EX-84120).

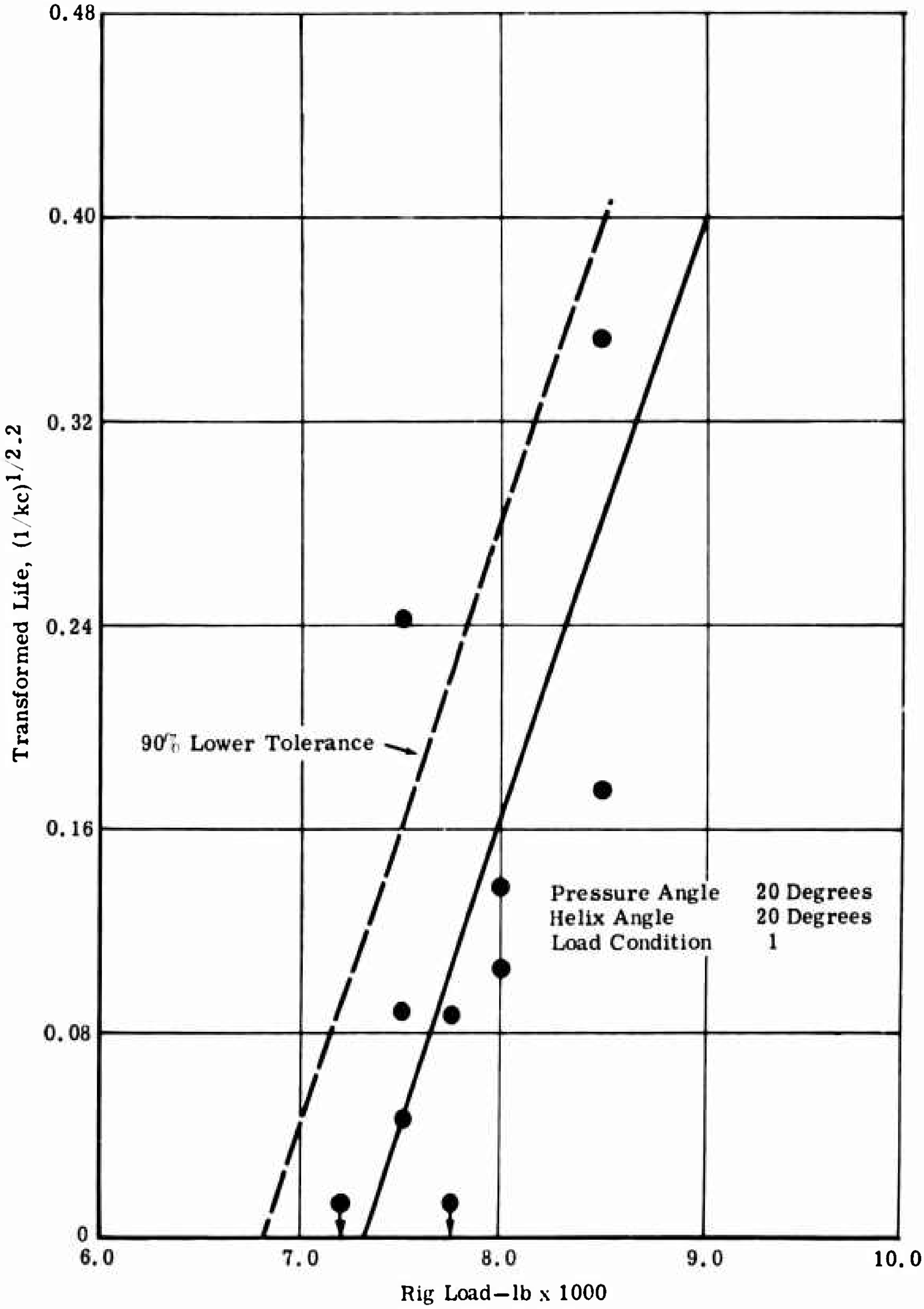

Figure 120. Fatigue Test Results—Applied Load Versus Transformed Life (EX-84117).

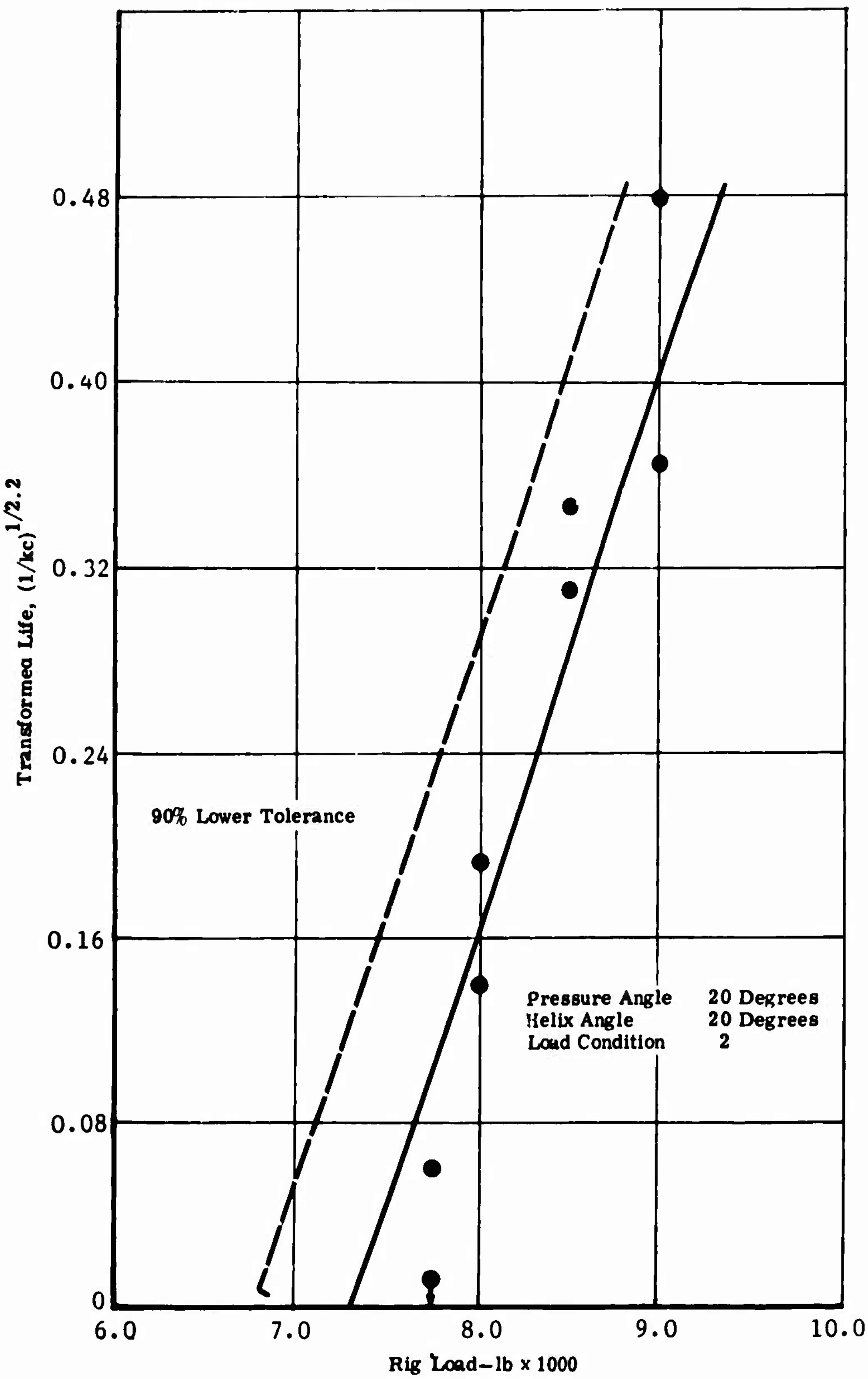

Figure 121. Fatigue Test Results—Applied Load Versus Transformed Life (EX-84117).

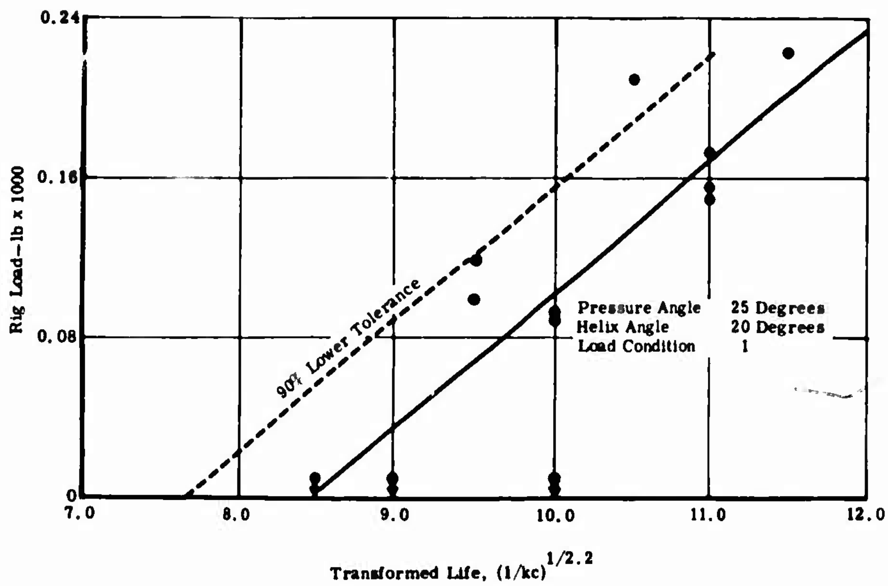

Figure 122. Fatigue Test Results—Applied Load Versus Transformed Life (EX-84118).

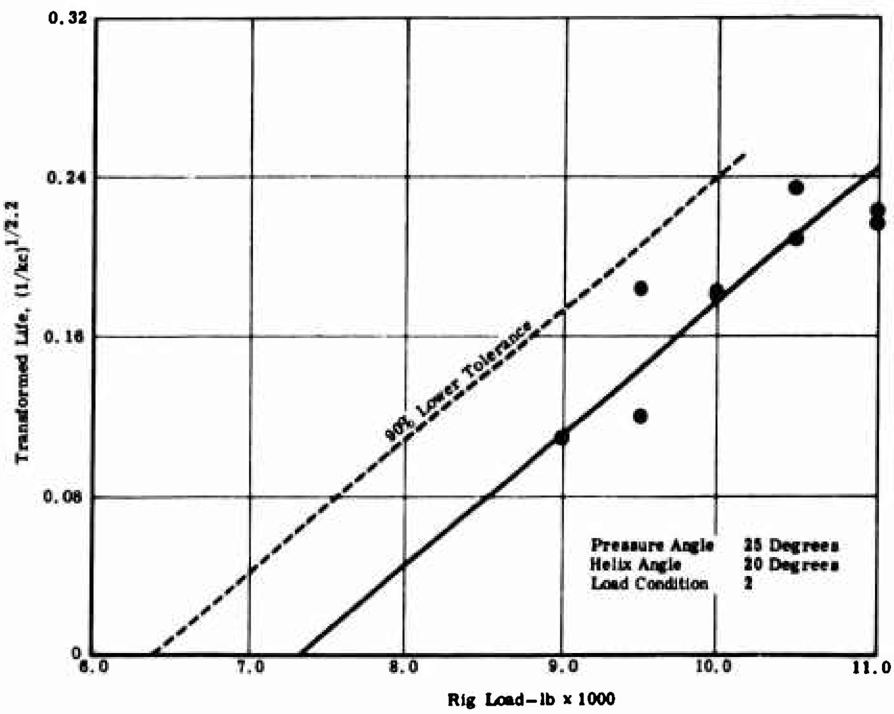

Figure 123. Fatigue Test Results—Applied Load Versus Transformed Life (EX-84118).

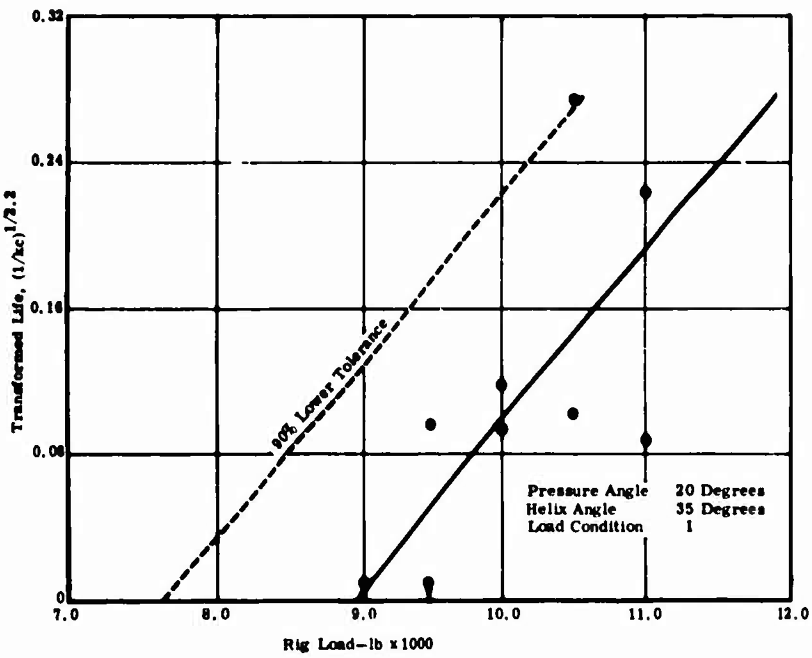

Figure 124. Fatigue Test Results—Applied Load Versus Transferred Life (EX-84119).

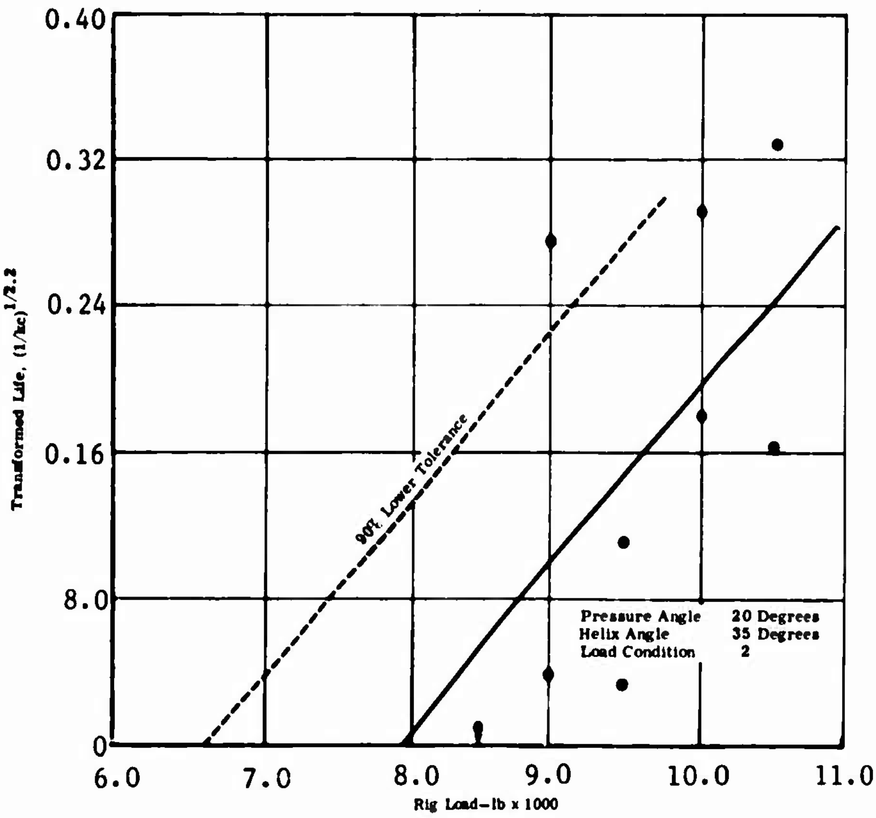

Figure 125. Fatigue Test Results—Applied Load Versus Transformed Life (EX-84119).

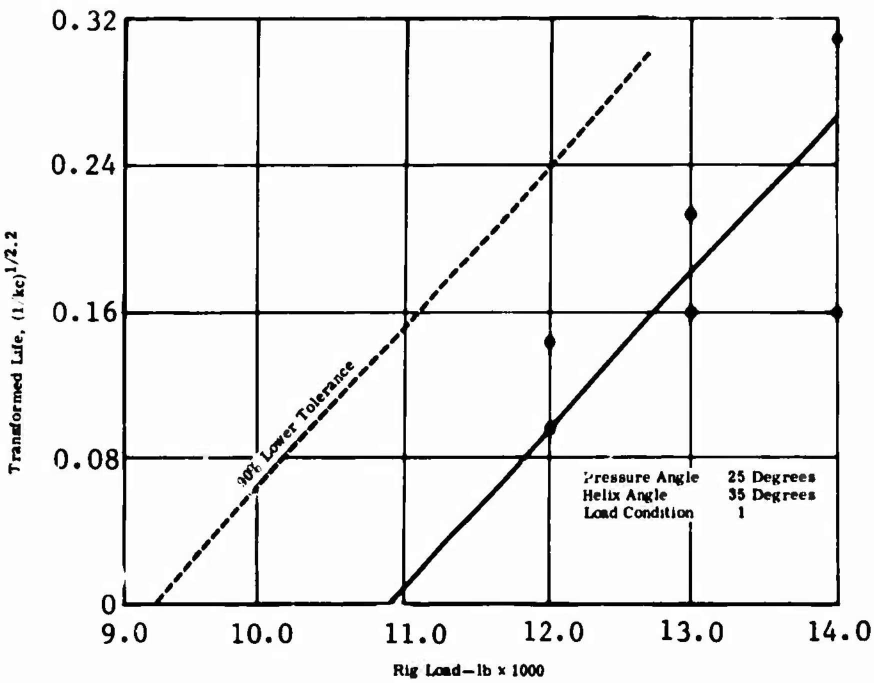

Figure 126. Fatigue Test Results—Applied Load Versus Transferred Life (EX-84120).

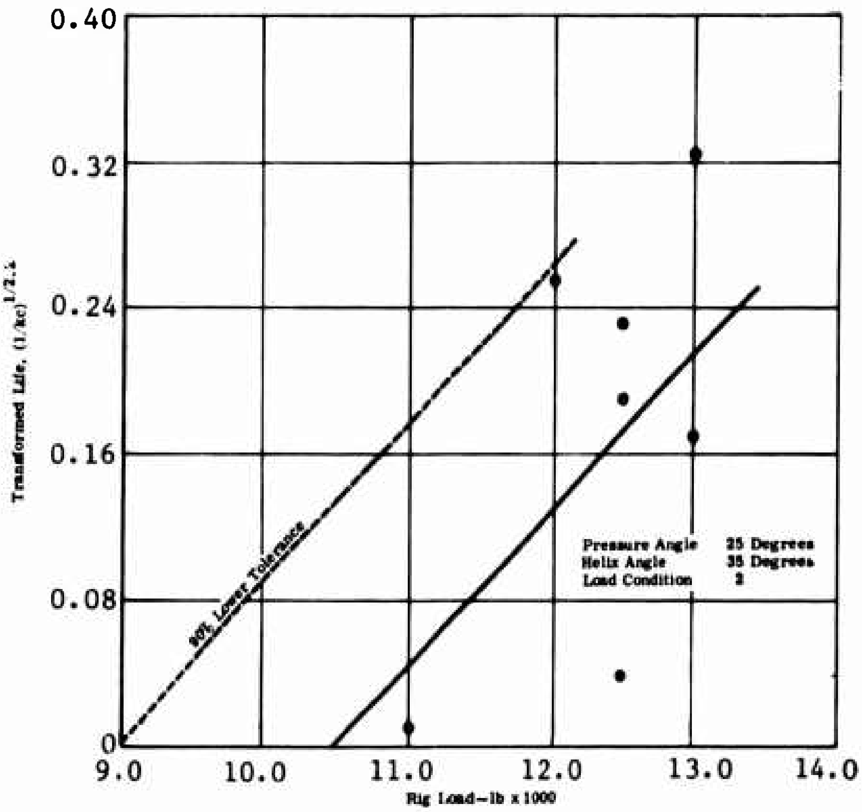

Figure 127. Fatigue Test Results—Applied Load Versus Transferred Life (EX-84120).

The lower 90 percent tolerance limit is the number of cycles that at least 90 percent of repeated tests will survive per given rig load. In the alternate connotation, the 90 percent lower tolerance is the rig load that will permit at least 90 percent of tests to survive to the infinite life region. The construction of a lower 90 percent tolerance limit on the endurance is outlined as follows:

- Variances and standard deviations for tolerance intervals were computed using the equations

$$V(T.L.) = \frac{S_e^2}{B^2} \left\{ 1 + \frac{1}{n} + \frac{(E.L. - \bar{X})^2}{\Sigma (X - \bar{X})^2} \right\} \tag{20}$$

(where all terms are as previously defined)

and

$$SD(T.L.) = \text{Standard deviation} = \left\{ V(T.L.) \right\}^{1/2} \tag{21}$$

- The lower 90 percent tolerance limit is obtained by subtracting (1.282)[SD(T.L.)]from the computed tolerance limit. The factor 1.282 was obtained from the one-tailed 't' table with $\alpha = 0.10$.

APPENDIX V

AGMA STANDARD 221.02

Following is a reprint of "Tentative AGMA Standard for Rating the Strength of Helical and Herringbone Gear Teeth," by permission of J. C. Sears, American Gear Manufacturers Association.

AGMA Standards represent minimum or average data, conditions or applications. The Standards are subject to constant improvement, revision or withdrawal as dictated by experience. Any person who refers to a Standard should satisfy himself that he has the latest information available from the Association on the subject matter of the Standard.

Personnel of

Gear Rating Committee

Technical Division

January, 1963

E. J. Wellauer, Chairman, The Falk Corp., Milwaukee, Wis.

D. L. Borden, The Falk Corp., Milwaukee, Wis.
W. Coleman, Gleason Works, Rochester, New York
D. W. Dudley, General Electric Co., West Lynn, Mass.
J. H. Glover, Ford Motor Co., Dearborn, Michigan
R. Hoffman, Tool Steel Gear & Pinion Co., Cincinnati, Ohio
J. B. Hopper, Lufkin Foundry & Machine Co., Lufkin, Texas
I. Koenig, Hewitt-Robins, Inc., Chicago, Illinois
W. L. Kriegs, Hewitt-Robins, Inc., Chicago, Illinois
J. K. Morris, Western Gear Corp., Lynwood, California
C. F. Schwan, Reliance Electric & Engineering Co., Cleveland, Ohio
J. C. Straub, Wheelabrator Corp., Mishawaka, Indiana
F. A. Thoma, De Laval Turbine, Inc., Trenton, New Jersey
N. A. Wilson, Morgan Construction Co., Worcester, Mass.
G. L. Scott, AGMA, Washington, D. C.

Tables or other self supporting sections may be quoted or extracted in their entirety. Credit lines should read: "Extracted from AGMA Tentative Standard Strength of Helical and Herringbone Gear Teeth, (AGMA 221.02) with the permission of the publisher, the American Gear Manufacturers Association, One Thomas Circle, Washington 5, D. C."

FOREWORD

This standard is for rating the strength of helical and herringbone gear teeth. It contains the following:

Basic Rating Formula

This section enumerates the factors known to affect strength. Numerical values are presented for those factors which have been evaluated by analytical means, test results or field experience. Suggestions are made for the factors which are not now capable of being expressed accurately. New knowledge and more definite measurement of these parameters will continually necessitate revisions and improvements.

In addition to the above, it is contemplated to publish design practices, such as AGMA 221.02A, having specific application under the heading of:

Design Practices for Specialized Applications

It is recognized that it is sometimes desirable to provide simplified design practice data applicable to a specialized field of application. These individual design practices will enable enclosed speed reducer, mill gear, aircraft or other specialized product designers to record the modifications and limitations they wish to use.

This tentative standard was initially printed as an AGMA paper for presentation at the June, 1960 Annual Meeting. It was approved by the AGMA membership in June, 1961. However, final printing of the standard was intentionally delayed in order to correlate copies of all the strength rating standards.

TENTATIVE

AGMA STANDARD

STRENGTH OF HELICAL & HERRINGBONE GEAR TEETH

Basic Rating Formula

1. Scope

1.1 This standard presents the fundamental formula for the strength of helical and herringbone gear teeth. It includes all of the factors which are known to affect gear tooth strength. This formula and standard is based on AGMA Information Sheet 225.01 and is therefore coordinated with strength ratings for spur and bevel gears.

1.2 Both pinion and gear teeth must be checked for bending strength rating to account for differences in geometry factors, material properties, and numbers of tooth contact cycles under load.

1.3 Other AGMA standards contain numerical values to be used to rate gears for specific applications. These should be consulted when applicable.

1.4 Where no applicable specific AGMA standard is established, numerical values for the factors may be estimated from the data given in this standard and the strength rating calculated.

1.5 The formulas presented in this standard apply to external gears unless otherwise noted.

1.6 The symbols used, wherever applicable, conform to AGMA Standard 111.03 "Letter Symbols for Gear Engineering" (ASA B6.5-1954) and "Letter Symbols for Mechanics of Solid Bodies" (ASA Z10.3-1948).

2. Fundamental Bending Stress Formula

2.1 The basic equation for the bending stress in a gear is calculated as follows:

$$s_t = \frac{W_t\, K_o}{K_v} \; \frac{P_d}{F} \; \frac{K_s\, K_m}{J}$$

Where:

s_t = calculated tensile stress at the root of the tooth, psi

Load:

- W_t = transmitted tangential load in pounds at operating pitch dia. (see section 4)
- K_o = overload factor (see section 9)
- K_v = dynamic factor (see section 8)

Tooth Size:

- P_d = transverse diametral pitch
- F = net face width, inches

Stress Distribution:

K_s = size factor (see section 7)

K_m = load distribution factor (see section 6)

J = geometry factor (see section 5)

2.1.1 Note that the above equation is divided into three groups of terms, the first of which is concerned with the load, the second with tooth size, and the third with stress distribution.

2.2 The relation of calculated stress to allowable stress is:

$$s_t \leq \frac{s_{at}\, K_L}{K_T\, K_R}$$

Where:

s_{at} = allowable stress for material, psi (see section 13)

s_t = calculated stress, psi (see section 2.1)

K_L = life factor (see section 11)

K_T = temperature factor (see section 12)

K_R = factor of safety (see section 10)

3. Fundamental Power Formula

3.1 In preparing handbook data, for gear designs already developed, the following formula can be used to directly calculate the power which can be transmitted by a given gear set.

$$P_{at} = \frac{n_P\, d\, K_v}{126{,}000\, K_o}\ \frac{F}{K_m}\ \frac{J}{K_s\, P_d}\ \frac{s_{at}\, K_L}{K_R\, K_T}$$

Where:

P_{at} = allowable power of gear set in horsepower

n_P = pinion speed, rpm

d = operating pitch diameter of pinion, inches.

4. Transmitted Tangential Load

4.1 The transmitted tangential load is calculated directly from the power transmitted by the gear set. (When operating near a critical speed of the drive, a careful analysis of conditions must be made). When the transmitted load is not uniform, consideration should be given not only to the peak load and its anticipated number of cycles, but also to intermediate loads and their number of cycles.

4.2 The transmitted tangential load is:

$$W_t = \frac{P \times 33{,}000}{v_t} = \frac{2T}{d} = \frac{P \times 126{,}000}{n_P\, d}$$

Where:

P = power transmitted in horsepower

T = pinion torque, pound inches

v_t = pitch line velocity, fpm

5. Geometry Factor – J

5.1 The geometry factor evaluates the shape of the tooth, the position at which the most damaging load is applied, stress correction due to geometric shape, and the sharing of load between oblique lines of contact.

5.2 See Appendix A for a further discussion of helical gear geometry factors.

5.3 In helical gears, the critical point of load application is determined by the position of the oblique line of contact. Figures 1, 2A and 2B show the approximate geometry factors for equal addendum involute helical gears for the contact condition of Figure A-2 of Appendix A.

6. Load Distribution Factor – K_m

6.1 The load distribution factor depends upon the combined effect of:

1) misalignment of axes of rotation;

2) lead deviations;

3) elastic deflection of shafts, bearings and housing.

6.2 Figures 3 and 4 illustrate misalignment and its effect on load distribution.

6.3 The effect of different rates of helical gear misalignment is shown in Figure 5.

6.4 When the misalignment is known, use Figure 5 to select K_m. F_m represents the face width having just 100 per cent contact for a given tangential load and alignment error. Generally F_m should exceed F. The misalignment represents the combined effect of the helix error of the pinion, helix error of the gear and misalignment of the pinion and gear axes under load.

6.5 Manufacturers of gears with face widths greater than 6 inches generally find it necessary to control misalignment by other means than allowed rates of misalignment. To handle such cases, Table 1 shows appropriate values of K_m.

6.6 When the estimated or actual misalignment is not known, the K_m factor may be obtained from Table 2.

Table 1 Load Distribution Factor for Wide Face Gears – K_m

Ratio of F/d	Contact	K_m
1.0 or less	95% face width contact obtained at 1/3 torque 95% face width contact obtained at full torque	1.4 at 1/3 torque 1.1 at full torque
	75% face width contact obtained at 1/3 torque 95% face width contact obtained at full torque	1.8 at 1/3 torque 1.3 at full torque
	35% face width contact obtained at 1/3 torque 95% face width contact obtained at full torque	2.5 at 1/3 torque 1.9 at full torque
	20% face width contact obtained at 1/3 torque 75% face width contact obtained at full torque	4.0 at 1/3 torque 2.5 at full torque
	Teeth are crowned 35% face width contact at 1/3 torque 85% face width contact at full torque	2.5 at 1/3 torque 1.7 at full torque
over 1 less than 2	Calculated combined twist and bending of pinion not over .001 in. over entire face Pinion not over 250 BHN hardness 75% contact obtained at 1/3 torque 95% contact obtained at full torque	2.0 at 1/3 torque 1.4 at full torque
	Calculated combined twist and bending of pinion not over .0007 in. over entire face Pinion not over 350 BHN hardness 75% contact obtained at 1/3 torque 95% contact obtained at full torque	2.0 at 1/3 torque 1.4 at full torque
	30% contact obtained at 1/3 torque 75% contact obtained at full torque	4.0 at 1/3 torque 3.0 at full torque
	Twist and bending exceeds .001 in. over entire face	Calculate effects of deflection and either adjust helix angle to compensate for deflection or increase K_m to allow for both alignment errors and deflection.

Table 2 Load Distribution Factor – K_m

Condition of Support	Face Width, Inches			
	2 and under	6	9	16 and over
Accurate mountings, low bearing clearances, minimum elastic deflection, precision gears	1.2	1.3	1.4	1.7
Less rigid mountings, less accurate gears, contact across full face	1.5	1.6	1.7	2.0
Accuracy and mounting such that less than full face contact exists	over 2			

7. Size Factor – K_s

7.1 The size factor reflects non-uniformity of material properties. It depends primarily on:

1) tooth size;

2) diameter of parts;

3) ratio tooth size to diameter of part;

4) face width;

5) area of stress pattern;

6) ratio of case depth to tooth size;

7) hardenability and heat treatment of materials.

7.2 The size factor may be taken as unity for most helical and herringbone gears provided a proper choice of steel is made for the size of the parts and the case depth or hardness pattern is adequate.

7.3 Standard size factors for helical teeth have not yet been established for cases where there is a detrimental size effect. In such cases some size factor greater than unity should be used.

8. Dynamic Factor – K_v

8.1 The dynamic factor depends on:

1) effect of tooth spacing and profile errors;

2) effect of pitch line speed and rpm;

3) inertia and stiffness of all rotating elements;

4) transmitted load per inch of face;

5) tooth stiffness.

8.2 Figure 6 shows some of the dynamic factors that are commonly used.

Curve 1 – Used for high precision helical gears where the items listed in 8.1 are such that no appreciable dynamic load is developed.

Curve 2 – Used for high precision helical gears where the items listed in 8.1 can develop a

dynamic load. This curve is recommended for commercial helical gears.

8.3 When milling cutters are used to cut the teeth or inaccurate teeth are generated, lower dynamic factors than shown in Figure 6 must be used.

9. Overload Factor – K_o

9.1 The overload factor makes allowances for the roughness or smoothness of operation of both the driving and driven apparatus. Specific overload factors can be established only after considerable field experience is gained in a particular application.

9.2 In determining the overload factor, consideration should be given to the fact that many prime movers develop momentary overload torques appreciably greater than those determined by the nameplate ratings of either the prime mover or the driven apparatus.

9.3 In the absence of specific overload factors, the values in Table 3 should be used.

Table 3 Overload Factors – K_o

Power Source	Load On Driven Machine		
	Uniform	Moderate Shock	Heavy Shock
Uniform	1.00	1.25	1.75 or higher
Light Shock	1.25	1.50	2.00 or higher
Medium Shock	1.50	1.75	2.25 or higher

9.4 Service factors have been established where field data is available for specific applications. These service factors include not only the overload factor, but also the life factor and factor of safety. Service factors for many applications are listed in AGMA standards, and should be used whenever applicable. If a specific service factor is used in place of the overload factor K_o, use a value of 1.0 for K_R and K_L.

10. Factor of Safety – K_R

10.1 The factor of safety is introduced in this equation to offer the designer an opportunity to design for high reliability or, in some instances, to design for a calculated risk. Table 4 shows a suggested list of factors of safety to be applied to the fatigue strength of the material rather than to the tensile strength. For this reason, the values are much smaller than customarily used in other branches of machine design.

10.1.1 Failure in the following table does not mean an immediate failure under applied load, but rather a shorter life than the minimum specified.

Table 4 Factors of Safety – K_R

Fatigue Strength

Requirements of Application	K_R
High Reliability	1.50 or higher
Fewer than 1 failure in 100	1.00
Fewer than 1 failure in 3	0.70

10.2 Table 5 shows safety factors to be applied to the yield strength of the material. These values must be applied to the maximum peak load to which the gears are subjected.

Table 5 Factors of Safety — K_R
Yield Strength

Requirements of Application	K_R
High Reliability	3.00 or higher
Industrial	1.33

11. Life Factor — K_L

11.1 The life factor adjusts the allowable loading for the required number of cycles. Table 6 shows typical values, for use with the lower allowable stress values of Figure 7 or Table 7.

Table 6 Life Factor — K_L

Number of Cycles	K_L			
	160 BHN	250 BHN	450 BHN	case carb.*
Up to 1000	1.6	2.4	3.4	2.7
10,000	1.4	1.9	2.4	2.0
100,000	1.2	1.4	1.7	1.5
1 million	1.1	1.1	1.2	1.1
10 million and over	1.0	1.0	1.0	1.0

*case carburized 55-63 R_c

12. Temperature Factor — K_T

12.1 When gears operate at oil or gear blank temperatures not exceeding 250 deg F, K_T, is generally taken as 1.0. In some instances, it is necessary to use a K_T value greater than 1.0 for case carburized gears at a temperature above 160 deg F. One basis of correction is:

$$K_T = \frac{460 + T_F}{620}$$

Where:

T_F = the peak operating oil temperature in degrees Fahrenheit.

13. Allowable Stress — s_{at} and s_{ay}

13.1 An allowable design stress for unity application factor and 10 million cycles of load application is determined by field experience, for each material and condition of that material. This stress is designated s_{at}.

13.2 The allowable stress for gear materials varies considerably with heat treatment, forging or casting practice, material composition, and with such treatment as shot peening.

13.3 The allowable fatigue design stress for steel is shown in Figure 7. The lower values are suggested for general design purposes. The upper values may be used when high quality material is used, when section size and design allows maximum response to heat treatment and when proper quality control is effected by adequate inspection.

13.4 The allowable fatigue design stress for case carburized steel and other materials is shown in Table 7.

Table 7 Allowable Fatigue Design Su

Material	Hardness	s_{at} - psi
Case Carburized and Hardened Steel		
General Design	55-63 R_c	55,000
Special Material, Heat treatment and Inspection	55-63 R_c	65,000
Cast Iron		
AGMA Grade 20		5,000
" " 30	175 BHN (Min.)	8,500
" " 40	200 BHN (Min.)	13,000

13.5 Use 70 per cent of the s_{at} values for idler gears and other gears where the teeth are loaded in both directions.

13.6 When the gear is subjected to infrequent momentary high overloads the maximum allowable stress is determined by the allowable yield properties rather than the fatigue strength of the material. This stress is designated as s_{ay}. Figure 8 shows suggested values for allowable yield strength. In these cases the design should be checked to make certain that the teeth are not permanently deformed. When yield is the governing stress, the stress concentration factor is sometimes considered ineffective.

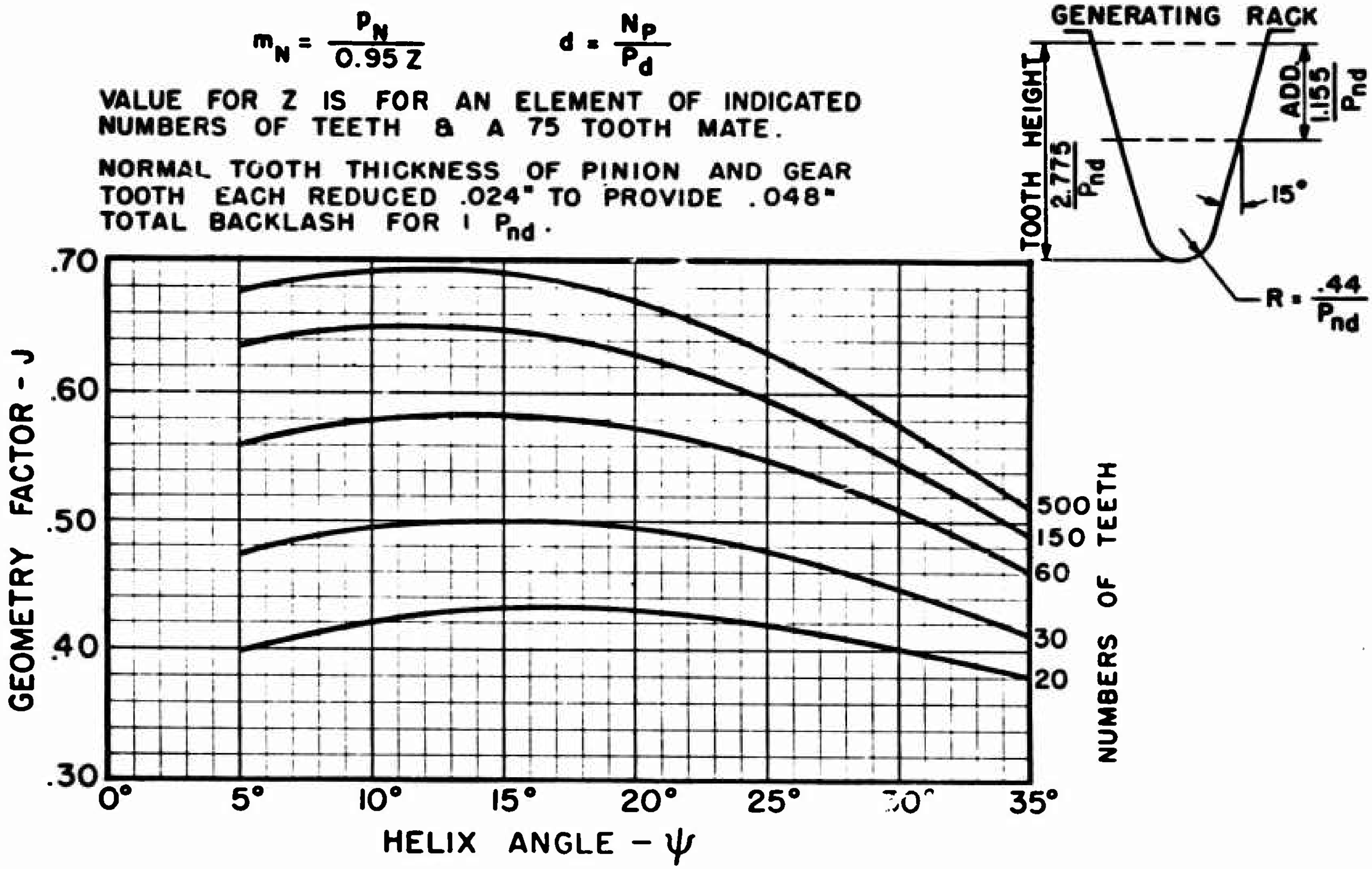

FIG. 1 GEOMETRY FACTOR (J) 15° NORMAL PRESSURE ANGLE - STANDARD ADDENDUM

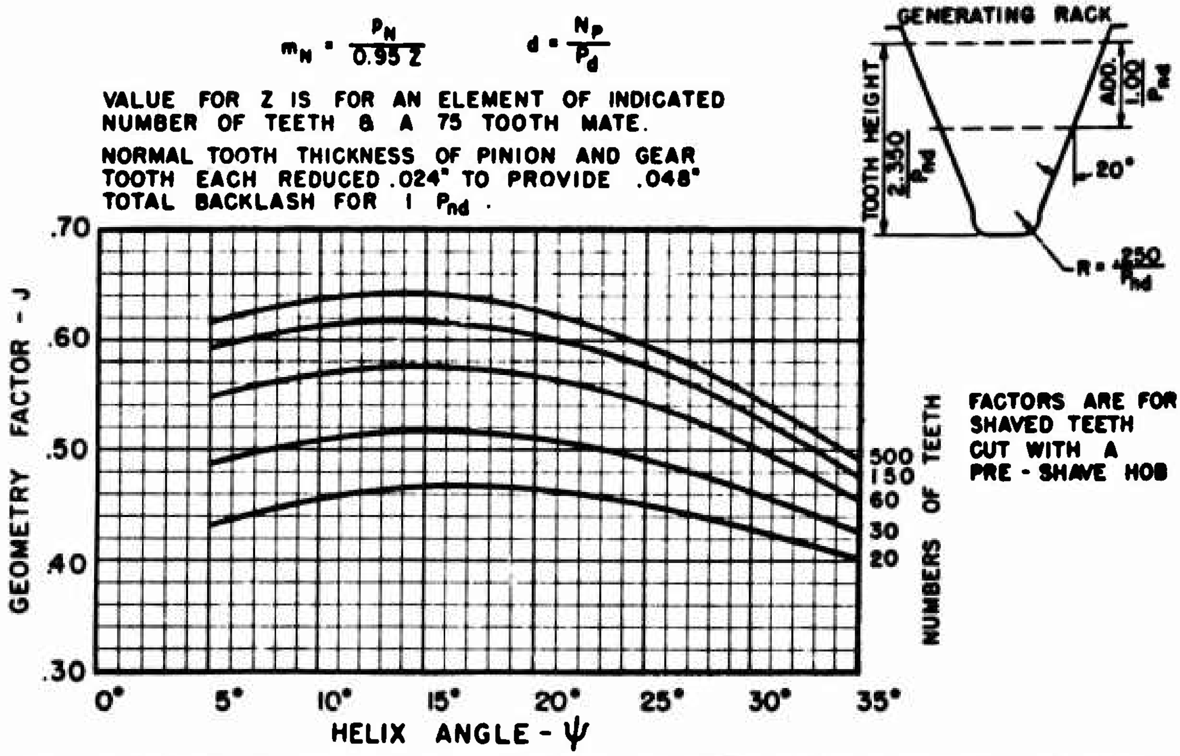

FIG. 2A GEOMETRY FACTOR (J) 20° NORMAL PRESSURE ANGLE-STANDARD ADDENDUM PRE-SHAVE HOB

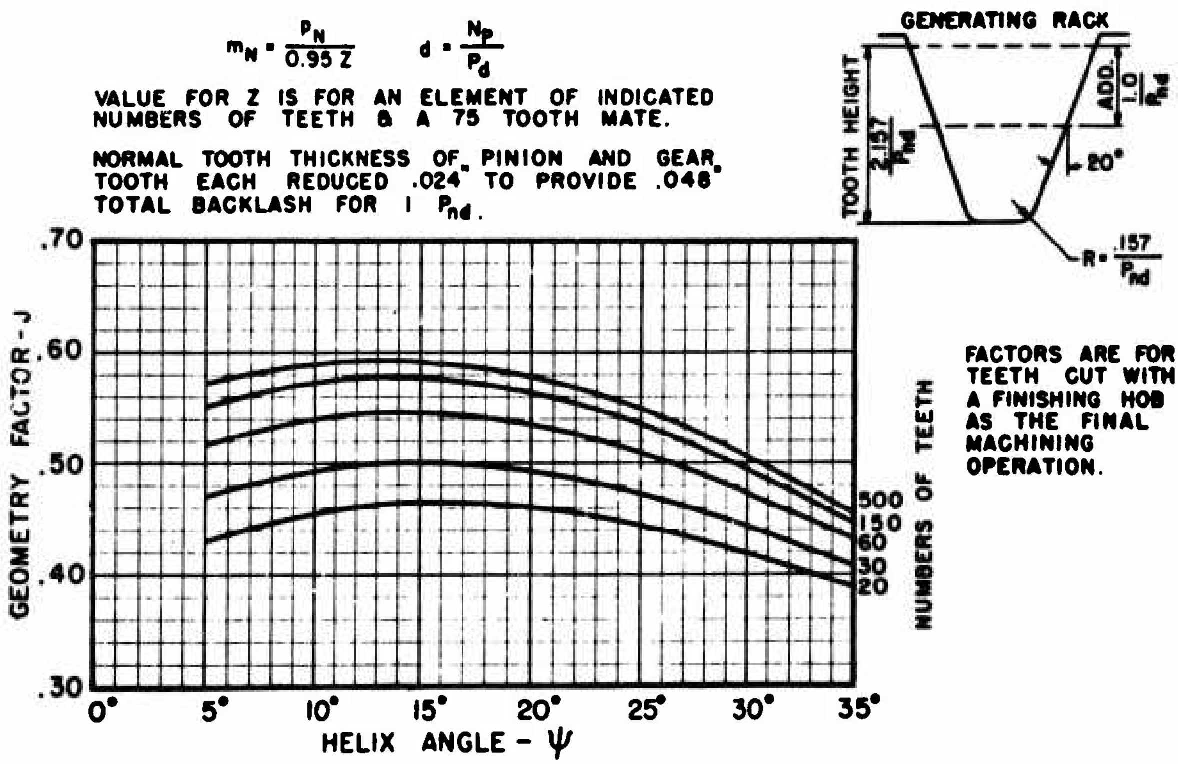

FIG. 2B GEOMETRY FACTOR (J) 20° NORMAL PRESSURE ANGLE-STANDARD ADDENDUM FINISHING HOB

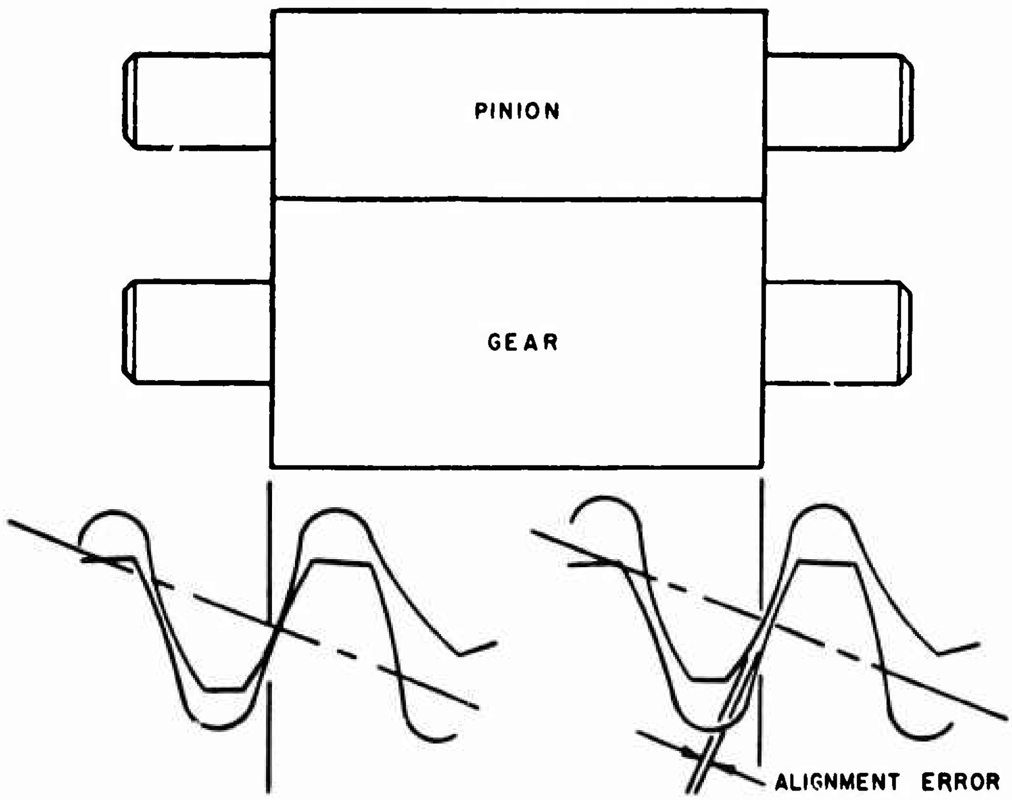

FIG. 3 Example of a Pinion and Gear Misaligned Under No Load. Teeth Contact at Left Hand End and Are Open at Right Hand End.

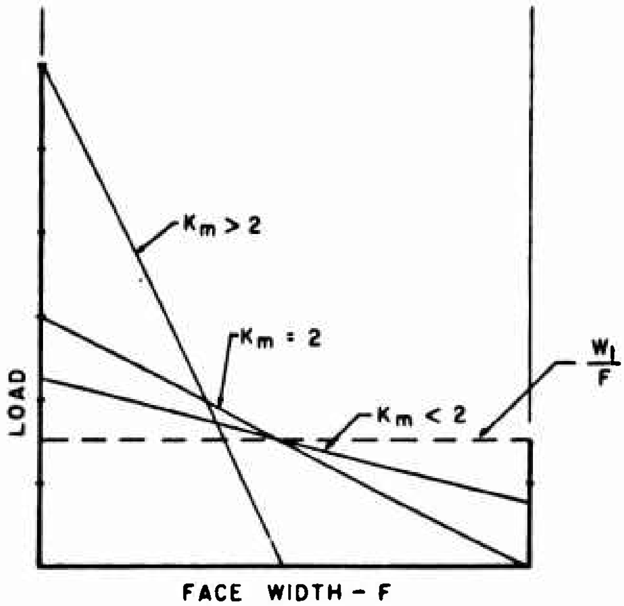

FIG. 4 Load Distribution Across Face Width for Various Contact Conditions

$C_e = \dfrac{W_t}{1000\ e}$	W_t = TANGENTIAL LOAD - LBS e = ALIGNMENT ERROR INCHES/INCH

Z = LENGTH OF LINE OF ACTION

p_b = BASE PITCH — NORMAL TO INVOLUTE, TRANSVERSE PLANE

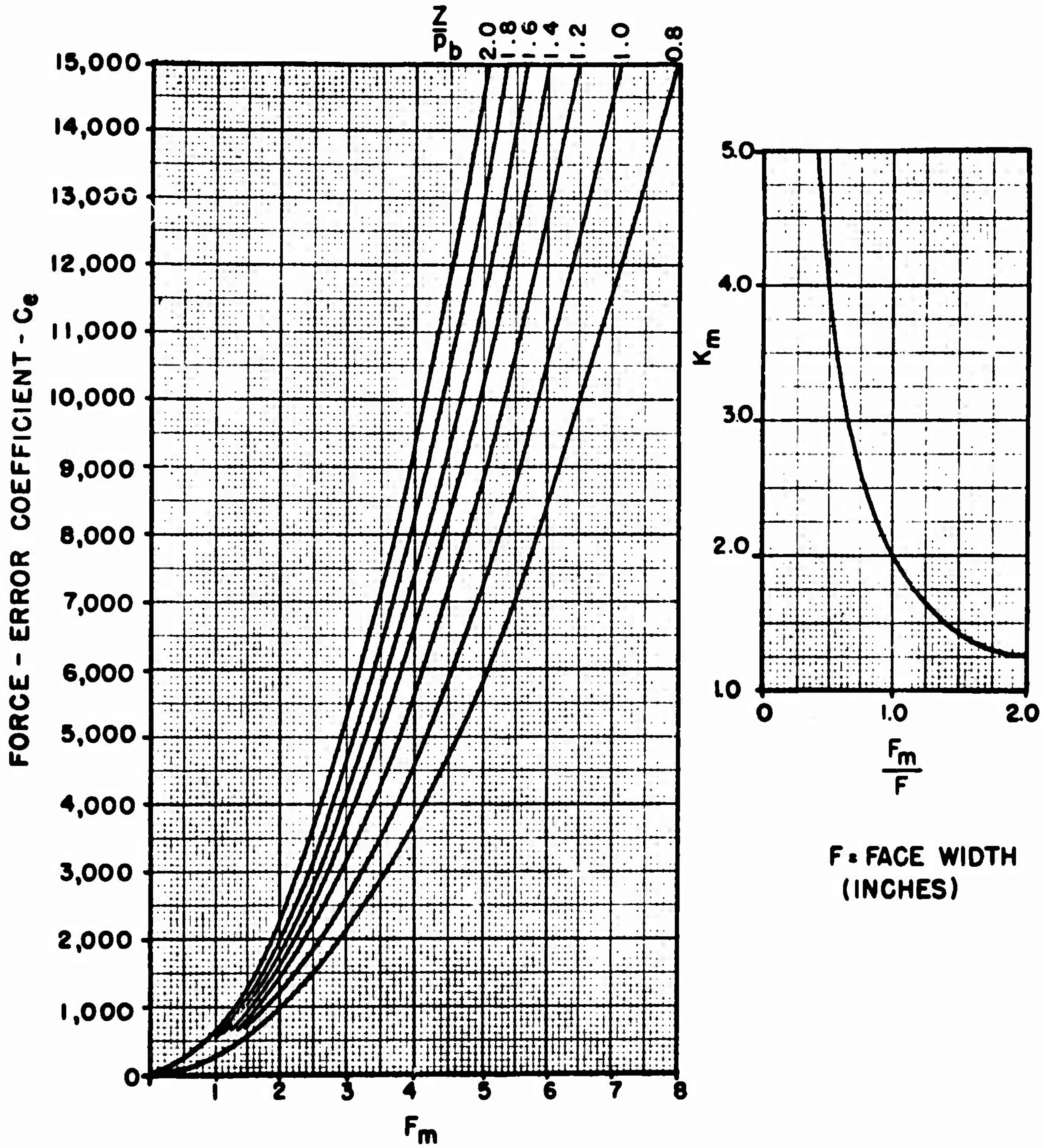

FIG. 5 HELICAL GEAR LOAD DISTRIBUTION FACTOR - K_m

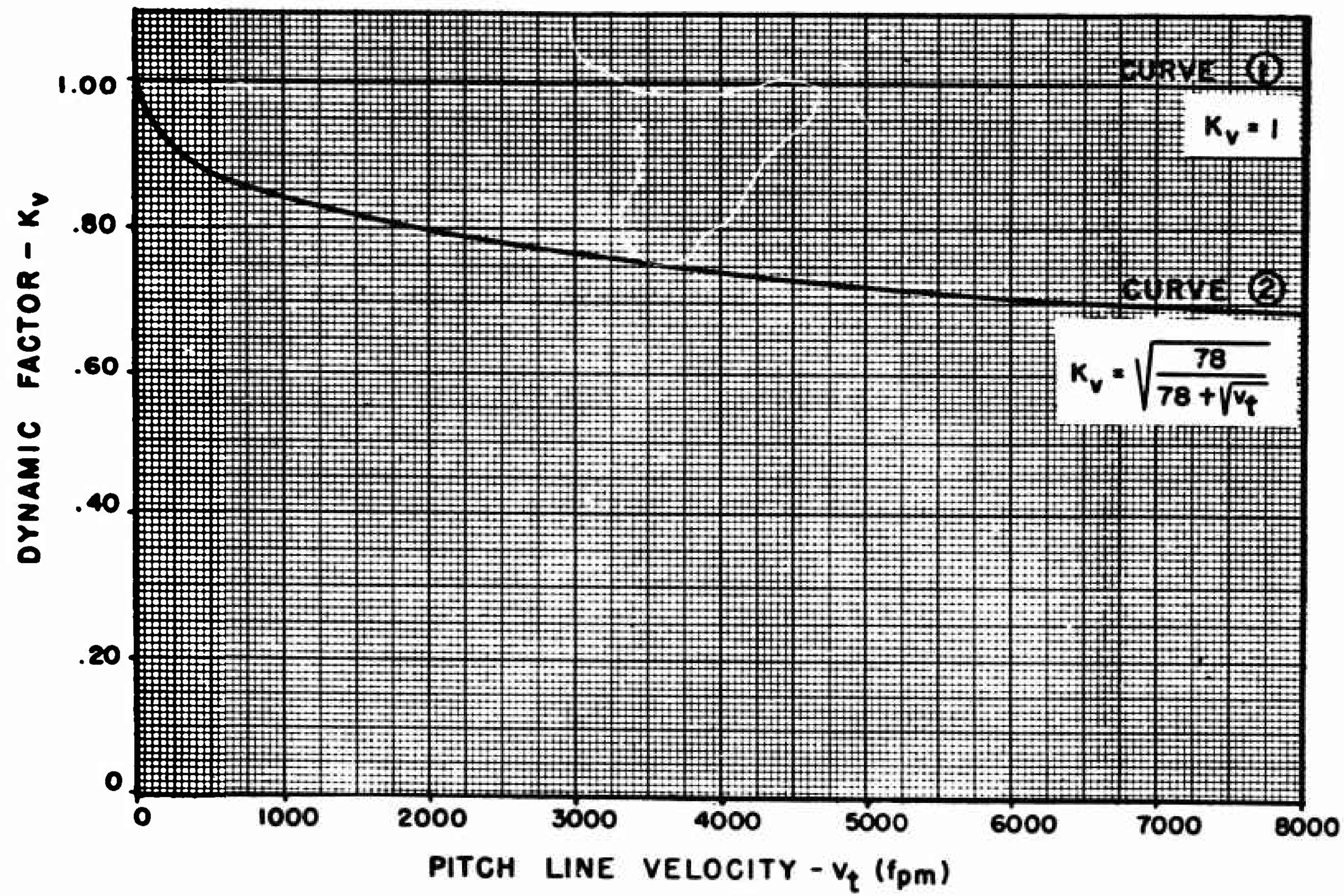

FIG.6 DYNAMIC FACTOR - K_v

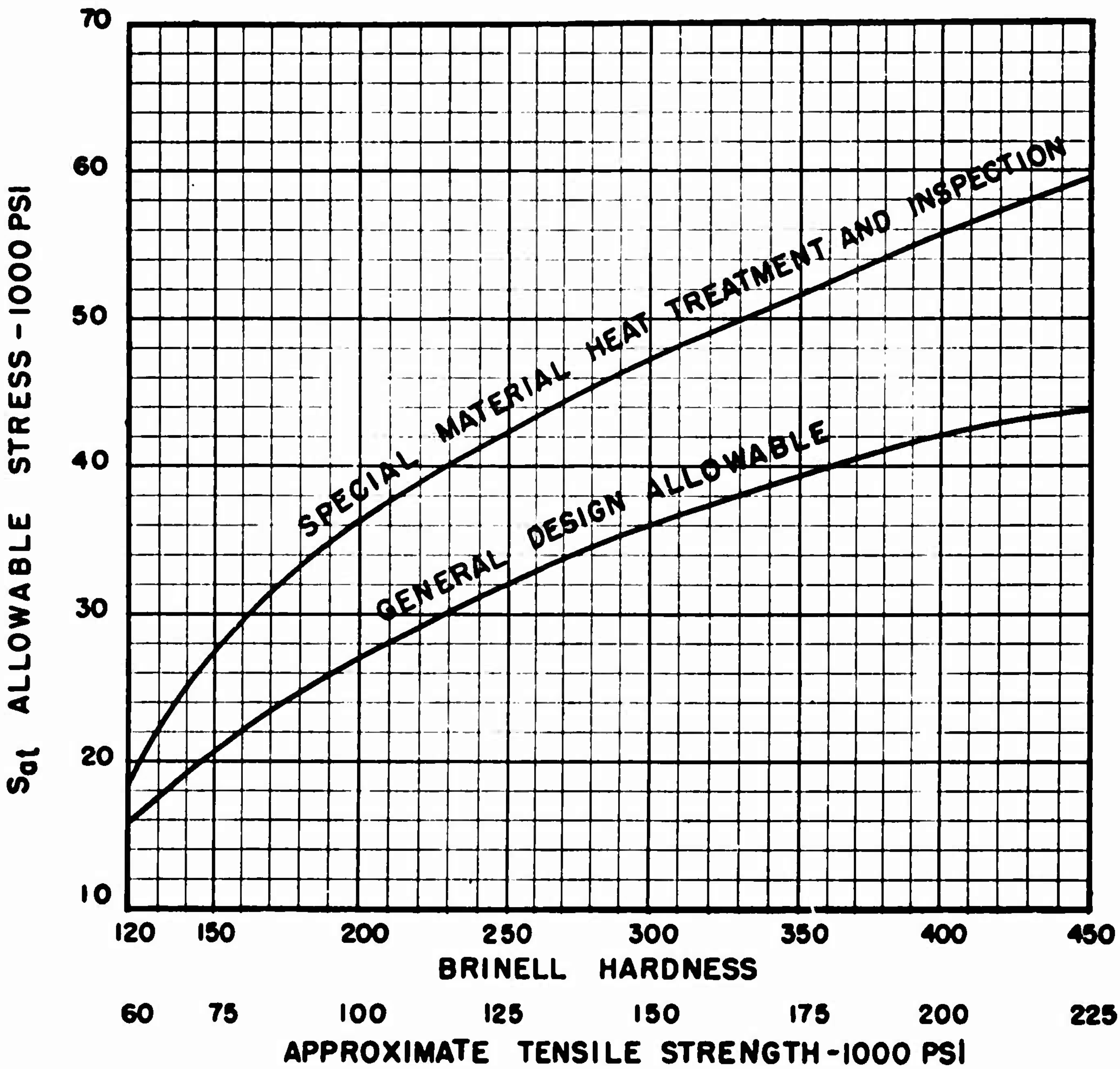

FIG.7 ALLOWABLE FATIGUE STRESS FOR STEEL GEARS - S_{at}

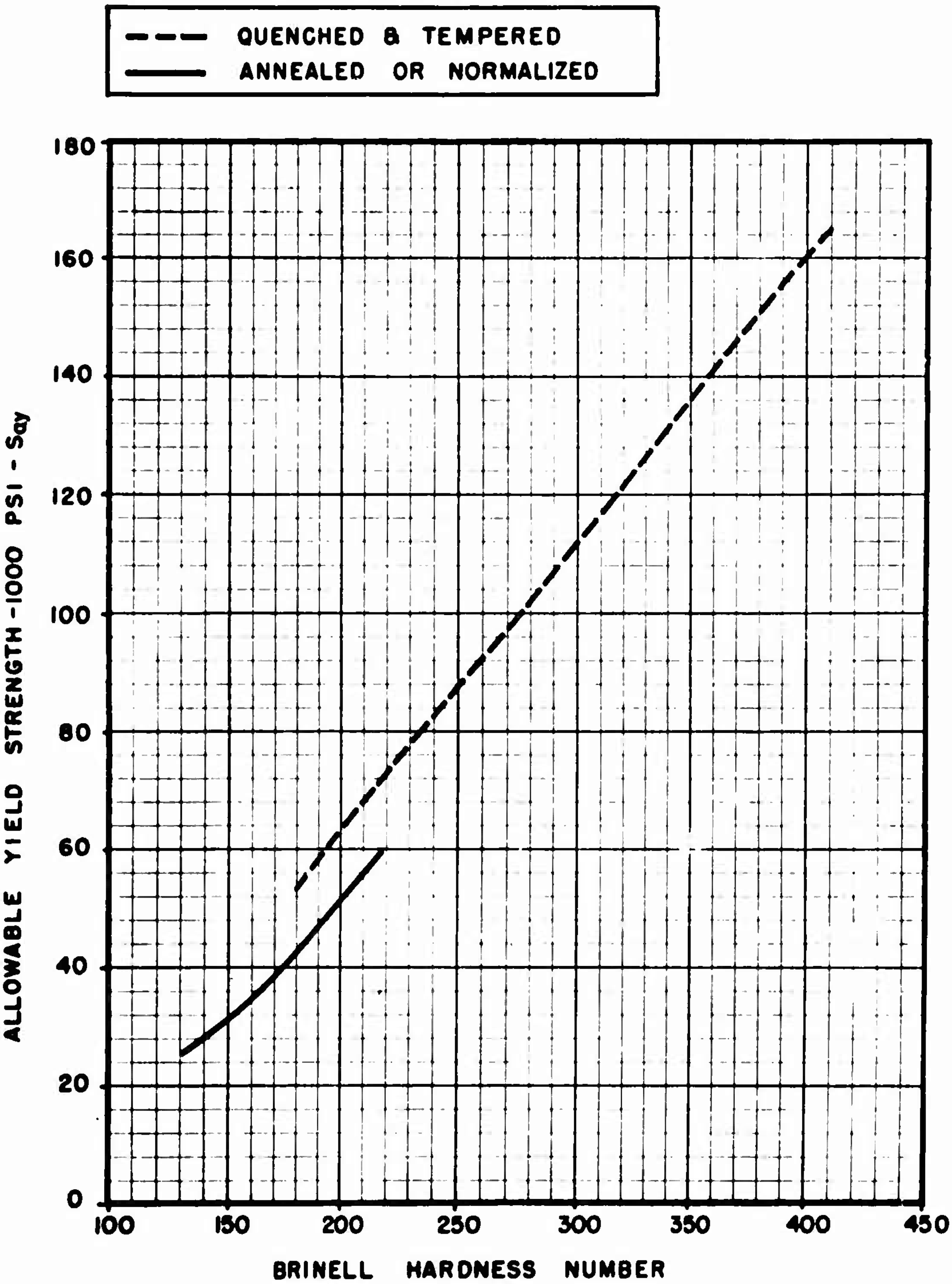

FIG. 8 ALLOWABLE YIELD STRENGTH - S_{ay}

APPENDIX A

GEOMETRY FACTOR

1. Geometry Factor – J

1.1 The geometry factor (J) is expressed : the following formula:

$$J = \frac{Y_c \cos^2 \psi}{K_f \, m_N}$$

where:

J = geometry factor

Y_c = tooth form factor

ψ = helix angle - degrees

K_f = stress correction factor

m_N = load sharing ratio

2. Stress Correction Factor – K_f

2.1 Stress correction factor depends on:

1) effective stress concentration;

2) location of load;

3) plasticity effects;

4) residual stress effects;

5) materials composition effects;

6) surface finish:

   a) resulting from gear production

   b) resulting from service

7) Hertz stress effects;

8) size effect;

9) end of tooth effects.

2.2 The stress correction factors used are those of Dolan and Broghamer and are as follows:

$$K_f = H + \left(\frac{t}{r_f}\right)^J \left(\frac{t}{h}\right)^L$$

The values of H, J and L are obtained from Table A-1. For other pressure angles, the values of H, J and L can be obtained by interpolation or extrapolation.

Table A-1 Values of H, J and L

Normal Pressure Angle	H	J	L
14½°	0.22	0.20	0.40
20°	0.18	0.15	0.45
25°	0.14	0.11	0.50

2.3 Plasticity reduces the effect of stress concentration and is partially measured by the life factor of Table 6. When more accurate data such as notch sensitivity values are available, they may be used.

3. Load Sharing Ratio – m_N

3.1 Load sharing ratio is composed of:

1) profile contact ratio;

2) face contact ratio;

3) crowning effect;

4) strengthening effect of unloaded ends.

APPENDIX A

3.2 The load sharing ratio for helical and herringbone gears is:

$$m_N = \frac{F}{L}$$

For a conservative estimate L can be taken as L_{min}. For most helical gears having a face contact ratio of 2 or more, $\frac{L_{min}}{L_{avg}}$ exceeds 0.95 and

$$m_N = \frac{p_N}{0.95\, Z}$$

where:

p_N = normal base pitch

Z = length of action in transverse plane-inches

F = net face width, inches

L = length of lines of contact for worst condition – inches

L_{min} = minimum contact length – inches

L_{max} = maximum contact length – inches

$$L_{avg} = \frac{L_{min} + L_{max}}{2}$$

This value may also be used for internal gears.

For pinions the worst condition of oblique loading at the edge of the tooth occurs with maximum length of contact.

4. Tooth Form Factor – Y_c

4.1 Y_c is determined for tip loading as shown in Figure A-1 using the generated layout of the tooth profile in the normal plane at a scale of one diametral pitch (P_{nd}). The tooth layout is made for the equivalent number of teeth. The form factor is calculated as follows:

$$Y_c = \frac{1}{\dfrac{\cos \phi_{Ln}}{\cos \phi_n}\left(\dfrac{1.5}{X\, C_h} - \dfrac{\tan \phi_{Ln}}{t}\right)}$$

5. Tooth Profile Layout Information

5.1 Nomenclature of the form factor formula and Figure A-1 are as follows:

d_{Re} = equivalent root diameter for equivalent number of teeth, inches

d_{be} = equivalent base diameter for equivalent number of teeth, inches

d_e = equivalent pitch diameter for equivalent number of teeth, inches

d_{oe} = equivalent outside diameter for equivalent number of teeth, inches

a = generated addendum to one normal diametral pitch – inches

b = generated dedendum to one normal diametral pitch – inches

ϕ_{Ln} = normal load pressure angle at tip of tooth

ϕ_n = tooth normal pressure angle

line ae = normal load line, tangent to equivalent base circle.

APPENDIX A

t = tooth thickness at section of maximum stress obtained by constructing kji tangent to fillet curvature at i so that $kj = ji$.

t_L = measured from layout

X = distance mn measured from layout

C_h = helical factor which is the ratio of the root bending moment produced by tip loading to the root bending moment produced by the same intensity of loading applied along the oblique helical contact line. Values for C_h are given by Fig. A-3. If the worst condition of load occurs where full buttressing exists, the value of C_h may be increased by 10 percent.

r_f = minimum fillet radius at root circle – inches

5.2 Factors that must be calculated may be computed as follows:

$$N_e = \frac{N}{\cos^3 \psi}$$

where:

N_e = equivalent number of teeth

N = actual number of teeth

$$d_e = N_e$$

$$a = \left(\frac{d_o - d}{2}\right)(P_{nd})$$

$$b = \left(\frac{d - d_R}{2}\right)(P_{nd})$$

where:

d = standard pitch diameter $\left(\frac{N_P}{P_d}\right)$ for the actual number of teeth and generated pitch – inches.

d_o = outside diameter for the actual number of teeth and generated pitch – inches.

d_R = root diameter for the actual number of teeth and generated pitch – inches.

P_{nd} = normal diametral pitch.

$$d_{be} = d_e (\cos \phi_n)$$

$$d_{oe} = d_e + 2a$$

$$d_{Re} = d_e - 2b$$

$$\phi_{Ln} = {}^*\cos^{-1}\left(\frac{d_{be}}{d_{oe}}\right) - \left(\frac{t_L}{d_{oe}}\right)(57.3)$$

$$r_f = \frac{(b - r_T)^2}{\frac{d_e}{2} + b - r_T} + r_T$$

where:

r_T = edge radius of generating hob to one normal diametral pitch, inches.

5.3 The minimum generated fillet radius, r_f tangent to the root circle is used to determine the stress correction factor K_f.

5.4 Having obtained the dimensions t, h, and r_f calculate t/h and t/r_f and determine the stress correction factor using the procedures as outlined.

$^*\cos^{-1}$ means "the angle whose cosine is".

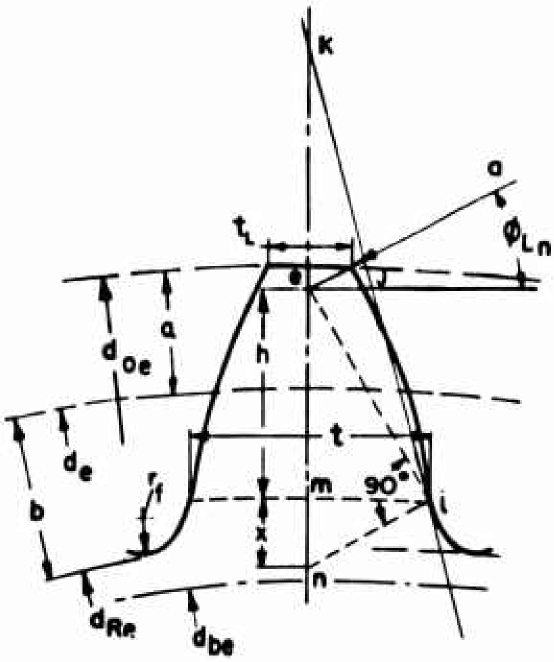

Fig A-1 Helical Tooth Form Factor Layout - Y_c

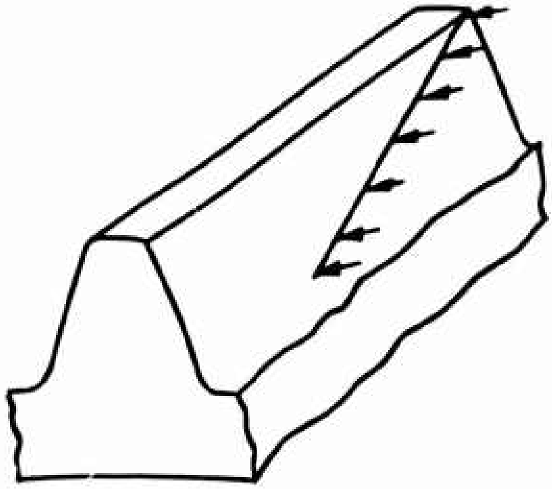

Fig A-2 Corner Loading

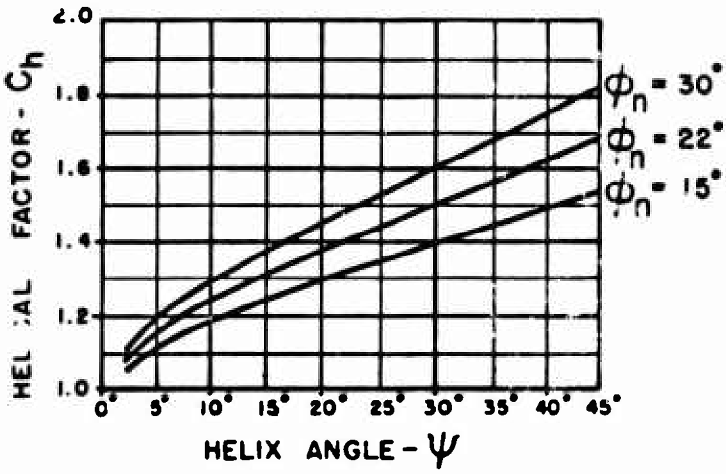

Fig. A-3 Helical Factor - C_h

$$C_h = \frac{1}{1-\sqrt{\frac{\nu}{100}\left(1-\frac{\nu}{100}\right)}}$$

FORMULA NOT APPLICABLE WHEN $\psi > 50^\circ$

ν = LOAD LINE INCLINATION ANGLE - DEGREES

$$\tan \nu = \tan \psi \sin \phi_n$$

DISTRIBUTION

US Army Materiel Command	6
US Army Aviation Materiel Command	5
United States Army, Pacific	1
US Army Forces Southern Command	1
Chief of R&D, DA	2
US Army R&D Group (Europe)	2
US Army Aviation Materiel Laboratories	33
US Army Ballistic Research Laboratories	2
Army Aeronautical Research Laboratory, Ames Research Center	1
US Army Test and Evaluation Command	1
US Army Combat Developments Command, Fort Belvoir	2
US Army Combat Developments Command Experimentation Command	1
US Army Combat Developments Command Transportation Agency	1
US Army Transportation School	1
US Army Aviation School	1
Assistant Chief of Staff for Force Development	1
US Army Tank-Automotive Command	2
US Army Aviation Test Board	2
US Army Aviation Test Activity, Edwards AFB	2
Air Force Flight Test Center, Edwards AFB	2
US Army Field Office, AFSC, Andrews AFB	1
Air Force Aero Propulsion Laboratory, Wright-Patterson AFB	1
Air Force Materials Laboratory, Wright-Patterson AFB	2
Air Force Flight Dynamics Lavoratory, Wright-Patterson AFB	1
Systems Engineering Group, Wright-Patterson AFB	2
Naval Air Systems Command, DN	15
Office of Naval Research	2
Commandant of the Marine Corps	1
Marine Corps Liaison Officer, US Army Transportation School	1
Lewis Research Center, NASA	1
Ames Research Center, NASA	2
NASA Scientific and Technical Information Facility	2
NAFEC Library (FAA)	2
US Army Board for Aviation Accident Research	1
Bureau of Aviation Safety, National Transportation Safety Board	2
US Naval Aviation Safety Center, Norfolk	1
US Naval Air Station, Norfolk	1
Federal Aviation Administration, Washington DC	2
US Government Printing Office	1
Defense Documentation Center	20
United States Army, Hawaii	1

Unclassified
Security Classification

DOCUMENT CONTROL DATA - R & D

(Security classification of title, body of abstract and indexing annotation must be entered when the overall report is classified)

1. ORIGINATING ACTIVITY (Corporate author) Allison Division of General Motors Indianapolis, Indiana	2a. REPORT SECURITY CLASSIFICATION Unclassified 2b. GROUP

3. REPORT TITLE

ADVANCEMENT OF HELICAL GEAR DESIGN TECHNOLOGY

4. DESCRIPTIVE NOTES (Type of report and inclusive dates)
Final Report (22 June 1966 through 22 February 1968)

5. AUTHOR(S) (First name, middle initial, last name)
Wayne L. McIntire
Terry A. Lyon

6. REPORT DATE	7a. TOTAL NO. OF PAGES	7b. NO. OF REFS
July 1968	257	23

8a. CONTRACT OR GRANT NO. DA 44-177-AMC-450(T) b. PROJECT NO. Task 1G125901A01410 c. d.	9a. ORIGINATOR'S REPORT NUMBER(S) USAAVLABS Technical Report 68-47 9b. OTHER REPORT NO(S) (Any other numbers that may be assigned this report) Allison EDR 5503

10. DISTRIBUTION STATEMENT
This document has been approved for public release and sale; its distribution is unlimited.

11. SUPPLEMENTARY NOTES	12. SPONSORING MILITARY ACTIVITY
	U.S. Army Aviation Materiel Laboratories Fort Eustis, Virginia

13. ABSTRACT

An analytical and experimental study to evaluate factors for accurate appraisal of gear tooth bending strength is described. A design analysis consisting of a thorough review of current methods of calculating bending strength is presented. A dynamic test at high speed and an experimental evaluation of strain gage measured stresses are also presented for substantiation of the theoretical stress analysis. Results from a designed static fatigue test are presented to evaluate the effect of two geometric variables, i.e., pressure angle and helix angle, and two load positions. A final computer program is described to calculate bending stress as substantiated by design analysis, experimental evaluation, and static fatigue test. It is shown that the thorough consideration of geometric variables permits a more precise assessment of bending strength for life expectance of lightweight aircraft gearing.

DD FORM 1 NOV 65 1473 REPLACES DD FORM 1473, 1 JAN 64, WHICH IS OBSOLETE FOR ARMY USE.

Unclassified
Security Classification

Unclassified

Security Classification

14 KEY WORDS	LINK A		LINK B		LINK C	
	ROLE	WT	ROLE	WT	ROLE	WT
Helical Gear Teeth						
Bending Strength						
Bending Stress						
Dynamic Factor						
Endurance Limit						
Calculation Method						
Material Stren 'h						
Speed Factor						

Unclassified

Security Classification

8054-68